

1-1-2013

A Comprehensive Research Framework for Geographic Parthenogenesis in Whiptail Lizards (Genus *Aspidoscelis*)

Adam Leland

University of Nevada, Las Vegas, adam.leland@gmail.com

Follow this and additional works at: <https://digitalscholarship.unlv.edu/thesesdissertations>



Part of the [Biology Commons](#), and the [Genetics Commons](#)

Repository Citation

Leland, Adam, "A Comprehensive Research Framework for Geographic Parthenogenesis in Whiptail Lizards (Genus *Aspidoscelis*)" (2013). *UNLV Theses, Dissertations, Professional Papers, and Capstones*. 1747.

<https://digitalscholarship.unlv.edu/thesesdissertations/1747>

This Dissertation is protected by copyright and/or related rights. It has been brought to you by Digital Scholarship@UNLV with permission from the rights-holder(s). You are free to use this Dissertation in any way that is permitted by the copyright and related rights legislation that applies to your use. For other uses you need to obtain permission from the rights-holder(s) directly, unless additional rights are indicated by a Creative Commons license in the record and/or on the work itself.

This Dissertation has been accepted for inclusion in UNLV Theses, Dissertations, Professional Papers, and Capstones by an authorized administrator of Digital Scholarship@UNLV. For more information, please contact digitalscholarship@unlv.edu.

A COMPREHENSIVE RESEARCH FRAMEWORK FOR GEOGRAPHIC PARTHENOGENESIS

IN WHIPTAIL LIZARDS (GENUS *ASPIDOSCELIS*)

by

Adam Bohrer Leland

Bachelor of Science & Bachelor of Arts
University of California, San Diego
2001

Master of Science
San Diego State University
2007

A dissertation submitted in partial fulfillment of
the requirements for the

Doctor of Philosophy in Biological Sciences

**School of Life Sciences
College of Sciences
The Graduate College**

**University of Nevada, Las Vegas
December 2012**

Copyright by Adam B. Leland, 2013
All Rights Reserved



THE GRADUATE COLLEGE

We recommend the dissertation prepared under our supervision by

Adam Leland

entitled

A Comprehensive Research Framework for Geographic Parthenogenesis in Whiptail Lizards (Genus *Aspidoscelis*)

be accepted in partial fulfillment of the requirements for the degree of

Doctor of Philosophy in Biological Sciences
School of Life Sciences

Brett Riddle, Ph.D., Committee Chair

Daniel Thompson, Ph.D., Committee Member

David Bradford, Ph.D., Committee Member

Matthew Lachniet, Ph.D., Graduate College Representative

Tom Piechota, Ph.D., Interim Vice President for Research &
Dean of the Graduate College

December 2012

ABSTRACT

A Comprehensive Research Framework for Geographical Parthenogenesis in Whiptail Lizards (genus *Aspidoscelis*)

by

Adam Bohrer Leland

Dr. Brett R. Riddle, Examination Committee Chair
Professor
University of Nevada, Las Vegas

One of the most compelling topics in biology has been the ubiquity of sexual reproduction in living organisms. Because the ecological and evolutionary advantages of sex are well founded, those organisms that reproduce asexually remain enigmatic. Parthenogenesis, the clonal reproduction of an all-female species without the need for males, is a relatively common form of asexual reproduction in vertebrates, and has been subject of numerous academic investigations. Many parthenogenic organisms also share aspects of their geographic distributions, such as inhabiting higher latitudes, higher altitudes, islands or island-like habitats, xeric environments, and marginal, disturbed or ecotonal habitats relative to their sexual congeners, a pattern termed “geographical parthenogenesis” (Vandel, 1928). This has led to the development of numerous hypotheses to account for the geographic distribution and persistence of parthenogenic organisms relative to their sexual relatives.

These hypotheses often consider overlapping biological processes, complicating efforts to create a simplified model accounting for parthenogenic reproduction. Instead

of treating hypotheses individually, a better approach is to categorize common biological patterns underlying the suite of hypotheses posited in the literature to develop a Comprehensive Research Framework that tests for overall patterns based on their commonalities and differences. In this way, we may tease apart the relative contribution of a particular hypothesis.

In this chapter, we review the hypotheses regarding geographic parthenogenesis generated in the literature and emphasize the underlying biological processes. Using these biological processes as our framework, we develop a five-part Comprehensive Research Framework that encompasses the range of biological phenomena acting on parthenogenic organisms: (1) the Population Genetics of Sexual Populations; (2) Hybridity and Heterosis; (3) Clonal Ecological Strategy; (4) Exclusion or Coexistence; and (5) Evolutionary History. In each section, we suggest potential methods and studies that explicitly test biological processes acting at that level, which have the potential to illuminate the biological conditions where parthenogenic reproduction is successful.

Using the Comprehensive Research Framework, we conclude with two test studies that each examine the expectations of one of the five parts identified above, using parthenogenic hybrid whiptail lizards (*genus Aspidoscelis*) as our model species. We explicitly test the Hybridity and Heterosis (Chapter Two) and Clonal Ecological Strategy (Chapter Three) sections, utilizing the methods suggested in the Comprehensive Research Framework. These studies demonstrate the utility of the framework we developed, supporting its use as a road-map for developing further research programs into additional taxa where parthenogenic reproduction occurs.

ACKNOWLEDGEMENTS

For the successful completion of this dissertation, I must thank all who served me through my academic career: Dr. Brett Riddle, my advisor who encouraged my research direction and focus, Dr. Daniel Thompson and Dr. David Bradford whose criticisms, suggestions and discussions improved the quality and content of the research and manuscript, and Dr. Matthew Lachniet (UNLV Geosciences), my graduate college representative whose solid advocacy provided me an anchor in difficult times. My deepest gratitude I also extend to Dr. Andrew Bohonak (SDSU Biology Department) who provided me with lab space and access to lab equipment while conducting genetics research in San Diego.

My research also greatly benefited from numerous discussions with colleagues. I thank members of the Riddle Lab: Sean Neiswenter for his expertise regarding AFLP protocols, Tereza Jezkova for the numerous discussions and suggestions regarding modeling and Maxent, and Mallory Eckstut for her selfless assistance with completing and submitting this document to the Graduate College. I also wish to recognize Cheryl Vanier, who not only provided invaluable statistical advice, but also served as a mentor for my teaching experiences.

The unwavering support of family and friends provided the foundation on which I could build my academic career, and all deserve my heartfelt appreciation. In particular I wish to thank my good friend Dean Leavitt, who participated in my first field trip and almost single handedly sparked my interest in herpetology. My parents and my mother-in-law were incredibly important to my successes and offered unsolicited support

throughout all stages of my pursuits. Finally I must also thank the support of my wife, Kelly, who was the bedrock on which I attached myself during this process, and she frequently held me fast when I was at risk of being washed away, even while she was enveloped in her own pursuit of a law degree.

This project couldn't have been completed without the financial support of ASIH Gaige Award (2008) and the UNLV Graduate & Professional Student Association Grants (2007 - 2009).

TABLE OF CONTENTS

Abstract	iii
Acknowledgements.....	v
Table of Contents	vii
List of Tables	ix
List of Figures	x
Chapter 1: A Comprehensive Research Framework on Geographical Parthenogenesis	1
<i>Introduction.....</i>	<i>1</i>
<i>Hypotheses.....</i>	<i>3</i>
<i>The Comprehensive Research Framework.....</i>	<i>8</i>
1. Population Genetics of Sexual Congeners	9
2. Hybridity and Heterosis	11
3. Clonal Ecological Strategy	14
4. Exclusion or Coexistence.....	15
5. Evolutionary History.....	17
<i>Case Studies</i>	<i>18</i>
<i>Conclusion</i>	<i>22</i>
Chapter 2: Hybridity & Heterosis in Geographical Parthenogenesis.....	25
<i>Abstract.....</i>	<i>25</i>
<i>Introduction.....</i>	<i>26</i>
<i>Methods</i>	<i>34</i>
Museum Records	35
Environmental Variable Data Sets	36
Maxent methodology	37
<i>Results</i>	<i>40</i>
PCA Results	41
ANOVA Results	42
Maxent Results	44
<i>Discussion.....</i>	<i>55</i>
Hypotheses: Hybridity & Heterosis.....	56
Modeling Considerations	61
Paleoclimate.....	64

Alternative Considerations	66
Further Work.....	69
<i>Conclusion</i>	70
Chapter 3. Clonal Ecological Strategy in <i>Aspidoscelis</i>	90
<i>Abstract</i>	90
<i>Introduction</i>	91
Hypotheses	92
<i>Methods</i>	96
<i>Results</i>	103
Genetic Results	103
Principal Components Analysis: <i>A. unipares</i> and <i>A. velox</i> only	106
Principal Components Analysis: All whiptails	108
<i>Discussion</i>	110
General Conclusions	110
Environmental Structure.....	114
Future Directions	118
<i>Conclusion</i>	120
Appendix A	134
Appendix B.....	165
Appendix C.....	166
Appendix D	168
Appendix E	172
Appendix F	175
Appendix G	177
Bibliography.....	183
Curriculum Vitae	193

LIST OF TABLES

Table 2.1. Academic institutions and natural history museums for specimen records obtained through the HerpNet data portal	73
Table 2.2. Initial Maxent contribution and permutation scores of each variable per species	74
Table 2.3. Variables removed iteratively during that variable reduction process	75
Table 2.4. Principal component analysis (PCA) result summary on 19 WorldClim variables extracted from eight focal whiptail species.	76
Table 2.5. Species pairwise significance for Tukey’s HSD test on PC1, PC2 and PC3.	77
Table 3.1. Sampling locations and abbreviations with geographic coordinates and location descriptions.....	123
Table 3.2. Selective AFLP primer pair combinations.....	124
Table 3.3. Principal Component Analysis PC scores	125
Table 3.4. Pairwise comparisons of environmental conditions occupied by AFLP clusters for <i>A. uniparens</i> based on the PCA using only <i>A. uniparens</i> and <i>A. velox</i>	126
Table 3.5. Pairwise comparisons of environmental conditions occupied by AFLP clusters for <i>A. uniparens</i> based on the PCA using all whiptail species.....	127

LIST OF FIGURES

Figure 1. Potential models of environmental niches along two hypothetical habitat variables	24
Figure 2.1. Phylogenetic relationships between sexual <i>Aspidoscelis</i>	78
Figure 2.2. Range maps for <i>Aspidoscelis</i> species.....	79
Figure 2.3. Geographic locations of museum specimens downloaded from HerpNet	80
Figure 2.4. Graph of mean PC scores from PCA of 8 whiptail species with 95% confidence intervals	81
Figure 2.5. Maxent predicted distributions for <i>A. burti</i>	82
Figure 2.6. Maxent predicted distributions for <i>A. exsanguis</i>	83
Figure 2.7. Maxent predicted distributions for <i>A. flagellicauda</i>	84
Figure 2.8. Maxent predicted distributions for <i>A. gularis</i>	85
Figure 2.9. Maxent predicted distributions for <i>A. inornata</i>	86
Figure 2.10. Maxent predicted distributions for <i>A. sonora</i>	87
Figure 2.11. Maxent predicted distributions for <i>A. uniparens</i>	88
Figure 2.12. Maxent predicted distributions for <i>A. velox</i>	89
Figure 3.1. Sampling localities for all specimens used	128
Figure 3.2. <i>Aspidoscelis uniparens</i> AFLP UPGMA clustering dendrogram	129
Figure 3.3. Geographic location of AFLP clusters for <i>A. uniparens</i>	130
Figure 3.4. <i>Aspidoscelis velox</i> AFLP UPGMA clustering dendrogram	131
Figure 3.5. Geographic location of AFLP clusters for <i>A. velox</i>	132
Figure 3.6. Principal Component scatter plots for AFLP clusters	133

CHAPTER 1:
A COMPREHENSIVE RESEARCH FRAMEWORK ON
GEOGRAPHICAL PARTHENOGENESIS

Introduction

One of the most compelling discussions in ecological and evolutionary theory regards the evolution and maintenance of sexual reproduction. In spite of the numerical advantage of asexual reproduction (Maynard Smith, 1978), sex is the rule rather than the exception based on its ubiquity in plant and animal taxa (Kearney, 2005). This is often attributed to the adaptive advantage of sexual recombination in changing environments and heterogeneous landscapes, and to competitive, predatory and parasitic pressures on populations (Maynard Smith, 1978; Bell, 1982).

Parthenogenesis, the clonal reproduction of an all-females species without the need for males, is a form of asexual reproduction in animals. Parthenogenesis is relatively rare in nature, occurring in less than 0.1 percent of described species (White, 1978; Kearney, 2005), but is found in a wide range of organisms, from insects to vertebrates (reviewed in: Glesener *et al.*, 1978; Bell, 1982; Kearney, 2005). Parthenogenic species are often found at higher latitudes, higher altitudes, islands or island-like habitats, xeric environments, and in marginal, disturbed or ecotonal habitats relative to their sexual progenitors, a pattern termed “geographical parthenogenesis” (Vandel, 1928; Glesener *et al.*, 1978; Maynard Smith, 1978; Lynch, 1984). Within taxonomic groups where parthenogenesis is found, parthenogenic organisms typically

occupy the terminal nodes of phylogenetic trees, indicating that these clonal organisms have arisen recently from sexual ancestors and do not result in a diversification of asexual lineages. As a result, parthenogenic organisms have been regarded as evolutionary “dead-ends” (Simon *et al.*, 2003), likely due to the long term negative effects of asexuality, such as the accumulation of deleterious mutations known as “Müller’s ratchet” and the lack of recombination in the face of environmental change, evolving parasites and competitors (the "Red Queen" hypothesis, Maynard Smith, 1978). However, the persistence and broad distribution of many parthenogenic organisms suggests that, under appropriate conditions, there may be an ecological and/or evolutionary advantage to this form of reproduction.

An additional complication regarding vertebrate parthenogenic organisms is that most are the result of hybridization between two historically separate groups of sexual species (Simon *et al.*, 2003; Kearney, 2005). As a result, explanations regarding the success of parthenogenic organisms needs to include the role that hybridization may have had on their evolution and ecology (Kearney, 2005). Further, many hybrid parthenogenic organisms are also polyploids (Kearney, 2005), containing more than the typical two sets of chromosomes of a diploid organism (one set from a maternal parent and one set from a paternal parent). Polyploidy has been shown to characterize organisms with increased geographic ranges and environmental tolerances (Cain, 1944; Glesener *et al.*, 1978). Studies regarding the success and geographic distributions of parthenogenic organisms need to disentangle the relative roles of asexuality, hybridity and polyploidy.

Hypotheses

Parthenogenic organisms are the focus of numerous studies regarding the origin, cellular biology, geographic distribution and evolutionary advantages of parthenogenesis relative to their sexual ancestors. As a result, a diverse array of biological explanations and hypotheses has been described in the literature. Many of the posited hypotheses vary in the degree to which they address the effects of asexuality, hybridity and polyploidy in parthenogenic organisms. Often, predictions of one or two of these hypotheses have been tested where one hypothesis is the alternative to another, despite the fact that contributing biological phenomena may not be exclusive to only one hypothesis. Below, nine hypotheses from the literature regarding the geographic distribution and persistence of parthenogenesis are summarized to describe the diversity and range of biological processes that may contribute to the success of parthenogenic organisms. The range of hypotheses also illustrates the complex interplay of biological processes and evolutionary theories that are difficult to disentangle when attempting to explain the advantages of parthenogenesis.

Reproductive Assurance: This hypothesis can be split into two different but related interpretations: First (1), newly colonizing parthenogenic individuals have an inherent advantage because they are not mate limited (Cuellar, 1977; Bell, 1982; Moore, 1984; Peck *et al.*, 1998). A single parthenogenic individual can establish a new population because males, which are necessary to the successful establishment of a sexual population, are not needed. Second (2), in marginal habitats where population

densities may be low, parthenogenic organisms will be better able to persist (less likely to be extirpated) because they are not mate limited (Cuellar, 1977; Bell, 1982; Peck *et al.*, 1998).

Biotic Interactions: This hypothesis posits that, relative to asexual taxa, sexual species can better adapt to the biotic pressures of parasites and predators because sexual recombination can generate novel genetic combinations (Levin, 1975; Glesener *et al.*, 1978; Maynard Smith, 1978) and maintain higher geometric fitness over time as fitness levels fluctuate (Hamilton 1980). This hypothesis predicts that asexual species will therefore only be able to persist in areas where such biotic interactions are weak, such as habitat where environmental factors only support low population densities and the influence of abiotic factors dominate biotic factors (Levin, 1975; Hamilton, 1980; Haag & Ebert, 2004).

Weed Hypothesis: Formulated directly from observations of environments inhabited by parthenogenic whiptail lizards, this hypothesis posits that whiptails are successful only in marginal, disturbed or ecotonal habitats (Wright & Lowe, 1968). Because of their superior colonizing ability and broad ecological tolerances, whiptails colonize these areas much like a “weed” (Wright & Lowe, 1968; Vrijenhoek, 1989). The areas containing parthenogenic whiptails are also characterized as historically unstable because of Pleistocene climate fluctuations, and the habitat and/or species distributions may still be expanding or shifting (Wright & Lowe, 1968; Wright & Vitt, 1993).

Intermediate Niche: Here, hybrids are expected to be phenotypically intermediate to their sexual progenitors because they have genes that evolved in

environmental conditions from each population, resulting in parthenogenic hybrids best suited to environmental niches intermediate to their sexual progenitors (Moore, 1984; Vrijenhoek, 1989; Vrijenhoek, 1998). Similar to hybrid superiority, this hypothesis also suggests that hybrids will have an advantage in intermediate or marginal habitats between sexual progenitors because sexual species may not be well adapted and unable to compete (Moore, 1984).

Generalist Genotype: Here, the success of parthenogenic organisms is hypothesized to be due to selection for the genotype which is most generally adapted to a wide range of environmental conditions (Vrijenhoek, 1998). While used to explain broad geographic distributions and tolerance to a wide range of environments (Parker Jr. *et al.*, 1977), this hypothesis also explains that the genotype with the highest geometric mean fitness (smallest variance) will replace more specifically adapted clones over evolutionary time in highly variable environments (Lynch, 1984; Vrijenhoek, 1998). Accordingly, it is expected that there will be few distinct hybrid clones distributed over a broad range of environmental conditions across the distribution of a parthenogenic hybrid.

Frozen Niche: In contrast to the generalist genotype, this hypothesis suggests that successful parthenogenic clones are genetically “frozen” to a specific range of environmental conditions (Vrijenhoek, 1998). Natural selection then acts on the array of clonal genotypes such that successful clones will have minimal niche overlap with other clones and their sexual relatives (Vrijenhoek, 1998). Through this process, one would expect to see multiple narrowly adapted clones with minimal environmental

overlap over the distribution of the parthenogenic species.

Hybridity and Heterosis (Hybrid Vigor): This hypothesis suggests that the high heterozygosity resulting from the initial hybridization event creates hybrids superior to their sexual progenitor species (Moore, 1984; Vrijenhoek, 1989; Whitlock *et al.*, 2000; Kearney, 2005). In the most extreme form, hybrids are more vigorous than either parent (as seen in many domesticated plants Moore, 1984), expanding their ranges far beyond the environmental constraints of their sexual relatives (Moore, 1984; Vrijenhoek, 1989). Additionally, hybridization has the potential to be adaptive because different combinations of progenitor genes may lead to hybrid genotypes of varying fitness (Barton, 2001) that potentially result in adaptations to new environments (Kearney, 2005). One complicating factor associated with this hypothesis is the occurrence of polyploidy in many hybrid vertebrates (Bell, 1982; Moore, 1984; Kearney, 2005). Polyploid species have been associated with tolerance of wider and more extreme environmental conditions relative to sexual species (Cain, 1944; Otto & Whitton, 2000; Hunter *et al.*, 2001). This success is attributed to the fact that polyploid species have a larger amount of genetic material on which natural selection can act (White, 1978; Otto & Whitton, 2000; Vrijenhoek, 2006). Under this hypothesis, it is expected that hybrid parthenogens expand their distribution beyond their sexual progenitors into novel environmental conditions. However, it must be stressed that separating the effects of polyploidy, heterozygosity and hybridity is very difficult because the preponderance of parthenogenic organisms are polyploid hybrids (Moore, 1984; Kearney, 2005).

Gene Flow: Populations of a particular species are theoretically expected to inhabit their fundamental niche if there are no barriers to individual movement and there is no competitive exclusion (Hutchinson, 1957). At the periphery, populations have a tendency to occur less frequently and to be less densely occupied (Brown, 1984), possibly because these populations are located in marginal environments. In the absence of gene flow, peripheral populations are expected to evolve to new ecological optima. If there is continued gene flow from central populations, theoretical models have shown that the effects of natural selection are arrested and peripheral populations are unable to adapt (Garcia-Ramos & Kirkpatrick, 1997). Under the gene flow hypothesis, parthenogenic species are expected to have an advantage in marginal habitats because successful parthenogens are derived from peripheral populations and are not subject to the deleterious effects of gene flow compared to their sexual progenitors (Peck *et al.*, 1998).

Metapopulation Model: Also known as the inbreeding hypothesis, this idea also operates on the premise that peripheral populations are located in marginal habitats, thus reducing the density and frequency of populations. Instead of the homogenizing effect of gene flow in sexual populations arresting selection, it is assumed that gene flow amongst peripheral populations is very low or non-existent, such that peripheral population act like metapopulations and genetic drift and inbreeding depression have the strongest effects (Haag & Ebert, 2004). The loss of genetic diversity and inbreeding depression have negative effects on the fitness (Charlesworth & Charlesworth, 1987; Amos & Balmford, 2001; Keller & Waller, 2002) and the evolutionary potential of sexual

species (Franklin, 1980; Soulé, 1980), and under this model, these effects would be strongest in peripheral populations. In contrast, asexual populations are protected from these effects because there is no sexual recombination (Vrijenhoek, 1998; Haag & Ebert, 2004) and because they can persist in marginal habitats with low density and frequency. In addition, hybridization between inbred populations of two sexual species may exhibit heterosis (Whitlock *et al.*, 2000), leading to high fitness hybrids. The combination of low fitness in sexual peripheral populations combined with higher maintained genetic diversity in asexual populations may allow parthenogenic hybrids to invade and persist in peripheral environments (Haag & Ebert, 2004).

The Comprehensive Research Framework

Studies that attempt to understand the geography and coexistence of parthenogenic species relative to their sexual progenitors are complicated by the processes and assumptions that are not exclusive to the individual hypotheses outlined in the previous section. While many researchers have studied predictions based on individual hypotheses, some have recognized the redundancy of published hypotheses and attempted to create classifications based on their commonalities (Moore, 1984; Haag & Ebert, 2004). However, there is a need for a simplifying pattern or explanation for the geographic distribution and persistence of parthenogenic hybrids.

Instead of treating each hypothesis individually, where interpretation of results is complicated by overlapping predictions, a better approach is to examine hypotheses collectively and identify consistent predictions to test. This section describes a

Comprehensive Research Framework where biological patterns relevant to described hypotheses are tested individually, and, in turn, the relative contribution of that hypothesis can be evaluated.

The scope of this framework is very large, encompassing research into ecological and evolutionary patterns at multiple scales (from the population to distributional scale) of both parthenogenic organisms and their sexual ancestors, or in case of parthenogenic hybrids, their sexual progenitors. This reflects the complexity in parthenogenesis research and requires multiple studies utilizing different data types with a wide array of methods. Current computational techniques combined with increasingly sophisticated molecular methods demonstrate promise for revealing biological patterns associated with the success of parthenogenesis. The framework outlined here provides a road map to design studies that will tease apart these biological processes to determine their relative effects on successful parthenogenic organisms.

The Comprehensive Research Framework outlined below is divided into five testable simplifying categories based on the biological processes identified in the nine hypotheses reviewed above, and the type of research methods necessary to study them. Each category is outlined individually below:

1. Population Genetics of Sexual Congeners

The Population Genetics category looks at the relative effects of inbreeding and gene flow on the adaptation of sexual populations in marginal habitat. The premise is that population genetic processes are acting on peripheral sexual populations such that they are unable to adapt to peripheral habitats, or experience the deleterious effects of

small population size on the periphery of their range (Haag & Ebert, 2004).

Parthenogenic hybrids, on the other hand, lock the high heterozygosity created by the combination of divergent genomes from their sexual progenitors in an asexual reproductive mode (Kearney, 2005) because there is no genetic recombination and hence loss of genetic diversity. The result is a genetically superior parthenogenic hybrid that can successfully compete with the relatively less adapted sexual progenitors on the periphery of the sexual species range. Here, population genetic processes acting on the periphery of a sexual population (especially in areas that overlap with parthenogenic congeners) are tested instead of a direct examination of parthenogenic species to illustrate patterns in sexual populations that may relate to the success of parthenogenic species.

One potential pattern hypothesizes that peripheral sexual populations are affected by inbreeding depression due to low densities and/or population size because peripheral habitat is marginal relative to habitat in the core of the species distribution. As a result, peripheral sexual populations are expected to be characterized by low diversity, low heterozygosity and high genetic substructure relative to more central populations (Haag & Ebert, 2004). If inbreeding is an important factor in the persistence and adaptation of peripheral populations, then the following expectations are hypothesized: (1) there is significantly less genetic diversity in peripheral populations relative to core populations; and (2) a significant amount of variance in population structure (F_{ST}) is located in peripheral populations, while a significant amount of the overall genetic variation is located core populations.

A second pattern hypothesizes that peripheral populations are affected by gene flow from core populations such that the effects of natural selection on the periphery are swamped by genes from core populations and peripheral populations are unable to adapt to peripheral environments (Garcia-Ramos & Kirkpatrick, 1997). The expected population genetic patterns contrast with the above inbreeding depression pattern, where (1) there are similar levels of genetic diversity and heterozygosity between core and peripheral populations, (2) there is high gene flow between core and peripheral populations, and (3) there is low genetic structure between core and peripheral populations because of shared genes due to ongoing gene flow.

Significance of these expectations can be analyzed by testing for deviations from a random distribution for population haplotype diversity (h) and nucleotide diversity (π) between core and peripheral populations using a chi-squared test. An Analysis of Molecular Variance (AMOVA: Excoffier *et al.*, 1992) can also test how genetic variation is partitioned between populations, and between peripheral and core groups of populations. In addition, isolation by distance plots would determine if there is a significant difference between the relationship of genetic distance and geographic distance between peripheral populations and between core populations, where genetic differences are higher in peripheral populations relative to geographic distance.

2. Hybridity and Heterosis

The Hybridity and Heterosis category is based on the relative effects of being a hybrid and experiencing hybrid vigor, and can be examined by analyzing niche breadth and overlap between parthenogenic hybrids and their sexual progenitor species. The

true ecological niche (*sensu* Hutchinson, 1957) of a species is difficult to measure because it isn't possible to account for all dimensions of a species niche. Previous studies used working definitions of the species niche based on research measurements, such as quantifying overlap in food resources or physiological tolerances, but these characteristics are only a subset of the characteristics that make up the fundamental niche. Hybridity and heterosis may best be explained by patterns occurring at landscape level if we aim to describe aspects of species distributions. For this reason, we treat the species niche based on spatial characteristics such as physical environment (temperature, precipitation, soil, aspect, *etc.*) and biotic variables (vegetation, biotic community, species presence, *etc.*). There is a large body of literature dedicated to species distribution modeling (SDM) or ecological niche modeling (ENM) using presence-only or presence/absence data, and we direct the reader to the primary literature for a full review of techniques available. These techniques can be used to evaluate hypothesized patterns described in the following paragraph regarding the niche of parthenogenic hybrid organisms relative to their sexual parents.

The first potential pattern (1) is that hybrid parthenogenic species occupy a niche that is intermediate to both of their sexual progenitors. Under this predicted pattern, the ecological breadth of the hybrid should overlap substantially with both progenitors, without inhabiting environmental space that would be novel to either sexual species (Figure 1A). A potential variant of this pattern (2) concerns genetic dosing in polyploid hybrids, where the hybrid niche should overlap most with the progenitor that contributed the most genetic material to a triploid (Figure 1B). The next potential

pattern (3) is that parthenogenic hybrids exhibit heterosis, or hybrid vigor, such that their environmental niche extends far beyond that of either sexual progenitor into novel environmental space (Figure 1C). Under this hypothesis, niche breadth of the hybrid parthenogen should be much wider than that of either parent. Here, the degree of niche overlap is not important and hybrids may or may not overlap substantially with their sexual progenitors. The final potential pattern (4) is that hybrid parthenogens are limited to a small subset of environmental conditions and are thus not widely adapted. In this case, genotypes frozen by asexual reproduction are limited to a very narrow range of environmental conditions (Figure 1D) and are unable to expand into novel environments. Again, the degree of niche overlap between the parthenogenic hybrid and the sexual progenitor is not important, as long as the niche of the hybrid is not widely different from the progenitors.

The method of Rissler and Apodaca (2007) is appropriate for this analysis. Environmental variable values are extracted from point locations for parthenogenic hybrid species and their sexual parent species and analyzed for significant differences in environmental preferences by Principal Component Analysis (PCA) and Analysis of Variance (ANOVA). The PCA will visualize the environmental variation according to PC factors, and the PC factors for each sample are used to examine the breadth or variance of environmental conditions unique to the niche of that species. The distribution and variance of each species along these axis scores is then statistically compared using ANOVA (Rissler & Apodaca, 2007) to distinguish between the possible outcomes listed above. In addition, SDMs that utilize popular modeling algorithms such as Maxent

(Phillips *et al.*, 2006; Phillips & Dudik, 2008) can make use of tools such as ENMTools (Warren & Seifert, 2011) that offer metrics to quantify distribution and niche overlap.

3. Clonal Ecological Strategy

The Ecological Strategy category examines the relative effects of clone diversity over the range of a hybrid species and how clones may be partitioning niche space (specialization or generalization). This results in a test of two previously posited hypotheses: the Generalist Genotype or the Frozen Niche Model.

To tease apart these two hypotheses, two sets of analysis are required. First (1), it needs to be determined whether there is cryptic clonal diversity within a particular parthenogenic hybrid. Cluster analysis or PCA should be conducted on clonal genetic variation to determine if there are distinct genetic groups of clones across the landscape. The type of marker used here is not necessarily important, but generating large amounts of variation in a potentially polyploid clonal organism is. As a result, Amplified Fragment Length Polymorphisms (AFLPs) are a good option because they generate highly variable, anonymous nuclear genetic data at a reasonable cost compared to other markers. Distinct genetic clusters are determined by analyzing individual band frequency using clustering algorithms such as PCA, UPGMA (Unweighted Pair Group Method with Arithmetic Mean) trees, and Bayesian genetic clustering algorithms implemented in STRUCTURE v.2.2 (Pritchard *et al.*, 2000; Falush *et al.*, 2007).

Distinct genetic groups can be used for the second part of the analysis (2), determining whether unique clones have partitioned environmental niche space into

non-overlapping units. Under the Generalist Genotype Model (A), there should be one or few unique clones with highly over-lapping environmental niches and geographic distributions. These clones will be widely distributed across the geographic distribution of a parthenogenic organism, with little evidence of geographically structured genetic variation. In contrast, under the Frozen Niche Model (B), many unique clones have partitioned niche and geographic space into unique and exclusive units. Here, clones (and genetic variation) will be environmentally and geographically structured, such that independent genetic clones occupy unique environments. Genetic clusters identified in part (1) of this analysis are visualized in geographic space to determine extent of spatial overlap. Environmental overlap of genetic clones is analyzed using the method of Rissler and Apodaca (2007) as described in the previous section, to determine if they occupy unique environmental space. Multivariate statistics (*i.e.* MANOVA) are used to compare environmental variables extracted from each specimen to assess environmental divergence across genetic clusters to determine if parthenogenic organisms meet the expectations of the Generalist Genotype or Frozen Niche model.

4. Exclusion or Coexistence

The Exclusion or Coexistence category involves assessing the role of competition (biotic interactions) between parthenogenic species and their sexual congeners in habitats where they coexist or where species ranges come into contact. Here, research into the competitive abilities of parthenogenic and sexual species allow insight into whether species exclude another on the basis of competitive ability. Ecological studies

have a long history of exclusion experiments to assess competition, and this includes parthenogenic species relative to sexual species (*e.g.* Cuellar, 1993). Field experiments designed to exclude a species in order to see a response to competitive release in another are good for determining local competitive behavior between coexisting parthenogenic and sexual species. These tests are more difficult to extrapolate over landscapes where there is environmental and habitat variation across the ranges of parthenogenic and sexual species of interest.

A more generalized approach is comparing the inferred fundamental environmental niches for parthenogenic species and their sexual congeners, assuming all species use the same set of ecological resources, and combining these niches with geographic distributions to infer respective realized niches due to the presence of other species (Hutchinson, 1957; Real *et al.*, 1991). There are four potential patterns under this analysis. The first (1) is that asexual species are competitively excluded from potential habitat as inferred from environmental niche models by sexual species. Under this scenario, the geographic distribution of asexual hybrids would not extend into potential habitat inhabited by sexual species. This would be consistent with hypotheses that suggest asexual species are inferior competitors which are forced to expand into marginal habitats to reduce competition. The second scenario (2) suggests the opposite: asexual species are competitively superior and exclude sexual species from potential habitat. The third potential pattern (3) is that both asexual and sexual species coexist in suitable habitat. Under this scenario, the potential habitat of both asexual and sexual species is occupied regardless of the presence of the other and indicates that

competitive exclusion is not occurring. The final pattern (4) is a combination of both exclusion and coexistence in different areas of suitable habitat. This pattern suggests that competitive exclusion may be possible in some habitats while, in others, coexistence is possible. In this case, it is necessary to look at the geographic areas of both coexistence and exclusion to see if there are environmental variables that explain the observed pattern.

Species distribution models may have the potential to test geographic predictions associated with competitive exclusion and competitive release according to the methods of Anderson *et al.* (2002) assuming that these models approximate the fundamental niche (*sensu* Hutchinson, 1957). Under this method, ENMs would be compared between parthenogenic hybrids and their sexual progenitors for areas of overlap and potential overlap (based on habitat suitability scores). By visualizing potential distributions (based on habitat suitability values) and actual distributions (based on sampling localities) of a focal species, it may be determined if a species is limited to a subset of available habitat due to the presence of another species.

5. Evolutionary History

Finally, it is important to examine patterns inferred from previous analyses within the context of the historical processes that shaped current genetic and distributional patterns of parthenogenic species and their closely related sexual congeners. The Evolutionary History category involves inferring phylogenetic processes and constructing paleo-distribution models based on historical climate scenarios.

Phylogenetic analyses infer the evolution of both parthenogenic hybrids and their sexual progenitors, and increase the understanding of current geographic and genetic patterns by describing the history underlying these patterns. The patterns are revealed through common analyses such as phylogeny building using molecular clocks to determine the time scale of evolutionary history (Bromham & Penny, 2003) and using statistical phylogeographic methods to determine past demographic patterns (Knowles & Maddison, 2002; Templeton, 2004; Drummond *et al.*, 2005).

Paleo-niche models can be used to infer the past distributions of a species by projecting current ecological niche models onto historical environmental conditions (Braconnot, 1999; Braconnot *et al.*, 2007b). When used in conjunction with phylogenetic methods, paleo-niche modeling provides insight into the stability of habitats over time and the evolution of populations in changing climatic conditions (Hugall *et al.*, 2002). Finally, paleo-niche models also provide a framework in which to test phylogenetic hypotheses by generating a historical distribution which can be used to model the evolution of populations (Carstens & Richards, 2007; Knowles *et al.*, 2007).

Case Studies

The Comprehensive Research Framework above describes a research program that can test the diverse range of biological processes that result in the successful establishment of parthenogenic species. To illustrate the utility of this approach, two case studies were conducted that each test two of the categories described above: the Hybridity and Heterosis (2) and Clonal Ecological Strategy (3) sections. These studies

utilized the diverse and widespread group of whiptail lizards in the Southwestern Deserts where parthenogenesis occurs frequently.

Whiptail lizards (genus *Aspidoscelis*, formerly *Cnemidophorus*) are a conspicuous group of teiid lizards abundant in the arid southwestern deserts of the U.S and Mexico (Wright & Vitt, 1993; Reeder *et al.*, 2002). These ecologically important lizards have diversified into approximately 50 recognized species, of which almost a third are parthenogenic hybrids (Wright & Vitt, 1993). Currently recognized whiptail hybrids include both diploid and triploid species resulting from hybridization between two (back crossing for triploid species) or three different sexual whiptail species (Dessauer & Cole, 1989). Often there are both diploid and triploid populations in the same hybrid species (*e.g. A. tessellatus*). All known hybrid parthenogenic whiptail species are found to exhibit a pattern consistent with geographical parthenogenesis by inhabiting arid, ecotonal and marginal habitats relative to their sexual progenitors (Wright & Lowe, 1968). The majority of parthenogenic hybrids are found within the same general vicinity: the southwestern deserts of Arizona, New Mexico, southern Utah, southwestern Colorado and northern Mexico (Wright & Vitt, 1993).

While the relationship between asexuality and sexuality in whiptails have been studied ecologically (Case, 1990; Cuellar, 1993; Price *et al.*, 1993; Paulissen, 2001) and physiologically (Cullum, 1997; Cullum, 2000), there is no clear consensus on what processes govern the geographic patterns of these species. Due to the high frequency and broad distribution of parthenogenesis in *Aspidoscelis*, whiptails have the potential to illuminate causal factors of geographical parthenogenesis that are not conclusively

inferred.

First, the role of Hybridity and Heterosis (part two of the Comprehensive Research Framework) was inferred for a subset of North American parthenogenic whiptails and their sexual parental species. Five recognized parthenogenic species in the American Southwest, *Aspidoscelis exsanguis*, *A. flagellicauda*, *A. sonora*, *A. uniparens*, and *A. velox*, share the same sexual progenitors species, *A. burti*, *A. gularis* and *A. inornata*, with some degree of distributional overlap, and based on their evolutionary and historical hybridization relationships, provide a suitable cohort of species on which to test predictions. Combining location data available in electronic databases of academic and museum specimens with free spatial physical environmental conditions from the WorldClim database (Hijmans *et al.*, 2005), we can visualize the relative roles that hybridity and heterosis have on parthenogenic whiptails according to hypothesized patterns described above (see Figure 1).

This study is detailed in Chapter Two and found patterns consistent with predictions. Three of the five parthenogenic whiptails, *A. exsanguis*, *A. flagellicauda*, and *A. sonora*, exhibited patterns consistent with the intermediate niche (Figure 1A) relative to their sexual progenitors. In contrast, the remaining parthenogenic species showed evidence of alternative patterns: *Aspidoscelis uniparens* displayed a patterned consistent with genetic dosing with the parent that contributed two haploid genomes (*A. inornata*), while *A. velox* displayed a pattern consistent with heterosis.

Second, we investigated how clones within a parthenogenic species may be dividing up environmental and geographic space according to the Clonal Ecological

Strategy section (section three) by conducting a genetic survey across the distributions of the parthenogenic hybrids *A. uniparens* and *A. velox*. Here, we used AFLPs to investigate genetic diversity on specimens sampled across their geographic ranges. Once genetic clusters were identified, the values of physical environmental variables from the WorldClim database (Hijmans *et al.*, 2005) were extracted at each location where an individual of a particular genetic cluster was sampled, to statistically determine if genetic cluster were found in unique environmental conditions.

This study is detailed in Chapter Three, and the results from cluster analyses (using UPGMA trees and STRUCTURE) identified unique genetic clusters in each species, but the degree to which those clusters divided up geographic space and environmental conditions differed between species. *Aspidoscelis uniparens* exhibited strong geographic structure of genetic clusters, and one of the four recognized genetic clusters was found in significantly different environmental conditions than the other clusters. This pattern is most consistent with the frozen niche hypotheses described above. In contrast, *A. velox* did not show the same extent of geographic structure, with one genetic cluster (G) displaying a wide distribution across the species range. There were also no significant differences in the environmental conditions occupied by genetic clusters, a pattern consistent with the genetic genotype.

These case studies demonstrate that the research structure advocated in the Comprehensive Research Structure results in the development of studies that can test different categories of biological processes in a coherent and organized way. These two studies successfully tested explicit predictions from previously posited hypotheses by

focusing on the underlying patterns identified by the Comprehensive Framework.

Further case studies on the other sections of the comprehensive framework are necessary to further evaluate the usefulness of the research strategy outlined here, but are beyond the time constraints and financial scope of the author. Future work should concentrate on untested categories of the framework for whiptail lizards, and on adding additional data to the test-cases described in the following chapters to further buttress the results and conclusions. Unpublished studies that have examined the evolutionary history of species of interest (*e.g.* Bell, 2003) should be incorporated into these investigations, but there is a need for additional work beyond that described here.

Conclusion

Geographical parthenogenesis is a common pattern that has attracted the attention of numerous ecological and evolutionary scientists since Vandel first coined the term in 1928 (Vandel, 1928). Based on their geographic distribution, whiptail lizards provide an excellent candidate species to study the ecology and evolution of geographical parthenogenesis. These parthenogenic species are ideal for this scientific exploration because of their close proximity, abundance and daily habits that allow for efficient collection.

The comprehensive research framework outlined in this chapter has the potential to streamline investigations into the geographic patterns and persistence of parthenogenic organisms relative to their sexual progenitors. Current techniques in molecular genetics, coupled with computer-based ecological analyses, have the exciting

potential to generate novel insights into the patterns and processes governing the distribution of parthenogenic hybrids and their sexual ancestors. Currently, no studies of geographical parthenogenesis have utilized these techniques together to tease apart the ecological, demographic and historical processes in parthenogenic organisms. The power of the current framework is the ability to examine the interactions of these factors, and to look at their individual and combined effects on the distribution of asexual hybrids. These methods, combined with the analytical framework described here, may be generalized to other organisms that share a pattern of geographic parthenogenesis and may potentially determine why geographical parthenogenesis is shared among so many different groups of organisms.

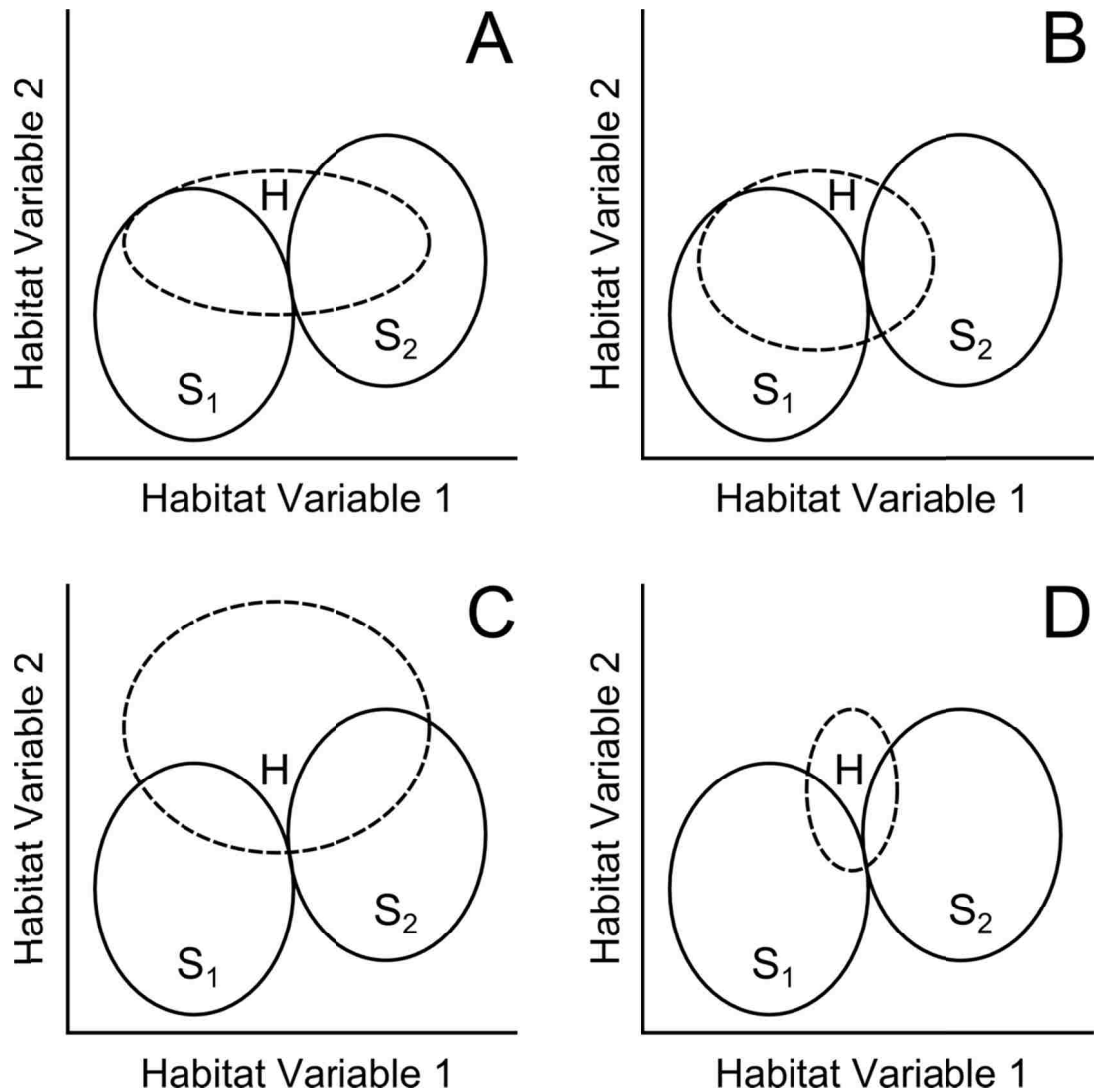


Figure 1. Potential models of environmental niches along two hypothetical habitat variables for a parthenogenic hybrid (H) and its sexual progenitors (S1 and S2): intermediate niche (A), where the niche of a hybrid is intermediate to both sexual progenitors; genetic dosing (B), where the niche of the hybrid overlaps most with the sexual parent that contributed the most genetic material (S1); heterosis (C), where the hybrid expands into environmental space novel to either parent; and narrowly adapted niche (D), where the hybrid is only adapted to a narrow set of conditions between sexual parent species.

CHAPTER 2:

HYBRIDITY & HETEROSIS IN GEOGRAPHICAL PARTHENOGENESIS

Abstract

Parthenogenesis is the clonal reproduction of an all-females species without the need for males, and is a relatively rare form of asexual reproduction in animals. Parthenogenic species are the result of hybridization between two sexual species (Kearney, 2005), and are distributed at higher latitudes, higher altitudes, islands or island-like habitats, xeric environments, and in marginal, disturbed or ecotonal habitats relative to their sexual progenitors, a pattern termed “geographical parthenogenesis” (Vandel, 1928; Glesener *et al.*, 1978; Maynard Smith, 1978; Lynch, 1984). This study examines four potential environmental distributional patterns of hybrid parthenogenic whiptails (genus *Aspidoscelis*): (1) the intermediate niche, (2) genetic dosing, (3) heterosis and (4) the narrowly adapted niche. Using specimen location records for five parthenogenic whiptail hybrids and three sexual parental species downloaded from online databases, the breadth and overlap in environmental conditions occupied (based on 19 WorldClim physical environmental variables) are compared by simplifying variation using Principal Components Analysis (PCA) and testing for significant differences between species using an ANOVA.

Evidence for three out of the four potential hypotheses was found. The intermediate niche was consistent with the environmental conditions occupied by three of parthenogenic hybrid whiptails and their sexual parental species. The remaining two

parthenogenic whiptails had different patterns; one occupied environmental conditions that were consistent with the predictions of genetic dosing, while the other showed evidence of heterosis. Current and historical Environmental Niche Models (ENMs) were created for each species, and the role of climate change since the Last Glacial Maximum (LGM) on the geographic distribution of parthenogenic whiptails was investigated during ENM creation.

This study represents a test-case for the Hybridity and Heterosis section of the Comprehensive Research Framework identified in Chapter One of this volume. This section identifies a subset of biological process related to a hybrid parthenogenic species' environmental tolerances that may contribute to the overall geographic distribution and persistence of parthenogenic organisms. The methodology employed here is successful at comparing parthenogenic hybrids relative to their sexual parents and identified patterns consistent with previously posited hypotheses.

Introduction

Parthenogenesis, the clonal reproduction of an all-females species without the need for males, is a form of asexual reproduction in animals. Parthenogenesis is relatively rare in nature, occurring in less than 0.1 percent of described species (White, 1978; Kearney, 2005), but is found in a wide range of organisms, from insects to vertebrates (reviewed in: Glesener *et al.*, 1978; Bell, 1982; Kearney, 2005).

Parthenogenic species are found at higher latitudes, higher altitudes, islands or island-like habitats, xeric environments, and in marginal, disturbed or ecotonal habitats

relative to their sexual congeners, a pattern termed “geographical parthenogenesis” (Vandel, 1928; Glesener *et al.*, 1978; Maynard Smith, 1978; Lynch, 1984).

Many hypotheses have been formulated to account for the geographic distribution and persistence of parthenogenic organisms relative to their sexual congeners (see Chapter One). Biological processes overlap between hypotheses that are treated independently, complicating attempts to study parthenogenesis. However, a Comprehensive Research Framework that sorts biological phenomena from these hypotheses into testable units can simplify the process and provide a reliable road-map for formulating a research plan. As a case study on the geographic distribution of parthenogenic hybrids relative to their sexual parent species, we utilized research suggestions from the “Hybridity and Heterosis” section of the comprehensive research plan outlined in Chapter One in a group of lizards from the American Southwest.

Parthenogenesis frequently occurs in organisms due to hybridization between sexual species, many times resulting in polyploid genomes, and the ecological success of these organisms may be consequence of their hybridity (Kearney, 2005). Many hybrid organisms are more vigorous than their sexual parent species and spread their distribution beyond the ranges of their parents into novel environments (Moore, 1984; Vrijenhoek, 1989), potentially because of the high heterozygosity that results from the combination of different genomes (Whitlock *et al.*, 2000; Kearney, 2005).

There are four potential patterns regarding environmental niche breadth and degree of niche overlap of hybrids relative to their progenitors: (1) intermediate niche, (2) intermediate niche with genetic dosing, (3) heterosis, and (4) narrowly adapted niche

(Figure 1).

The intermediate niche hypothesis (1) suggests that because parthenogenic hybrids have genes that evolved in environmental conditions from each parental population, the ecological breadth of the hybrid should be intermediate to, and overlap substantially with both progenitors, without inhabiting environmental space that would be novel to either sexual species (Figure 1A; Moore, 1984; Vrijenhoek, 1989; Vrijenhoek, 1998). The result will be a hybrid species whose environmental requirements should overlap substantially with both sexual parent species. This hypothesis also suggests that hybrids will have an advantage in intermediate or marginal habitats between sexual progenitors because sexual species may not be well adapted and unable to compete (Moore, 1984).

The genetic dosing hypothesis (2) is a variant of the intermediate niche hypothesis, with the hybrid niche overlapping most with the progenitor species that contributed the most genetic material (Figure 1B). Genetic dosing is found in triploid parthenogens that result from a back cross with one of the original parent species after the initial hybridization event. The expectation is that because the hybrid can draw from more genetic material from the parent donating two haploid genomes, it will be phenotypically most similar to that parent. Dosage effects have been found in morphological characteristics (Schultz, 1969; Kearney & Shine, 2004) and climatic tolerances (Kearney *et al.*, 2003; Kearney & Shine, 2004) of triploid hybrids relative to their progenitors.

In contrast to the previous hypotheses, the heterosis hypothesis (3), often

referred to as hybrid vigor, suggests that the high heterozygosity resulting from the initial hybridization event creates hybrids superior to their sexual progenitor species (Moore, 1984; Vrijenhoek, 1989; Whitlock *et al.*, 2000; Kearney, 2005). Hybridization has the potential to be adaptive because different combinations of progenitor genes may lead to hybrid genotypes of varying fitness (Barton, 2001) that potentially result in adaptations to new environments (Kearney, 2005). The pattern expected under heterosis is that the environmental preferences of hybrids extend beyond that of their progenitor species into novel environmental space unavailable to either parent (Figure 1C). Here, the niche breadth of the hybrid should encompass novel environmental conditions, with similar or reduced environmental overlap compared to the intermediate niche hypothesis (Figure 1C).

Finally, the narrowly adapted niche (4) is developed from the hypothesis that hybrid parthenogenic genotypes are frozen to a small subset of environmental conditions and are thus not widely adapted (Vrijenhoek, 1998). It follows that the environmental niche of the parthenogenic hybrid is narrower than either parental species (Figure 1D) such that the range of environmental conditions occupied by the hybrid is smaller than that of either parental species individually and the overlap with its parents is small. This pattern has been found in hybrid species (Semlitsch *et al.*, 1997) including unisexual hybrids (Gray & Weeks, 2001).

Whiptail lizards (genus *Aspidoscelis*, previously *Cnemidophorus*), a conspicuous group of teiid lizards abundant in the arid southwestern deserts of the U.S and Mexico (Anderson *et al.*, 1993; Leaché & Reeder, 2002), have been the subject of intense study

due to the occurrence of numerous parthenogenic species. Nearly one third of the 64 known species of whiptails are parthenogenic hybrids (Anderson *et al.*, 1993). Parthenogenic whiptails tend to inhabit warmer and dryer, marginal, disturbed, transitional, or ecotonal habitats relative to their sexual progenitors (Wright & Lowe, 1968; Wright & Vitt, 1993), a pattern consistent with geographical parthenogenesis. This observation has been termed the “Weed hypothesis” (Wright & Lowe, 1968) and it theorizes that because the American southwest has experienced high climatic and vegetation community change since the last glacial maximum (*ca.* 21,000 calendar years before present; Thompson *et al.*, 1994; Thompson & Anderson, 2000), the superior colonizing ability and broad ecological tolerances of parthenogenic whiptails allows these species to colonize areas characterized as historically unstable, much like a “weed” (Wright & Lowe, 1968).

In their phylogenetic study of the genus *Cnemidophorus*, Reeder *et al.* (2002) recognized three distinct groups of sexual North American *Aspidoscelis*: the *A. deppii*, *A. tigris* and *A. sexlineata* groups. For the purposes of this study, only whiptails of the *A. sexlineata* group (*A. burti*, *A. costata*, *A. gularis*, *A. inornata*, and *A. sexlineata*) and their parthenogenic hybrid daughter species (*A. exsanguis*, *A. flagellicauda*, *A. sonora*, *A. uniparens*, and *A. velox*) are used. Other North American parthenogenic whiptails involve hybridization with the wide spread, morphologically and genetically diverse Tiger Whiptail, *A. tigris* (Reeder *et al.*, 2002). These species have been excluded from this study because *A. tigris* may be composed of multiple distinct species (Marshall & Reeder, 2005) in different habitats that have not been determined at this time.

Hybrid relationships between focal species are complex and are summarized in Figure 2.1. The initial diploid hybridization for all focal parthenogenic hybrid species occurred between the Little Striped Whiptail, *A. inornata*, and species belonging to the paraphyletic *A. burti/costata* complex (Reeder *et al.*, 2002; Bell, 2003). Because of the paraphyletic nature of the species relationships (Reeder *et al.*, 2002; Bell, 2003) and the uncertainty whether hybridization occurred with the Canyon Spotted Whiptail, *A. burti*, or the Western Mexico Whiptail, *A. costata* (for *A. exsanguis* and *A. velox*; Moritz *et al.*, 1989; Reeder *et al.*, 2002), these species are treated collectively as the single taxon *A. burti* through the rest of this study.

Hybridization events that resulted in each parthenogenic whiptail species with descriptions of their ranges are described below:

Aspidoscelis uniparens & *A. velox*: The Desert Grassland Whiptail, *A. uniparens*, and the Plateau Striped Whiptail, *A. velox*, are triploid parthenogenic hybrid species with largely allopatric distributions except for co-occurrence along the Mogollon Rim of Arizona and the Rio Grande river valley in the vicinity of Magdalena, New Mexico (Figure 2.2A). These two species share the same sexual progenitors, the Little Striped Whiptail *A. inornata*, distributed in the grasslands of the Chihuahuan, desert and the *A. burti* complex, distributed in the Sonoran Desert of Arizona and western Mexico (Figure 2.2B). The initial hybridization even was followed by a back cross with *A. inornata* resulting in the triploid genome (Reeder *et al.*, 2002). They are morphologically very similar, leading to suggestions that they are clonal variants (Densmore III *et al.*, 1989), but they differ in

maternal ancestry. The maternal ancestor to *A. uniparens* is *A. inornata* (Densmore III *et al.*, 1989), while the maternal ancestor to *A. velox* is the western Mexico whiptail, *A. costata* (Bell, 2003) of the *A. burti* complex.

Aspidoscelis flagellicauda & *A. sonorae*: The Gila Spotted Whiptail, *A. flagellicauda*, and the Sonoran Spotted Whiptail, *A. sonorae*, are largely allopatric, morphologically similar triploid hybrid species that share the same sexual progenitors as *A. uniparens* and *A. velox* (Reeder *et al.*, 2002). However, the maternal ancestor to both hybrids is *A. inornata* (Densmore III *et al.*, 1989) with two paternal crosses with the *A. burti* complex (Dessauer & Cole, 1986; Densmore III *et al.*, 1989). *Aspidoscelis flagellicauda* is distributed along the Mogollon Rim of Arizona, similar to the distribution of *A. uniparens*, while *A. sonorae* is distributed further south in the creosote and mesquite scrub of the Sonoran Desert (Figure 2.2C).

Aspidoscelis exsanguis: The Chihuahuan Spotted Whiptail, *A. exsanguis*, is a triploid hybrid of three sexual ancestors, the *A. burti* complex, *A. inornata*, and the Common Spotted Whiptail, *A. gularis* (Dessauer & Cole, 1986). In this species however, the precise maternal ancestor is unknown (Reeder *et al.*, 2002). *Aspidoscelis exsanguis* has a widely overlapping range in the Chihuahuan Desert grasslands with its sexual parent *A. inornata*, while its unique parent species *A. gularis* is distributed further to the east in Texas and eastern Mexico (Figure 2.2D).

Because of the frequency of hybridization events, high density of species and relative ease in locating specimens, whiptail lizards offer a unique opportunity to investigate hypotheses regarding hybridity and heterosis in parthenogenic hybrids. Using recently developed computational methods and freely available, high-resolution environmental data in conjunction with information maintained by natural history museums and research institutions available in online databases, it is possible to combine species location information with continuous layers of physical environmental data to calculate and compare spatial distribution maps of suitable conditions for a suite of species of interest.

This study will quantify the environmental conditions inhabited by parthenogenic whiptails relative to their sexual progenitors using a statistical analysis first proposed by Rissler and Apodaca (2007), and by examining Environmental Niche Models (ENMS) developed using the program Maxent (Phillips *et al.*, 2006). Using Principal Components Analysis (PCA) on environmental data extracted from the specimen location data of museum records, the breadth and overlap of environmental niches for parthenogenic whiptails and their sexual progenitors will be visualized and statistically compared. The results of these analyses will be contrasted with the expected patterns derived from hypotheses regarding hybridity and heterosis identified above in parthenogenic whiptails: (1) the intermediate niche, (2) genetic dosing, (3) heterosis, and (4) narrowly adapted niche (Figure 1). In addition, ENMs calculated from specimen location information and physical environmental variables will visualize the current spatial distribution of parthenogenic species and their sexual progenitors, and

evaluate the relative importance of each variable in model construction. By hind-casting ENMs onto historical climates from the Last Glacial Maximum (LGM), we may tease apart the role of environmental change on the distribution of parthenogenic hybrids. By developing climate change variables that spatially quantify the difference between current and LGM environments and incorporating them into ENMs, the importance of climate change in predicting the distribution of parthenogenic hybrids can be evaluated as suggested by the “weed” hypothesis.

Methods

To examine hypotheses regarding hybridity and heterosis of parthenogenic hybrids relative to their sexual progenitors, two separate analyses were used. First (1), we employed a PCA method first outlined by Rissler and Apodaca (2007), where PC scores based on multivariate environmental data were statistically compared between species using an Analysis of Variance (ANOVA) to determine if a parthenogenic hybrid’s environmental preferences overlap with those of their sexual parent species. Second (2), ENMs were constructed for each species to quantify favorable environmental conditions, to project a distribution of suitable habitat onto current and historical climates, and to compare environmental conditions and distributions between species. The ENMs were calculated using the Maxent v.3.3.3 (Phillips *et al.*, 2006) modeling software which has been shown to provide reliable predictions of species distributions for presence-only data relative to other methods (Elith *et al.*, 2006), even when sample size is small (Pearson *et al.*, 2007). Each of these analyses is described in detail below.

Museum Records

Specimen records were downloaded through the HerpNet data portal (<http://www.herpnet.org/>, accessed 6 June, 2011) from academic institutions and museums (Table 2.1) for all species of interest. Records that had a written location description but no geographic coordinates were georeferenced using GEOLocate v.3.2 (Rios & Bart, 2010). All resulting coordinates were cross-checked and corrected by hand using written location information in searches conducted in Google Earth v.6.0 (accessed June-August, 2011) using MaNIS georeferencing guidelines (<http://manisnet.org/GeorefGuide.html>). Additional specimen localities of *A. uniparens* and *A. velox* collected by the author for a genetic study (Chapter Three) were included.

The georeferenced dataset was cleaned by removing incorrect or uncertain records using the following criteria:

- Records that had a calculated geographic uncertainty greater than five km or were in a grossly incorrect location (*ie*: water bodies, states with no known occurrences).
- Specimen records outside the known species range, based on Stebbins (2003), Brennan *et al.* (2006), Degenhardt *et al.* (2005) and IUCN Red List (IUCN, 2010), were considered potentially misidentified if they occurred within the range of morphologically similar species.
- Specimens identified by collectors with high numbers of uncertain records based on the above criteria.

Finally, species records with unique coordinates but occurring within the same sampled

5 km x 5 km environmental pixel were removed so that each environmental data point was sampled only once for each species. The final set of georeferenced specimens is listed in Appendix A.

Environmental Variable Data Sets

Statistical analyses and ENMs used temperature and precipitation data available in the 19 bioclimatic variables downloaded from the WorldClim database (Appendix B; Hijmans *et al.*, 2005). These data are derived from observations over 50 years at climate stations worldwide, interpolated over the landscape using a thin-plate smoothing spline (Hijmans *et al.*, 2005). Raster layer data were downloaded at a resolution of 2.5 arc-minutes (approximately 5 km²).

Paleoclimatic data used to reconstruct past distributions were derived from simulations of the last glacial maximum (LGM, *ca.* 21,000 calendar years before present) based on ocean, atmosphere, land and ice simulations available from the Paleoclimate Modelling Intercomparison Project Phase II (Braconnot *et al.*, 2007a; Braconnot *et al.*, 2007b). Two climate models of the LGM were used: Community Climate System Model v.3 (Otto-Bliesner *et al.*, 2006) and the Model for Interdisciplinary Research on Climate v.3.2 (Hasumi & Emori, 2004). Both CCSM and MIROC models have been applied to previous ENM studies by converting the data to the 19 bioclimatic variables and 2.5 arc-minute resolution of the Worldclim dataset (Peterson & Nyári, 2007; Waltari *et al.*, 2007).

Because parthenogenic species have been hypothesized to occur in areas that

experienced high environmental change since the LGM (Wright & Lowe, 1968), environmental change between now and the LGM was quantified by calculating the difference between pixels of the WorldClim data set from the two paleoclimate models (CCSM and MIROC) using ArcMap 9.2 (ESRI Inc., 2006) across an area encompassing the distributions of all species of interest. To reduce the variance in 19 difference calculations, a PCA was calculated in ArcMap to describe the environmental change in 19 variables on four independent, orthogonal variables for each paleo-model. Each PC variable describes a portion of environmental change since the LGM and layers were exported to ascii file format for use in later Maxent analyses.

The environmental values of all 19 WorldClim variables were extracted for each georeferenced specimen using DIVA-GIS 7.3.0.1 (<http://www.diva-gis.org/>). The resulting matrix of environmental values for each specimen location was analyzed using PCA to reduce the variation in 19 partially correlated variables to four independent principle component axes that describe different aspects of the environment. Principal component (PC) scores were analyzed using ANOVA with species as a fixed factor to determine if species significantly differed for each component axis. Once species was confirmed as a significant factor, Tukey's Honestly-Significant-Difference (HSD) Post-Hoc test was used to examine which pairs of species differed significantly from each other. All statistical analyses were conducted in SYSTAT 12 (SYSTAT software, Inc. 2007).

Maxent methodology

Maxent ENM models were constructed for each species using the 19 WorldClim

environmental variables. Maxent predictions have been shown to be robust when correlated environmental variables are used, but interpretation of variable importance within the model becomes complicated by covariation, and models run the risk of being over-fit. As a result, two separate sets of WorldClim variables were used for species ENMs: A model using all available variables, and a model using a reduced set where redundant variables were removed. Variable choice in the reduced set was based on a series of metrics described below.

First, each principle component axis from the first section of this study was examined to determine the variables that loaded most strongly on each PC factor. Once variable loadings were known, this information was used to insure that the climatic variation identified by each PC factor is represented in the final reduced data set during the variable reduction decision-making. Second, a Pairwise Pearson correlation matrix between all extracted WorldClim variables was constructed in Systat 12 to identify highly correlated variables ($R > 0.75$, Appendix C) to preferentially remove redundant variables. Finally, an initial Maxent model using all WorldClim variables and a mask based on the Nature Conservancy ecoregions (http://maps.tnc.org/gis_data.html, accessed December, 2011) was built for each species using default parameters with the following modifications: create response curves, jackknife of variable response, random seed and 10 replicates using cross validation. The mask was used to limit the background sampling of Maxent to areas that specimens could be while eliminating areas specimens would obviously be absent from (*i.e.*: high mountains, swamp, *etc.*) to insure a more accurate model (VanDerWal *et al.*, 2009). Two metrics from the Maxent

models were considered to determine variable importance. The first metric, variable contribution, keeps track of the increase in model gain (a goodness of fit metric used in Maxent) as model features are modified, and attributes the change in each iteration to the modified variable. For the second metric, variable permutation, each variable value is permuted and the resulting change in the Area Under the Curve (AUC) is recorded as a normalized percentage. The results of these metrics are shown in Table 2.2, and while the results from these metric often agreed, this pattern was not always consistent and the results were evaluated separately.

The above information was used to create a series of Maxent models that iteratively removed redundant variables. Variables that had high contribution and/or permutation scores were preferentially retained during the variable reduction decision making process, while highly correlated variables were removed. The series of retained and removed variables is shown in Table 2.3.

The fit of each iterative model relative to all other models was assessed using the metrics AIC, AICc and BIC calculated by ENM tools v.1.3 (Warren & Seifert, 2011). The AICc in particular has been shown to perform best at estimating true model complexity and evaluating variable importance (Warren & Seifert, 2011). The resulting model fit scores for each set of reduced variables are shown in Appendix D for each species where the variables removed is shown in the row labels and model scores across species are summed and averaged. Higher model scores have increasingly darker highlighting, with the top three further highlighted by white text. The full set of WorldClim variables had some of the highest model fit scores based on AICc and BIC,

but the highest scores overall were for the a reduced model that removed all high correlations ($R > 0.75$) by omitting the following variables: BIO3, BIO6, BIO7, BIO10, BIO11, BIO12, BIO13, BIO16, and BIO17 (underlined values, Appendix D). These two models were used in further analysis.

For the full and reduced variable sets, final Maxent models were rerun using default parameters with the following adjustments: random seed, create response curves, randomly set aside 25% of points to test the model, logistic output, and 25 replicated models using subsampling. Jackknife of variable importance was also included in Maxent model runs to measure variable importance, where models were run using all but a single variable, and again with solely that variable, and model fit assessed by model training gain, test gain and AUC scores. Because this calculation is time consuming, a subset of 5 replicates was used for jackknife calculations.

The resulting logistic output of Maxent models were then visualized in ArcGIS 9.2 using three thresholds of logistic output scores: A low threshold (least stringent) by balancing training omission, area and threshold; a middle threshold by equating the entropy of thresholded and original distributions; and a high threshold (most stringent) setting training sensitivity and specificity equal. Currently, there is no consensus on which thresholds are the most appropriate, so the choices here are based on fit to known distributions and illustrating high versus low logistic output.

Results

A total of 1753 specimen records were retained after museum specimens were

downloaded, georeferenced and cleaned for uncertain samples. The following number of specimens for each species was used for all analyses and Maxent models: 179 *A. burti* (includes samples of *A. costata*), 239 *A. exsanguis*, 73 *A. flagellicauda*, 324 *A. gularis*, 235 *A. inornata*, 241 *A. sonora*, 264 *A. uniparens* and 198 *A. velox* (See Appendix A). The spatial distribution of specimen localities is shown in Figure 2.3.

PCA Results

The PCA on environmental data extracted from museum specimen locations resulted in 4 PC factors that had eigen values greater than one. Principal component one (PC1) explains 45.07% of the total variation in the data set (Table 2.4), and describes increasing temperature and precipitation, and decreasing temperature variation and seasonality (BIO1, BIO4, BIO6, BIO7, BIO11, BIO12, BIO13, BIO16, and BIO18). Principal component two (PC2) explains 21.45% of the variation (Table 2.4) and describes decreasing daily temperature range and increasing overall precipitation with less seasonality (BIO2, BIO3, BIO14, BIO15, BIO17, and BIO19). Principal component three (PC3) explains 16.70% of the variation (Table 2.4) and describes decreasing temperatures (BIO5, BIO8, and BIO10). The last component, principle component four (PC4), explains 5.77% of the variation in the data (Table 2.4), and describes increasing temperature of the driest quarter (BIO19).

Scatter plot distributions for the PCA scores for all species are shown graphically in Figure 2.4A and B where PC score means are graphed with corresponding 95% confidence intervals for each component axis. These graphs depict the range of

environmental conditions (as represented by PCA scores) occupied by each of the focal species in this study. Because the variance explained by PC4 is less than 6%, comparisons with PC4 have been excluded.

ANOVA Results

For each of the four PC axes, species was a significant factor in explaining the variation in the dataset (PC1 $F_{7,1745} = 388.347$, $p < 0.001$; PC2 $F_{7,1745} = 236.402$, $p < 0.001$; PC3 $F_{7,1745} = 37.357$, $p < 0.001$; PC4 $F_{7,1745} = 217.858$, $p < 0.001$) and pairwise comparisons of each species for each PC axis is summarized in Table 2.5. The degree of environmental overlap between related parthenogenic hybrids and their sexual progenitors is described separately below.

Aspidoscelis uniparens and *A. velox*

Scatter plots depicting the range of environmental conditions on PC1 and PC2 occupied by the parthenogenic hybrids *A. uniparens* and *A. velox*, and their sexual progenitors *A. burti* and *A. inornata* is shown in Figure 2.4C, and for PC1 and PC3 in Figure 2.4D. Results of the Tukey HSD test are shown in Table 2.5. Overall, there are significant differences in the environmental conditions occupied between *A. uniparens*, *A. velox*, *A. burti* and *A. inornata*, with notable exceptions. First, *A. uniparens* is not significantly different from *A. inornata* on PC1 or PC2. Second, *A. uniparens* is not significantly different from *A. burti* on PC2 or PC3. Finally, the sexual progenitors are not significantly different from each other on PC2.

These results indicate that *A. velox* is different from its parent species on all PC

axes, occupying different environmental conditions relative to both of its parental species, while the environmental conditions *A. uniparens* occupies overlaps with each of its parental species, most notably *A. inornata* on PC1 (Figure 2.4C and D). Therefore, *A. velox* appears to have a distribution most consistent with heterosis (Figure 1C), while *A. uniparens* appears to be most consistent with the genetic dosing hypothesis based on its high overlap with the parent who contributed two haploid genomes, *A. inornata* (Figure 1B).

Aspidoscelis flagellicauda and *A. sonorae*

Scatter plots for PC1 and PC2 of the parthenogenic hybrids *A. flagellicauda* and *A. sonorae*, and their sexual progenitors *A. burti* and *A. inornata* are shown in Figure 2.4E, and for PC1 and PC3 in Figure 2.4F. Pairwise HSD tests are shown in Table 2.5. Similar to the pattern described above, the environmental conditions occupied by *A. flagellicauda*, *A. sonorae*, *A. burti* and *A. inornata* are significantly different with the following exceptions. First, *A. flagellicauda* is not significantly different from its sexual progenitor *A. inornata* on PC1. Second, both *A. flagellicauda* and *A. sonorae* are not significantly different from each other on PC3, nor are they significantly different from their sexual progenitor *A. burti*. Finally, as was stated above, both *A. burti* and *A. inornata* are not significantly different from each other on PC2.

Here, in contrast to patterns seen above, no parthenogenic hybrids occupy environments that are significantly different from their progenitors like *A. velox*, but appear to occupy conditions that overlap to a large extent with both progenitors (Figure 2.4E and F). Because these distributions are within the range of conditions of both

parents, this is most consistent with an intermediate distribution hypothesis (Figure 1A).

Aspidoscelis exsanguis

The final set of scatter plots shows the environmental conditions occupied by the parthenogenic hybrid *A. exsanguis* relative to its three sexual progenitors *A. burti*, *A. gularis*, and *A. inornata* on PC1 and PC2 (Figure 2.4G), and on PC1 and PC3 (Figure 2.4H). Pairwise HSD tests are shown in Table 2.5. These species are all significantly different from each other on PC1, but only *A. gularis* is significantly different from the other species on PC2. Finally, on PC3, *A. burti* and *A. exsanguis* are not significantly different at $p < 0.05$ level, but are significantly different at $p < 0.1$.

Again, *A. exsanguis* does not inhabit environmental conditions outside the range of its progenitors, but instead appears to be within their ranges despite significant differences in pairwise comparisons (Figure 2.4G and H]. The distribution appears to be most consistent with the intermediate distribution (Figure 1A).

Maxent Results

The resulting ENMs for the full and reduced environmental data sets for all species, plus their projections to the environmental conditions of the last LGM, are shown in Figures 2.5 - 2.12. The ENMs for full and reduced models that included environmental change PCA variables did not show any notable difference in predicted distribution from ENMs that did not include environmental change variables, and the figures are not included.

Model fit scores for full, reduced and environmental change data sets are shown

in Appendix E. The first two sets of scores are AUCs calculated by Maxent on the training and test data, with higher scores highlighted by darker colors. Overall, models that included more variables (full data set with paleo-climate change data), resulted in higher scores. The final three sets of scores are model fit metrics calculated by ENMTools that penalize models for having too many variables. In particular, AICc has been shown to provide a better estimator of true model complexity than other scores (Warren & Seifert, 2011). Models that include paleo-climate change data have overall lower scores, indicating that these variables didn't increase model fit any more than the original variables and aren't adding unique information to the modeling process.

Important variables for each species model according to the contribution and permutation metrics from the Maxent modeling process are shown in. Descriptions of the Maxent model results are described for each species individually below.

Aspidoscelis burti

Maxent distributions for *A. burti* for the full data set are shown in Figure 2.5A and Figure 2.5B for the reduced variable data set, and appear very similar in extent. These distributions also fit well with published range maps.

BIO9 (mean temperature of the driest quarter) and BIO4 (temperature seasonality) consistently result in the largest effects on Maxent models, regardless of the model run (full, reduced, or environmental change), in terms of variable contribution and permutation importance (Appendix F). Both variables had large effects on the model (as measured by gain) during jackknife tests when used as the sole variable, and also resulted in the lowest model fit when excluded.

BIO14 (precipitation of the driest month) also had a large effect on Maxent models regardless of the variable set used, but the largest effect was seen in the permutation importance. None of the other measures indicated notable effects of BIO14 on the Maxent models.

The projection of Maxent distributions onto paleo-climate models is shown in Figure 2.5C and D for CCSM on full and reduced variable models respectively, and Figure 2.5E and F for MIROC on full and reduced variable models respectively. Again, both the full and reduced models agree on predicted distributions, but while CCSM shows a reduction in suitable environmental conditions into central Mexico, the MIROC model shows little change except for a slight shift to the west in the northern portion of the distribution.

The environmental PCA variables did not have a notable effect on Maxent models and as a result were not deemed important in predicting the distribution of *A. burti*.

Aspidoscelis exsanguis

Maxent distributions for the full environmental data set of *A. exsanguis* is shown in Figure 2.6A and the reduced data set is shown in Figure 2.6B. These distributions are very similar in predicted area, with the reduced variable data showing a slightly larger distribution, and both correspond well to published range maps.

In terms of contribution and permutation, BIO15 (precipitation seasonality) is the most important variable for *A. exsanguis* across models where PCA variables derived from the MIROC paleoclimate models are not used. BIO15 also results in low model

performance when excluded and high model performance when it is the sole variable. In addition, BIO6 (minimum temperature of the coldest month) is important in all models built using the full set of variables, while variables that BIO6 is highly correlated to, BIO1 (annual mean temperature) and BIO4 (temperature seasonality), become important in all reduced models (including those with PCA variables derived from MIROC) based on contribution and permutation measures. However, while BIO6 results in high model fit when used as the sole variable and lower model fit when excluded, BIO1 and BIO4 don't have this effect on the reduced models.

Projections of the Maxent models onto the CCSM paleoclimate are shown in Figure 2.6C for the full environmental data set and Figure 2.6D for the reduce data set, and onto the MIROC paleoclimate in Figure 2.6E for the full data set and Figure 2.6F for the reduced data set. All paleoclimate projections indicate that distributions are pushed further south into areas not currently inhabited, and in the case of MIROC, severely reduce the extent of the distributions. Species distribution from the CCSM model are also split between regions of the Sonoran desert in Arizona and Chihuahuan desert of Mexico just south of the Mexican border, except for the reduced model, where lower threshold areas include a large part of the current distribution. In contrast, the MIROC predictions indicate species distribution along the border with Mexico for the reduced model, and virtually no distribution under the full model.

Models that included the effects of environmental change found that PCA variables had high effects on the Maxent model. For variables derived from CCSM, PC2 was important based on all measures; contribution and permutation score were high,

and there was low model performance when excluded and high model performance when it was the sole variable. For PCA variables derived from MIROC, PC2 and PC3 had the highest contribution and permutation scores of all variables, had high model fit when they were the sole variables, but PC3 was the only variable that resulted in lower model fit when excluded.

Aspidoscelis flagellicauda

Maxent distributions for *A. flagellicauda* are shown in Figure 2.7A for the full variable dataset, and Figure 2.7B for the reduced variable dataset. Again, the predicted distributions are very similar and correspond to published species ranges.

The models for *A. flagellicauda* are generally noisy with low consistency on which variables are important during model construction. This especially true for the model built on the full suite of WorldClim variables where there is little agreement on variable importance based on contribution and permutation. Generally speaking however, BIO15 (precipitation seasonality) and BIO19 (precipitation of the coldest quarter) score highly in both contribution and permutation across all models, regardless of the variables used. BIO15 also consistently has the lower model performance when excluded, though it does not perform well when it is the sole variable. Similarly, BIO19 generally leads to poorer model performance when absent (but not to the same extent as BIO15), but has high model fit when it is the sole variable in the full models. BIO9 (mean temperature of the driest quarter) is another important variable in terms of contribution and permutation for all models built. It results in low model performance when excluded from models built using PCA variables (but not the reduced WorldClim

only), but doesn't have high model fit when it is the sole variable.

Projections of the Maxent models into the CCSM paleoclimate are shown in Figure 2.7C for the full variable dataset and Figure 2.7D for the reduced dataset, and indicates that there was a slight reduction in species distribution without a real shift in any direction. The MIROC paleoclimate model is shown in Figure 2.7E for the full data set and Figure 2.7F for the reduced dataset, and has a similar pattern to the CCSM, though there was less reduction in overall area and a slight shift to the west.

Overall PCA variables from either CCSM or MIROC do not contribute any unique information to the Maxent models for *A. flagellicauda*.

Aspidoscelis gularis

Maxent ENM distributions for *A. gularis* are shown in Figure 2.8A for the full model and Figure 2.8B for the reduced model. While the overall distributions look quite similar, the reduced model shows a much larger extent of suitable environmental conditions at the highest threshold (equal training sensitivity and specificity).

BIO1 (annual mean temperature) and BIO14 (precipitation of the driest month) had the largest contribution and permutation effects regardless of the variables used. BIO1 had a large effect on model fit when it was the sole variable, but had little change in model fit when it was excluded, indicating that it may have little unique information to add. In contrast, BIO14 had little effect on model fit when it was the sole variable, but had decreased model fit when it was excluded, indicating that it may contribute unique information to the overall model.

In addition, BIO17 (precipitation of the driest quarter) had high contribution and

permutation values for models using the full suite of variables. BIO17 did not have notable effects on models where they were excluded or were the sole variables used.

The paleoclimate distributions for CCSM are shown in Figure 2.8C for the full variable dataset and Figure 2.8D for the reduced dataset, and shows a large contraction into the southern portion of its distribution, regardless of the number of variables used. The MIROC paleoclimate model is shown in Figure 2.8E for the full data set and Figure 2.8F for the reduced dataset, and has a similar pattern to the CCSM, though the range contraction isn't as severe as the CCSM paleoclimate model.

Overall, including PCA environmental change variables did not change model fit and variables were not important during model construction based on permutation and contribution scores.

Aspidoscelis inornata

Maxent ENM distributions for *A. inornata* are shown in Figure 2.9A for the full model and Figure 2.9B for the reduced model. Similar to the *A. gularis* model, the overall extent of the distribution is the same between the two models, but the reduced variable set shows a much greater distribution of suitable climates at the highest threshold (equal training sensitivity and specificity).

Aspidoscelis inornata appears to be strongly dependent on precipitation with BIO19 (precipitation of the coldest quarter) having the highest importance based on contribution and permutation scores regardless of the variables used, and BIO18 (precipitation of the warmest quarter) being important in all models that used the reduced WorldClim variables. Both BIO19 and BIO18 had low model fit when excluded

from the model and the highest model fit when it was the sole variable used. Temperature also had an effect on models for *A. inornata* in that BIO8 (mean temperature of the wettest quarter) and BIO9 (mean temperature of the driest quarter) had high contribution for the full model.

The distribution of *A. inornata* projected into the CCSM paleoclimate is shown in Figure 2.9C for the full variable dataset, and Figure 2.9D for the reduced dataset. These figures also show a pattern similar to *A. gularis* with a contraction of suitable environmental conditions into the southern portion of its range. The distribution for the MIROC paleoclimate models is shown in Figure 2.9E for the full variable dataset, and Figure 2.9F for the reduced variable dataset. Similar to the CCSM projection, there is a strong contraction of the species distribution, though this effect is even more pronounced in the MIROC dataset.

Environmental change was important when considering the MIROC model, where PC3 had high importance both in terms of contribution and permutation in the full and reduced models. This variable also resulted in lowered model performance when excluded, but didn't have high fit when it was the sole variable, indicating that it contributed unique information when predicting the distribution of *A. inornata*.

Aspidoscelis sonorae

The ENM distributions for *A. sonorae* are shown in Figure 2.10A for the full model and Figure 2.10B for the reduced model. These models are very similar in extent and are consistent with published range information.

BIO4 (temperature seasonality) and BIO19 (precipitation of the coldest quarter)

consistently have the highest importance in Maxent models based on contribution and permutation, regardless of the variables used. BIO4 also leads to the lowest model performance when excluded and the highest model performance when it is the sole variable, while BIO19 has similar but lower magnitude effects.

Projections of the Maxent distribution to the CCSM paleoclimate model are shown in Figure 2.10C for the full model, and Figure 2.10D for the reduced model. Again, these distributions show a contraction of the species distribution to the southern portion of its current distribution. The MIROC projections are shown in Figure 2.10E for the full data set and Figure 2.10F for the reduced data set and in contrast to the CCSM projection, show a shift in distribution to the west with no noticeable difference in overall area.

When PCA variables are included, additional variables contribute to the Maxent model. Under the CCSM paleoclimate PCA variables, BIO14 (precipitation of the driest month) have high model importance based on the contribution and permutation.

In contrast to the CCSM PCA variables which were not important in the model, MIROC variables PC1 and PC2 had high importance based on contribution and permutation scores. Neither of these variables resulted in large changes when excluded or was the sole variable, indicating that they may not have added information that was unique to the model.

Aspidoscelis uniparens

The ENM distributions for *A. uniparens* are shown in Figure 2.11A for the full model and Figure 2.11B for the reduced model. These models are very similar in extent

and are consistent with published range information.

BIO4 (temperature seasonality) is consistently the most important variable across all models regardless of variables used, both in terms of contribution and permutation. It also consistently results in poor model fit when excluded, and has the highest model fit when it is the sole variable. BIO3 (isothermality) and BIO9 (mean temperature of the driest quarter) are also consistently important variables across all full models, but with the exception of BIO9 resulting in the lowest model performance when excluded, these variables don't have any further notable effect.

Projections of Maxent models to the CCSM paleoclimate is shown in Figure 2.11C for the full variable data set, and Figure 2.11D for the reduced variable dataset. There is a contraction of suitable environmental conditions to the southwest of the current distribution. A similar pattern is shown in projections to the MIROC paleoclimate using the full (Figure 2.11E) and reduced (figure 2.11F) variable datasets, though the contraction are not as great in magnitude as the CCSM projection.

PCA variables are important in this species only based on the MIROC paleoclimate model, where PC1 has high importance based on contribution. Despite this, none of the PCA variables resulted in large model changes when excluded or used as the sole variable indicating relatively low importance to model construction overall.

Aspidoscelis velox

The ENM distributions for *A. velox* are shown in Figure 2.12A for the full model and Figure 2.12B for the reduced model. These models are very similar in extent, but appear to show suitable environmental conditions outside the published range. This

may indicate that *A. velox* has the potential to spread further, or that there are other factors limiting the distribution of this parthenogenic hybrid.

BIO1 (annual mean temperature) is consistently the most important variable regardless of the model used, based on contribution and permutation. This variable also results in the worst model fit when excluded and the highest model fit when it is the sole variable. In addition, BIO18 (precipitation of the warmest quarter) is important across all models according to the same measures as above, although the magnitude of its effect is much lower than that of BIO1. BIO19 (precipitation of the coldest quarter) also had some effect on models, though the overall effect of this variable is relatively low in magnitude with regard to contribution and permutation.

Projections of Maxent models to the CCSM paleoclimate model is shown in Figure 2.12C for the full variable dataset, and Figure 2.12D for the reduced variable dataset. Species distribution has a marked shift to the south into areas where this species is not currently present, manifesting to the southwest of its current distribution into the Sonoran desert and extending into the Mojave Desert area of southern Nevada. There is an additional area of high suitability appearing in southern Texas. The MIROC projection is shown in Figure 2.12E for the full variable dataset, and Figure 2.12F for the reduced variable dataset. Again, suitable habitat appears to the south and west of its current distribution, in Southern Nevada and along the bottom of the Mogollon Rim in Arizona.

The only PCA variables that had an effect on the Maxent model were those derived from the MIROC paleoclimate model, where PC2 had high effects based on

contribution and permutation, and on model fit when excluded and the sole variable. While the effect of PCA variables derived from CCSM didn't have high scores based on contribution and permutation, it deserves to be mentioned that PC1 and PC3 did result in relatively low model fit when excluded from the overall model.

Discussion

This study provides a test case of the Hybridity and Heterosis section of the Comprehensive Research Framework on the spatial distribution and persistence of parthenogenic organisms relative to their sexual progenitors outlined in Chapter One. We used landscape level environmental variables in conjunction with specimen localities to examine the distribution of parthenogenic hybrid whiptail lizards relative to their sexual progenitors using models of their environmental niched by testing expectations regarding the role of hybridity and heterosis, and the ecological expectations of geographic parthenogenesis.

Do the distributions of parthenogenic whiptail correspond to patterns associated with geographic parthenogenesis by inhabiting arid, xeric environments, and marginal, disturbed or ecotonal habitat? The answer is yes. Figure 2.4A shows that parthenogenic hybrids cluster towards the bottom left corner of the graph of PC1 and PC2, corresponding to drier conditions with greater seasonal variation in both temperature and precipitation relative to sexual progenitors. Arid conditions are often cited as a defining characteristic for geographic parthenogenesis (Kearney *et al.*, 2009). On PC1, the precipitation based WorldClim variables BIO12 (annual precipitation), BIO13

(precipitation of the wettest month), BIO16 (precipitation of the wettest quarter), and BIO18 (precipitation of the warmest quarter) increase as the PC1 score increases, so drier values are found on the left side of the graph. Likewise, the precipitation variables BIO14 (precipitation of the driest month), BIO17 (precipitation of the driest quarter) and BIO19 (precipitation of the coldest quarter) on PC2 increase as the score increases, leaving drier values towards the bottom of the scale. Principal component 2 also includes a precipitation seasonality variable, BIO15, that negatively loads with PC2, resulting in high seasonality at low PC2 scores with decreasing seasonality as PC2 scores increase. The result is a clear section of arid environments in the bottom left quarter of the PC1 and PC2 scatterplot, where parthenogenic whiptails cluster.

Patterns seen on PC2 are more ambiguous than PC1 because the sexual species *A. burti* and *A. inornata* overlap to a large extent with the parthenogenic hybrids at the low end of the PC2 score, indicating that they too inhabit dry habitats. But, because parthenogenic hybrids clearly cluster on the negative side PC1, parthenogenic hybrids can be characterized as inhabiting more arid climates as observed in descriptions of geographic parthenogenesis.

Hypotheses: Hybridity & Heterosis

How do the environmental conditions that parthenogenic hybrids occupy relate to the conditions occupied by their parents? The patterns observed here vary among hybrids and correspond to patterns of the intermediate niche, genetic dosing and heterosis, depending on the species. In fact, the only pattern not observed among

parthenogenic whiptails from the four shown in Figure 1 is the narrow niche hypothesis. Each observed pattern is described further below.

Three out of the five hybrid parthenogens considered in this study are consistent with patterns of the intermediate niche hypothesis, where the environmental conditions they inhabit are within the range of, and intermediate to their parental species (see Figure 1A). The parthenogenic hybrids *A. flagellicauda* and *A. sonora* and their sexual progenitors *A. burti* and *A. inornata* provide the best examples of this pattern.

Aspidoscelis flagellicauda overlaps with (is not significantly different from) *A. inornata* on PC1, and with *A. burti* on PC3, demonstrating a great degree of overlap with the environmental conditions of both parents. Beyond the statistical pattern, closer inspection of Figures 2.4E and F shows that the 95% confidence intervals around the mean for *A. flagellicauda* tends to overlap substantially with one or both parental species on all PC axes, indicating that *A. flagellicauda* inhabits a subset of the environmental conditions of both sexual progenitors in agreement with the intermediate niche hypothesis.

The environmental conditions that *A. sonora* inhabits also overlaps substantially with those of its parents, with its mean centered almost directly between the means of its parents on PC1 (Figure 2.4E and F). However, unlike *A. flagellicauda*, *A. sonora* is significantly different from its parents on PC axes 1 and 2. Despite this pattern, the degree of overlap of 95% confidence intervals, combined with the fact that the environmental conditions *A. sonora* inhabits is largely between the environmental conditions of its parents (on PC1), suggests that it is in fact intermediate to its parents.

Aspidoscelis exsanguis also appears to conform to a pattern expected by the intermediate niche hypothesis. While it is not significantly different from two (*A. burti* and *A. inornata*) of its three (*A. gularis* being the third) sexual parent species on PC2, the range of environmental conditions it inhabits overlaps with a subset of the conditions inhabited by all three of its parents (figure 2.4G and H]. While the overlap with *A. gularis* is weaker than its other parents (95% confidence interval only overlapping on PC3), this pattern of partial environmental overlap with its parents suggests that it inhabits an environmental niche intermediate to all three of its parents.

Patterns within the *A. uniparens* and *A. velox* hybrid group appear to deviate from the intermediate niche hypothesis identified in other parthenogenic hybrids examined in this study, even while sharing the same sexual progenitors. First, close examination of *A. uniparens* indicates that it overlaps substantially with one of its parent species, *A. inornata*, rather than a more intermediate pattern. *Aspidoscelis uniparens* is not significantly different from *A. inornata* on both PC1 and PC2, accounting for substantial overlap over 66% of the total variation in the environmental data set (PC1 accounts for 45% and PC2 for 21%). While *A. uniparens* is not significantly different from only *A. burti* on PC3 (16% of the variation), there is also substantial overlap of its 95% confidence interval with the mean of *A. inornata*. Combining this pattern of environmental overlap with the fact that two of three of its haploid genomes are donated by *A. inornata* (as a result of a back cross with *A. inornata* after an initial hybridization between *A. burti* and *A. inornata*), this pattern is most consistent with the genetic dosing hypothesis, where the hybrid overlaps most with the parental species

that contributed the most genetic information (Figure 1B).

In contrast with all other parthenogenic hybrids, *A. velox* doesn't overlap with the environmental conditions of any other species of whiptail considered in this study. Despite being of the same general hybridization origin as *A. uniparens*, *A. velox* inhabits environmental conditions well outside the 95% confidence intervals of either of its parents by having more negative scores on PC1 and higher scores on PC2 (Figure 2.4A). Only PC3 shows *A. velox* having any substantial overlap with the environmental conditions of its parents, where it occupies a subset of conditions occupied by *A. burti* and a small portion of the conditions occupied by *A. inornata*. These patterns show that *A. velox* is occupying a novel set of environmental conditions relative to its parents, a pattern consistent with heterosis (Figure 1C).

The contrasting patterns within the *A. uniparens* and *A. velox* hybrid group are particularly unique considering that other hybrids with the sexual progenitors *A. burti* and *A. inornata* inhabit intermediate environmental niches. *Aspidoscelis uniparens* is sympatric with all of the other parthenogenic hybrids examined in this study in some portion of its range, and yet is the only species to show a pattern consistent with genetic dosing. In contrast, *A. velox* is found in habitats that are not inhabited by other parthenogens, except for the southernmost portions of that range in Arizona and New Mexico, indicating that it has invaded areas that are not available to other related whiptail species. The *uniparens/velox* hybrid group has a back cross with *A. inornata* rather than *A. burti* or *A. gularis* in common, but this study is unable to address this observation further. This pattern should be considered in additional investigations of

parthenogenesis in whiptail lizards.

Of further interest is the apparent retraction and decline of *A. inornata* across much of its historical range. *Aspidoscelis inornata* is a widespread species that exhibits wide variation in morphological and ecological characteristics, and has been subdivided into numerous subspecies (Wright & Lowe, 1993). Within Arizona, such subspecies are represented in disjunct populations, including *A. inornata pai* found around Flagstaff, Arizona, and *A. i. arizonae* found around the Wilcox Playa in Southeastern Arizona (Wright & Lowe, 1993; Brennan & Holycross, 2006). These populations, while often recognized as distinct species by many taxonomists (*e.g.* Sullivan *et al.*, 2005; Brennan & Holycross, 2006) represent ancestral populations of a once more widely distributed species that may have declined as habitat degraded due to overgrazing in the last 100 years (Wright & Lowe, 1993). Habitat degradation may have also facilitated the spread of its parthenogenic hybrids, but this assertion has yet to be tested and the results of this study do not explicitly examine the effects of degraded habitat on the ENMs of parthenogenic and sexual species. An ongoing decline of *A. inornata* has been described across southwestern New Mexico (Wright & Lowe, 1993; Degenhardt *et al.*, 2005), also potentially due to habitat degradation. This is further supported by the author's own observations, where *A. inornata* was not found in previously identified locations despite multiple search days during collecting trips across western New Mexico.

Museum specimens of *A. inornata* for some of these disjunct populations were used in developing the ENM models for this species, although these samples only account for 2.5% of the total specimen records (6 out of the total 235 records) and may

not have a large effect on the model outcome. Environmental niche model results of *A. inornata* (Figure 2.9A and B) shows that suitable environmental conditions extend into areas of northern Arizona that are not currently occupied by *A. inornata*, suggesting that *A. inornata* may not be inhabiting the full area available to it. This is important when considering the distributions of its parthenogenic hybrids *A. uniparens* and *A. velox*, along with the conclusions drawn about the climatic niches they inhabit. It may be that these hybrids have a greater degree of environmental overlap with *A. inornata* (further evidence of genetic dosing for *A. uniparens*, but potentially impacting a conclusion of heterosis for *A. velox*) than the current analysis suggests. Also, the absence of *A. inornata* from areas inhabited by its parthenogenic hybrids may suggest competitive exclusion if habitat degradation can be excluded as the cause for the decline of *A. inornata*. This is a pattern in need of further research.

Modeling Considerations

Overall, ENM models created using the reduced set of variables (removing high correlations) were in agreement with ENM models created using the full set of WorldClim variables. Generally, reduced models tended to predict a larger extent of suitable environmental conditions, but this difference was quite minor and didn't change overall predictions. Reduced variable models also tended to show larger areas at the highest (most stringent) threshold, but this effect was only pronounced in a subset of the taxa studied here (e.g. *A. flagellicauda*, *A. inornata*, *A. gularis*, and *A. velox*). These patterns suggest that overall, full and reduced models are generally equivalent.

The reduction of correlations within the environmental data set reduced some of the specificity in the predictions, but may have provided more generalized results. Reducing the variable data set also had the advantage of being able to accurately evaluate the effect of individual variables on the model because those effects were not complicated by correlations with other variables.

The use of thresholds to provide calculated presence/absence predictions is an important concept for practical use in conservation and management practices, and has been investigated for many modeling methods that use presence/absence data (Liu *et al.*, 2005). However, thresholds have received relatively little attention for presence-only models such as Maxent, and a wide variety the thresholds have been reported in the literature. Use of thresholds generally depends on the types of questions being asked in a given study, and the types of error one is willing to accept (*i.e.* are false positives more acceptable than false negatives? Fielding & Bell, 1997; Loiselle *et al.*, 2003; Rondinini *et al.*, 2006).

Rather than reporting one threshold, we chose to use different thresholds in the present study to provide some indication of how models fit known distributions. A low threshold was used that insured that all training samples were included in suitable areas predicted by the ENM (omission rate of less than 1% of training samples). A high threshold was also chosen to visualize higher suitability values that were most likely to be inhabited by the species of interest by choosing a threshold where training sensitivity and specificity are equal. A similar metric, minimizing the difference between sensitivity and specificity, has been show to produce accurate predictions (Jiménez-Valverde &

Lobo, 2007).

Generally, high threshold areas fell within known and published ranges for all sexual species within this study, with the exception of *A. inornata* where suitable environmental conditions were predicted in northern Arizona (Figure 2.9C-F). The lower threshold tended to predict suitable environmental conditions beyond published ranges, but these predictions do not seem unreasonable given that range boundaries are not rigid in nature.

In contrast to the sexual whiptails, predictions from parthenogenic species often found suitable environmental conditions beyond published ranges, suggesting that they are not inhabiting the full area available to them. This is especially true of *A. velox*, where the lower threshold extends broadly beyond known distribution into portions of the Great Basin Desert in Nevada, and the Chihuahuan Desert in southwestern New Mexico.

Related parthenogenic hybrids (*e.g. A. flagellicauda/A. sonorae* or *A. uniparens/A. velox*) also appear to have a greater degree of overlap of suitable environmental conditions with each other than their current distributions would otherwise indicate. Environmental niche models here only consider the effect of environmental variables on the distribution of species and ignore other important aspects that define the realized niche, like biotic interactions (such as competition, facilitation, or vegetation requirements; Pulliam, 2000; Soberón & Peterson, 2005). The fact that there is over-prediction of suitable conditions could be an indication that there is some degree of competitive exclusion occurring (Anderson *et al.*, 2002), but there are

areas where these species occur sympatrically in great numbers in the same types of habitats (pers. obs.) with little evidence of competition.

Aspidoscelis sonora and *A. flagellicauda* have nearly allopatric distributions, except for areas of sympatry in the vicinity of Oracle and Duncan, Arizona, along the borders between Pinal and Pima, and between Cochise and Graham counties. Visual inspections of ENMs (Figure 2.7A and B for *A. flagellicauda*, and Figure 2.10A and B for *A. sonora*) suggest there are a greater amount of potential overlap than collection records indicate, particularly along the Mogollon Rim and the Sonoran Desert region of southeastern Arizona. This is also true of *A. uniparens* and *A. velox*, where there is a greater amount of overlap suggested by the ENM than has been observed. The models suggest that *A. uniparens* and *A. velox* should overlap extensively along the Mogollon Rim of Arizona and across a broad stretch of Chihuahuan Desert in the southwestern quarter of New Mexico. These species have been confirmed sympatric by the author (pers. obs.) after numerous field trips in the vicinity of Magdalena, NM. Other locations where published ranges overlap have been visited, but only one species was collected and/or seen in those areas. This may suggest that competitive exclusion is occurring, but more field work is required. These ENM maps can provide additional information necessary to develop studies into the role of competition in the distributions of related parthenogenic hybrids, and between hybrids and their sexual parent species.

Paleoclimate

We also attempted to quantify environmental change since the LGM for

WorldClim variables by calculating PCA variables on the difference between current and LGM (CCSM and MIROC) data sets. These variables were incorporated into separate Maxent models to determine if environmental change was an important factor in calculating ENMs for parthenogenic hybrids.

These PCA variables were important variables in the ENMs for some whiptail species, but the expected pattern of increased importance for parthenogenic lizards rather than their sexual progenitors did not emerge. Variables derived from the MIROC model were more important in the ENM models than variables derived from the CCSM model, and they were important in both sexual whiptails (*A. inornata*, 1 out of 3 sexual whiptails) and 3 out of 5 parthenogenic hybrids (*A. exsanguis*, *A. sonora* and *A. velox*). In addition, when PCA variables were important, it was often the 2nd and/or 3rd PC variables that contributed to ENM development, rather than the first which describes more of the variation in the data. It may be that environmental change does not play a decisive role in the distributions of parthenogenic hybrids, or that the data do not have the resolution to adequately detect the role of climate change since the LGM. The observations of Wright and Lowe (1968) that parthenogenic species inhabit ecotonal and disturbed habitats related to climate change since the Pleistocene are based on vegetation communities, for which we used climate as a proxy. Future investigations would benefit by quantifying habitat/vegetation changes once data of sufficient resolution exist.

There was substantial variation in the paleo-distribution predictions from the CCSM and MIROC models. Examination of Figures 2.5 - 2.12 show that CCSM and

MIROC predictions differ in terms of the amount of suitable environmental conditions available (CCSM greater for *A. inornata*; MIROC greater for *A. gularis*, *A. exsanguis*, *A. sonorae*, *A. uniparens*) and in the actual geographic locations of those suitable conditions (*A. burti*, *A. exsanguis*, *A. velox*). Because these models are built on global scale simulations of ocean and atmospheric circulation patterns, there is likely to be a lot of variability in predictions at the local scale due to error or artifacts in the modeling process and downscaling calculations. The PCA calculations may therefore better quantify differences in the modeling process rather than actual changes in climates since the LGM, a possibility that would explain the variation seen between CCSM and MIROC models. As a result, paleo-distribution models are best viewed as providing working hypotheses on the past distributions of species. Furthermore, because parthenogenic hybrids are viewed as very recent in origin (during the Pleistocene; Densmore III *et al.*, 1989; Moritz *et al.*, 1989; Wright & Vitt, 1993), it is also likely that current parthenogenic whiptail species had no paleo-distributions to reconstruct, and projecting ENMs to the LGM serves little purpose.

Alternative Considerations

This study serves as test case for the Comprehensive Research Framework on the geographic distribution and persistence of parthenogenesis outlined in Chapter One, and the methods outlined for testing biological processes are supported by the results here. While the current study has evaluated the distributions of hybrid parthenogenic whiptails relative to their sexual progenitors using environmental characterizations of

their niches, there are additional potential explanations of hybrid distributions that were not specifically examined or discussed.

Previous studies have indicated that parthenogenic hybrids are relatively recent in origin, probably only arising as climates and ranges shifted to their current conditions since the LGM (Densmore III *et al.*, 1989; Moritz *et al.*, 1989; Wright & Vitt, 1993). Overall, the ENMs of the sexual species suggest that at the LGM, suitable environmental conditions were restricted in area (range contraction) and/or shifted to the south (range shift) compared to current distributions. In fact, ENMs suggest that ancestral distributions between hybridizing species did not touch, or had much more limited contact than their current distributions. As environmental conditions changed, hybridizations would have occurred as ranges between sexual species began expanding and/or shifting into their current positions.

For hybridization opportunities between the *A. burti/costata* complex and *A. inornata*, there is no contact in ENMs of the LGM, regardless of the model used, and they only show very limited overlap under current climate conditions in southeast corner of Arizona and southwest corner New Mexico. Also, based on past mitochondrial studies, the most likely maternal candidate is *A. inornata arizonae* (Densmore III *et al.*, 1989) who currently occupies an area not included in the hypothesized historical range suggested by the ENMs. These patterns suggest that hybridization opportunities for current parthenogenic whiptails were not possible until after their sexual parents expanded to their current distributions. This leads to the conclusion that current distributions of successful hybrids may be very recent in origin, as suggested by previous

studies, and potentially their ranges are still expanding.

Based on LGM ENM models for *A. inornata* and *A. gularis*, there was overlap during the LGM in the vicinity of the Mexican states of Coahuila and Nuevo Leon (though surprisingly not further north into Texas), allowing opportunity to hybridize. However, there is no evidence that these two species resulted in an F1 hybrid, only as a back cross of *A. gularis* with an *A. burti* complex and *A. inornata* 2N hybrid. This also suggests that *A. exsanguis* would have a recent origin as the other parthenogenic hybrids in this study.

The conclusions of this study may be further complicated by the evolutionary dynamics within sexual progenitors (addressed in section five of the research framework in Chapter One). It has been recognized that the diversity within whiptails is the result of fragmentation and rapid evolution (Wright & Vitt, 1993). The sexual whiptail species examined in this study are complex, and within the *A. burti* complex (Bell, 2003) and *A. inornata* (Wright & Lowe, 1993), many subspecies have been recognized on the basis of ecology and morphology and fragmented ranges. Given better phylogenies and definitions of subspecies, it may be better to analyze subspecies separately rather than as a single unit because one subspecies may not be adapted to the same set of environmental conditions as another. As a result, a parthenogenic hybrid may only overlap with the environmental conditions of the specific subspecies from which it originated. Because there are few published phylogenetic studies for the sexual species in this study, and because there is still a lot of variation in the literature and museum records regarding subspecies designations, the level of specificity necessary to use

subspecies in the current investigation is not available. Comprehensive phylogenies are necessary to further elucidate evolutionary patterns and dynamics as they relate to hybridization and parthenogenesis within North American whiptail lizards.

Further Work

This study examined patterns at the landscape level, only considering broad patterns of climatic variables. In reality, landscapes are more complex and heterogeneous than the variables used here imply. Within areas that species appear sympatric in maps, lizard species may not be found sympatrically at all, instead sticking to particular vegetation and/or soil types that are not distinguishable at a resolution of five square kilometers. As a result, the ENMs used here may not truly represent the biology of these lizards and are ignoring very important biological processes.

Additional models should attempt to incorporate habitat, vegetation and soil variables at a local level to assess the true degree of niche overlap between parthenogenic hybrids and their parental species. These studies should be able to more accurately determine if hybrids are found in transitional or ecotonal habitats consistent with geographic parthenogenesis. It should also be easier to tease apart the role of competition between species.

To adequately conduct these more specific niche models, specimen records with more accurate location data and variables at a higher resolution are needed. This study looked at patterns over the landscape where a five square kilometer resolution was appropriate, but to adequately examine finer scale biological patterns such as habitat

choice and competitive interactions, the data need to reflect the scale at which those processes interact (Soberón & Peterson, 2005). If we can't adequately pin point what types of habitat particular species are found in with a good degree of accuracy, then we can't hope see the patterns operating at that scale. These models may be more localized, but in conjunction with a landscape scale study such as this, there is great potential to further our understanding of parthenogenesis in whiptails.

Finally, there are other hypotheses posited for the success of parthenogenic whiptail that weren't addressed by this study, and these were outlined further in Chapter One. For example, the Ecological Strategy section suggests that particular clones of parthenogenic taxa are adapted to a wide range of environmental conditions and quickly colonize habitat that meet those conditions. This is the generalist genotype, and has been supported in other asexual taxa (Parker Jr. *et al.*, 1977; Van Doninck *et al.*, 2002). Alternatively, the patterns associated with a frozen niche model may be a better fit, where particular clones in a parthenogenic taxon are narrowly adapted to a set of environmental conditions, and clones divide a landscape based on the conditions to which it is most adapted (Semlitsch *et al.*, 1997; Gray & Weeks, 2001). These alternative hypotheses are addressed by an additional case study in Chapter Three.

Conclusion

Geographic parthenogenesis describes the tendency for parthenogenic hybrids to inhabit arid, disturbed, marginal or ecotonal habitats relative to their sexual progenitors, a pattern that has been proposed in parthenogenic whiptail lizards. There

are potentially many biological processes involved in the geographic distribution and persistence of parthenogenic hybrid species, many of which interact between hypotheses generated in previous studies. A Comprehensive Research Framework has been stressed by the authors (see Chapter One) as a streamlined program to test these biological processes in an organized manner, and the current study serves as a test case for the “Hybridity and Heterosis” section of this framework.

This section suggests that environmental conditions inhabited by hybrid parthenogens are a consequence of the environmental preferences of their sexual parent species. Using location records from museums with WorldClim environmental data, we found evidence for three out of four proposed hypotheses regarding the climatic niche of hybrids relative to their sexual parents: the intermediate niche for *A. flagellicauda*, *A. sonorae* and *A. exsanguis*, genetic dosing for *A. uniparens*, and heterosis for *A. velox*. In addition, in line with geographic parthenogenesis, parthenogenic whiptails were found to inhabit more arid regions than related sexual species. Because the success of parthenogenic hybrids has also been hypothesized to be a result of climate and vegetation changes during the Pleistocene, we attempted to quantify the importance of climate change since the LGM and did not get significant results. While this conclusion may be true, it is more likely the result of insufficient resolution in paleoclimate data or more related to actual vegetation changes, for which we used climate as a proxy. This study also shed some light on the potential time frame for the initial 2N hybridization events for all parthenogenic hybrids examined here, between the sexual species *A. inornata* and the *A. burti* complex. Environmental niche

models indicate no potential for contact between these sexual species when projected onto LGM paleo-climate data, suggesting that hybridizations were only possible once the distributions of sexual species reached their modern extent. Further work is necessary to more accurately address additional ecological processes that may factor into the distribution of parthenogenic whiptails, such as biotic interactions like competition and vegetation community composition. The resulting distribution maps and environmental preferences determined here provide the framework on which future studies can be designed, and provide support for developing studies on geographic parthenogenesis based on a comprehensive research framework.

Table 2.1. Academic institutions and natural history museums for specimen records obtained through the HerpNet data portal. The abbreviation given here is used in the specimen's ID in Appendix B.

Abbr.	Museum Name
ASU	Arizona State University
CAS	California Academy of Sciences, San Francisco, CA
CM	Carnegie Museum of Natural History, Pittsburgh, PA
CU	Cornell University Museum of Vertebrates
KUNHM	University of Kansas Natural History Museum and Biodiversity Research Center
LACM	Natural History Museum of Los Angeles County
LSU	Louisiana Museum of Natural History, Louisiana State University
MCZ	Museum of Comparative Zoology, Harvard University
MPM	Milwaukee Public Museum
MSU	Division of Vertebrate Natural History, Michigan State University Museum
MVZ	Museum of Vertebrate Zoology, University of California, Berkeley
OMNH	Sam Noble Oklahoma Museum, University of Oklahoma
PSM	James R. Slater Museum, University of Puget Sound
ROM	Royal Ontario Museum, Toronto, Ontario
SDNHM	San Diego Natural History Museum, San Diego, CA
TCWC	Texas Cooperative Wildlife Collection, Texas A & M University
UAZ	Amphibian and Reptile Collection, University of Arizona
UCM	University of Colorado Museum
UTEP	The Centennial Museum, University of Texas at El Paso
YPM	Peabody Museum, Yale University

Table 2.2. Initial Maxent contribution and permutation scores of each variable per species. Species abbreviations are shown across the top: *A. burti* (b); *A. exsanguis* (e); *A. flagellicauda* (f); *A. gularis* (g); *A. inornata* (i); *A. sonorae* (s); *A. uniparens* (u); and *A. velox* (v). The top three values are shown in bold, and the sum and average of scores is given for each variable

Contribution:

	b	e	f	g	i	s	u	v	Sum	Ave
BIO 1	0.70	0.94	3.80	25.85	1.00	0.02	5.12	34.90	72.33	9.04
BIO 2	3.63	4.18	9.43	4.32	0.74	0.21	0.03	0.61	23.13	2.89
BIO 3	0.91	15.54	14.68	0.17	1.09	0.09	27.68	0.87	61.04	7.63
BIO 4	15.06	4.93	8.98	2.14	1.74	25.63	19.90	1.41	79.80	9.97
BIO 5	0.78	1.65	0.01	1.16	3.31	0.02	0.19	0.64	7.76	0.97
BIO 6	0.08	25.81	0.98	7.81	0.40	3.04	0.52	3.55	42.18	5.27
BIO 7	4.00	7.48	0.00	5.96	0.39	0.11	0.19	1.02	19.15	2.39
BIO 8	0.79	4.23	0.49	10.78	11.92	1.24	4.87	2.21	36.52	4.57
BIO 9	30.52	3.27	6.96	3.96	10.56	7.78	12.08	2.91	78.03	9.75
BIO 10	0.40	1.19	0.00	0.03	1.86	0.01	0.66	1.30	5.46	0.68
BIO 11	12.45	3.73	3.18	1.74	1.80	0.15	14.99	11.90	49.94	6.24
BIO 12	6.03	7.32	0.18	0.65	28.15	5.25	0.13	0.42	48.13	6.02
BIO 13	2.80	0.14	0.02	1.06	3.14	1.63	2.89	0.14	11.81	1.48
BIO 14	10.93	0.04	1.57	9.25	0.47	12.47	2.64	0.11	37.49	4.69
BIO 15	5.22	18.51	14.11	6.92	5.14	10.69	0.50	1.19	62.29	7.79
BIO 16	1.27	0.23	0.32	0.22	4.40	2.02	2.56	7.10	18.12	2.27
BIO 17	2.82	0.50	0.38	11.54	0.75	1.48	0.04	0.61	18.11	2.26
BIO 18	1.28	0.10	1.78	1.96	3.00	2.01	0.79	23.96	34.87	4.36
BIO 19	0.33	0.22	33.13	4.49	20.14	26.15	4.23	5.16	93.85	11.73

Permutation:

	b	e	f	g	i	s	u	v	Sum	Ave
BIO 1	2.10	0.49	0.00	6.95	0.38	0.27	15.81	27.14	53.14	6.64
BIO 2	2.45	0.76	0.18	0.65	4.37	0.58	0.07	0.63	9.68	1.21
BIO 3	0.31	5.35	1.10	1.04	1.68	0.07	5.76	2.10	17.42	2.18
BIO 4	3.98	3.06	0.37	6.50	7.81	11.14	18.90	1.30	53.06	6.63
BIO 5	1.39	0.30	0.01	0.99	6.12	0.39	0.21	7.50	16.90	2.11
BIO 6	0.05	9.14	3.96	7.89	2.50	1.46	1.25	5.19	31.42	3.93
BIO 7	5.46	7.29	0.00	3.64	3.28	0.04	0.26	1.20	21.16	2.65
BIO 8	3.27	2.36	0.20	4.62	0.73	3.67	4.14	2.31	21.30	2.66
BIO 9	41.63	6.01	21.87	9.00	5.47	14.00	28.61	6.70	133.29	16.66
BIO 10	0.60	1.22	0.00	0.06	5.86	0.01	0.63	1.15	9.52	1.19
BIO 11	3.10	0.75	24.67	4.24	0.42	4.69	3.63	10.85	52.36	6.55
BIO 12	7.35	6.05	1.04	0.47	10.65	0.42	0.14	3.66	29.77	3.72
BIO 13	2.63	6.47	0.00	6.94	4.96	0.07	3.22	0.23	24.51	3.06
BIO 14	14.66	0.49	20.05	0.53	1.86	6.54	2.52	0.64	47.27	5.91
BIO 15	1.15	41.72	21.69	10.51	4.06	25.64	8.16	0.64	113.56	14.20
BIO 16	1.36	0.31	1.79	0.50	5.04	0.65	0.74	2.81	13.19	1.65
BIO 17	4.87	2.77	0.05	16.51	3.15	2.21	0.28	0.97	30.82	3.85
BIO 18	2.89	1.02	0.17	9.08	10.33	2.56	0.39	7.39	33.83	4.23
BIO 19	0.78	4.45	2.85	9.91	21.35	25.58	5.28	17.59	87.78	10.97

Table 2.3. Variables removed iteratively during that variable reduction process. WorldClim variables are listed in rows and columns are listed in the order of variables were removed. Variables removed are indicated by an “X” and the final set of removed variables is shown in bold.

	1	2	3	4	5	6	7	8	9	10	11	12	13	14	15	16
BIO1																
BIO2																
BIO3				X			X	X		X		X	X	X	X	X
BIO4																
BIO5																
BIO6			X								X	X	X	X		X
BIO7	X	X	X	X	X	X	X	X	X	X	X	X	X	X	X	X
BIO8																
BIO9															X	X
BIO10	X	X		X	X	X	X	X	X	X	X	X	X	X	X	X
BIO11			X		X		X		X	X	X	X	X	X	X	X
BIO12													X		X	X
BIO13	X	X	X	X	X	X	X	X	X	X	X	X	X	X	X	X
BIO14																
BIO15																
BIO16			X			X		X	X	X	X	X	X	X	X	X
BIO17		X		X	X	X	X	X	X	X	X	X	X	X	X	X
BIO18														X		
BIO19																

Table 2.4. Principal component analysis (PCA) result summary on 19 WorldClim variables extracted from eight focal whiptail species. The first line describes the percent of variation described by each principal component (1-4), followed by the loading scores for each variable on that PC. Bold values indicate the variable that loads most heavily for each component.

	PC1	PC2	PC3	PC4
% variation explained:	45.068	21.447	16.704	5.774
BIO1	0.864	0.087	-0.467	-0.125
BIO2	-0.523	-0.638	0.026	0.306
BIO3	0.570	-0.648	0.306	0.023
BIO4	-0.860	0.229	-0.280	0.164
BIO5	0.351	0.069	-0.844	0.194
BIO6	0.952	0.068	-0.220	-0.097
BIO7	-0.906	-0.042	-0.172	0.207
BIO8	0.588	-0.109	-0.636	0.064
BIO9	0.571	-0.240	-0.191	0.653
BIO10	0.567	0.232	-0.766	-0.009
BIO11	0.948	-0.034	-0.251	-0.111
BIO12	0.707	0.520	0.412	0.088
BIO13	0.838	0.101	0.445	0.102
BIO14	0.000	0.937	0.057	-0.094
BIO15	0.544	-0.720	0.143	0.031
BIO16	0.826	0.047	0.475	0.070
BIO17	0.018	0.955	0.076	-0.025
BIO18	0.745	0.003	0.492	0.098
BIO19	0.022	0.679	0.195	0.620

Table 2.5. Species pairwise significance for Tukey's HSD test on PC1, PC2 and PC3. Sets of parthenogenic hybrids and their sexual progenitors (indicated with “*”) are grouped. Insignificant results ($p > 0.1$) are shown in *italics*, and marginally significant results ($0.1 > p > 0.05$) are shown in **bold**, and significant scores ($p < 0.05$) shown with no bold or *italics* (where 0 indicates $p < 0.001$.)

<u>PC1</u>				<u>PC2</u>			
	<i>burti*</i>	<i>inornata*</i>	<i>uniparens</i>		<i>burti*</i>	<i>inornata*</i>	<i>uniparens</i>
<i>inornata*</i>	0			<i>inornata*</i>	0.91		
<i>uniparens</i>	0	0.856		<i>uniparens</i>	0.997	0.998	
<i>velox</i>	0	0	0	<i>velox</i>	0	0	0
<u>PC3</u>				<u>PC2</u>			
	<i>burti*</i>	<i>inornata*</i>	<i>uniparens</i>		<i>burti*</i>	<i>inornata*</i>	<i>uniparens</i>
<i>inornata*</i>	0			<i>inornata*</i>	0.91	0	
<i>uniparens</i>	0.402	0		<i>inornata*</i>	0	0.033	0
<i>velox</i>	0	0	0	<i>sonorae</i>	0		
<u>PC1</u>				<u>PC2</u>			
	<i>burti*</i>	<i>flagellicauda</i>	<i>inornata*</i>		<i>burti*</i>	<i>flagellicauda</i>	<i>inornata*</i>
<i>flagellicauda</i>	0			<i>flagellicauda</i>	0		
<i>inornata*</i>	0	0.41		<i>inornata*</i>	0.91	0	
<i>sonorae</i>	0	0	0	<i>sonorae</i>	0	0.033	0
<u>PC3</u>				<u>PC2</u>			
	<i>burti*</i>	<i>flagellicauda</i>	<i>inornata*</i>		<i>burti*</i>	<i>flagellicauda</i>	<i>inornata*</i>
<i>flagellicauda</i>	1			<i>flagellicauda</i>	0		
<i>inornata*</i>	0	0		<i>inornata*</i>	0.91	0	
<i>sonorae</i>	0.999	1	0	<i>sonorae</i>	0	0.033	0
<u>PC1</u>				<u>PC2</u>			
	<i>burti*</i>	<i>exsanguis</i>	<i>gularis*</i>		<i>burti*</i>	<i>exsanguis</i>	<i>gularis*</i>
<i>exsanguis</i>	0			<i>exsanguis</i>	0.552		
<i>gularis*</i>	0	0		<i>gularis*</i>	0	0	
<i>inornata*</i>	0	0	0	<i>inornata*</i>	0.91	0.998	0
<u>PC3</u>				<u>PC2</u>			
	<i>burti*</i>	<i>exsanguis</i>	<i>gularis*</i>		<i>burti*</i>	<i>exsanguis</i>	<i>gularis*</i>
<i>exsanguis</i>	<i>0.064</i>			<i>exsanguis</i>	0.552		
<i>gularis*</i>	0	0		<i>gularis*</i>	0	0	
<i>inornata*</i>	0	0	0.043	<i>inornata*</i>	0.91	0.998	0

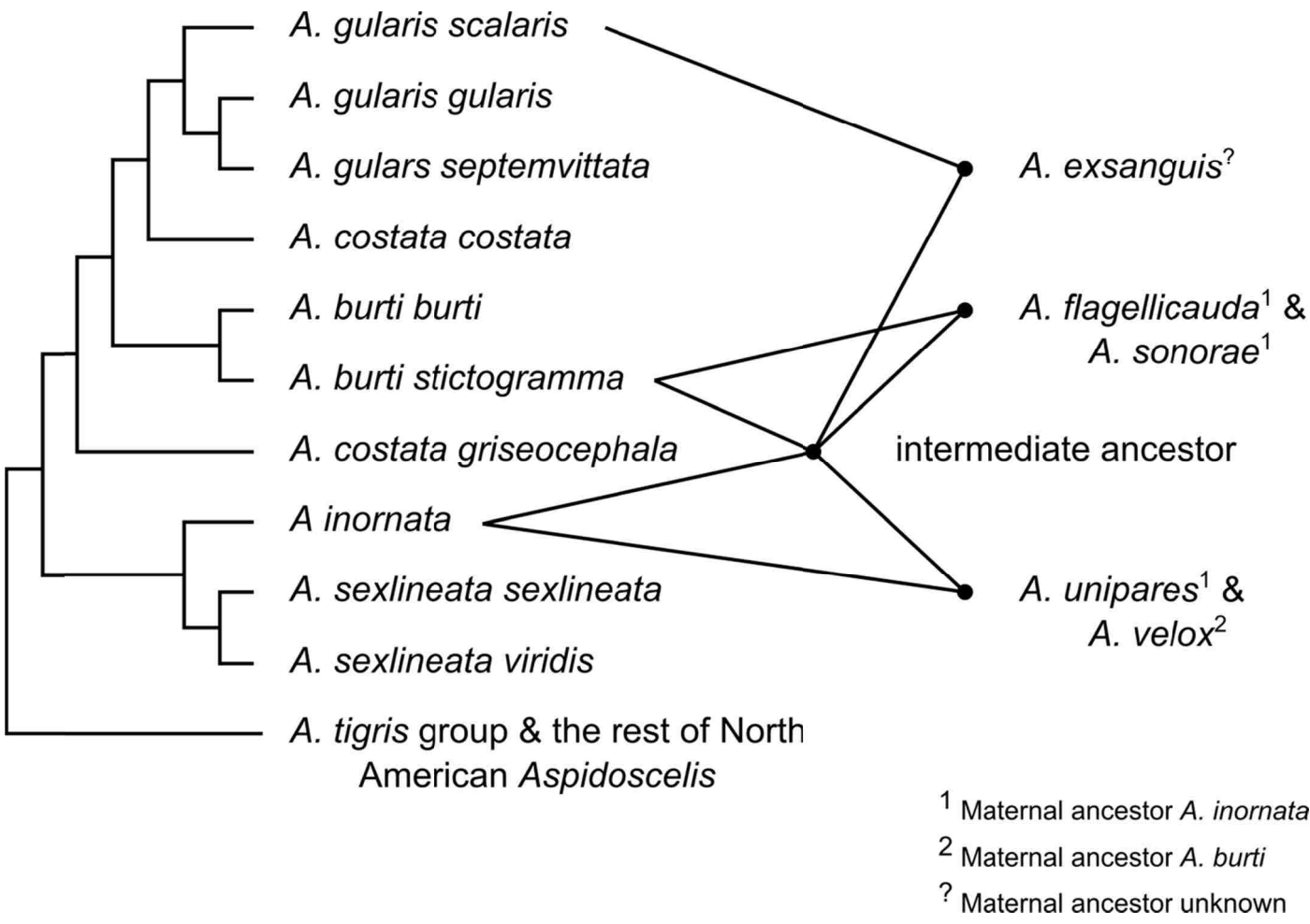


Figure 2.1. Phylogenetic relationships between sexual *Aspidoscelis* belonging to the *sexlineata* group and their parthenogenetic hybrids. All hybrids are the result of an initial hybridization between *A. burti* and *A. inornata* represented by the intermediate ancestor node, followed by an additional back cross. Adapted from Reeder *et al.* (2002)

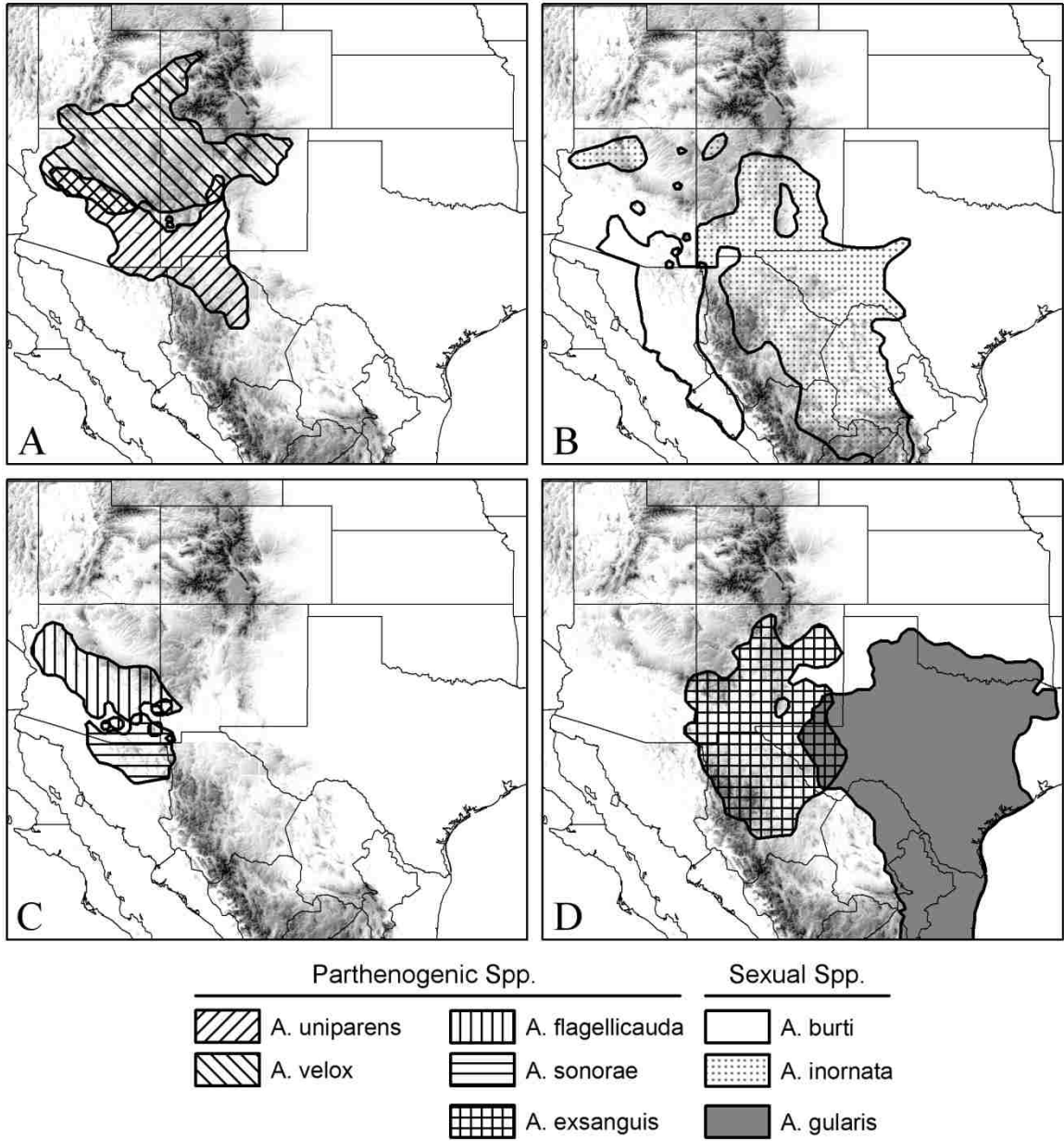


Figure 2.2. Range maps for *Aspidoscelis* species: (A) parthenogenic hybrids *A. uniparens* and *A. velox*, (B) sexual *A. burti* and *A. inornata*, (C) parthenogenic hybrids *A. flagellicauda* and *A. sonorae*, and (D) parthenogenic *A. exsanguis* and sexual *A. gularis*. Maps are based on Stebbins (2003).

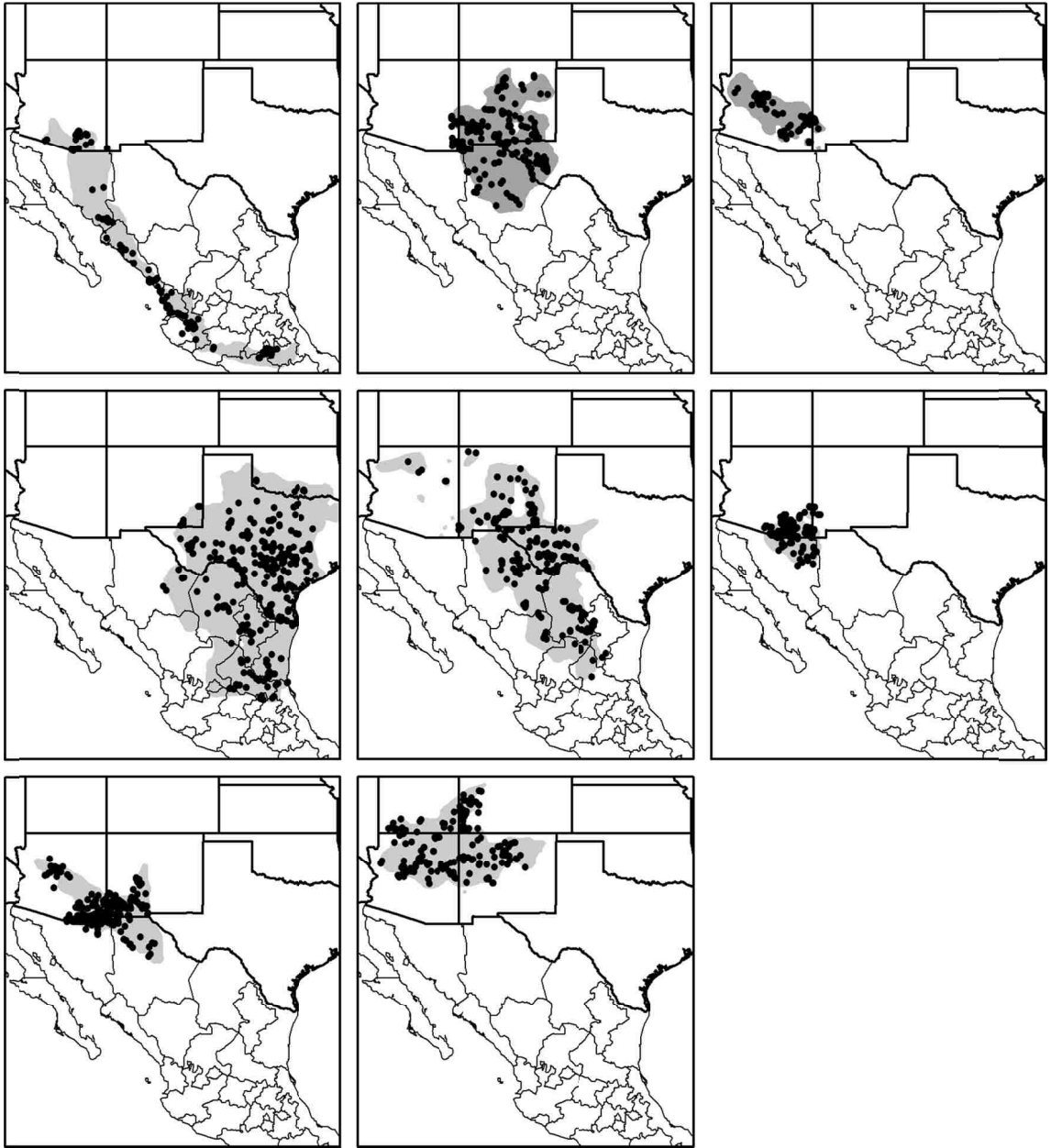


Figure 2.3. Geographic locations of museum specimens downloaded from HerpNET. Grey shading indicates known species range based on Stebbins (2003), Degenhardt *et al.* (2005) and IUCN Red List (2010).

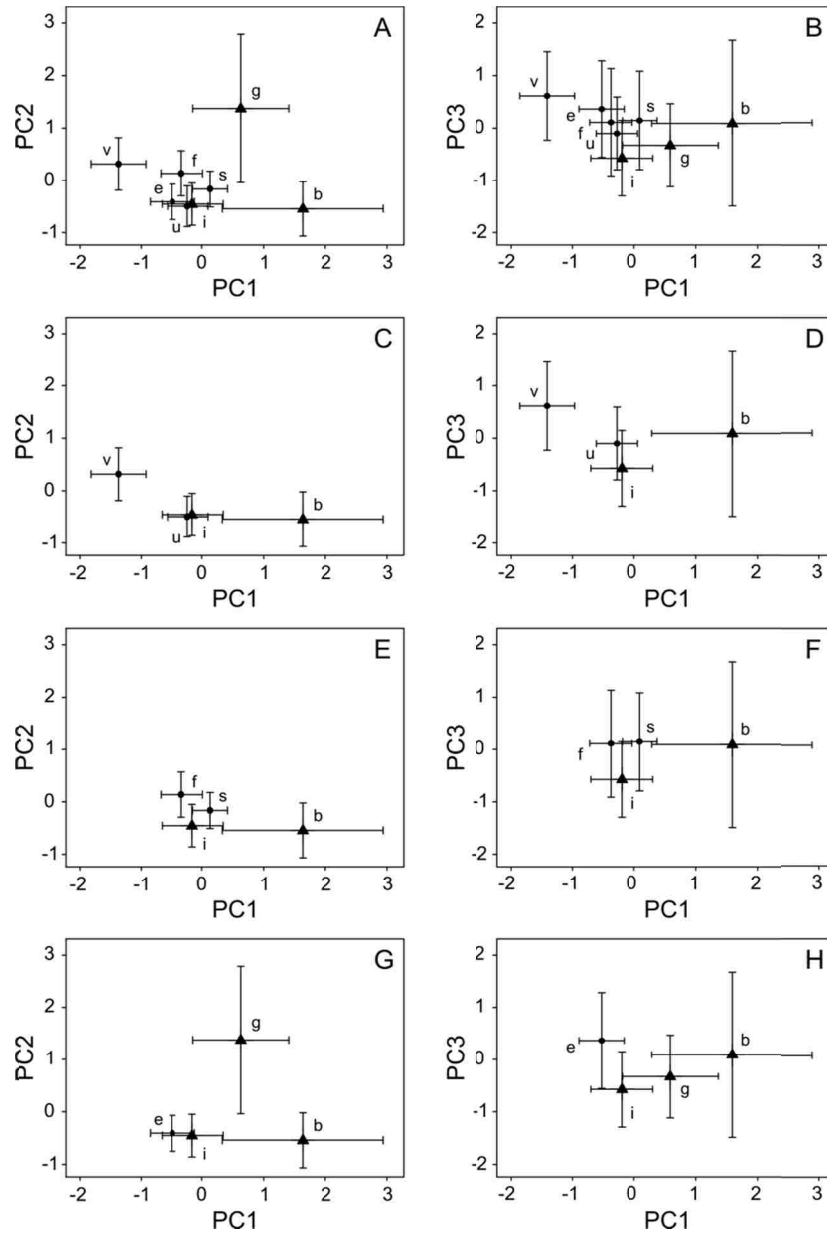


Figure 2.4. Graph of mean PC scores from PCA of 8 whiptail species with 95% confidence intervals. Means for a given species are indicated by the first letter of the species name: (b) *A. burti*, (e) *A. exsanguis*, (f) *A. flagellicauda*, (g) *A. gularis*, (i) *A. inornata*, (s) *A. sonorae*, (u) *A. uniparens*, and (v) *A. velox*. Parthenogenetic species means are indicated by a dot and sexual species means by a triangle. All species are graphed together for (A) PC1 and PC2, and (B) PC1 and PC3. The parthenogenetic hybrids *A. uniparens* and *A. velox* are graphed with their sexual progenitors *A. burti* and *A. inornata* for (C) PC1 and PC2, and (D) PC1 and PC3. The parthenogenetic hybrids *A. flagellicauda* and *A. sonorae* are graphed with their sexual progenitors *A. burti* and *A. inornata* for (E) PC1 and PC2, and (F) PC1 and PC3. The parthenogenetic hybrid *A. exsanguis* is graphed with its sexual progenitors *A. burti*, *A. gularis* and *A. inornata* for (G) PC1 and PC2, and (H) PC1 and PC3.

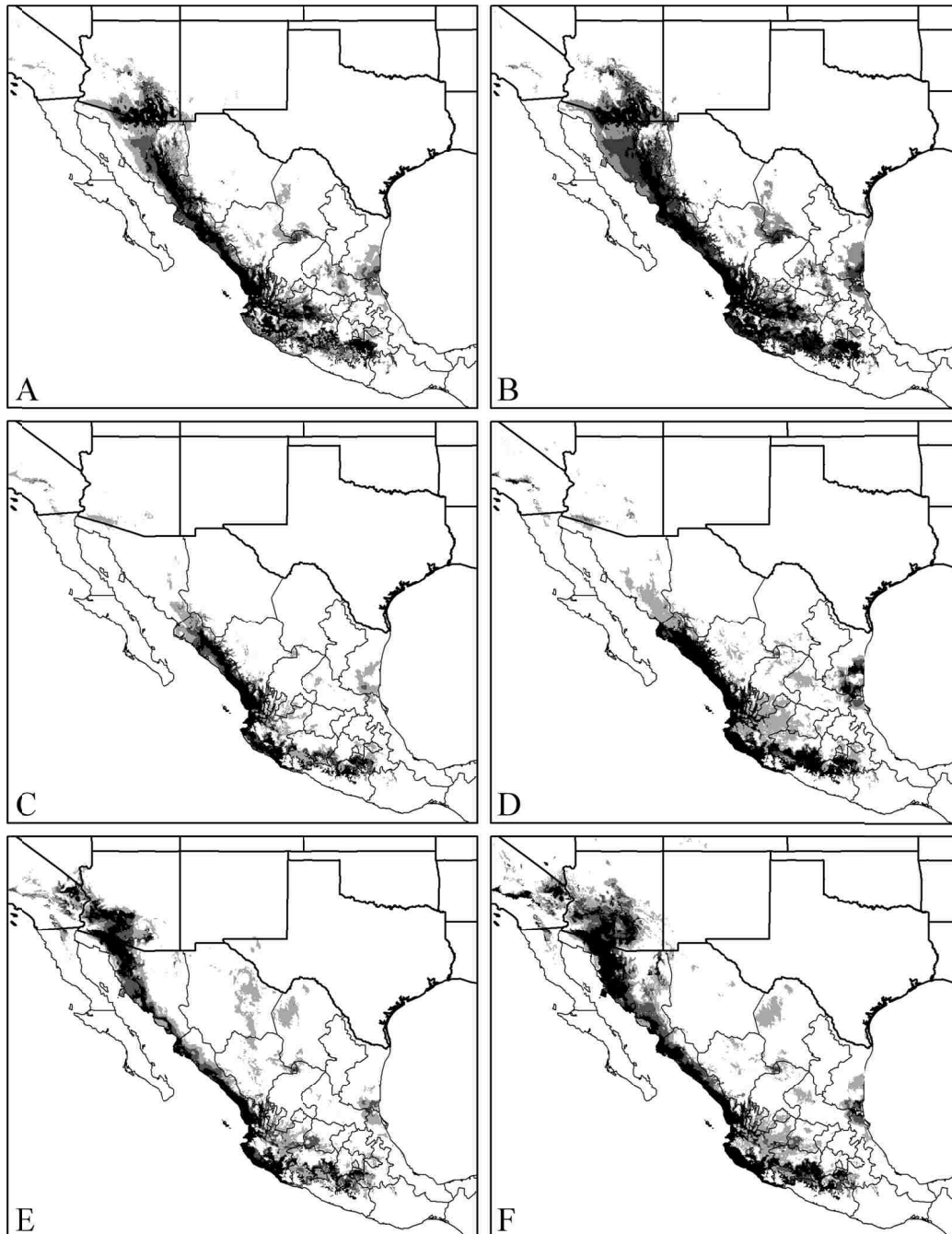


Figure 2.5. Maxent predicted distributions for *A. burti* based on (A) the full variable data set for present day, (B) reduced variable data set for present day, projected into the CCSM paleoclimate for full (C) and reduced (D) Maxent models, and projected into the MIROC paleoclimate for full (E) and reduced (F) Maxent models. Predicted distributions represent suitable habitat based continuous habitat suitability scores. The range of suitability scores are shown by cut-off value threshold: most stringent based on equal training sensitivity and specificity (black), medium stringency based on equal entropy of thresholded and original distributions (dark gray), and least stringent based on balancing training omission, area and threshold (light gray).

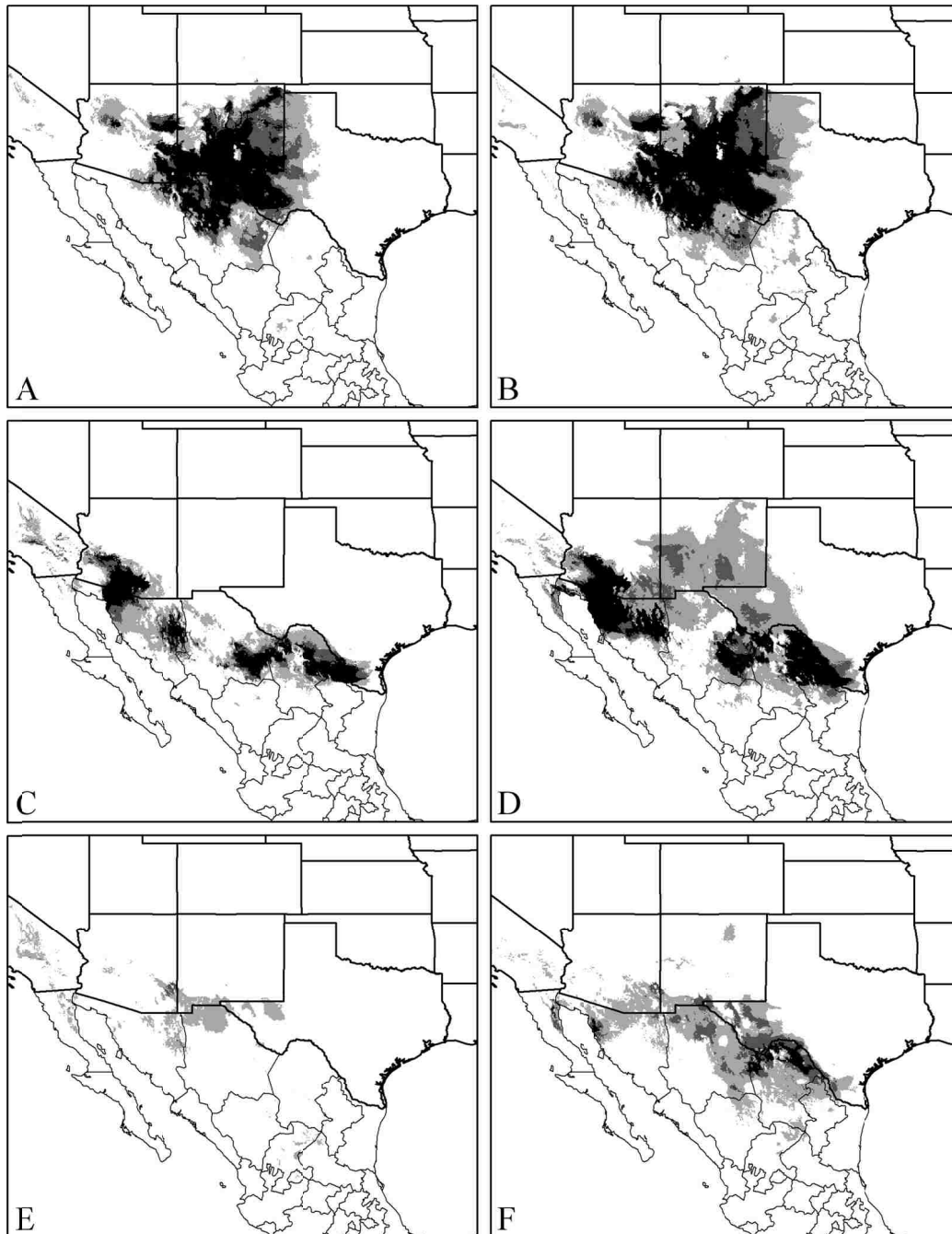


Figure 2.6. Maxent predicted distributions for *A. exsanguis* based on (A) the full variable data set for present day, (B) reduced variable data set for present day, projected into the CCSM paleoclimate for full (C) and reduced (D) Maxent models, and projected into the MIROC paleoclimate for full (E) and reduced (F) Maxent models. Predicted distributions represent suitable habitat based continuous habitat suitability scores. The range of suitability scores are shown by cut-off value threshold: most stringent based on equal training sensitivity and specificity (black), medium stringency based on equal entropy of thresholded and original distributions (dark gray), and least stringent based on balancing training omission, area and threshold (light gray).

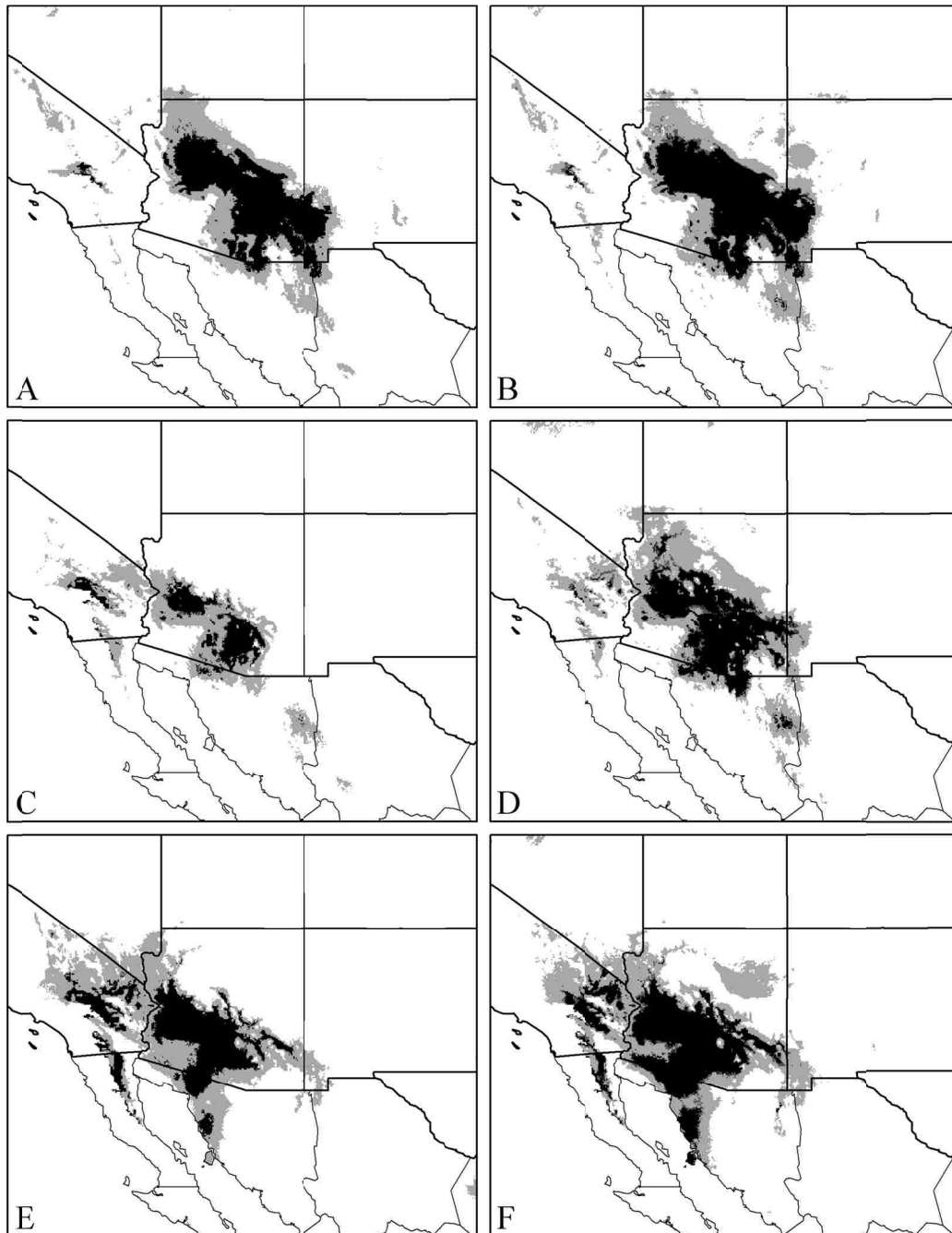


Figure 2.7. Maxent predicted distributions for *A. flagellicauda* based on (A) the full variable data set for present day, (B) reduced variable data set for present day, projected into the CCSM paleoclimate for full (C) and reduced (D) Maxent models, and projected into the MIROC paleoclimate for full (E) and reduced (F) Maxent models. Predicted distributions represent suitable habitat based continuous habitat suitability scores. The range of suitability scores are shown by cut-off value threshold: most stringent based on equal training sensitivity and specificity (black), medium stringency based on equal entropy of thresholded and original distributions (dark gray), and least stringent based on balancing training omission, area and threshold (light gray).

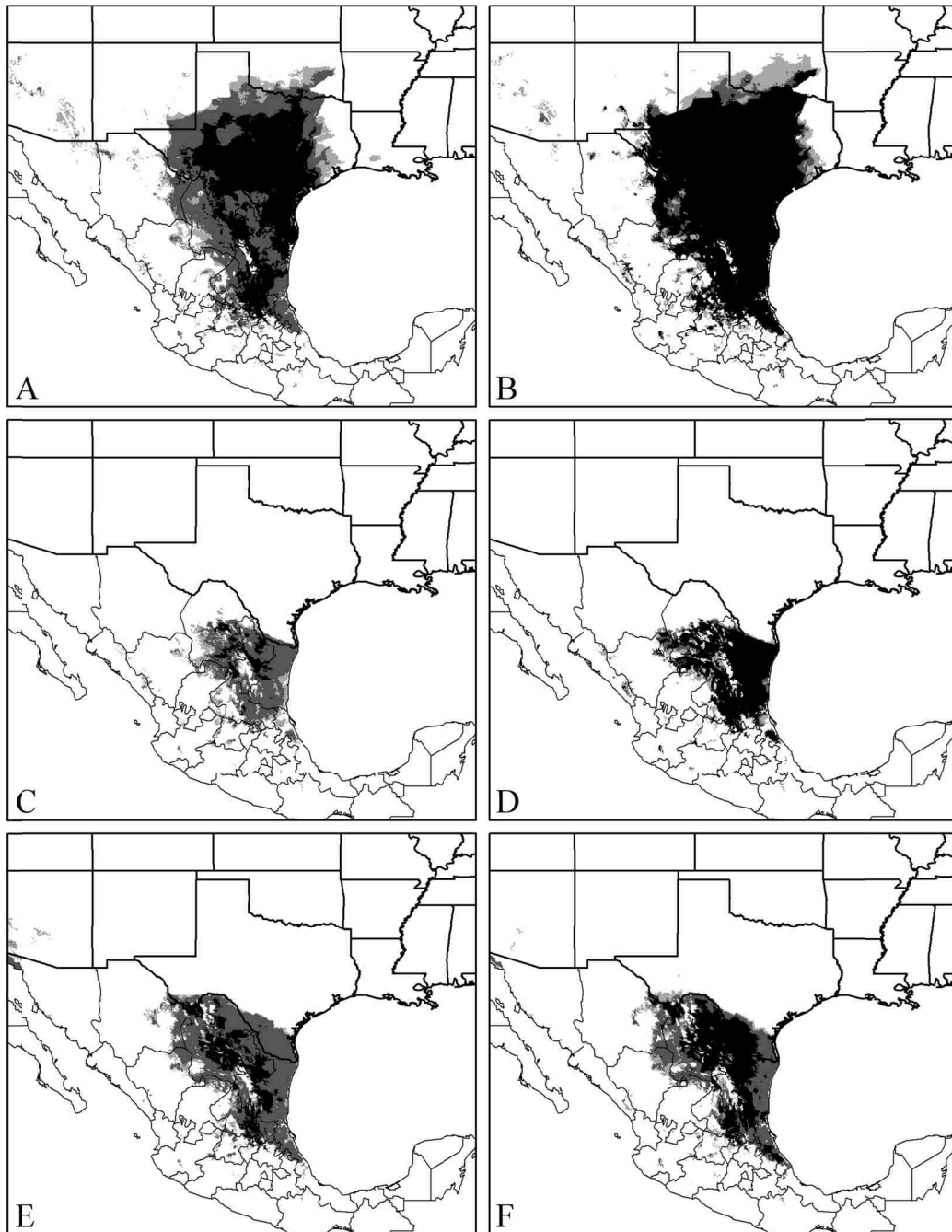


Figure 2.8. Maxent predicted distributions for *A. gularis* based on (A) the full variable data set for present day, (B) reduced variable data set for present day, projected into the CCSM paleoclimate for full (C) and reduced (D) Maxent models, and projected into the MIROC paleoclimate for full (E) and reduced (F) Maxent models. Predicted distributions represent suitable habitat based continuous habitat suitability scores. The range of suitability scores are shown by cut-off value threshold: most stringent based on equal training sensitivity and specificity (black), medium stringency based on equal entropy of thresholded and original distributions (dark gray), and least stringent based on balancing training omission, area and threshold (light gray).

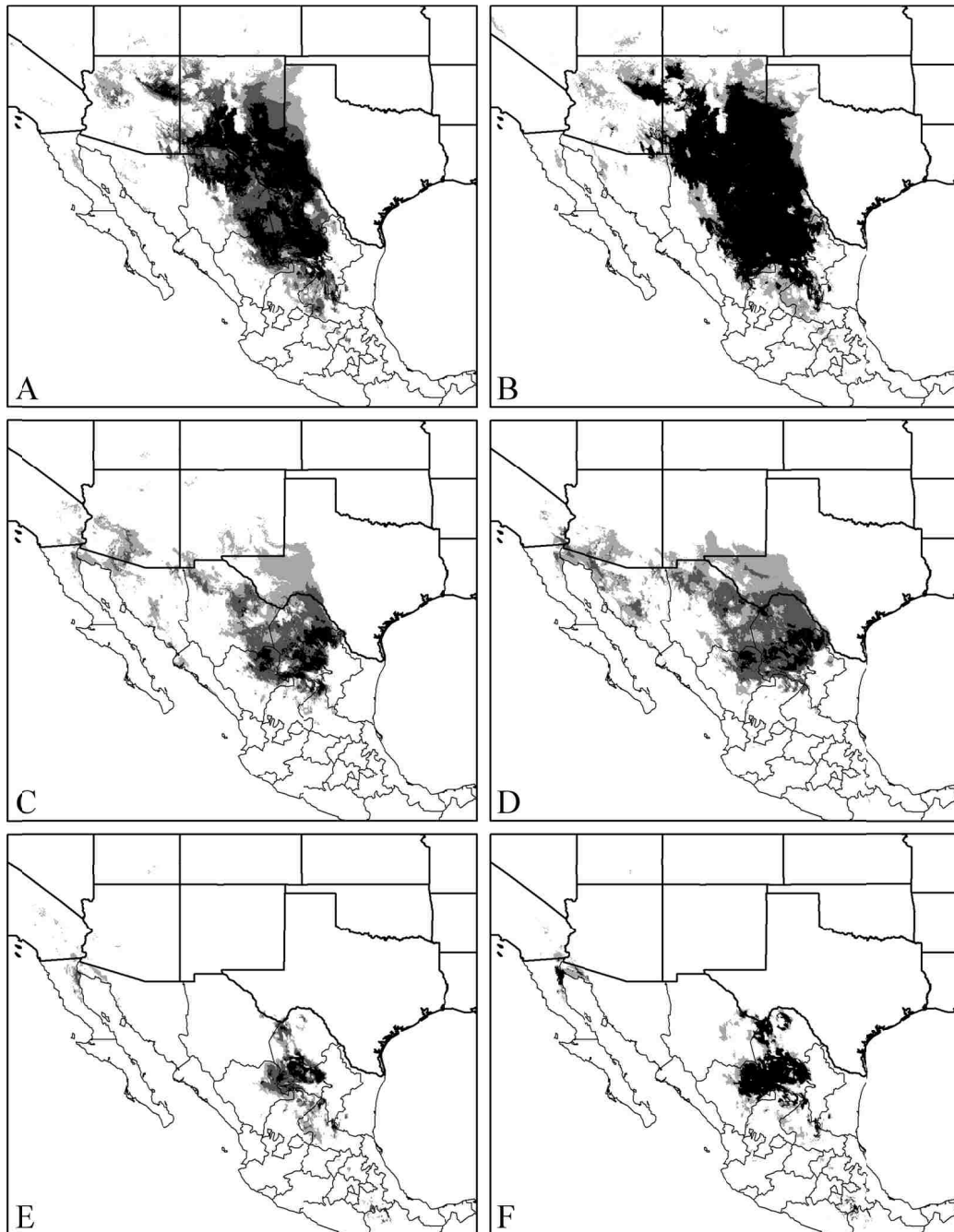


Figure 2.9. Maxent predicted distributions for *A. inornata* based on (A) the full variable data set for present day, (B) reduced variable data set for present day, projected into the CCSM paleoclimate for full (C) and reduced (D) Maxent models, and projected into the MIROC paleoclimate for full (E) and reduced (F) Maxent models. Predicted distributions represent suitable habitat based continuous habitat suitability scores. The range of suitability scores are shown by cut-off value threshold: most stringent based on equal training sensitivity and specificity (black), medium stringency based on equal entropy of thresholded and original distributions (dark gray), and least stringent based on balancing training omission, area and threshold (light gray).

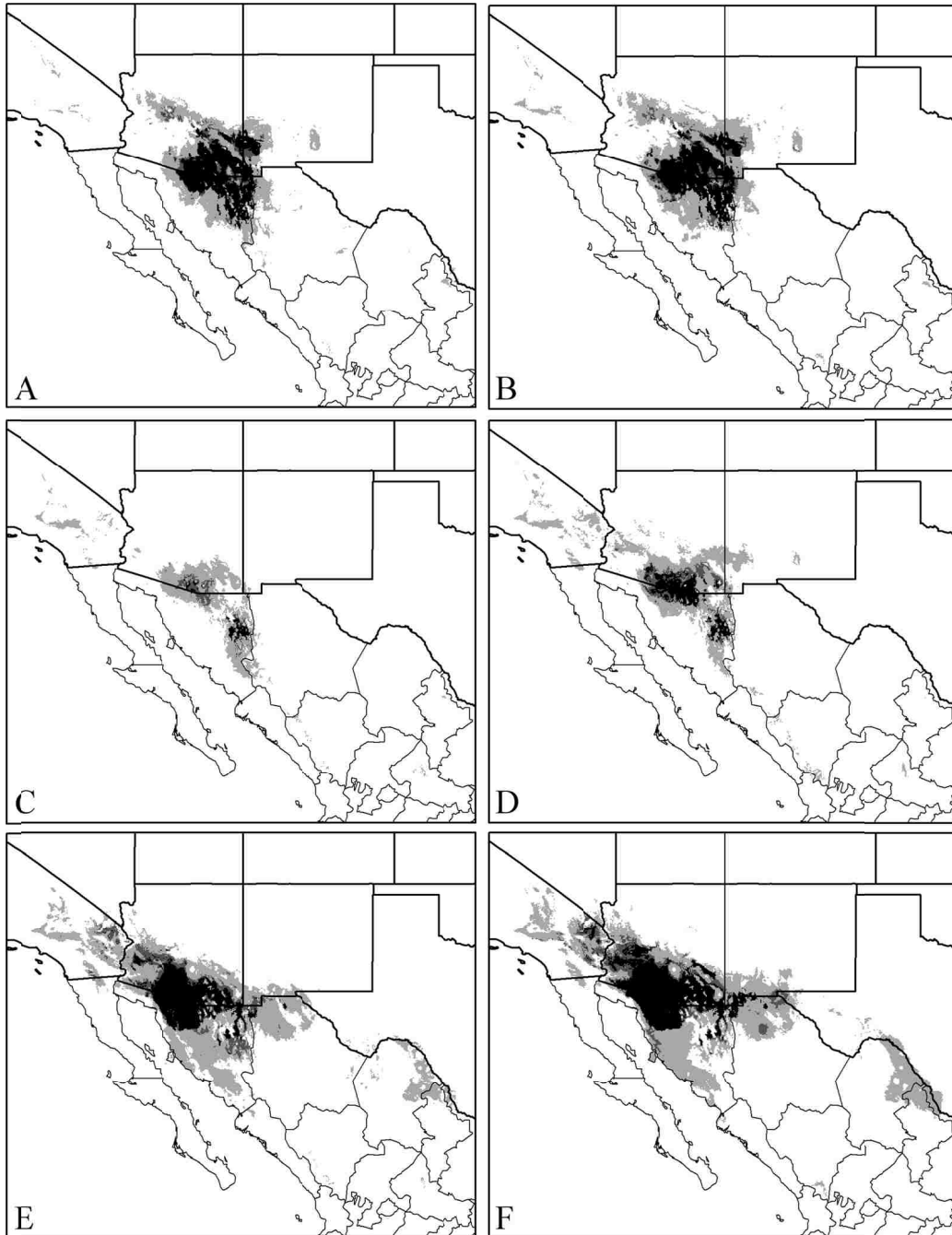


Figure 2.10. Maxent predicted distributions for *A. sonoreae* based on (A) the full variable data set for present day, (B) reduced variable data set for present day, projected into the CCSM paleoclimate for full (C) and reduced (D) Maxent models, and projected into the MIROC paleoclimate for full (E) and reduced (F) Maxent models. Predicted distributions represent suitable habitat based continuous habitat suitability scores. The range of suitability scores are shown by cut-off value threshold: most stringent based on equal training sensitivity and specificity (black), medium stringency based on equal entropy of thresholded and original distributions (dark gray), and least stringent based on balancing training omission, area and threshold (light gray).

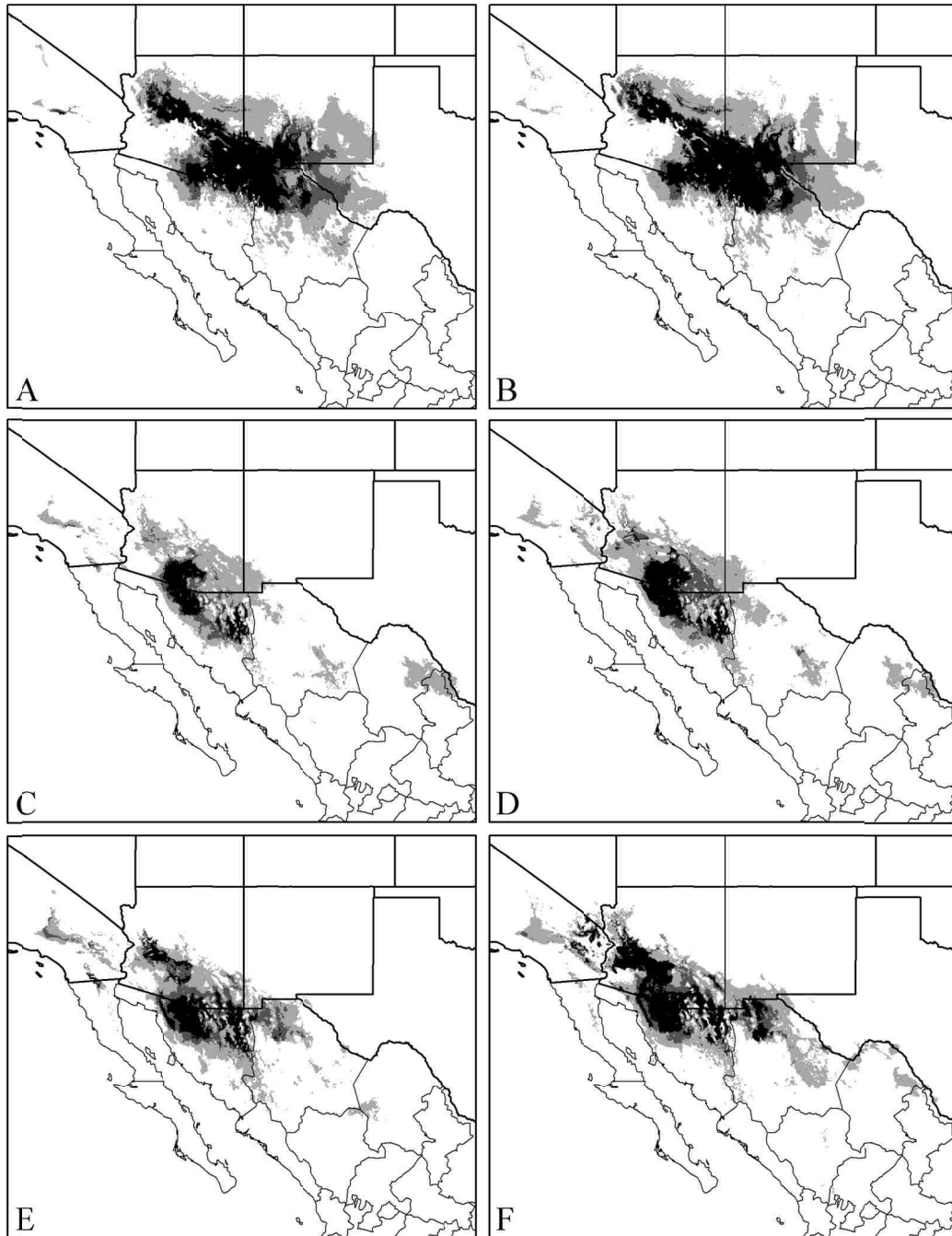


Figure 2.11. Maxent predicted distributions for *A. uniparens* based on (A) the full variable data set for present day, (B) reduced variable data set for present day, projected into the CCSM paleoclimate for full (C) and reduced (D) Maxent models, and projected into the MIROC paleoclimate for full (E) and reduced (F) Maxent models. Predicted distributions represent suitable habitat based continuous habitat suitability scores. The range of suitability scores are shown by cut-off value threshold: most stringent based on equal training sensitivity and specificity (black), medium stringency based on equal entropy of thresholded and original distributions (dark gray), and least stringent based on balancing training omission, area and threshold (light gray).

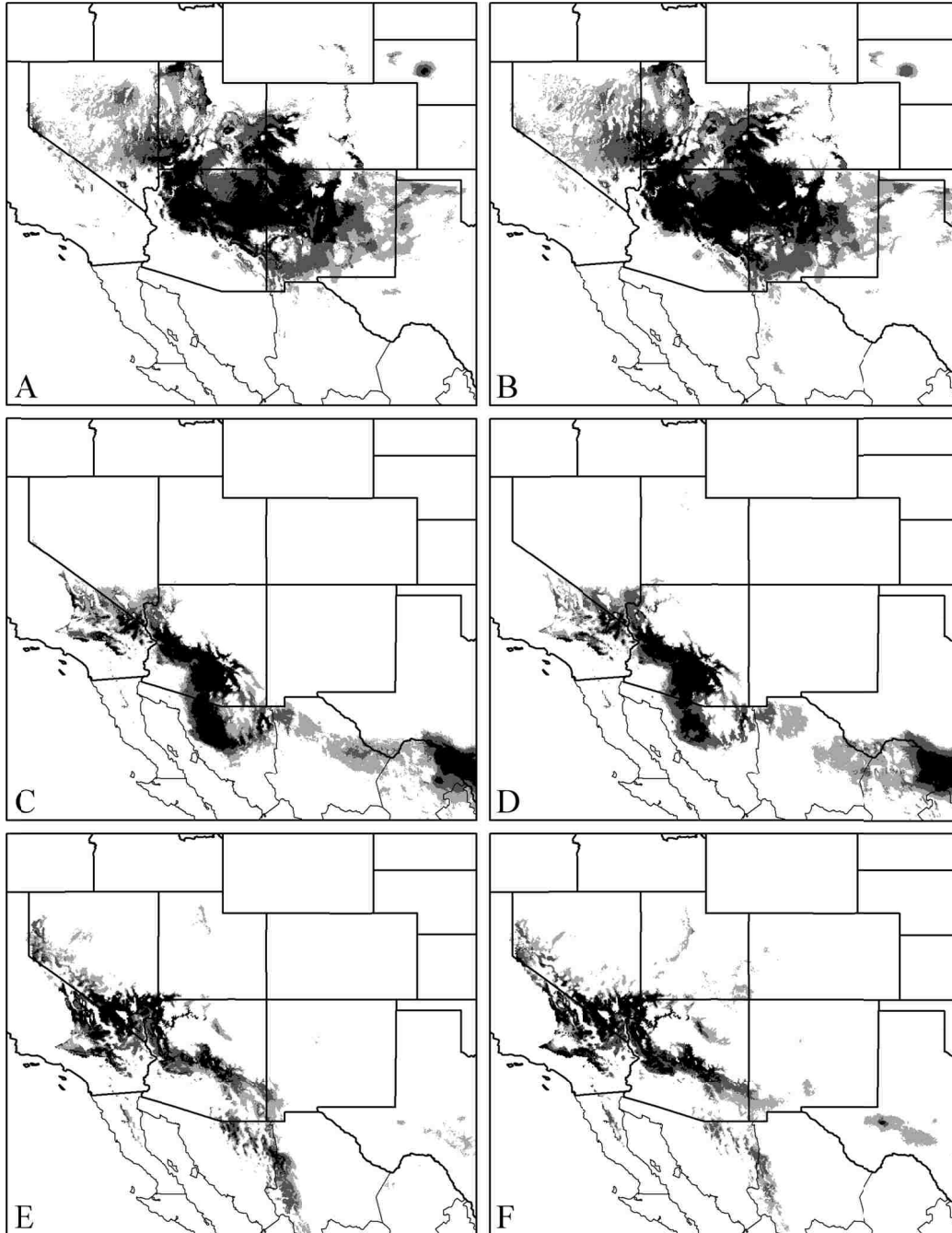


Figure 2.12. Maxent predicted distributions for *A. velox* based on (A) the full variable data set for present day, (B) reduced variable data set for present day, projected into the CCSM paleoclimate for full (C) and reduced (D) Maxent models, and projected into the MIROC paleoclimate for full (E) and reduced (F) Maxent models. Predicted distributions represent suitable habitat based continuous habitat suitability scores. The range of suitability scores are shown by cut-off value threshold: most stringent based on equal training sensitivity and specificity (black), medium stringency based on equal entropy of thresholded and original distributions (dark gray), and least stringent based on balancing training omission, area and threshold (light gray).

CHAPTER 3.

CLONAL ECOLOGICAL STRATEGY IN *ASPIDOSCELIS*

Abstract

The key to understanding the evolutionary importance of sex is determining how genetic variation within a species interacts with the environment. This gene-environment interaction was investigated across the distribution of two parthenogenic hybrid whiptail species, *A. uniparens* and *A. velox*, and their sexual parents *A. inornata* and *A. burtti*. Geographic variation in the nuclear genome sampled across evenly distributed populations throughout each species range was described by Amplified Fragment Length Polymorphism (AFLP) data to test two competing hypotheses regarding the ecological adaptation of parthenogenic clones. The first hypothesis, termed the generalist genotype, suggests that there is one broadly adapted asexual genotype distributed throughout the entire range of a hybrid species (Vrijenhoek, 1998). The alternative is the frozen niche hypothesis, where uniquely adapted clones divide the environmental niche space into non-overlapping units (Lynch, 1984; Vrijenhoek, 1998).

These predictions were tested according to the method of Rissler and Apodaca (2007) by employing a Principle Components Analysis (PCA) on the 19 physical environmental variables from the WorldClim dataset extracted from the locations of unique genetic clusters identified during the AFLP analysis. An analysis of variance (ANOVA) on the resulting PCA scores was used to determine if unique genetic clusters are found in significantly different environments. *Aspidoscelis uniparens* was found to

have highly geographically structured genetic clusters, some of which were found in significantly different environments than other clusters, consistent with the frozen niche hypothesis. In contrast, genetic clusters from *A. velox* were found to exhibit weaker geographic structure and there were no significant differences in the environmental conditions occupied by each genetic cluster, consistent with the generalist genotype.

This study represents a test-case for the Ecological Strategy of Clones subsection of the Comprehensive Research Framework regarding the geographic distribution and persistence of parthenogenic organisms identified in Chapter One. As part of a road-map whose aim is to identify a large number of potentially important biological processes in parthenogenic organisms relative to their sexual relatives, this section represents a focused research plan into genetic processes acting on parthenogenic organisms contributing to their apparent ecological success in certain environments. This study successfully identified two hypothesized population level genetic patterns acting in related parthenogenic hybrid whiptails.

Introduction

The evolution and maintenance of sexual reproduction in biological organisms is a widely discussed and important concept in ecological and evolutionary theory. Sexual reproduction is dominant form of reproduction in most plant and animal species (Kearney, 2005), despite the numerical advantages of asexual reproduction because males, who don't directly contribute to the next generation with offspring of their own, are absent (Maynard Smith, 1978). One form of asexual reproduction in vertebrates is

parthenogenesis, the clonal reproduction of an all-female species without the need for males. Though relatively rare in natural populations, parthenogenesis often occurs as a consequence of hybridization between sexual species (Kearney, 2005), occurring in insects and vertebrates such as fish and reptiles (reviewed in: Glesener *et al.*, 1978; Bell, 1982; Kearney, 2005). Hybrid parthenogenic organisms have been recognized as sharing distributional characteristics relative to their sexual relatives, a pattern termed “geographical parthenogenesis” (Vandel, 1928). These organisms are found at higher latitudes, higher altitudes, islands or island-like habitats, xeric environments, and in marginal, disturbed or ecotonal habitats compared to their sexual congeners (Glesener *et al.*, 1978; Maynard Smith, 1978; Lynch, 1984). Because these asexual organisms are vulnerable to the accumulation of deleterious mutations known as “Müller’s ratchet” and cannot rapidly evolve in the face of environmental change, parasitism and competition because of their lack of genetic recombination (the “Red Queen” hypothesis; Maynard Smith, 1978), they are often viewed as evolutionary “dead-ends.” However, the broad distribution and persistence of parthenogenic hybrids in some taxonomic groups, such as the whiptail lizards (genus *Aspidoscelis*) suggest there may be an adaptive advantage to this form of reproduction under restricted but perhaps predictable conditions.

Hypotheses

The success of parthenogenic hybrids relative to their sexual progenitors has been addressed by a diverse array of ecological and evolutionary hypotheses. However, the biological processes that underlie these hypotheses often overlap, complicating

efforts to test one hypothesis to the exclusion of another. To address this complexity in an organized way, a Comprehensive Research Framework (see Chapter One) was developed that categorized biological processes into testable groups, allowing the geographic distribution and persistence of parthenogenic organisms to be examined in a consistent and comprehensive manner. Using parthenogenic whiptail lizards as the organism of interest, the present study will act as a test case for the Comprehensive Research Framework by examining biological processes described in the “Ecological Strategy” section that characterizes the ecological adaptation of parthenogenic clones to the landscape across a hybrid’s distribution. The genetic patterns inferred here will be contrasted with patterns predicted by generalist genotype or the frozen niche hypotheses.

Under the generalist genotype hypothesis, the success of parthenogenic hybrids is predicted to result from the selective success of a clone that is widely adapted to a general range of biological conditions and can thus spread over a large geographical area or a range of environments (Vrijenhoek, 1989). While used to explain broad geographic distributions and tolerance to a wide range of environments (Parker Jr. *et al.*, 1977), this hypothesis also posits that the genotype with the highest geometric mean fitness (smallest variance) will replace more specifically adapted clones over evolutionary time in highly variable environments (Lynch, 1984; Vrijenhoek, 1998). Support for this hypothesis has been demonstrated for asexual organisms in previous studies (Haack *et al.*, 2000; Van Doninck *et al.*, 2002). The expectation in a widely distributed asexual species is that there will be one or a few widely distributed clones

throughout the distribution. If there is more than one clone, then these clones will overlap widely with little evidence of geographic, environmental or habitat structure.

In contrast to the generalist genotype, the frozen niche hypothesis suggests that successful parthenogenic clones are genetically “frozen” to a specific and narrow range of environmental conditions (Vrijenhoek, 1998). The expectation is that natural selection will act on an array of clonal genotypes such that successful clones will be adapted to a narrow range of conditions that have minimal niche overlap with other clones and their sexual relatives (Vrijenhoek, 1998). The predictions of the frozen niche hypothesis have been tested in a number of asexual taxa with closely related sexual congeners, which both support (Semlitsch *et al.*, 1997; Gray & Weeks, 2001) and reject (Jensen *et al.*, 2002) the predictions of this model. It is expected that in an asexual species distributed widely across a number of habitats, many clones will be found across the species range in non-overlapping geographic distributions that correspond to unique environmental conditions or habitat types.

Whiptail lizards (genus *Aspidoscelis*) are a widespread and conspicuous group of lizards that are found throughout the American southwest (Wright & Vitt, 1993; Reeder *et al.*, 2002). While parthenogenesis has been found in a wide variety of lizard taxa (Kearney, 2005), whiptails are unique because of the high frequency of parthenogenic species; of the approximately 50 recognized species nearly a third are parthenogenic (Wright & Vitt, 1993). Parthenogenic whiptails are the result of hybridization between sexual species (reviewed in: Reeder *et al.*, 2002) and include diploid species, and most frequently triploid species that result from a diploid hybrid back crossing with a sexual

species (Dessauer & Cole, 1989). Parthenogenic whiptail species also exhibit a pattern of geographic parthenogenesis (Vandel, 1928) by inhabiting arid, ecotonal and marginal habitats relative to their sexual progenitors (Wright & Lowe, 1968). The majority of parthenogenic hybrids are also found within the same general vicinity: the southwestern deserts of Arizona, New Mexico, southern Utah, southwestern Colorado and northern Mexico (Wright & Vitt, 1993).

This study will test the genetic and environmental expectations of the generalist genotype and frozen niche hypotheses across the distribution of two parthenogenic whiptail species *A. uniparens* and *A. velox*. The desert grassland whiptail, *A. uniparens*, and the plateau striped whiptail, *A. velox*, are triploid parthenogenic hybrid species with largely allopatric distributions except for known co-occurrence along the Mogollon Rim of Arizona and in the Rio Grande River valley in New Mexico. These two species share the same sexual progenitors, *A. inornata* and the *A. burti/costata* complex, and are morphologically very similar, leading to suggestions that they are clonal variants (Densmore III *et al.*, 1989). However, they differ in maternal ancestry. The maternal ancestor to *A. uniparens* is the little striped whiptail, *A. inornata* (Densmore III *et al.*, 1989), while the maternal ancestor to *A. velox* is the western Mexico whiptail, *A. costata* (Bell, 2003). Because *A. costata* belongs to the paraphyletic *burti/costata* complex (Bell, 2003), which includes the canyon spotted whiptail, *A. burti*, and the red-backed whiptail, *A. xanthonota*, I refer to this group of species as the *A. burti* complex. Because these two species share the same ancestors and are thus closely related, they provided a useful comparison assessing the strength of patterns found in the distribution of

clones across a given species distribution.

The triploid genomes, hybrid origin and asexual reproduction of *A. uniparens* and *A. velox* make it potentially difficult to analyze the evolutionary history and population genetic structure of these species. Mitochondrial DNA has been previously examined in *A. velox*, but the amount of diversity is relatively low compared to sexual species (Bell, 2003). The genomes of hybrid species are further complicated because it has been recently found that high heterozygosity is maintained in parthenogenic whiptails (Lutes *et al.*, 2010). Amplified fragment length polymorphisms (AFLPs) is a genetic technique with potential to generate the genetic variation necessary to analyze genetic structure in organisms as complex as whiptails.

Using AFLP profiles and freely available spatial environmental information, expectations of the generalist genotype versus frozen niche hypothesis will be tested in *A. uniparens* and *A. velox*. These parthenogenic hybrids may be generally adapted to a broad range of environmental conditions across their range, where a few clones have highly overlapping environmental niches and geographic distributions, consistent with the generalist genotype. Alternatively, multiple hybrid clones may be narrowly adapted to a small set of non-overlapping environmental conditions, partitioning the landscape as in the frozen niche model.

Methods

Two sets of analyses will be conducted in order to distinguish between the generalist genotype and frozen niche hypotheses. First, the number of distinct genetic

units, or clones, will be determined by assessing genetic variation in AFLP markers across the range of each parthenogenic hybrid. Distinct genetic clusters will be determined by analyzing individual band frequency using UPGMA trees and Bayesian genetic clustering algorithms implemented in STRUCTURE v.2.2 (Pritchard *et al.*, 2000; Falush *et al.*, 2007). Once the appropriate number of distinct genetic clusters has been identified, and each specimen assigned to an appropriate group, these groups will be visualized in geographic space to determine extent of spatial overlap using a Geographic Information System. The environmental niche will then be compared according to the method of Rissler and Apodaca (2007), as described in the previous chapter, to determine if they occupy unique environmental space. Multivariate statistics (*i.e.* ANOVA) will be used to compare environmental variables extracted from each species to assess environmental divergence.

Specimens of *A. uniparens* and *A. velox* were collected across their respective ranges on public lands of Arizona, New Mexico, Utah and Colorado (see Figure 3.1, Table 3.1). Locations were chosen to evenly sample genetic variation across each species range. At each location, 3 to 5 specimens were collected, liver and heart tissues were preserved in liquid nitrogen or 95% ethanol, and the specimens retained and vouchered. In total, 49 *A. uniparens* were collected from 13 localities, and 76 *A. velox* were collected from 16 localities during the summers of 2007-2009 (Appendix G). All specimens were collected according to the Guidelines for Use of Live Amphibians and Reptiles in Field Research (available at: [http://iacuc.ucsd.edu/PDF_References/ASIH-HL-SSAR Guidelines for Use of Live Amphibians and Reptiles.htm](http://iacuc.ucsd.edu/PDF_References/ASIH-HL-SSAR%20Guidelines%20for%20Use%20of%20Live%20Amphibians%20and%20Reptiles.htm)),

the Institutional Animal Care and Use Committee (IUCAC) of the University of Nevada, Las Vegas (UNLV; Protocol No: R701-0307-215), and the American Veterinary Medical Association (2000).

Genomic DNA was extracted from preserved tissues using the DNeasy Tissue Kit (Qiagen) according to the manufacturer's standard protocol, and stored in the provided buffer at 4°C. To ensure that extracted DNA was of high quality, 2µl of extraction product was run on a 0.8 percent agarose gel to verify the presence of high molecular weight DNA. Initial screening of AFLP markers was conducted using the AFLP Plant Mapping Kit (Applied Biosystems) followed by the AFLP protocol made available by Paul Wolf (Wolf, 2000).

Digestion of genomic DNA and ligation of adaptors was conducted as a single reaction overnight using 5.5µl of genomic DNA, 5 units EcoRI (New England Biolabs), 1 unit MseI (New England Biolabs), 1 unit T4 DNA ligase (New England Biolabs), 1.1µl 10x ligase buffer, 1.1µl 0.5M NaCl, 0.55µl 1mg/mL BSA, 1µl each of 5mM forward and reverse MseI (Mse_F: 5'gACgATgAgTCCTgAG3'; Mse_R: 5'TACTCaggACTCAT3') and EcoRI (Eco_F: 5'CTCgTAgACTgCgTACC3'; Eco_R: 5'AATTggTACgCAGTCTAC3') adaptors, and PCR water to a total reaction volume of 11µl. Resulting digestion/ligation products were then diluted with 94.5µl of TE_{0.1} buffer. Preselective amplifications of samples used 3µl of digestion/ligation product with 0.2µl GoTaq (Promega), 0.6µl 5mM dNTPs, 5µl of 5x reaction buffer and 0.5µl each of the 5mM preselective primers EcoA (5'gACTgCgTACCAATTCA3') and MseC (5'gATgAgTCCTgAgTAAC3') in a 25µl total reaction volume. The thermocycler conditions for preselective amplifications consisted of a two

minute hold at 72°C, 20 cycles of 94°C for 20 seconds, 56°C for 30 seconds and 72°C for 2 minutes, followed by a 30 minute hold at 60°C. The resulting preselective product was then used in all selective amplifications using all possible combinations of selective EcoRI primers (5'gACTgCgTACCAATTC3' with terminal 3' bases: AAC, ACT, AgC) with 6FAM fluorescent tags, and MseI primers (5'gATgAgTCCTgAgTAA3' with terminal 3' bases: CAA, CAC, CAg, CAT, CTA, CTC, CTg, and CTT; Table 3.2). For the 12.5µl selective amplifications, 3µl of preselective product was combined with 0.3µl 5mM dNTPs, 0.1µl Platinum Taq (invitrogen), 1.25µl 10x reaction buffer, 1µl 25mM MgCl₂, 0.1µl 1mg/mL BSA, 0.05µl of the selective EcoRI primer (10µM), and 0.25µl of the selective MseI primer (10µM). The thermocycler protocol for selective amplifications consisted of a 2 minute hold at 94°C, 12 cycles of 94°C for 30 seconds, 65°C for 30s with a 0.7°C temperature drop each following cycle, and 72°C for 2 minutes, followed by 23 cycles of 94°C for 30 seconds, 56°C for 30 seconds, and 72°C for 2min, concluding with a 72°C hold for 10 minutes. Approximately 20% of the amplifications for primer pairs were repeated starting from the tissue extraction step to assess reproducibility of the AFLP protocol from restriction enzyme digestion to selective amplification. The final selective amplification products were sent to the Nevada Genomics Center at the University of Nevada, Reno, where genotyping was conducted on an Applied Biosystems 3730 DNA Analyzer using a LIZ 500 size standard.

The intensity and size of peaks from the raw chromatographs were detected using the freely available Peak Scanner software v.1 (Applied Biosystems, 2006) with default values except for light smoothing of peaks, where each peak represents a band

of AFLP DNA. The resulting data matrix was filtered for low quality samples and automatically scored using the free R CRAN library RawGeno (Arrigo *et al.*, 2009). Automated scoring is preferable to scoring by eye because scoring peaks is not subject to human error or bias, is repeatable, and requires less time with large datasets. Following recommendations from the RawGeno manual and Arrigo *et al.* (2009), the following range of parameters were used for the scoring algorithm (parameters varied by primer pair and bin refers to the lower and upper size defining a given peak): minimum band size = 100bps, maximum band size = 350-500bps, minimum bin width = 1 - 1.5bps, maximum bin width = 1.5 - 2bps, minimum peak intensity = 100 rfu, and minimum frequency of peak bin between samples = 3. Optimum parameters were determined by maximizing the information content per bin (maximizing I_{bin} , defined as the average number of bins differing between a focal sample and other samples data set, divided by the total number of bins in the dataset; Arrigo *et al.*, 2009), by iterating the analysis across several parameter values. Error, as determined by replicated samples, was generally below 8%, with two primer sets having 11% error (Table 3.2). Size homoplasy among similar sized bands was examined by looking for a significant negative correlation between bin frequencies to fragment size for each primer set (Vekemans *et al.*, 2002). Scored datasets for each primer pair was then exported to presence/absence data matrices for polymorphic loci.

Similarities between AFLP genotypes were assessed using hierarchical clustering of a distance matrix of total pairwise differences by calculating UPGMA (Unweighted Pair Group Method with Arithmetic Mean) dendrograms in PAUP* v.4b10 (Swofford,

2002). Support for each branch was assessed using 1000 bootstrap replicates. Dendrograms were created using all specimens for each primer pair separately, on a concatenated data set for each species separately, and on a concatenated data set of all loci.

Additional genotype clustering was employed using assignment tests in STRUCTURE v.2.3 (Pritchard *et al.*, 2000) for dominant markers (Falush *et al.*, 2007). Considering that these species reproduce asexually and dominant AFLP markers were amplified, the following parameters were used on a concatenated data set of all primer sets: Polyploidy = 3, no admixture, independent allele frequencies, recessive alleles = 1, burnin = 1,000 generations, and Markov Chain Monte Carlo (MCMC) generations = 10,000. The number of genetic clusters assumed (k, often referred to as the number of populations) ranged from 1 to 10, and three replicates of each k were run for each species using a batch script in Perl. Specimen assignments to genetic clusters from all runs were then compared to determine the total number of clusters and the likely assignment of that specimen to a genetic cluster in each species. For *A. uniparens*, the number of clusters converged on 4 and assignment was unambiguous for all specimens. While the number of genetic clusters for *A. velox* converged on 5, cluster assignment for a number of specimens was ambiguous and additional analyses were necessary. STRUCTURE was run 100 times for *A. velox* using the same settings as above but assuming a k of 5, and the probability of assignment to each genetic cluster was averaged to give the probability of a specimen being assigned to a given cluster.

To distinguish between the frozen niche and generalist genotype hypotheses,

the environmental characteristics of genotypic clusters were analyzed for each species using the method of Rissler and Apodaca (2007) and described in the Chapter Two. The following expectations were examined: if individual genotypes are found in unique environmental conditions (frozen niche), then there will be statistical differences between the environmental conditions occupied by each recognized genotype; alternatively, if there are one or few genotypes that are broadly distributed across the range of environmental conditions the species inhabits (generalist genotype), then there will be no statistical difference in the environmental conditions occupied by each recognized genotype because they will overlap across environmental values.

First, the environmental values for the 19 WorldClim (Hijmans *et al.*, 2005) bioclimatic variables (Appendix B) were extracted using DivaGIS v.7.5 (Hijmans *et al.*, 2012) from a large georeferenced data set of parthenogenic and sexual whiptail lizards (see Chapter Two for details) that included the localities sampled in this study. The matrix of extracted variables was then analyzed using principal components analysis (PCA) in SYSTAT 12 (SYSTAT software Inc., 2007) to reduce the variation inherent in 19 variables, and the resulting matrix of Principal Component (PC) scores for each of the first four Principal Component Axes were used in further statistical analyses .

Two separate PCAs were used: one analysis built using only the focal species in this study (*A. uniparens* and *A. velox*), and one that included all parthenogenic and sexual species from the previous study (8 species including *A. uniparens* and *A. velox*). The first PCA describes the environmental variation found across the distributions of only the two focal species on independent orthogonal axes. In contrast to the first PCA,

the environmental variation described by the second PCA is extended to include conditions inhabited by parental and sympatric parthenogenic whiptail species ranges. The environmental conditions described by PC factors in these two PCAs differ because each is describing a different range of environmental conditions. The latter may be more generalizable because environmental variation is described over a suite of related parthenogenic hybrid whiptails and their sexual progenitors that are found in same general geographic location, and better describes the environmental condition of the entire geographic region where parthenogenesis occurs. This is potentially useful when comparing how genotypic clusters may differ in their environmental distribution.

The resulting PC scores were analyzed using an analysis of variance (ANOVA) with genotypic cluster assignment as the fixed factor for both species together and separately. For those sampling localities that contained more than one genotypic cluster, or if there was uncertainty regarding the assignment of specimens to a particular cluster, that sampling locality was duplicated to include its PC score for the environmental analysis of each genotypic cluster.

Results

Genetic Results

All possible combinations of primers, 24 total, were scored for the presence and absence of peaks using RawGeno and the resulting matrices were analyzed for signal using UPGMA trees for each primer individually. Of the 24 primer pairs, 21 provided results that clearly divided samples into the two recognized species, *A. velox* and *A.*

uniparens, and demonstrated population structure by grouping specimens from the same populations together. The remaining 3 primer sets (Eco_AAC, Mse_CAC; Eco_ACT, Mse_CAC; and Eco_AgC, Mse_CAA) were discarded as too noisy after examining the raw chromatographs and output from RawGeno based on too many peaks, low peak height and/or high background noise obscuring peaks. These primer pairs will not be addressed further in this study.

The remaining 21 primers were concatenated into a final data set that contained 1403 informative loci. *Aspidoscelis uniparens* and *A. velox* clearly separate into clades based on a UPGMA dendrogram of all samples and loci (not shown), confirming their independent origins as parthenogenic hybrids, and all subsequent analyses are performed on each species separately.

The results of the UPGMA and STRUCTURE analyses for *A. uniparens* are shown in Figure 3.2. The UGMA dendrograms are shown with bootstrap support values above the node of interest for distinct clusters of specimens, and the assigned cluster from the STRUCTURE analysis is shown as the coded box at the terminal ends of the dendrogram. There was no uncertainty in the assignment of specimens to genotypic clusters in the STRUCTURE analysis, so the probability of assignment is not shown. For *A. uniparens*, specimens were unambiguously assigned to 4 distinct clusters of genotypes (Figure 3.2) that are consistent with population sampling: all specimens within a population belong to the same genotype cluster with two exceptions: the population sampled at Cienegas (Ci) contains two genotypic clusters, A and B, and the population sampled at Duncan (Du) contains two genotypic clusters, B and C.

The geographic distribution of genotypic clusters is shown in Figure 3.3 and shows a distinct geographic structure in the distribution of clusters where members of a genetic cluster are found in neighboring populations. The populations with two genotypes (Ci and Du) occupy positions between the distributions of the two genotypes, and may represent an area where the two genotypes meet and overlap. The geographic structure found in *A. uniparens* is consistent with a pattern predicted by the frozen niche hypothesis, where specific genotypes are found narrowly distributed in a small geographic area relative to the species range.

Genetic structure of *A. velox* from the UPGMA and STRUCTURE analyses is shown in Figure 3.4. The UPGMA tree with bootstrap support and clusters of genotypes from STRUCTURE are shown as described above. STRUCTURE settled on 5 genetic clusters in the dataset, but because assignment of particular specimens was uncertain, the analysis was repeated 100 times with the number of clusters set to 5 ($k = 5$). The proportion of assignments to a particular cluster for each specimen is shown in the right most columns of Figure 3.4. Uncertainty between genetic clusters I and J existed in the population Williams (WI) where the probability of being assigned to a particular cluster (the high value) ranged from 0.81 to 0.55. The uncertainty between genetic clusters G and H existed in the populations Pilar (Pi) and Naturita (Na) where the probability of being assigned to a particular cluster ranged from 0.68 to 0.47.

The geographic distribution of genotypic clusters is shown in Figure 3.5 and, in contrast to the patterns seen in *A. uniparens*, particular clusters are more spread out across the species distribution indicating a weaker pattern of geographic structure. The

most geographically contained genotypic clusters (those populations whose nearest neighbors share genetic clusters) are cluster I, found in the populations Escalante (Es), Kanab (Ka), Jacob (Ja), and Williams (Wl) on the western edge of the species range (although specimens from Wl have uncertain assignment to genotypic cluster I or J), and genotypic cluster F, found in the populations Grants (Ga), Magdalena (Ma) and Ysidro (Ys, although this population is shared with another genotypic cluster G). Cluster J is also found narrowly distributed in the population Winslow (Wn) and potentially Wl (as described above). The remaining genotypic clusters are distributed broadly across the species distribution. Genotypic cluster G is the most widely distributed, found in the northern populations of Bridge (Br) and Bloomfield (Bl), the eastern populations of Pilar (Pi) and Santa Fe (Sf), and the southwestern population of Flagstaff (Fl). The specimens of the northern most population of Naturita (Na) are uncertain regarding their assignment to G or the less widely distributed genotypic cluster H. Unambiguously identified cluster H is largely found in the more southerly distributed specimens of the populations in Church (Ch) and Springer (Sp) while its assignment is uncertain with regard to cluster G in Pi and Na. While the genetic structure in *A. velox* appears to have restricted geographic structure of some genotypic clusters similar to that of *A. unipares*, there is a widespread genotypic cluster (G) that is consistent with the generalist genotype hypothesis.

Principal Components Analysis: *A. unipares* and *A. velox* only

Three Principal Component (PC) axes for the combined museum and field specimens of only *A. unipares* and *A. velox* had eigen values greater than 1, and the

results are shown in Table 3.3A. Principal component 1 (PC1) explains 54.9% of the variation in the data set, and describes the effect of all but 4 of the 19 WorldClim variables (BIO1, BIO3, BIO4, BIO6, BIO7, BIO8, BIO9, BIO10, BIO11, BIO13, BIO14, BIO15, BIO16, BIO17, and BIO18). Generally, increasing PC1 values correspond to increasing temperatures at all times of the year, decreasing temperature seasonality, and increasing precipitation seasonality. Principal component 2 (PC2) explains 24.1% of the variation in the data set and describes decreasing overall precipitation (BIO5, BIO12, and BIO19). Finally, principal component 3 (PC3) describes 8.8% of the variation in the data and is described by a single variable, the mean temperature diurnal range (BIO20).

The results of the PCA are shown graphically in Figure 3.6, where PC score means for the entire data set are graphed with corresponding 95% confidence intervals for each component axis. The PCA scores for each sampled genetic cluster are graphed with a symbol corresponding to the cluster's identity to show the environmental range occupied. Comparisons of PC1 and PC2 are shown in Figure 3.6A while comparison of PC1 and PC3 are shown in Figure 3.6B.

Genetic cluster is a significant factor at $p < 0.01$ (PC1 $F_{3,10} = 2.948$, $p = 0.085$; PC2 $F_{3,10} = 4.001$, $p = 0.041$; PC3 $F_{3,10} = 7.622$, $p = 0.006$) for *A. uniparens*. There are significant differences between the environmental conditions occupied by each genetic cluster, and the pairwise differences as calculated using Tukey's Honestly Significant Difference (HSD) test are shown in Table 3.4. For all PCs, genetic cluster A is significantly different from C, and C is significantly different from D (but, only one sample location) on PC3. Because of the small sample size in the ANOVA analysis, statistical test were

repeated using the non-parametric Kruskal-Wallis test. Genetic cluster is only a significant factor for PC2 and PC3 (PC1 $H = 5.73$, d.f. = 3, $p = 0.125$; PC2 $H = 7.516$, d.f. = 3, $p = 0.047$; PC3 $H = 10.211$, d.f. = 3, $p = 0.017$). Pairwise comparisons of genetic clusters from PC1 and PC2 reveal that cluster A and C are significantly different for PC2, while C is significantly different from A and B for PC3 (Table 3.4).

In contrast to *A. uniparens*, genetic cluster for *A. velox* is not a significant factor (PC1 $F_{4,14} = 2.113$, $p = 0.133$; PC2 $F_{4,14} = 0.627$, $p = 0.651$; PC3 $F_{4,14} = 1.822$, $p = 0.181$), indicating that there is no difference in the environmental conditions between the distributions of recognized genetic clusters. Once again, because of the small sample size, the ANOVA analysis was repeated using the non-parametric Kruskal-Wallis test. Similar to the ANOVA and in contrast to *A. uniparens*, the environmental conditions over the distribution of genetic clusters is not significantly different from one another (PC1 $H = 6.539$, d.f. = 4, $p = 0.162$; PC2 $H = 3.665$, d.f. = 4, $p = 0.455$, PC3 $H = 7.193$, d.f. = 4, $p = 0.126$).

Principal Components Analysis: All whiptails

When the PCA included the environmental distributions of additional whiptails species, four PC axes had eigen values greater than 1 (Table 3.3B). Principal component 1 (PC1) explains 45.07% of the total variation in the data set, and describes increasing temperature and precipitation, and decreasing temperature variation and seasonality (BIO1, BIO4, BIO6, BIO7, BIO11, BIO12, BIO13, BIO16, and BIO18). Principal component 2 (PC2) explains 21.45% of the variation and describes decreasing daily temperature range and increasing overall precipitation with less seasonality (BIO2, BIO3, BIO14,

BIO15, BIO17, and BIO19). Principal component 3 (PC3) explains 16.70% of the variation and describes decreasing temperatures (BIO5, BIO8, and BIO10). The last component, principle component 4 (PC4), explains 5.77% of the variation in the data, and describes increasing temperature of the driest quarter (BIO9).

The results of the PCA built using the suite of whiptail species is shown in Figure 3.6, but only the PC score means are graphed for *A. uniparens* and *A. velox* with corresponding 95% confidence intervals. The PCA scores for each sampled genetic cluster are graphed with a symbol corresponding to the cluster's identity, and comparisons of PC1 and PC2 are shown in Figure 3.6C while comparison of PC1 and PC3 are shown in Figure 3.6D.

Genetic cluster is a significant factor for the first two PCs for *A. uniparens* (PC1 $F_{3,10} = 4.781$, $p = 0.026$; PC2 $F_{3,10} = 5.783$, $p = 0.015$; PC3 $F_{3,10} = 1.189$, $p = 0.363$; PC4 $F_{3,10} = 2.224$, $p = 0.148$). Tukey's HSD indicates that for PC1, genetic cluster C is significantly different from A and B, and C is significantly different from A for PC2 (Table 3.5). Similar to the ANOVA, the Kruskal-Wallis test indicate that genetic cluster is a significant factor for PC1 and PC2 (PC1 $H = 6.29$, d.f. = 3, $p = 0.098$; PC2 $H = 10.368$, d.f. = 3, $p = 0.016$; PC3 $H = 2.785$, d.f. = 3, $p = 0.426$; PC4 $H = 4.572$, d.f. = 3, $p = 0.206$). Pairwise calculations indicate that genetic cluster C is significantly different from A and B for PC1, and that C and B are significantly different from A for PC2 (Table 3.5).

Genetic cluster assignment for *A. velox* was only a significant factor on PC2 (PC1 $F_{4,14} = 1.662$, $p = 0.214$; PC2 $F_{4,14} = 2.636$, $p = 0.079$; PC3 $F_{4,14} = 0.561$, $p = 0.695$; PC4 $F_{4,14} = 1.98$, $p = 0.153$), and within PC2, the only significant difference was between genetic

clusters F and G (Table 3.5). Results from the Kruskal-Wallis test differed from the ANOVA. Only PC4 had significant differences between genetic clusters (PC1 $H = 5.419$, d.f. = 4, $p = 0.247$; PC2 $H = 6.858$, d.f. = 4, $p = 0.144$; PC3 $H = 1.319$, d.f. = 4, $p = 0.858$; PC4 $H = 7.892$, d.f. = 4, $p = 0.096$), where genetic cluster J was significantly different from all other clusters.

Discussion

This study provides the first detailed investigation into clonal structure of the parthenogenic whiptail using highly variable AFLP nuclear markers. Using this genetic information, we attempted to address expectations regarding previously posited hypotheses for the distribution of asexual species, the generalist genotype and frozen niche hypotheses.

General Conclusions

Genetic analysis on the morphologically similar parthenogenic whiptail lizards *A. uniparens* and *A. velox* found significant genetic structure between and within these hybrid species. These lizards are notoriously difficult to differentiate in the field when they occur sympatrically, and identification relies on published accounts of scale counts (also highly geographically variable within a hybrid species) and slight differences in color. Despite the genomic complexities of a triploid, asexually reproducing hybrid, the AFLP profiles were able to unambiguously assign specimens to a particular hybrid species, and correct misidentified specimens once in the lab, after the author separated morphologically variable lizards at one location into two species.

Because these two hybrid species were distinguishable at every AFLP primer pair, all subsequent analyses were conducted on each species separately. Significant genetic structure was identified in both species. Because parthenogenesis is a form of asexual reproduction where female lizards lay eggs containing complete genetic clones without the need for males, genetic structure is significant because it confirms that there are multiple distinct clones within each hybrid species. While it has not been determined if these particular clones are of independent origin, meaning that multiple hybridizations (and hence many clones) have occurred at the initial F1 hybridization event, or at the back cross of the F1 hybrid with a parent species, previous studies indicate that this is not the case (Bell, 2003). Despite the large number of parthenogenic hybrid species that occur in the American southwest (Wright & Vitt, 1993; Reeder *et al.*, 2002) which suggests hybridization occurs frequently, it seems unlikely that there were multiple hybridizations per parthenogenic species given the difficulties in replicating hybridization events in the laboratory (Cole *et al.*, 2010; Moritz & Bi, 2011). The results for each species are addressed separately below.

Genetic variation across the distribution of *A. uniparens* is highly structured, with four distinct clusters of genotypes recognized, hereafter referred to as clones, based on UPGMA and STRUCTURE analyses (Figure 3.2). These clones are highly supported, as indicated by the high bootstrap support of nodes between clusters in the UPGMA tree, and by the consistent assignment of specimens to groups in the STRUCTURE analysis.

The distribution of clones on the landscape is highly structured, with like clones distributed in close proximity in distinct areas (Figure 3.3). Clone A is distributed in the

southwestern Arizona section of *A. uniparens* range in the mesquite scrub of Arivaca and Sonita in the south, to the rocky slopes around Tuscon and Oracle in the Sonoran desert, and as far north as Clifton. Clone B is also distributed in the mesquite grasslands of southern Arizona in the area of Tombstone, up to Duncan further north, but is generally distributed to the east of clone A with overlap at Sonita and Cienegas where both clones were collected. Clone C is found throughout the Chihuahuan grasslands and desert scrub of New Mexico, from the southwest near Hachita, up the Rio Grande River Valley to the juniper savannah of Magdalena in the north where it is sympatric with *A. velox*. Clone C also crosses the Arizona, New Mexico border and coexists with clone B at Duncan, but this is the only sampled location in Arizona where it occurs. The final clone, clone D, appears to be more limited in distribution, located at the northwestern limit of the *A. uniparens* range along the Mogollon Rim of Arizona. Presumably, this clone is found at other locations along the Mogollon Rim, but multiple searches in these areas failed to find specimens to sample. It may be that *A. uniparens* is distributed in patches in this topographically complex area, but locating and accessing suitable sites is difficult.

Genetic patterns within *A. velox* are not as clear cut as they are in *A. uniparens*. Both the UPGMA and STRUCTURE analyses agree that there are 5 unique clones within *A. velox*, although there is some ambiguity on the assignment to particular clones between the two analyses (Figure 3.4). The UPGMA dendrogram clearly shows five distinct clusters of AFLP genotypes, but STRUCTURE had trouble assigning particular specimens to specific clones. In particular, certain specimens could be assigned to either clone G or H from Naturita, CO and Pilar, NM, or clone I or J in Williams, AZ. This

indicates that the AFLP profiles from these specimens are more intermediate than other specimens, but since we used clustering algorithms in this study, the precise nature of these relationships cannot be determined at this point.

Similar to the distribution of clones in *A. uniparens*, there was some geographic structuring of clones across the distribution of *A. velox*, though this pattern is weaker than *A. uniparens*. In particular, the structure of clones is strongest at the western edge and southeastern quarter of the species range. Clone I is largely found to the northwest, separated from the rest of clones by the Colorado River canyon system, with the exception of specimens from Williams, AZ that are intermediate to clone I and clone J. Unambiguous specimens of clone J are found in a single location along the south edge of the Colorado Plateau in Arizona in the vicinity of Winslow, Arizona. The final clone that showed a strong geographic affinity was clone F distributed along the Rio Grande River valley in New Mexico from Magdalena where it occurs in sympatry with *A. uniparens*, to San Ysidro, NM.

The remaining clones G and H are much more wide spread than the other clones, distributed across the central and northern portions of the distribution of *A. velox*. Clone G is particularly wide spread, found at six sampling localities in Arizona, Utah and New Mexico. In contrast, clone H is found at two locations in the south-central portion of the distribution, at Springer, AZ and Church Rock in northwestern New Mexico. This may seem geographically restricted, but the assignment of specimens from the northern most location in Naturita, CO, and Pilar, NM are ambiguous with regard to their assignment to Clone H or the wide spread clone G. As a consequence, we chose to view

clone H as potentially widespread, especially since a large portion of northeastern Arizona hasn't been sampled (these areas are tribal reservations and collecting permissions were not obtained).

The geographic AFLP patterns seen in the present study are in agreement with previous phylogenetic studies of *A. velox* using mitochondrial DNA markers conducted by Bell (2003). In particular, the haplotype network constructed by Bell describes a widespread mtDNA haplotype spread throughout the Colorado plateau, consistent with clones G and H, and a distinct clade of haplotypes on the western edge of the distribution of *A. velox*, consistent with the clones I and J. The distinction of these clones is further supported by close examination of the UPGMA tree which indicates that while the exact clustering arrangements of I and J versus the rest of clones is ambiguous (<50% bootstrap support as indicated by the polytomy), all other clones cluster together as more similar to each other than to either I or J (Figure 3.5). This pattern supports the distinction of I and J from the rest of the clones in the more central portions of *A. velox*'s distribution.

Environmental Structure

To disentangle patterns predicted by the generalist versus frozen niche genotype hypotheses, PCAs on the environmental variation occupied by each clone were analyzed using an ANOVA and parametric and non-parametric pairwise comparisons. While the sample sizes of specimens per species were relatively large, the numbers of samples involved in comparisons across clones were the actual sampling localities rather than the number of specimens collected, which results in a much smaller sample size. As a

result, these analyses are not very powerful in determining significant differences between clones, but are still useful in determining if clones are found in different environmental conditions. Further, because small sample sizes makes it difficult to determine if data are distributed normally, both parametric and non-parametric tests were used.

Two separate PCA analyses were used based on a large set of georeferenced whiptail lizard museum specimens, one where the PCA was run the environmental variables found across the distributions of only *A. uniparens* and *A. velox*, and another PCA where environmental variation was assessed across a wide set of related sexual and parthenogenic whiptail lizards that included *A. uniparens* and *A. velox*. There were important differences between the two PCAs. First, for the PCA based on only *A. uniparens* and *A. velox*, PC1 described over half of the variation in the data set (54.9%) and loads 15 out of the 19 WorldClim variables, while PC2 described an additional quarter of the variation in the data set (24.1%) and loaded a remaining 3 out of 4 WorldClim variables. As a result, the majority of the environmental variation in *A. uniparens* and *A. velox* is described by the PC1. In contrast, the PCA based on a full suite of *Aspidoscelis* species more evenly divided up environmental variation between PC factors. The first PC factor accounted for less than half of the variation (45%) and is more specific of what environmental variables are described (Table 3.3B). The second PC factor also described less than a quarter of the variation (21%) and loads a larger number of the variables than the PCA based only on *A. uniparens* and *A. velox*. Finally, PC3 described a greater amount of the variation in the data set (17%), loading 3

variables compared to the one of the PCA based on *A. uniparens* and *A. velox*. Using more species in the PCA results in a scatter plot that clearly differentiates *A. uniparens* and *A. velox* at PC2 and PC3 (Figure 3.6) when they appear relatively equivalent in the PCA based solely on those species.

The PC factor scores for each sampling locality at which a particular clone was found is shown in the PCA scatter plots with the species mean and 95% confidence intervals (Figure 3.6). The statistical results for each species are addressed separately below.

Clones in *A. uniparens* overall appear to be in significantly different environmental conditions based on multivariate analysis with clone as a fixed factor, regardless of the PCA used, or parametric versus non-parametric tests, with one exception: the Kruskal-Wallis test for PC1 on the PCA using only *A. uniparens* and *A. velox* (Table 3.4). Closer examination of the pairwise comparisons in Table 3.4 shows that this pattern is being driven primarily by clone C. In the PCA based on *A. uniparens* and *A. velox*, clone C is significantly different from A on PC1 (parametric test only), PC2 and PC3. For the PCA based on the suite of whiptail species, clone C is significantly different from both clones A and B on PC1 and PC2, regardless of the test used.

The fact that clones within *A. uniparens* are geographically structured and appear to inhabit environments that are different lends support for the frozen niche hypothesis, where narrowly adapted clones are found in unique environments. As stated in the previous paragraph, clone C seems to be driving this pattern and deserves closer inspection. Clone C is distributed in the Chihuahuan Desert grasslands of

southwestern New Mexico, separate from other clones found in the Sonoran Desert regions of Arizona. The division between Sonoran and Chihuahuan taxa in this region is well documented, having been shown to be a phylogenetic break in a wide variety of reptile taxa (Castoe *et al.*, 2007; Leaché & Mulcahy, 2007; Mulcahy, 2008), including a sexual whiptail (Marshall & Reeder, 2005). Therefore, it may be likely that the difference in environmental conditions inhabited by clone C is a function of differences on either side of divide between Sonoran and Chihuahuan Deserts. However, genetic breaks in other taxa in this region are also much older than the hypothesized age of parthenogenic whiptails (possibly only existing since the last glacial maximum [Chapter Two]; Densmore III *et al.*, 1989; Moritz *et al.*, 1989; Wright & Vitt, 1993). However, the clear structuring of other clones in *A. uniparens* within the Sonoran Desert does suggest that clones are dividing up geographic regions, though no significant differences in the environmental conditions occupied were found between other clones.

As stated above, there is weak geographic structuring of clones in *A. velox*, compared to *A. uniparens*, with highly structured clones I and J on the western edge of the distribution, and clone F in the Rio Grande River valley. There were also no significant differences in the environmental conditions occupied by different clones, regardless of the PCA or statistical test used. This pattern, combined with the broad distribution of the two clones G and H (and G in particular), suggests that the spatial and environmental distribution of clones in *A. velox* and most consistent with patterns under the generalist genotype. The distinct structure seen in the western edge of the species distribution could likely be the result of geographic barriers such as the Colorado River

Canyon system.

Other patterns revealed in additional studies of *A. velox* found patterns consistent with the generalist genotype. An investigation from Chapter Two found that the environmental conditions inhabited by *A. velox* relative to its sexual progenitors *A. burti* and *A. inornata* fit a pattern of heterosis. The high heterozygosity that results from hybridization creates hybrids that are superior to their parents, and who then invade areas unavailable to their parent species (Moore, 1984; Vrijenhoek, 1989; Kearney, 2005). The expansion of a vigorous hybrid from an initial hybridization is likely to fit a scenario of a widely distributed genetic clone, rather than a series geographically structured clones frozen a narrow subset of environmental conditions as suggested by the frozen niche hypothesis (Vrijenhoek, 1989).

Future Directions

This study serves as a test-case for the Clonal Ecological Strategy section (section three) of Comprehensive Research Framework on the geographic distribution and persistence of parthenogenic organisms described in Chapter One. We conducted a genetic and environmental survey of two related parthenogenic hybrid whiptail species to determine if inferred patterns fit with the expectation of the generalized genotype or frozen niche hypothesis. The results of this study lead to some additional questions and considerations.

The sample size is clearly a problem for making conclusions regarding whether clones have partitioned the environmental conditions across the range of a hybrid. Because multiple specimens were collected in a given environmental pixel from the

WorldClim data, the number of localities became the independent units used in the statistical tests rather than the number specimens collected. This is the first study to use a highly variable genetic marker in these parthenogenic whiptail lizard species, so there was little information regarding how many clones would be distributed across the landscape and potentially shared at sampling locations. Sampling was conducted like a population study with multiple samples per site, and an even distribution of sampling sites. This way, we could see how many clones were found together, and how those clones were distributed. The fact that largely only one clone (sometimes two) was found at a given location is a little surprising given the potential for whiptails to disperse (these are highly active lizards that constantly travel over wide areas), and reinforces the notion that these species are highly geographically-structured (in particular *A. uniparens*). The study may have been better served by collecting only a couple specimens per site and extending the geographic extent of sampling as traditionally done in phylogenetic studies. Additional sampling should be conducted in these species to increase the sample size beyond that used here and reexamine the difference in environmental conditions occupied by each clone.

This study is also unable to further elucidate the hybridization events that led to the formation of these parthenogenic whiptail species. There are two reasons for this. First, no specimens of parental species were analyzed using AFLPs, partly because the parental species are located in Mexico (in the case of the *A. burti/costata* ancestor; Bell, 2003) and searches for *A. inornata* in New Mexico were unsuccessful. Second, the anonymous nature of AFLPs complicates phylogenetic analysis in a triploid asexual

species and is beyond the scope of this study. Phylogenies have been constructed using AFLP markers (*e.g.* Després *et al.*, 2003; Pellmyr *et al.*, 2007), but disentangling markers for related parental specimens would be complex given the sheer amount of genetic material in these hybrid lizards. While the hybridization relationship has been studied in *A. velox* (Bell, 2003), a similar examination is not available for *A. uniparens*. Future studies of this group of whiptail hybrids should include a phylogenetic study of *A. uniparens*.

Conclusion

This study examined the genetic or clonal structure of two closely related parthenogenic hybrid whiptail species, *A. uniparens* and *A. velox*, to test the predictions of two hypotheses regarding the environmental adaptation of a unisexual hybrid: the generalist genotype versus the frozen niche hypotheses. This examination represents a subset of studies necessary to evaluate the geographic distribution and persistence of parthenogenic organisms from the Comprehensive Research Framework identified in Chapter One. This research framework has been stressed as a comprehensive and streamlined approach for testing the underlying biological processes of previously posited hypotheses for parthenogenic organisms.

The results from this test study demonstrate that genetic patterns differ between closely related parthenogenic hybrid species. Despite the fact that they share the same sexual progenitors, the population structures differed between the two parthenogenic lizards: *Aspidoscelis uniparens* conforms to expectations of the frozen

niche hypothesis while *A. velox* conforms to expectations of the generalist genotype. These results demonstrate that evolutionary processes differed between these lizard species in their respective ranges, despite a shared origin. To further understand the context in which these patterns arose, the evolutionary history of both the parthenogenic hybrids and their sexual parent species need to be determined so that the genetic patterns inferred here can be interpreted based on their evolutionary histories. The patterns found here can serve as the foundation on which to design additional studies, such as refining the geographic genetic patterns, adding additional environmental sampling localities to increase the sample size, or starting genetic surveys on additional species of parthenogenic whiptails.

Because of the hybrid and triploid nature of these parthenogenic whiptails, AFLPs are an ideal marker for this type of study. We were able to successfully differentiate genetic clusters within these species using this genetic technique in combination with an automated peak calling software in RawGeno. AFLPs are advantageous in being able to generate a large amount of variable markers with little preliminary work and overhead cost. These markers are also highly repeatable, as indicated by the low error scores, and can be applied to future expansion of the current study or to additional whiptail species.

There is still a need for additional studies on parthenogenic organisms to investigate biological processes that were not addressed by this study. This includes population level genetic studies of the sexual parental species, and the potential role of competition between parthenogenic species and their sexual relatives. The

Comprehensive Research Framework provides the necessary road-map for designing these studies in an organized and comprehensive way, and future studies can use this framework for evaluating past studies and to design their own experiments to address biological processes in need of investigation.

Table 3.1. Sampling locations and abbreviations with geographic coordinates and location descriptions.

Abbr.	Name	Description	Lattitude	Longitude
Ar	Arivaca	3.66 mi NW of Arivaca	31.59810	-111.36815
Bl	Bloomfield	13.4mi SE of Bloomfield	36.54359	-107.86199
Br	Bridge	3.1mi ESE from Natural Bridges National Monument	37.59702	-109.92271
Bp	Bridgeport	4.32 mi S of Bridgeport	34.65916	-111.98496
Ch	Church	9mi SE of Church Rock	35.46676	-108.46759
Ci	Cinegas	Las Cinegas; 5 mi E of HW 83	31.76203	-110.61953
Cl	Clifton	13 mi N, 13.8 mi W of Clifton	33.09705	-109.53458
De	Deming	15mi NE of Deming	32.42871	-107.5913
Du	Duncan	3.5 mi S, 8.5 mi W of Duncan	32.77304	-109.25142
Es	Escalante	5.9mi ESE of Escalante	37.73607	-111.50279
Fl	Flagstaff	16.1 mi N, 6 mi E of Flagstaff	35.43245	-111.53940
Ga	Grants	12.5mi SSE of Grants	34.97037	-107.81017
Ge	Green	3.8 mi S, 11.5 mi E of Green Valley	31.79808	-110.80010
Ha	Hachita	10.59 mi SSW of Hachita	31.76972	-108.36761
Ja	Jacob	21.5 mi SSE of Jacob Lake	36.45152	-112.00338
Ka	Kanab	13.1mi NE of Kanab	37.16544	-112.35601
Ma	Magdalena	3.5mi NNE of Magdalena	34.16576	-107.22326
Mo	Monticello	5.1 mi NE of Monticello	33.44805	-107.38435
Na	Naturita	1.7mi SW of Naturita	38.19804	-108.58636
Pe	Pepper	5 mi S, 3 mi E of Oracle: Peppersauce campground	32.53736	-110.72133
Pi	Pilar	6mi NNW of Pilar	36.35283	-105.82237
Sf	SantaFe	2.5 mi W of Santa Fe Municiple Airport	35.61259	-106.13969
Sp	Springer	2.6 mi ENE of Springerville	34.15183	-109.21302
To	Tombstone	9.3 mi N, 3.7 mi E of Tombstone	31.85121	-110.00358
Tu	Tucson	8.8 mi N, 21 mi E Tucson	32.34807	-110.54076
Wl	Williams	9.8 mi N, 20 mi W of Williams	35.39376	-112.54567
Wn	Winslow	23 mi S of Winslow	34.68342	-110.72118
Ys	Ysidro	5.5 mi SW of San Ysidro	35.49235	-106.84924

Table 3.2. Selective AFLP primer pair combinations. Each pair used one EcoRI and MseI primer, and the selective three base terminal end of the primer is listed. Parameters and results from the RawGeno analysis include the number of peaks and error based on replicated samples. From RawGeno, the minimum and maximum width of a bin used for calling a peak, and the lbin score (defined as the average number of bins differing between a focal sample and other samples data set, divided by the total number of bins in the dataset) for each primer pair are listed. Highlighted primer pairs were problematic after visual examination of chromatographs and removed from the final dataset

Primer		Min bin width	Max bin width	lbin	# peaks	error
EcoRI	MseI					
AAC	CAA	1.0	2.0	0.222	78	0.0513
AAC	CAC	1.0	2.0	0.291	50	N/A
AAC	CAg	1.0	1.5	0.170	59	0.0508
AAC	CAT	1.0	2.0	0.190	55	0.0545
AAC	CTA	1.0	2.0	0.203	52	0.0673
AAC	CTC	1.5	2.0	0.211	56	0.0357
AAC	CTg	1.0	2.0	0.197	58	0.0776
AAC	CTT	1.0	1.5	0.228	54	0.0556
ACT	CAA	1.0	2.0	0.155	45	0.0444
ACT	CAC	1.5	2.0	0.143	105	0.0667
ACT	CAg	1.5	2.0	0.202	123	N/A
ACT	CAT	1.0	1.5	0.211	35	0.1143
ACT	CTA	1.0	2.0	0.157	54	0.1111
ACT	CTC	1.5	2.0	0.179	83	0.0783
ACT	CTg	1.5	2.0	0.152	78	0.0128
ACT	CTT	1.0	2.0	0.309	62	N/A
AgC	CAA	1.0	2.0	0.274	57	N/A
AgC	CAC	1.0	2.0	0.267	65	N/A
AgC	CAg	1.0	2.0	0.299	92	N/A
AgC	CAT	1.0	2.0	0.218	46	0.0652
AgC	CTA	1.0	2.0	0.292	82	N/A
AgC	CTC	1.0	1.5	0.256	74	N/A
AgC	CTg	1.0	1.5	0.238	78	0.0705
AgC	CTT	1.0	2.0	0.239	55	0.0364

Table 3.3. Principal Component Analysis PC scores, including the percent of variation in the environmental dataset explained by that score, with factor loading scores for each variable. Highest loading scores for each variable are highlighted by bold text. (A) PCA conducted on only *A. uniparens* and *A. velox*, (B) PCA conducted on all whiptail species. See text for further details

A	PC1	PC2	PC3	B	PC1	PC2	PC3	PC4
% variation explained:	54.933	24.087	8.786	% variation explained:	45.068	21.447	16.704	5.774
BIO1	0.901	0.333	0.218	BIO1	0.864	0.087	-0.467	-0.125
BIO2	0.317	0.393	-0.596	BIO2	-0.523	-0.638	0.026	0.306
BIO3	0.851	-0.067	-0.373	BIO3	0.570	-0.648	0.306	0.023
BIO4	-0.876	0.429	0.126	BIO4	-0.860	0.229	-0.280	0.164
BIO5	0.569	0.695	0.302	BIO5	0.351	0.069	-0.844	0.194
BIO6	0.938	0.037	0.310	BIO6	0.952	0.068	-0.220	-0.097
BIO7	-0.778	0.521	-0.163	BIO7	-0.906	-0.042	-0.172	0.207
BIO8	0.698	0.301	-0.016	BIO8	0.588	-0.109	-0.636	0.064
BIO9	0.743	0.110	0.335	BIO9	0.571	-0.240	-0.191	0.653
BIO10	0.714	0.575	0.337	BIO10	0.567	0.232	-0.766	-0.009
BIO11	0.970	0.128	0.158	BIO11	0.948	-0.034	-0.251	-0.111
BIO12	0.221	-0.912	0.209	BIO12	0.707	0.520	0.412	0.088
BIO13	0.756	-0.600	-0.157	BIO13	0.838	0.101	0.445	0.102
BIO14	-0.841	-0.383	-0.051	BIO14	0.000	0.937	0.057	-0.094
BIO15	0.871	0.042	-0.413	BIO15	0.544	-0.720	0.143	0.031
BIO16	0.730	-0.635	-0.188	BIO16	0.826	0.047	0.475	0.070
BIO17	-0.770	-0.527	0.175	BIO17	0.018	0.955	0.076	-0.025
BIO18	0.720	-0.614	-0.242	BIO18	0.745	0.003	0.492	0.098
BIO19	0.065	-0.720	0.530	BIO19	0.022	0.679	0.195	0.620

Table 3.4. Pairwise comparisons of environmental conditions occupied by AFLP clusters for *A. uniparens* based on the PCA using only *A. uniparens* and *A. velox*. Significant ($p < 0.1$) pairwise comparisons are indicated in bold. The first column are the parametric tests (ANOVA and Tukey HSD), while the second column are the non-parametric tests (Kruskal-Wallis test).

PC1: $F_{3,10} = 2.948$, $p = \mathbf{0.085}$

	A	B	C
B	1.000		
C	0.098	0.180	
D	0.621	0.674	0.991

PC1: $H = 5.73$, d.f. = 3, $p = 0.125$

	A	B	C
B	0.881		
C	0.047	0.072	
D	0.380	0.180	0.770

PC2: $F_{3,10} = 4.001$, $p = \mathbf{0.041}$

	A	B	C
B	0.777		
C	0.042	0.331	
D	0.220	0.538	0.994

PC2: $H = 7.516$, d.f. = 3, $p = \mathbf{0.047}$

	A	B	C
B	0.456		
C	0.016	0.134	
D	0.143	0.180	0.770

PC3: $F_{3,10} = 7.622$, $p = \mathbf{0.006}$

	A	B	C
B	0.387		
C	0.006	0.188	
D	0.986	0.540	0.063

PC3: $H = 10.211$, d.f. = 3, $p = \mathbf{0.017}$

	A	B	C
B	0.101		
C	0.009	0.036	
D	0.770	0.180	0.143

Table 3.5. Pairwise comparisons of environmental conditions occupied by AFLP clusters for *A. uniparens* based on the PCA using all whiptail species. Significant ($p < 0.1$) pairwise comparisons are indicated in bold. The first column are the parametric tests (ANOVA and Tukey HSD), while the second column are the non-parametric tests (Kruskal-Wallis test).

PC1: $F_{3,10} = 4.781$, $p = \mathbf{0.026}$

	A	B	C
B	0.966		
C	0.022	0.099	
D	0.603	0.801	0.855

PC1: $H = 6.29$, d.f. = 3, $p = \mathbf{0.098}$

	A	B	C
B	0.655		
C	0.028	0.072	
D	0.380	0.655	0.380

PC2: $F_{3,10} = 5.783$, $p = \mathbf{0.015}$

	A	B	C
B	0.250		
C	0.012	0.518	
D	1.000	0.584	0.159

PC2: $H = 10.368$, d.f. = 3, $p = \mathbf{0.016}$

	A	B	C
B	0.053		
C	0.009	0.720	
D	0.380	0.180	0.143

PC3: $F_{3,10} = 1.189$, $p = 0.363$

	A	B	C
B	1.000		
C	0.999	1.000	
D	0.315	0.380	0.354

PC3: $H = 2.785$, d.f. = 3, $p = 0.426$

	A	B	C
B	0.655		
C	0.754	0.764	
D	0.143	0.180	0.143

PC4: $F_{3,10} = 2.224$, $p = 0.148$

	A	B	C
B	0.962		
C	0.197	0.525	
D	0.903	0.782	0.275

PC4: $H = 4.572$, d.f. = 3, $p = 0.206$

	A	B	C
B	0.456		
C	0.175	0.368	
D	0.143	0.180	0.143

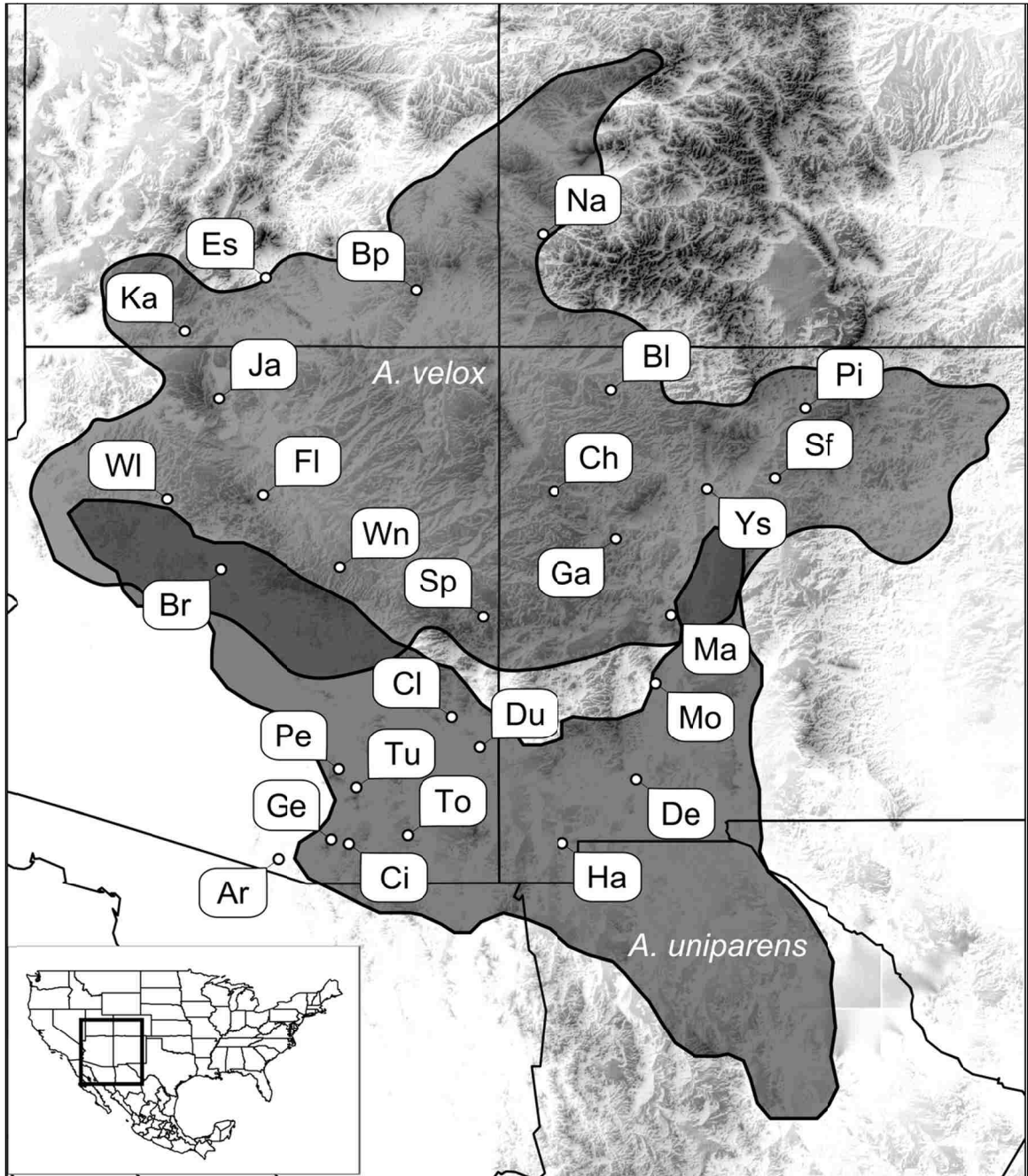


Figure 3.1. Sampling localities for all specimens used in this study across Arizona, New Mexico, Utah and Colorado. Species ranges are shown over a hill-shaded digital elevation model. The locations are Arivaca (Ar), Bloomfield (Bl), Natural Bridges National Monument (Br), Bridgeport (Bp), Church Rock (Ch), Las Cienegas (Ci), Clifton (Cl), Deming (De), Duncan (Du), Escalante (Es), Flagstaff (Fl), Grants (Ga), Green Valley (Ge), Hachita (Ha), Jacob Lake (Ja), Kanab (Ka), Magdalena (Ma), Monticello (Mo), Naturita (Na), Peppersauce campground (Pe), Pilar (Pi), Santa Fe (Sf), Springerville (Sp), Tombstone (To), Tucson (Tu), Williams (WI), Winslow (Wn), and San Ysidro (Ys).

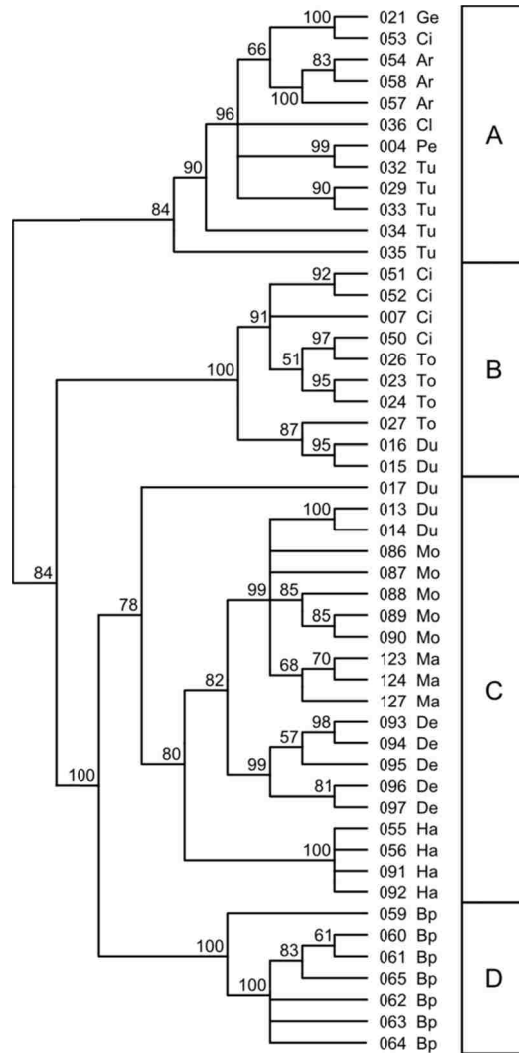


Figure 3.2. *Aspidoscelis uniparens* AFLP UPGMA clustering dendrogram. Bootstrap values are shown above the node of interest and nodes with < 50% support has been collapsed into a polytomy. Specimen number (last three digits) and location code are shown at the terminal ends of the dedrogram. STRUCTURE cluster assignments for each specimen are shown as boxes on the right hand side, including cluster name (A-D).

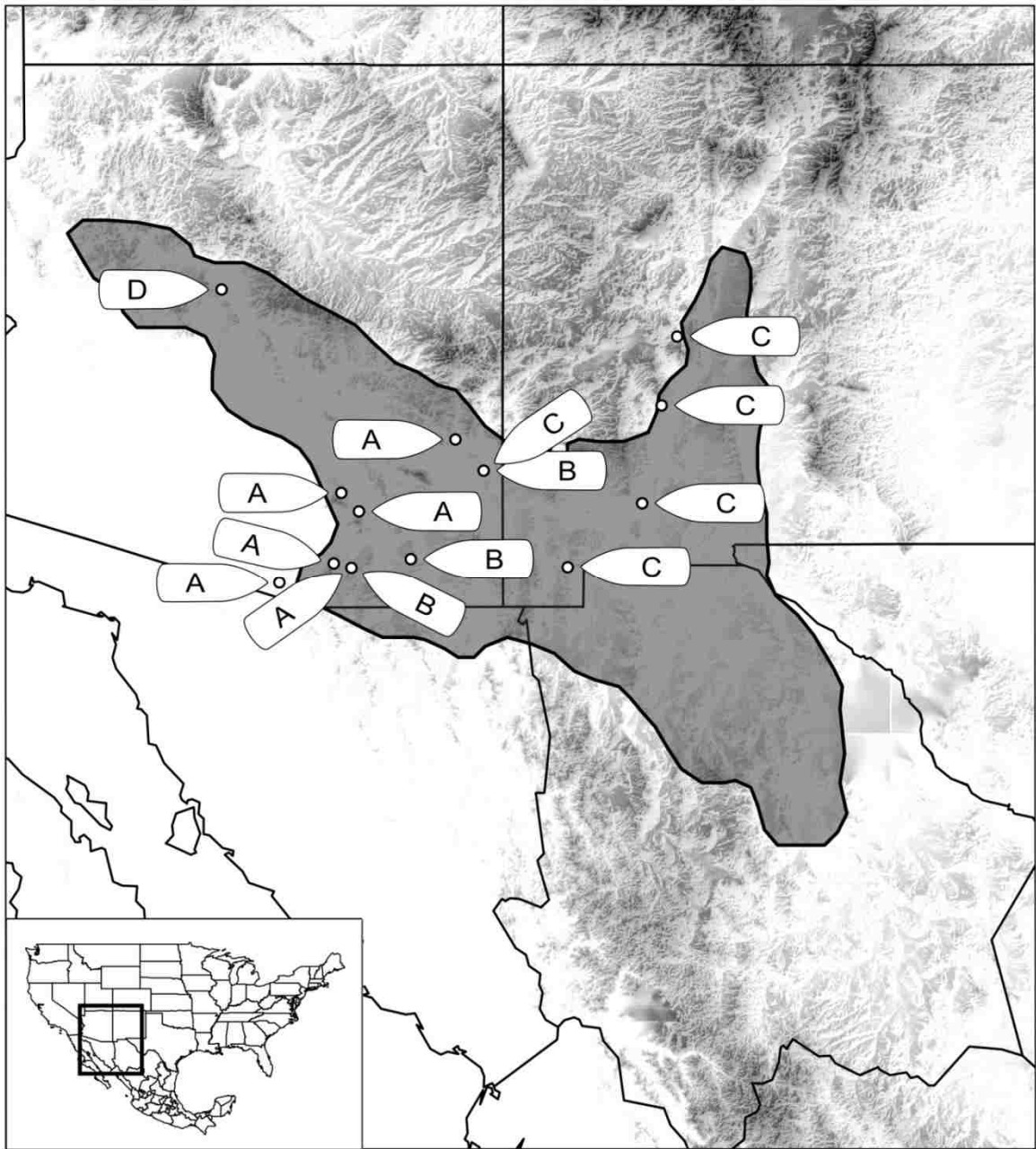


Figure 3.3. Geographic location of AFLP clusters (A-D) for *A. uniparens*. Species range based on Stebbins (2003) is shown as a dark colored polygon.

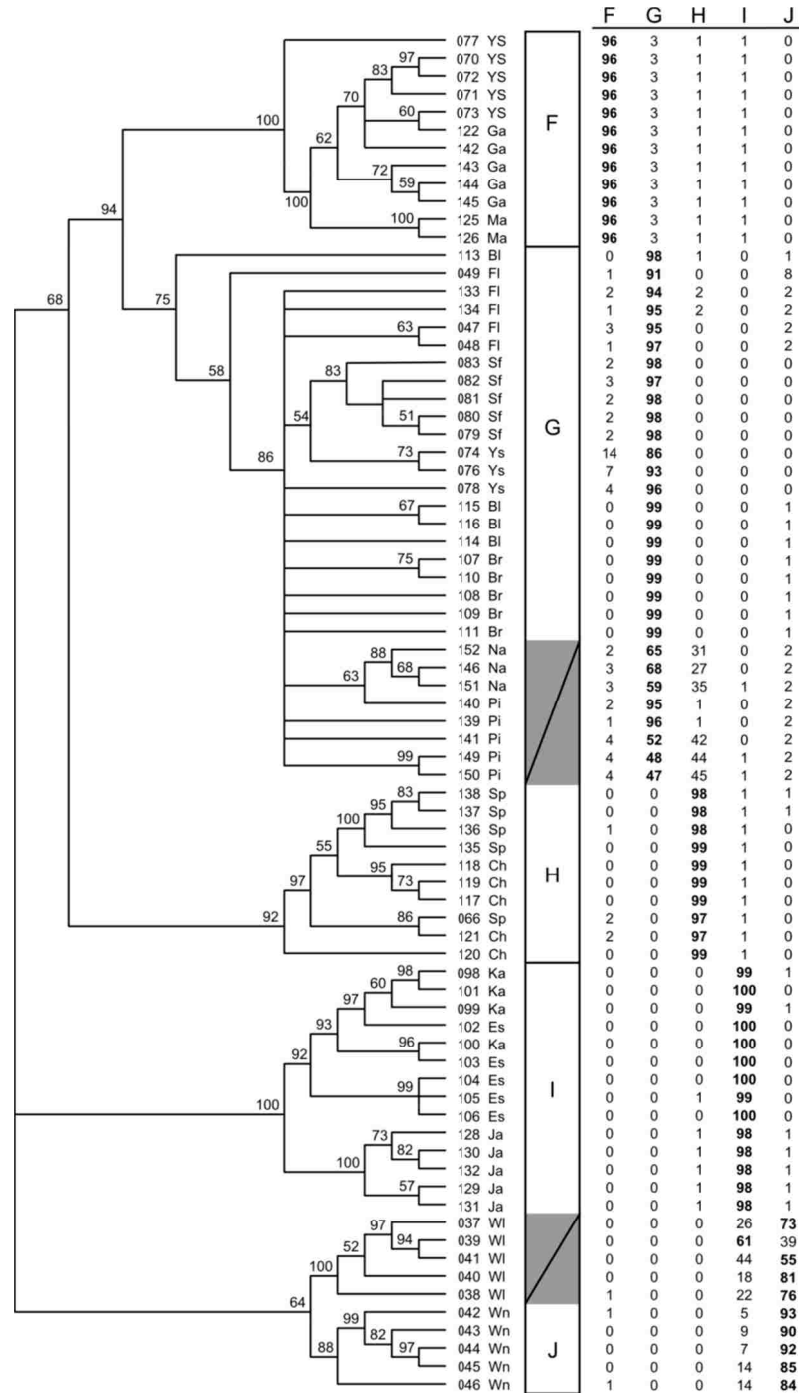


Figure 3.4. *Aspidoscelis velox* AFLP UPGMA clustering dendrogram. Bootstrap values are shown above the node of interest and nodes with < 50% support has been collapsed into a polytomy. Specimen number (last three digits) and location code are shown at the terminal ends of the dendrogram. STRUCTURE cluster assignments for each specimen are shown as boxes on the right hand side, including cluster name (F-G). Because there was some uncertainty regarding cluster assignment, the probability of a specimen's assignment to a particular STRUCTURE cluster is shown in the columns to the right, with the highest percentages shown in bold. Uncertain assignments are also highlighted by gray shading in the STRUCTURE assignment boxes.

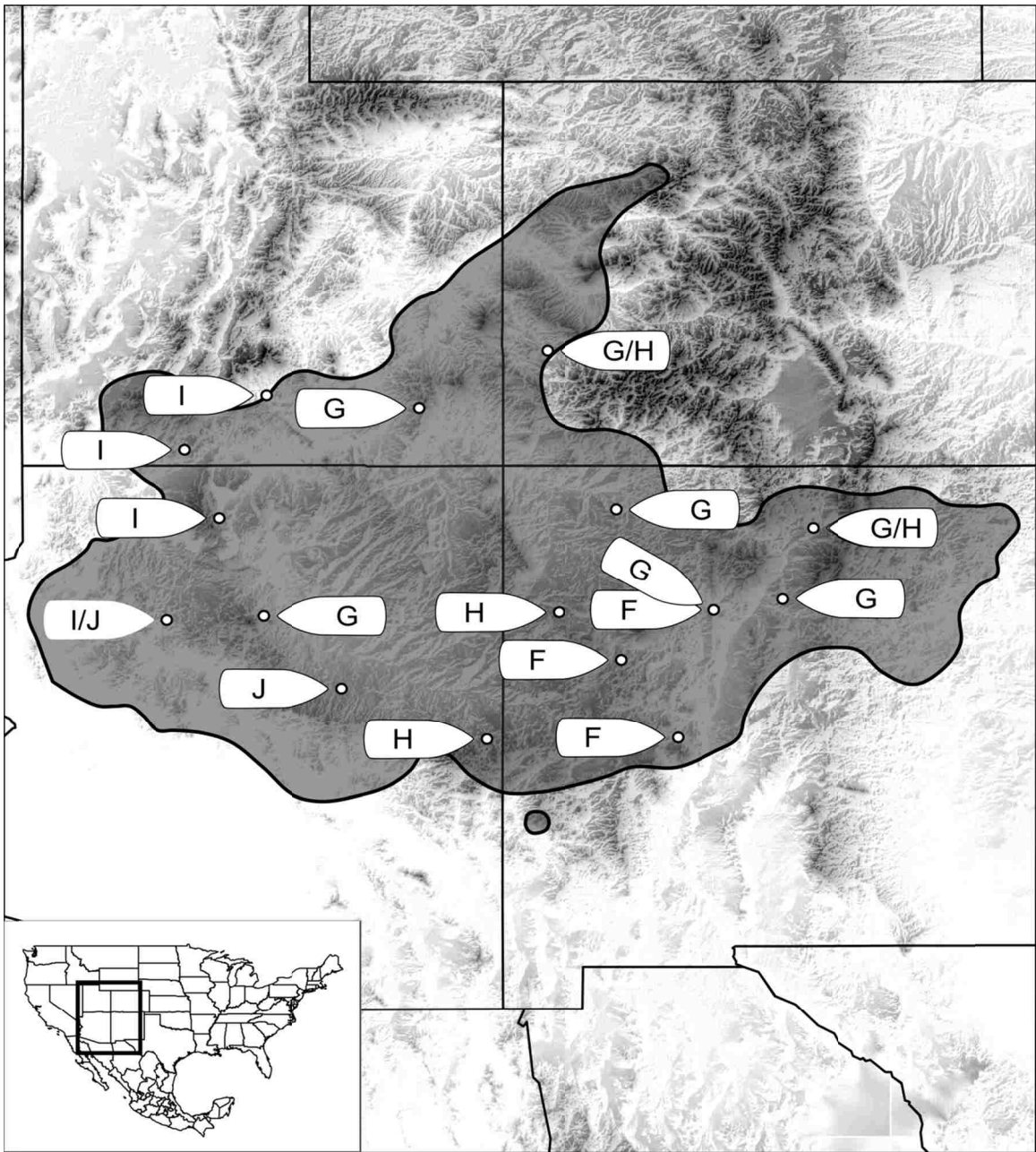


Figure 3.5. Geographic location of AFLP clusters for *A. velox*. Species range based on Stebbins (2003) is shown as a dark colored polygon. Uncertain cluster assignments are indicated by two cluster assignments separated by a “/,” while two separate clusters found at the same location are indicated by separate flags.

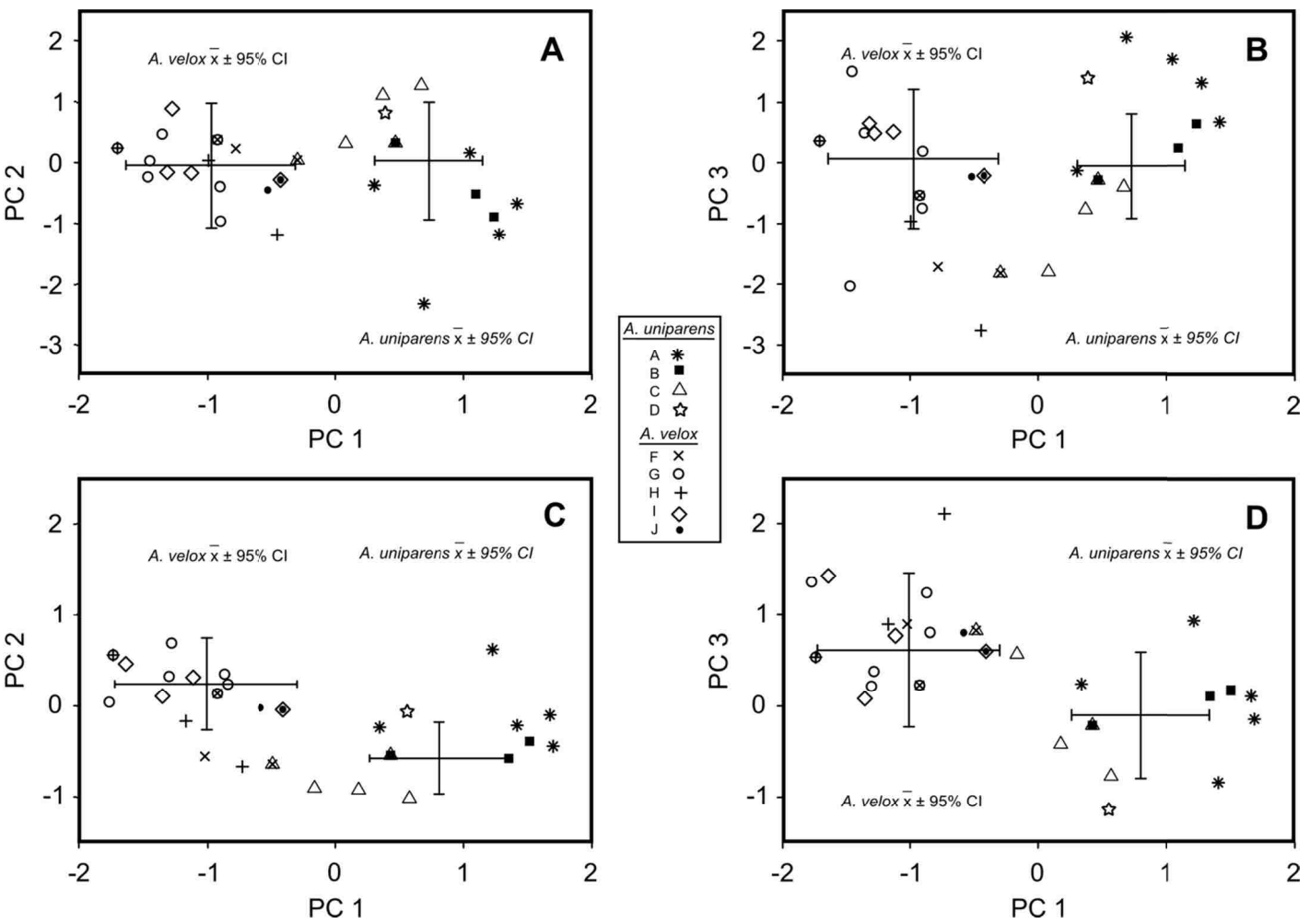


Figure 3.6. Principal Component scatter plots for AFLP clusters. The mean PC scores with 95% confidence intervals are shown for museum specimens for *A. uniparens* on the right and *A. velox* on the left. The locations where a particular AFLP cluster was found are shown by individual points, with each cluster indicated by a unique symbol. (A) PC1 and PC2 for the PCA using localities for *A. uniparens* and *A. velox* only. (B) PC1 and PC3 for the PCA using localities for *A. uniparens* and *A. velox* only. (C) PC1 and PC2 for the PCA using localities for all whiptails. (D) PC1 and PC3 for the PCA using localities for all whiptails.

APPENDIX A:

Specimen Records from Museum and Academic Collections down loaded from HerpNet (<http://www.herpnet.org/>, accessed 6 June, 2011). The species, museum abbreviation, collection number, country, state, county, and georeferenced latitude and longitude of specimens are listed. Written location data and other specimen information can be down loaded from HerpNet using the museum collection and specimen number, or contacting the author directly. Specimens are listed in order of species name, then museum abbreviation and finally specimen collection number.

Spp	Inst.	Specimen#	Country	State/Province	County	Latitude	Longitude
burti	CAS	2141	USA	Arizona	Pima	32.2596	-110.8732
burti	CAS	10107	USA	Arizona	Pima	32.3293	-110.7929
burti	CAS	189038	USA	Arizona	Santa Cruz	31.4422	-111.1798
burti	CM	19293	USA	Arizona	Pima	32.0765	-110.9258
burti	CM	25218	USA	Arizona	Santa Cruz	31.5292	-110.7676
burti	CM	53698	USA	Arizona	Cochise	31.9192	-109.9856
burti	KUNHM	6921	USA	Arizona	Pima	32.4322	-110.8872
burti	KUNHM	13108	USA	Arizona	Pima	32.3293	-110.7929
burti	KUNHM	48430	USA	Arizona	Santa Cruz	31.4429	-111.0538
burti	KUNHM	318097	USA	Arizona	Pima	32.3542	-110.9381
burti	KUNHM	318098	USA	Arizona	Pima	32.3383	-110.9042
burti	LACM	75844	USA	Arizona	Pima	32.0667	-112.7254
burti	LACM	112760	USA	New Mexico	Hidalgo	31.5179	-109.0145
burti	LACM	114743	USA	Arizona	Pinal	32.5903	-110.7946
burti	LACM	132297	USA	Arizona	Pima	32.3293	-110.7929
burti	LACM	132302	USA	Arizona	Pima	32.3196	-110.7805
burti	LACM	132304	USA	Arizona	Pima	32.3293	-110.7929
burti	LACM	132306	USA	Arizona	Santa Cruz	31.4422	-111.1798
burti	LACM	132307	USA	Arizona	Santa Cruz	31.4984	-110.8037
burti	LACM	134756	USA	Arizona	Pima	32.0667	-112.7254
burti	LACM	135444	USA	Arizona	Pima	32.3293	-110.7929
burti	LACM	141905	USA	Arizona	Pima	32.3293	-110.7929
burti	LACM	144361	USA	Arizona	Pima	32.3196	-110.7805
burti	LACM	144362	USA	Arizona	Pima	32.3293	-110.7929
burti	LACM	144363	USA	Arizona	Pima	32.3293	-110.7929
burti	LACM	144404	USA	Arizona	Pima	32.3293	-110.7929
burti	LACM	153255	USA	Arizona	Pima	32.3293	-110.7929
burti	LACM	153259	USA	Arizona	Pima	32.3293	-110.7929
burti	LSU	9818	USA	Arizona	Santa Cruz	31.3481	-111.1046
burti	LSU	28624	USA	Arizona	Pima	32.3542	-110.9381
burti	MVZ	49847	USA	Arizona	Santa Cruz	31.3886	-111.0917
burti	MVZ	57048	USA	Arizona	Pima	32.0667	-112.7254
burti	OMNH	6243	USA	Arizona	Cochise	32.3389	-110.2364
burti	OMNH	6247	USA	Arizona	Cochise	32.3902	-110.2971
burti	OMNH	6253	USA	Arizona	Cochise	32.3574	-110.2583
burti	SDNHM	4901	USA	Arizona	Cochise	31.7125	-110.3229
burti	SDNHM	15028	USA	Arizona	Pima	32.3293	-110.7929
burti	SDNHM	22942	USA	Arizona	Pinal	32.6108	-110.7703
burti	SDNHM	35261	USA	Arizona	Pima	32.3293	-110.7929
burti	SDNHM	62726	USA	Arizona	Santa Cruz	31.4422	-111.1798
burti	SDNHM	72377	USA	Arizona	Pima	32.3293	-110.7929
burti	TCWC	64529	USA	Arizona	Pima	32.0667	-112.7254
burti	UAZ	530	USA	Arizona	Pima	32.0667	-112.7254
burti	UAZ	5536	USA	Arizona	Pima	32.3293	-110.7929
burti	UAZ	5547	USA	Arizona	Pima	32.3347	-110.8313
burti	UAZ	5549	USA	Arizona	Pima	32.2972	-110.7144
burti	UAZ	5550	USA	Arizona	Graham	32.4274	-110.3188
burti	UAZ	5552	USA	Arizona	Pinal	32.5963	-110.7703
burti	UAZ	5553	USA	Arizona	Pima	32.3293	-110.7929
burti	UAZ	5557	USA	Arizona	Pinal	32.5903	-110.7946
burti	UAZ	5559	USA	Arizona	Pima	32.2773	-110.6335
burti	UAZ	5560	USA	Arizona	Pima	32.3293	-110.7929
burti	UAZ	5562	USA	Arizona	Pima	32.3293	-110.7929
burti	UAZ	5565	USA	Arizona	Pima	32.0667	-112.7254
burti	UAZ	5566	USA	Arizona	Pima	32.0667	-112.7254
burti	UAZ	5567	USA	Arizona	Pima	32.0667	-112.7254
burti	UAZ	5568	USA	Arizona	Pima	32.0667	-112.7254
burti	UAZ	5569	USA	Arizona	Pima	32.0667	-112.7254

Spp	Inst.	Specimen#	Country	State/Province	County	Latitude	Longitude
burti	UAZ	5573	USA	Arizona	Pima	31.9709	-112.8285
burti	UAZ	5574	USA	Arizona	Pima	32.0667	-112.7254
burti	UAZ	5575	USA	Arizona	Pima	32.0667	-112.7254
burti	UAZ	5576	USA	Arizona	Pima	32.0667	-112.7254
burti	UAZ	5580	USA	Arizona	Pima	32.0667	-112.7254
burti	UAZ	11118	USA	Arizona	Pinal	32.5408	-110.7089
burti	UAZ	11901	USA	Arizona	Pinal	32.5903	-110.7946
burti	UAZ	13824	USA	Arizona	Santa Cruz	31.3995	-111.1647
burti	UAZ	14118	USA	Arizona	Pima	32.3293	-110.7929
burti	UAZ	14951	USA	Arizona	Pima	32.3293	-110.7929
burti	UAZ	15548	USA	Arizona	Pima	32.3293	-110.7929
burti	UAZ	22092	USA	Arizona	Pima	32.3196	-110.7805
burti	UAZ	24755	USA	Arizona	Santa Cruz	31.4422	-111.1798
burti	UAZ	29300	USA	Arizona	Pinal	32.6108	-110.7703
burti	UAZ	29749	USA	Arizona	Pima	32.0667	-112.7254
burti	UCM	14626	USA	Arizona	Pinal	32.5800	-110.7337
burti	UCM	26989	USA	Arizona	Pima	32.3293	-110.7929
burti	YPM	808	USA	Arizona	Pima	32.3293	-110.7929
costata	ASU	6003	Mexico	Sonora		27.0166	-109.0475
costata	ASU	6433	Mexico	Sonora		27.1457	-109.0000
costata	ASU	6515	Mexico	Sonora		26.9005	-108.9333
costata	ASU	6517	Mexico	Sonora		27.0166	-109.0475
costata	ASU	6616	Mexico	Sonora		27.0457	-108.9333
costata	ASU	6618	Mexico	Sonora		27.0167	-108.9007
costata	ASU	6635	Mexico	Sonora		27.0166	-109.0475
costata	ASU	6661	Mexico	Sonora		27.0167	-108.9333
costata	CAS	100213	Mexico	Jalisco		19.9050	-104.3323
costata	CAS	104995	Mexico	Sinaloa		23.2167	-106.3850
costata	CAS	114281	Mexico	Nayarit		21.9676	-105.5423
costata	CAS	114288	Mexico	Nayarit		22.4672	-104.9744
costata	CAS	114290	Mexico	Nayarit		21.9824	-105.4584
costata	CAS	114317	Mexico	Nayarit		21.9736	-105.5003
costata	CAS	114329	Mexico	Nayarit		21.5401	-105.0731
costata	CAS	114377	Mexico	Nayarit		21.2298	-104.9293
costata	CM	38226	Mexico	Sinaloa		23.4083	-105.8973
costata	KUNHM	2735	Mexico	Michoacan		18.9624	-102.4030
costata	KUNHM	27278	Mexico	Jalisco		20.6171	-104.0630
costata	KUNHM	27280	Mexico	Jalisco		20.4181	-103.6798
costata	KUNHM	27283	Mexico	Jalisco		20.6512	-103.7536
costata	KUNHM	27730	Mexico	Nayarit		21.5343	-105.2816
costata	KUNHM	29278	Mexico	Jalisco		20.2804	-103.5296
costata	KUNHM	29290	Mexico	Michoacan		19.0833	-102.3962
costata	KUNHM	29298	Mexico	Michoacan		19.0833	-102.3654
costata	KUNHM	29304	Mexico	Jalisco		20.4972	-103.5812
costata	KUNHM	29736	Mexico	Sinaloa		23.2569	-106.3985
costata	LACM	6723	Mexico	Sinaloa		23.9417	-106.4280
costata	LACM	6734	Mexico	Sinaloa		22.8721	-105.8435
costata	LACM	6761	Mexico	Sinaloa		23.2676	-106.3219
costata	LACM	6762	Mexico	Sinaloa		22.5183	-105.7153
costata	LACM	14715	Mexico	Sonora		27.1193	-109.0486
costata	LACM	25841	Mexico	Jalisco		20.2300	-103.9700
costata	LACM	25843	Mexico	Jalisco		20.2100	-103.6300
costata	LACM	25857	Mexico	Sinaloa		23.3184	-106.4167
costata	LACM	25859	Mexico	Sinaloa		25.3297	-108.0769
costata	LACM	25861	Mexico	Sinaloa		25.9100	-109.0300
costata	LACM	162536	Mexico	Sinaloa		22.8721	-105.8435
costata	LSU	8434	Mexico	Sinaloa		24.3241	-107.3584
costata	LSU	36187	Mexico	Morelos		18.9667	-99.1472

Spp	Inst.	Specimen#	Country	State/Province	County	Latitude	Longitude
costata	LSU	36208	Mexico	Nayarit		22.4256	-105.6389
costata	LSU	36210	Mexico	Nayarit		21.1833	-104.5944
costata	LSU	38248	Mexico	Jalisco		19.5414	-103.4642
costata	LSU	38251	Mexico	Jalisco		19.5548	-103.4646
costata	LSU	72868	Mexico	Jalisco		20.8430	-103.3473
costata	LSU	72873	Mexico	Sinaloa		23.3450	-105.9742
costata	LSU	72875	Mexico	Sinaloa		23.3450	-105.9742
costata	LSU	72878	Mexico	Sinaloa		23.3450	-105.9742
costata	LSU	72879	Mexico	Sinaloa		23.2833	-106.2090
costata	MSU	4167	Mexico	Sinaloa		23.3319	-105.9893
costata	MSU	4366	Mexico	Sinaloa		23.2833	-106.0429
costata	MSU	4367	Mexico	Nayarit		21.6788	-105.1974
costata	MSU	6019	Mexico	Nayarit		21.2051	-105.0889
costata	MSU	7204	Mexico	Sinaloa		23.2552	-106.1427
costata	MSU	7205	Mexico	Nayarit		21.5412	-105.2221
costata	MSU	9208	Mexico	Sinaloa		23.3979	-105.9333
costata	MVZ	28922	Mexico	Sonora		27.0627	-109.0584
costata	MVZ	28924	Mexico	Sonora		26.9028	-108.6942
costata	MVZ	36598	Mexico	Morelos		18.7422	-99.2500
costata	MVZ	50714	Mexico	Sonora		26.9722	-109.0538
costata	MVZ	50716	Mexico	Sonora		27.1939	-109.5597
costata	MVZ	56300	Mexico	Jalisco		20.3190	-103.5336
costata	MVZ	57446	Mexico	Morelos		18.7277	-99.2500
costata	MVZ	59182	Mexico	Sinaloa		23.3475	-106.4167
costata	MVZ	59206	Mexico	Sinaloa		25.4612	-108.1914
costata	MVZ	71278	Mexico	Sonora		26.9345	-108.8411
costata	TCWC	4073	Mexico	Morelos		18.7500	-99.3333
costata	TCWC	4076	Mexico	Morelos		18.7500	-99.3333
costata	TCWC	4077	Mexico	Morelos		18.6164	-99.3193
costata	TCWC	6724	Mexico	Morelos		18.8830	-98.8623
costata	TCWC	6725	Mexico	Morelos		18.9454	-98.9500
costata	TCWC	6726	Mexico	Morelos		18.8167	-98.7500
costata	TCWC	6727	Mexico	Morelos		18.8833	-99.1589
costata	TCWC	6733	Mexico	Morelos		18.9833	-99.1000
costata	TCWC	6738	Mexico	Morelos		18.9276	-98.8151
costata	TCWC	6744	Mexico	Morelos		18.6440	-99.3196
costata	TCWC	6762	Mexico	Morelos		18.7114	-99.1072
costata	TCWC	6776	Mexico	Morelos		18.5766	-98.8475
costata	TCWC	6793	Mexico	Morelos		18.6653	-98.8000
costata	TCWC	7519	Mexico	Guerrero		18.3965	-99.6000
costata	UAZ	6233	Mexico	Morelos		18.6887	-99.2839
costata	UAZ	6248	Mexico	Morelos		18.7352	-99.2333
costata	UAZ	6257	Mexico	Morelos		18.5766	-98.8475
costata	UAZ	6258	Mexico	Morelos		18.6440	-99.3196
costata	UAZ	6263	Mexico	Sinaloa		25.1989	-107.8621
costata	UAZ	6264	Mexico	Sinaloa		25.1989	-107.8621
costata	UAZ	6266	Mexico	Sinaloa		25.1989	-107.8621
costata	UAZ	6267	Mexico	Sinaloa		25.1989	-107.8621
costata	UAZ	6274	Mexico	Nayarit		22.2078	-105.2661
costata	UAZ	6285	Mexico	Nayarit		21.1504	-104.4899
costata	UAZ	6294	Mexico	Nayarit		21.0333	-104.3266
costata	UAZ	6295	Mexico	Nayarit		21.9792	-105.4366
costata	UAZ	6304	Mexico	Jalisco		21.0274	-104.1364
costata	UAZ	6669	Mexico	Sonora		27.0838	-109.2357
costata	UAZ	6673	Mexico	Sonora		27.0714	-109.2828
costata	UAZ	6679	Mexico	Sonora		27.0936	-109.1676
costata	UAZ	6693	Mexico	Puebla		18.9667	-98.4667
costata	UAZ	6697	Mexico	Sonora		29.0500	-109.2333

Spp	Inst.	Specimen#	Country	State/Province	County	Latitude	Longitude
costata	UAZ	6704	Mexico	Sonora		28.9060	-109.9294
costata	UCM	12725	Mexico	Sinaloa		24.9566	-107.4313
costata	UCM	47374	Mexico	Sinaloa		22.6301	-105.6032
costata	UCM	48420	Mexico	Morelos		18.7500	-99.0000
costata	UCM	49529	Mexico	Guerrero		18.4225	-99.5331
exsanguis	CM	18209	USA	New Mexico	Hidalgo	31.5810	-108.7367
exsanguis	CM	18225	USA	New Mexico	Hidalgo	31.6450	-108.7553
exsanguis	CM	18231	USA	New Mexico	Hidalgo	31.4169	-108.9292
exsanguis	CM	43129	USA	New Mexico	Catron	33.2166	-108.8825
exsanguis	CM	43133	USA	New Mexico	Grant	33.1823	-108.8239
exsanguis	CM	48813	USA	New Mexico	Grant	33.1461	-108.8111
exsanguis	CM	48824	USA	New Mexico	Grant	33.1461	-108.8111
exsanguis	CM	54972	USA	New Mexico	Grant	32.5903	-107.9753
exsanguis	CM	58107	USA	Arizona	Greenlee	33.2105	-109.1916
exsanguis	CM	58115	USA	New Mexico	Catron	33.3794	-108.9028
exsanguis	CM	65683	USA	New Mexico	Lincoln	33.6786	-105.9210
exsanguis	CM	65684	USA	New Mexico	Santa Fe	35.4067	-106.1519
exsanguis	CM	67226	USA	New Mexico	Hidalgo	34.9247	-103.9706
exsanguis	CM	71053	USA	Arizona	Graham	32.8933	-109.4778
exsanguis	CM	75466	USA	New Mexico	Sierra	32.9208	-107.6217
exsanguis	CM	75468	USA	New Mexico	Sierra	32.9208	-107.6632
exsanguis	CM	75471	USA	New Mexico	Grant	32.8100	-107.8383
exsanguis	CM	75501	USA	New Mexico	Grant	32.8100	-108.0179
exsanguis	CM	107305	USA	New Mexico	Bernalillo	35.0844	-106.6506
exsanguis	CU	5527	USA	New Mexico	Bernalillo	35.0844	-106.6506
exsanguis	KUNHM	13007	USA	New Mexico	Bernalillo	35.0844	-106.6506
exsanguis	KUNHM	15419	USA	New Mexico	Eddy	32.4206	-104.2283
exsanguis	KUNHM	33761	Mexico	Chihuahua		31.1922	-106.5133
exsanguis	KUNHM	49575	USA	New Mexico	Grant	32.7700	-108.2797
exsanguis	KUNHM	49651	USA	New Mexico	Eddy	32.2017	-104.2525
exsanguis	KUNHM	50186	Mexico	Chihuahua		30.5734	-106.8355
exsanguis	KUNHM	50222	USA	New Mexico	Grant	32.6394	-108.2797
exsanguis	KUNHM	51881	Mexico	Chihuahua		29.5833	-104.4629
exsanguis	KUNHM	51888	Mexico	Chihuahua		28.7361	-107.9535
exsanguis	KUNHM	51889	Mexico	Chihuahua		28.7777	-108.0683
exsanguis	KUNHM	56205	Mexico	Chihuahua		27.9244	-106.7298
exsanguis	KUNHM	62891	USA	Texas	Culberson	31.9792	-104.7542
exsanguis	KUNHM	72233	USA	New Mexico	Guadalupe	35.1640	-105.0631
exsanguis	KUNHM	72253	USA	New Mexico	Eddy	32.6216	-104.3270
exsanguis	KUNHM	73291	USA	New Mexico	Otero	32.9508	-105.8696
exsanguis	KUNHM	73292	USA	New Mexico	Otero	33.0034	-105.9108
exsanguis	KUNHM	73293	USA	New Mexico	Dona Ana	32.2449	-106.8210
exsanguis	KUNHM	73294	USA	New Mexico	Dona Ana	35.4578	-105.1453
exsanguis	KUNHM	73299	USA	New Mexico	Chaves	33.1261	-104.3584
exsanguis	KUNHM	98370	USA	Arizona	Greenlee	33.1959	-109.2956
exsanguis	KUNHM	176630	USA	Texas	Brewser	30.3583	-103.6438
exsanguis	KUNHM	318103	USA	New Mexico	Hidalgo	31.9181	-108.3197
exsanguis	LACM	7687	USA	New Mexico	Lincoln	34.2916	-105.5525
exsanguis	LACM	7690	USA	New Mexico	Dona Ana	32.3122	-106.7778
exsanguis	LACM	7691	USA	New Mexico	Dona Ana	32.3122	-106.8293
exsanguis	LACM	7694	USA	New Mexico	Dona Ana	32.3993	-106.7778
exsanguis	LACM	7695	USA	New Mexico	Dona Ana	32.3122	-106.7263
exsanguis	LACM	7696	USA	New Mexico	Dona Ana	32.3658	-106.8041
exsanguis	LACM	7698	USA	New Mexico	Dona Ana	32.3121	-106.6061
exsanguis	LACM	14720	USA	New Mexico	Santa Fe	35.8758	-106.1419
exsanguis	LACM	14724	USA	New Mexico	Sierra	33.1791	-107.5636
exsanguis	LACM	14726	USA	New Mexico	Socorro	33.7736	-106.2708
exsanguis	LACM	28529	USA	New Mexico	Dona Ana	32.2531	-106.8350

Spp	Inst.	Specimen#	Country	State/Province	County	Latitude	Longitude
exsanguis	LACM	28774	USA	Texas	Jeff Davis	30.7242	-103.7845
exsanguis	LACM	66280	USA	Texas	El Paso	31.9203	-106.0381
exsanguis	LACM	66281	USA	Texas	Jeff Davis	30.8555	-103.9855
exsanguis	LACM	66284	USA	Texas	Jeff Davis	30.7772	-103.7439
exsanguis	LACM	99833	USA	Texas	Jeff Davis	30.5478	-103.9135
exsanguis	LACM	115679	USA	Texas	Jeff Davis	30.5333	-104.0628
exsanguis	LACM	115680	USA	Texas	Presidio	30.5871	-104.6985
exsanguis	LACM	121669	USA	Texas	Jeff Davis	30.6745	-104.2357
exsanguis	LACM	128287	USA	Arizona	Cochise	31.8646	-109.3953
exsanguis	LACM	131762	USA	Arizona	Cochise	31.8828	-109.1771
exsanguis	LACM	131772	USA	Arizona	Cochise	31.8686	-109.0129
exsanguis	LACM	131775	USA	Arizona	Cochise	31.9064	-109.1614
exsanguis	LACM	134306	USA	Texas	El Paso	31.7589	-106.3520
exsanguis	LACM	135893	Mexico	Chihuahua		29.8600	-107.4400
exsanguis	LACM	146349	USA	Texas	Jeff Davis	30.6339	-103.8558
exsanguis	LACM	147559	USA	Arizona	Cochise	31.8646	-109.3953
exsanguis	LACM	178617	USA	Arizona	Cochise	31.8520	-109.2134
exsanguis	LACM	178651	USA	Texas	El Paso	31.8969	-106.5997
exsanguis	LSU	9799	USA	New Mexico	Dona Ana	32.2531	-106.8350
exsanguis	LSU	9801	USA	New Mexico	Chaves	32.9429	-105.1610
exsanguis	LSU	10256	USA	Texas	Brewser	30.1104	-103.6247
exsanguis	LSU	23452	USA	Arizona	Cochise	31.9134	-109.3973
exsanguis	LSU	28627	USA	Texas	Hudspeth	31.2156	-105.4923
exsanguis	LSU	30683	USA	Texas	El Paso	31.7586	-106.4864
exsanguis	LSU	72955	USA	New Mexico	Lincoln	33.7237	-105.9753
exsanguis	LSU	72956	USA	Texas	Brewser	30.1802	-103.5841
exsanguis	LSU	72959	USA	Texas	Jeff Davis	31.0176	-104.2010
exsanguis	LSU	73102	USA	Texas	Brewser	30.1104	-103.6247
exsanguis	MCZ	78567	Mexico	Chihuahua		29.0667	-107.8500
exsanguis	MCZ	78568	Mexico	Chihuahua		29.0572	-107.8010
exsanguis	MCZ	114590	USA	New Mexico	Otero	32.8994	-105.9597
exsanguis	MPM	25714	USA	New Mexico	Eddy	32.2973	-104.3742
exsanguis	MVZ	7881	USA	Arizona	Cochise	31.9683	-109.3264
exsanguis	MVZ	7882	USA	Arizona	Cochise	31.9683	-109.3264
exsanguis	MVZ	7886	USA	Arizona	Cochise	31.9683	-109.3264
exsanguis	MVZ	24372	Mexico	Chihuahua		30.6167	-106.5504
exsanguis	MVZ	26960	USA	New Mexico	Quay	34.8606	-103.5630
exsanguis	MVZ	37006	USA	Texas	El Paso	31.9203	-105.9526
exsanguis	MVZ	46673	Mexico	Chihuahua		30.0163	-108.4340
exsanguis	MVZ	49858	USA	New Mexico	Otero	32.8994	-105.9597
exsanguis	MVZ	49859	USA	New Mexico	Chaves	33.3942	-104.5573
exsanguis	MVZ	55783	USA	New Mexico	Socorro	33.8599	-106.3719
exsanguis	MVZ	65903	Mexico	Chihuahua		30.5737	-106.7910
exsanguis	MVZ	66033	Mexico	Chihuahua		28.7059	-106.0833
exsanguis	MVZ	67084	USA	Arizona	Cochise	31.8825	-109.2161
exsanguis	MVZ	68785	Mexico	Chihuahua		30.7578	-107.4837
exsanguis	MVZ	68790	Mexico	Chihuahua		29.3226	-106.4500
exsanguis	MVZ	70883	Mexico	Chihuahua		29.2543	-107.0167
exsanguis	MVZ	70899	Mexico	Chihuahua		29.4667	-106.3167
exsanguis	MVZ	76755	USA	Arizona	Cochise	31.9347	-109.2183
exsanguis	MVZ	98807	USA	New Mexico	Hidalgo	31.9489	-108.8067
exsanguis	SDNHM	15767	USA	Arizona	Cochise	31.9347	-109.2183
exsanguis	SDNHM	24253	USA	New Mexico	Grant	32.8561	-107.9792
exsanguis	SDNHM	26000	USA	New Mexico	Grant	32.9074	-108.0402
exsanguis	SDNHM	26111	USA	New Mexico	Grant	32.9577	-107.9792
exsanguis	TCWC	645	USA	Texas	Jeff Davis	30.7772	-103.6594
exsanguis	TCWC	649	USA	Texas	Presidio	30.2485	-103.8172
exsanguis	TCWC	12959	USA	Texas	Jeff Davis	30.8555	-103.9855

Spp	Inst.	Specimen#	Country	State/Province	County	Latitude	Longitude
exsanguis	TCWC	14265	USA	Texas	Jeff Davis	30.6086	-103.9180
exsanguis	TCWC	18125	USA	Texas	Culberson	31.3432	-104.9029
exsanguis	TCWC	22648	USA	New Mexico	Dona Ana	32.2531	-106.8350
exsanguis	TCWC	25650	USA	Texas	Brewser	30.1263	-103.5795
exsanguis	TCWC	25658	USA	Texas	Brewser	30.1211	-103.5810
exsanguis	TCWC	25665	USA	Texas	Culberson	31.9792	-104.7542
exsanguis	TCWC	25670	USA	Texas	Culberson	31.9792	-104.7542
exsanguis	TCWC	25672	USA	Texas	Brewser	30.3415	-103.7189
exsanguis	TCWC	25673	USA	Texas	Brewser	30.3583	-103.6606
exsanguis	TCWC	27623	USA	Texas	Presidio	30.2307	-104.5782
exsanguis	TCWC	27624	USA	Texas	Presidio	30.2204	-104.5900
exsanguis	TCWC	35435	USA	Texas	Jeff Davis	30.8280	-103.7889
exsanguis	TCWC	37951	USA	New Mexico	Grant	33.1750	-108.2045
exsanguis	TCWC	42353	USA	Texas	Culberson	31.1638	-104.6853
exsanguis	TCWC	57906	USA	New Mexico	Chaves	32.8584	-104.9340
exsanguis	TCWC	61976	USA	New Mexico	Hidalgo	31.5621	-108.9292
exsanguis	TCWC	62827	USA	Texas	Presidio	30.5981	-104.0186
exsanguis	TCWC	63602	USA	Arizona	Cochise	31.8471	-109.1993
exsanguis	TCWC	63603	USA	Texas	El Paso	31.9203	-106.0381
exsanguis	TCWC	63605	USA	New Mexico	Catron	33.2722	-108.8722
exsanguis	TCWC	64374	USA	Texas	El Paso	31.7586	-106.4864
exsanguis	TCWC	64521	USA	Texas	El Paso	31.8952	-106.5152
exsanguis	TCWC	72775	USA	Texas	Brewser	30.0388	-103.5723
exsanguis	TCWC	76348	USA	Texas	Reeves	30.9544	-103.7769
exsanguis	TCWC	76349	USA	Texas	Brewser	30.5180	-103.6606
exsanguis	TCWC	79089	USA	Texas	Brewser	30.1480	-103.7108
exsanguis	TCWC	83974	USA	New Mexico	Harding	36.0321	-104.3750
exsanguis	UAZ	4772	USA	Arizona	Greenlee	33.4697	-109.4835
exsanguis	UAZ	4773	USA	Arizona	Greenlee	33.4490	-109.4931
exsanguis	UAZ	4774	USA	Arizona	Greenlee	33.4490	-109.4931
exsanguis	UAZ	4776	USA	Arizona	Greenlee	33.4697	-109.4835
exsanguis	UAZ	4777	USA	Arizona	Greenlee	33.5120	-109.4826
exsanguis	UAZ	4778	USA	Arizona	Greenlee	33.4490	-109.4931
exsanguis	UAZ	4779	USA	Arizona	Greenlee	33.4490	-109.4931
exsanguis	UAZ	4782	USA	Arizona	Greenlee	33.3732	-109.4846
exsanguis	UAZ	4785	USA	Arizona	Greenlee	33.3732	-109.4846
exsanguis	UAZ	4895	USA	Arizona	Cochise	31.9136	-109.1408
exsanguis	UAZ	4896	USA	Arizona	Cochise	31.9136	-109.1408
exsanguis	UAZ	4901	USA	Arizona	Cochise	31.9683	-109.3264
exsanguis	UAZ	4907	USA	Arizona	Cochise	31.9683	-109.3264
exsanguis	UAZ	4909	USA	Arizona	Cochise	31.9683	-109.3264
exsanguis	UAZ	4912	USA	Arizona	Cochise	31.9683	-109.3264
exsanguis	UAZ	4913	USA	Arizona	Cochise	31.7589	-109.3450
exsanguis	UAZ	4914	USA	Arizona	Cochise	31.7589	-109.3450
exsanguis	UAZ	5075	USA	New Mexico	Dona Ana	32.4333	-106.5556
exsanguis	UAZ	5076	USA	New Mexico	Socorro	33.9688	-107.4218
exsanguis	UAZ	5085	USA	New Mexico	Grant	32.9935	-108.5431
exsanguis	UAZ	5086	USA	New Mexico	Socorro	33.9318	-107.1517
exsanguis	UAZ	10493	USA	Arizona	Greenlee	33.0450	-109.1115
exsanguis	UAZ	10500	USA	New Mexico	Sandoval	35.3069	-106.4153
exsanguis	UAZ	13597	USA	New Mexico	Lincoln	33.3875	-105.2442
exsanguis	UAZ	13598	Mexico	Chihuahua		28.3000	-105.4833
exsanguis	UAZ	13599	USA	New Mexico	Lincoln	33.3875	-105.2442
exsanguis	UAZ	13604	Mexico	Chihuahua		30.1693	-108.0667
exsanguis	UAZ	13626	Mexico	Chihuahua		30.1693	-108.0667
exsanguis	UAZ	14241	Mexico	Chihuahua		28.4552	-105.7389
exsanguis	UAZ	14242	Mexico	Chihuahua		28.4552	-105.7389
exsanguis	UAZ	15331	USA	New Mexico	Grant	32.9040	-108.2208

Spp	Inst.	Specimen#	Country	State/Province	County	Latitude	Longitude
exsanguis	UAZ	16188	USA	New Mexico	Socorro	33.9319	-106.9489
exsanguis	UAZ	16614	USA	Texas	Brewser	30.2862	-103.5938
exsanguis	UAZ	17921	USA	Texas	Brewser	30.3583	-103.6606
exsanguis	UAZ	17932	USA	Texas	Jeff Davis	30.6714	-104.0042
exsanguis	UAZ	25705	USA	Arizona	Cochise	31.8646	-109.3953
exsanguis	UAZ	30869	USA	Texas	Hudspeth	31.2078	-105.4677
exsanguis	UAZ	30885	Mexico	Chihuahua		30.0652	-108.4966
exsanguis	UAZ	30892	USA	Texas	Jeff Davis	30.5881	-103.8942
exsanguis	UAZ	30896	Mexico	Chihuahua		30.0457	-108.5191
exsanguis	UAZ	30902	USA	Texas	Jeff Davis	30.5881	-103.8942
exsanguis	UAZ	30972	USA	New Mexico	Eddy	32.8422	-104.4028
exsanguis	UAZ	30985	USA	New Mexico	Sandoval	35.2353	-106.5889
exsanguis	UAZ	31003	USA	New Mexico	Eddy	32.8103	-104.7840
exsanguis	UAZ	31012	USA	New Mexico	Catron	33.3747	-108.8825
exsanguis	UAZ	31013	USA	New Mexico	Socorro	33.7736	-106.3336
exsanguis	UAZ	31014	USA	New Mexico	Socorro	33.7438	-106.3719
exsanguis	UAZ	31015	USA	New Mexico	Otero	33.3192	-105.9199
exsanguis	UAZ	34072	Mexico	Chihuahua		29.0667	-107.8500
exsanguis	UAZ	34944	Mexico	Chihuahua		29.5566	-107.7474
exsanguis	UAZ	43721	USA	Texas	Hudspeth	31.2156	-105.4923
exsanguis	UCM	6085	USA	Texas	El Paso	31.9203	-106.0381
exsanguis	UCM	6103	USA	New Mexico	Grant	32.7719	-108.1169
exsanguis	UCM	6791	USA	New Mexico	Harding	35.9438	-104.3747
exsanguis	UCM	10023	USA	New Mexico	Lincoln	33.5453	-105.5717
exsanguis	UCM	11983	USA	Arizona	Cochise	31.9644	-109.1408
exsanguis	UCM	11984	USA	Arizona	Cochise	31.9347	-109.2183
exsanguis	UCM	23296	USA	Arizona	Cochise	31.6657	-109.4292
exsanguis	UCM	24814	USA	New Mexico	Socorro	33.6794	-106.3431
exsanguis	UCM	24876	USA	New Mexico	Socorro	33.9317	-107.2112
exsanguis	UCM	24878	USA	New Mexico	Socorro	33.9317	-107.2112
exsanguis	UCM	29196	USA	New Mexico	Dona Ana	32.2531	-106.8350
exsanguis	UCM	29445	USA	New Mexico	Santa Fe	35.9090	-106.1814
exsanguis	UCM	29471	USA	New Mexico	Santa Fe	35.9090	-106.1814
exsanguis	UCM	29472	USA	New Mexico	Sandoval	35.7883	-106.3022
exsanguis	UCM	29670	USA	New Mexico	Torrence	34.6569	-106.3569
exsanguis	UCM	30097	USA	New Mexico	Eddy	32.2239	-104.0891
exsanguis	UCM	30146	USA	New Mexico	Socorro	33.6794	-106.3431
exsanguis	UCM	36274	USA	New Mexico	Sandoval	35.6216	-106.3375
exsanguis	UCM	37439	Mexico	Chihuahua		28.2614	-105.4807
exsanguis	UCM	37442	Mexico	Chihuahua		28.0155	-105.2915
exsanguis	UCM	40890	USA	Arizona	Cochise	32.1514	-109.4527
exsanguis	UCM	45911	USA	New Mexico	Hidalgo	31.9489	-108.8067
exsanguis	UCM	61725	USA	New Mexico	Catron	33.3167	-108.8825
exsanguis	UCM	61728	USA	New Mexico	Santa Fe	35.9090	-106.1814
exsanguis	UCM	61731	USA	New Mexico	Sandoval	35.7883	-106.3022
exsanguis	UCM	61857	USA	New Mexico	Torrence	34.6569	-106.3569
exsanguis	UCM	61860	USA	New Mexico	Sandoval	35.3000	-106.5683
exsanguis	UTEP	302	USA	New Mexico	Eddy	32.3627	-104.4858
exsanguis	UTEP	1534	USA	New Mexico	Eddy	32.3773	-104.4858
exsanguis	UTEP	1537	USA	New Mexico	Eddy	32.3627	-104.4174
exsanguis	UTEP	1538	USA	New Mexico	Eddy	32.3627	-104.4002
exsanguis	UTEP	1539	USA	New Mexico	Eddy	32.3627	-104.4002
exsanguis	UTEP	1540	USA	New Mexico	Eddy	32.3627	-104.4002
exsanguis	UTEP	1897	USA	Texas	Hudspeth	30.9375	-105.0500
exsanguis	UTEP	1905	USA	Texas	Hudspeth	30.9083	-105.0500
exsanguis	UTEP	1948	USA	New Mexico	Grant	32.7271	-108.5008
exsanguis	UTEP	2798	USA	Texas	El Paso	31.8972	-106.1500
exsanguis	UTEP	4400	USA	New Mexico	Otero	32.5681	-105.7377

Spp	Inst.	Specimen#	Country	State/Province	County	Latitude	Longitude
exsanguis	UTEP	5668	USA	New Mexico	Luna	32.5249	-107.6876
exsanguis	UTEP	9977	USA	New Mexico	Luna	32.1163	-107.6401
exsanguis	UTEP	10619	USA	New Mexico	Hidalgo	31.4805	-108.4385
exsanguis	UTEP	10664	USA	New Mexico	Sierra	32.9026	-107.2551
exsanguis	UTEP	10809	USA	New Mexico	Hidalgo	31.4342	-108.9798
exsanguis	UTEP	10817	USA	New Mexico	Hidalgo	31.4633	-108.9970
exsanguis	UTEP	10837	USA	New Mexico	Hidalgo	31.5215	-109.0142
exsanguis	UTEP	11497	USA	New Mexico	Grant	32.5529	-108.4837
exsanguis	UTEP	11518	USA	New Mexico	Otero	32.0006	-105.5600
exsanguis	UTEP	11935	USA	New Mexico	Dona Ana	32.2347	-106.5730
exsanguis	YPM	838	USA	Arizona	Cochise	31.9136	-109.1408
exsanguis	YPM	2833	USA	Texas	Jeff Davis	30.6026	-103.8942
flagellicauda	CAS	35107	USA	Arizona	Cochise	31.9347	-109.2183
flagellicauda	CAS	204046	USA	Arizona	Greenlee	33.0247	-109.1400
flagellicauda	CM	43128	USA	New Mexico	Catron	33.2166	-108.8825
flagellicauda	CM	43134	USA	New Mexico	Grant	33.1823	-108.8239
flagellicauda	CM	48706	USA	Arizona	Graham	32.7043	-109.7852
flagellicauda	CM	48819	USA	New Mexico	Grant	33.1461	-108.8111
flagellicauda	CM	48822	USA	New Mexico	Grant	33.1461	-108.8111
flagellicauda	CM	65686	USA	Arizona	Coconino	34.8842	-111.7603
flagellicauda	CM	65688	USA	Arizona	Yavapai	34.6776	-112.0841
flagellicauda	CM	71185	USA	Arizona	Greenlee	33.2983	-109.4183
flagellicauda	CM	90151	USA	Arizona	Yavapai	34.6856	-111.9821
flagellicauda	CU	10048	USA	Arizona	Yavapai	34.6776	-112.0841
flagellicauda	KUNHM	6509	USA	New Mexico	Catron	33.3892	-108.8825
flagellicauda	KUNHM	6819	USA	Arizona	Pima	32.3293	-110.7929
flagellicauda	KUNHM	6920	USA	Arizona	Pima	32.4322	-110.8872
flagellicauda	KUNHM	49560	USA	Arizona	Cochise	31.8969	-109.0934
flagellicauda	LACM	112397	USA	Arizona	Graham	32.9572	-110.3544
flagellicauda	LACM	114802	USA	Arizona	Pinal	32.5903	-110.7946
flagellicauda	LACM	130657	USA	Arizona	Yavapai	34.8958	-112.4800
flagellicauda	LACM	131758	USA	Arizona	Cochise	31.8471	-109.1993
flagellicauda	LACM	153315	USA	Arizona	Greenlee	33.6036	-109.1138
flagellicauda	LSU	29670	USA	Arizona	Yavapai	34.7711	-112.0572
flagellicauda	LSU	29671	USA	Arizona	Gila	34.3627	-111.4544
flagellicauda	LSU	29680	USA	Arizona	Yavapai	34.9278	-112.0092
flagellicauda	LSU	29681	USA	Arizona	Yavapai	34.3619	-112.0481
flagellicauda	LSU	29683	USA	Arizona	Yavapai	34.6776	-112.0841
flagellicauda	LSU	30863	USA	Arizona	Yavapai	34.9278	-112.0092
flagellicauda	LSU	31181	USA	Arizona	Yavapai	34.3619	-112.0481
flagellicauda	LSU	31189	USA	Arizona	Yavapai	34.2657	-112.1007
flagellicauda	LSU	36820	USA	Arizona	Gila	34.3569	-111.4544
flagellicauda	MVZ	204274	USA	Arizona	Pima	32.3542	-110.9381
flagellicauda	TCWC	63570	USA	New Mexico	Catron	33.2577	-108.8722
flagellicauda	UAZ	4775	USA	Arizona	Greenlee	33.4972	-109.4714
flagellicauda	UAZ	4786	USA	Arizona	Greenlee	33.3732	-109.4846
flagellicauda	UAZ	4790	USA	Arizona	Yavapai	34.8364	-111.7863
flagellicauda	UAZ	4794	USA	Arizona	Pinal	32.5903	-110.7946
flagellicauda	UAZ	4802	USA	Arizona	Pinal	32.5963	-110.7703
flagellicauda	UAZ	4878	USA	Arizona	Graham	32.6514	-109.8039
flagellicauda	UAZ	5064	USA	Arizona	Graham	32.6514	-109.8039
flagellicauda	UAZ	9270	USA	Arizona	Greenlee	33.0468	-109.4360
flagellicauda	UAZ	10504	USA	Arizona	Greenlee	33.0534	-109.0842
flagellicauda	UAZ	10789	USA	Arizona	Yavapai	34.2072	-112.7467
flagellicauda	UAZ	10800	USA	Arizona	Mohave	35.2423	-113.6059
flagellicauda	UAZ	11061	USA	Arizona	Graham	32.5957	-109.8962
flagellicauda	UAZ	13745	USA	Arizona	Pima	32.3356	-110.6958
flagellicauda	UAZ	14410	USA	Arizona	Pima	32.3356	-110.6958

Spp	Inst.	Specimen#	Country	State/Province	County	Latitude	Longitude
flagellicauda	UAZ	15248	USA	Arizona	Graham	32.6514	-109.8039
flagellicauda	UAZ	18574	USA	Arizona	Pima	32.3293	-110.7929
flagellicauda	UAZ	18750	USA	Arizona	Yavapai	34.7579	-112.5741
flagellicauda	UAZ	29636	USA	Arizona	Pima	32.3293	-110.7929
flagellicauda	UAZ	36798	USA	Arizona	Maricopa	33.9651	-111.8685
flagellicauda	UAZ	37093	USA	Arizona	Maricopa	33.9651	-111.8685
flagellicauda	UAZ	37515	USA	Arizona	Yavapai	34.2552	-112.2987
flagellicauda	UAZ	37520	USA	Arizona	Gila	33.7370	-111.3301
flagellicauda	UAZ	43163	USA	Arizona	Maricopa	33.6449	-111.1710
flagellicauda	UAZ	43714	USA	Arizona	Maricopa	33.6449	-111.1541
flagellicauda	UAZ	43718	USA	Arizona	Yavapai	34.7392	-111.7603
flagellicauda	UAZ	43719	USA	Arizona	Yavapai	34.4784	-112.3931
flagellicauda	UAZ	43720	USA	Arizona	Graham	32.9284	-109.5536
flagellicauda	UAZ	46546	USA	Arizona	Graham	33.5254	-109.7129
flagellicauda	UAZ	48794	USA	Arizona	Greenlee	33.0468	-109.4360
flagellicauda	UAZ	51757	USA	Arizona	Pinal	32.5483	-110.9917
flagellicauda	UAZ	52004	USA	Arizona	Pima	32.3356	-110.6958
flagellicauda	UAZ	52751	USA	Arizona	Greenle	33.2152	-109.1955
flagellicauda	UAZ	52752	USA	New Mexico	Grant	32.7706	-108.6209
flagellicauda	UAZ	52767	USA	Arizona	Pinal	32.8240	-110.4916
flagellicauda	UAZ	52769	USA	Arizona	Graham	32.4374	-110.3261
flagellicauda	UAZ	54480	USA	Arizona	Pima	32.1304	-110.6101
flagellicauda	UAZ	54879	USA	Arizona	Gila	33.6973	-110.8308
flagellicauda	UAZ	55536	USA	Arizona	Graham	32.9492	-110.3878
flagellicauda	UAZ	56467	USA	Arizona	Pinal	32.6108	-110.7703
flagellicauda	UCM	23297	USA	New Mexico	Catron	33.3269	-108.8702
flagellicauda	UCM	61782	USA	New Mexico	Catron	33.2287	-108.8722
gularis	CM	12988	USA	Texas	Williamson	30.6325	-97.6769
gularis	CM	22837	USA	Texas	Bexar	29.4479	-98.4501
gularis	CM	25854	USA	Texas	Travis	30.2669	-97.7428
gularis	CM	25855	USA	Texas	Travis	30.2669	-97.7428
gularis	CM	39581	USA	Texas	Bexar	29.6305	-98.6136
gularis	CM	43136	USA	Oklahoma	Greer	34.9006	-99.7307
gularis	CM	43147	Mexico	Coahuila		27.0336	-101.7167
gularis	CM	43148	Mexico	Coahuila		27.0359	-101.7052
gularis	CM	43159	Mexico	Coahuila		27.0336	-101.7167
gularis	CM	43169	Mexico	Coahuila		27.0031	-101.8410
gularis	CM	48364	Mexico	Coahuila		26.8798	-102.1620
gularis	CM	59444	Mexico	Coahuila		28.6833	-102.8666
gularis	CM	61889	USA	Texas	Young	33.1911	-98.6475
gularis	CM	65691	USA	Texas	Kenedy	26.6706	-97.7758
gularis	CM	65692	USA	Texas	Jim Hogg	27.1314	-98.7803
gularis	CM	65693	USA	Texas	Hidalgo	26.3231	-98.3250
gularis	CM	73300	USA	TEXAS	HAYS	29.9972	-98.0983
gularis	CM	75388	USA	Texas	Maverick	28.8221	-100.5214
gularis	CM	75397	USA	Texas	Terrell	30.0443	-101.9532
gularis	CM	P1018	USA	Texas	McLennan	31.5492	-97.1464
gularis	CM	P1020	USA	Texas	McLennan	31.5492	-97.1464
gularis	CM	P244	USA	Texas	Cameron	25.9014	-97.4972
gularis	CM	P249	USA	Texas	Cameron	25.9014	-97.4972
gularis	CM	P63	USA	Texas	Hidalgo	26.1494	-97.9133
gularis	CM	P75	USA	Texas	Matagorda	28.9825	-95.9692
gularis	CM	P87	USA	Texas	Cameron	26.0783	-97.8492
gularis	CM	P95	USA	Texas	Bosque	31.7822	-97.5764
gularis	CM	S8113	Mexico	Nueva Leon		25.5001	-99.4968
gularis	CM	S9779	Mexico	Coahuila		25.4413	-100.7748
gularis	CU	547	USA	Texas	Cameron	25.9014	-97.4972
gularis	CU	585	USA	Texas	Bexar	29.4933	-98.6961

Spp	Inst.	Specimen#	Country	State/Province	County	Latitude	Longitude
gularis	CU	621	USA	Texas	Cameron	25.9014	-97.4972
gularis	CU	1545	USA	Texas	Burnet	30.7581	-98.2281
gularis	CU	1595	USA	Texas	Hidalgo	26.3014	-98.1631
gularis	CU	8109	USA	Texas	Crockett	30.7100	-101.2003
gularis	CU	8110	USA	Texas	Wilson	29.2731	-98.0564
gularis	CU	8112	USA	Texas	Jeff Davis	30.5985	-103.9267
gularis	CU	8181	USA	Texas	Comal	29.7113	-98.1308
gularis	CU	8247	USA	Texas	Karnes	29.1281	-97.7847
gularis	CU	8534	USA	Texas	Comal	29.7028	-98.1242
gularis	CU	12712	USA	Oklahoma	Greer	34.8249	-99.7317
gularis	CU	12717	USA	Texas	Taylor	32.2353	-99.8797
gularis	CU	13280	USA	Texas	Brazos	30.6278	-96.3342
gularis	KUNHM	585	USA	Texas	Eastland	32.3881	-98.9789
gularis	KUNHM	616	USA	Texas	Burnet	30.7581	-98.2281
gularis	KUNHM	6928	USA	Texas	McLennan	31.5491	-97.0442
gularis	KUNHM	6931	USA	Texas	Travis	30.2669	-97.7428
gularis	KUNHM	6933	USA	Texas	Travis	30.2669	-97.7428
gularis	KUNHM	8976	USA	Texas	Val Verde	29.3933	-100.9317
gularis	KUNHM	8978	USA	Texas	Webb	27.5061	-99.5072
gularis	KUNHM	8979	USA	Texas	Starr	26.3794	-98.8200
gularis	KUNHM	8982	USA	Texas	Reeves	31.2051	-103.4928
gularis	KUNHM	8993	USA	Texas	Val Verde	29.6994	-101.3711
gularis	KUNHM	9042	USA	Texas	Cameron	25.9014	-97.4972
gularis	KUNHM	12738	USA	Texas	McLennan	31.5492	-97.1464
gularis	KUNHM	13087	USA	Texas	Cameron	25.9014	-97.4972
gularis	KUNHM	16071	USA	Texas	Bexar	29.5778	-98.6894
gularis	KUNHM	24059	Mexico	San Luis Potosi		22.2167	-98.4000
gularis	KUNHM	35081	Mexico	Tamaulipas		23.7692	-98.2055
gularis	KUNHM	35092	Mexico	Tamaulipas		23.7692	-98.2055
gularis	KUNHM	38290	Mexico	Coahuila		27.5418	-102.1755
gularis	KUNHM	38297	Mexico	Coahuila		27.5876	-102.1433
gularis	KUNHM	38350	Mexico	Coahuila		26.5823	-102.7424
gularis	KUNHM	39929	Mexico	Coahuila		28.3863	-100.5853
gularis	KUNHM	49655	USA	New Mexico	Eddy	32.2017	-104.2525
gularis	KUNHM	62675	Mexico	Tamaulipas		23.3167	-99.0008
gularis	KUNHM	62676	Mexico	Tamaulipas		22.8894	-98.9752
gularis	KUNHM	62677	Mexico	Tamaulipas		22.5698	-98.9705
gularis	KUNHM	62826	Mexico	Nueva Leon		25.6849	-100.5347
gularis	KUNHM	68113	Mexico	Nueva Leon		25.2281	-100.0573
gularis	KUNHM	92616	Mexico	Nueva Leon		25.4500	-100.2000
gularis	KUNHM	95712	Mexico	San Luis Potosi		22.4974	-99.7435
gularis	KUNHM	95714	Mexico	Tamaulipas		23.6288	-99.0749
gularis	KUNHM	105826	Mexico	San Luis Potosi		22.8695	-100.5049
gularis	KUNHM	199738	USA	Oklahoma	Johnston	34.2361	-96.6783
gularis	KUNHM	199813	USA	Oklahoma	Johnston	34.2794	-96.7040
gularis	KUNHM	199878	USA	Oklahoma	Johnston	34.2417	-96.7511
gularis	KUNHM	318110	USA	Texas	Frio	28.8919	-99.0947
gularis	KUNHM	318113	USA	Texas	Jeff Davis	30.7772	-103.7439
gularis	KUNHM	318122	Mexico	Nueva Leon		23.6666	-100.2944
gularis	LACM	7718	USA	Texas	Val Verde	29.6166	-100.9465
gularis	LACM	7725	USA	Texas	Glasscock	31.9655	-101.4808
gularis	LACM	7731	USA	Texas	Jeff Davis	30.5881	-103.8942
gularis	LACM	14688	USA	Texas	Tom Green	31.4635	-100.6068
gularis	LACM	14698	USA	Texas	Jeff Davis	30.7142	-103.7819
gularis	LACM	14699	USA	Texas	Eastland	32.3876	-98.7759
gularis	LACM	14700	USA	Texas	Eastland	32.3876	-98.7759
gularis	LACM	14703	USA	Texas	Eastland	32.4697	-98.6786
gularis	LACM	27436	USA	Texas	Kleberg	27.5156	-97.8558

Spp	Inst.	Specimen#	Country	State/Province	County	Latitude	Longitude
gularis	LACM	62047	USA	Texas	Sutton	30.5666	-100.7543
gularis	LACM	62049	Mexico	Tamaulipas		23.6665	-99.1333
gularis	LACM	62092	USA	Texas	Hidalgo	26.1709	-98.3830
gularis	LACM	62094	USA	Texas	Zavala	29.0744	-99.8494
gularis	LACM	66312	USA	Texas	Travis	30.3431	-97.8609
gularis	LACM	66313	USA	Texas	Blanco	30.0978	-98.3708
gularis	LACM	66315	USA	Texas	Sutton	30.4941	-100.6431
gularis	LACM	66316	USA	Texas	Hays	29.9561	-98.1772
gularis	LACM	66324	USA	Texas	Gonzales	29.6950	-97.2983
gularis	LACM	66326	Mexico	Tamaulipas		22.5358	-99.1260
gularis	LACM	75847	Mexico	San Luis Potosi		22.1135	-100.7690
gularis	LACM	99835	USA	New Mexico	Eddy	32.0984	-104.3929
gularis	LACM	99837	USA	New Mexico	Eddy	32.0987	-104.4296
gularis	LACM	99839	USA	Texas	Denton	33.3340	-97.1736
gularis	LACM	99844	Mexico	Coahuila		26.9497	-101.8063
gularis	LACM	106952	USA	Texas	Uvalde	29.3472	-99.0578
gularis	LACM	106953	USA	Texas	Burnet	30.7581	-98.2281
gularis	LACM	106954	USA	Texas	Bastrop	29.9956	-97.3973
gularis	LACM	112775	USA	Texas	Knox	33.5839	-99.7049
gularis	LACM	114825	USA	Texas	Brewser	30.3583	-103.6606
gularis	LACM	116202	Mexico	Nueva Leon		25.7941	-100.6138
gularis	LACM	128292	USA	Texas	Brazos	30.6185	-96.5257
gularis	LACM	128409	USA	Texas	Brazos	30.6185	-96.5257
gularis	LACM	131661	USA	Texas	Kendall	29.8958	-98.6575
gularis	LSU	2354	Mexico	San Luis Potosi		21.9667	-100.3833
gularis	LSU	2359	Mexico	San Luis Potosi		21.8500	-101.1370
gularis	LSU	2360	Mexico	San Luis Potosi		21.3976	-98.6296
gularis	LSU	2361	Mexico	San Luis Potosi		23.6744	-100.6960
gularis	LSU	2584	Mexico	San Luis Potosi		21.8872	-101.3971
gularis	LSU	2588	Mexico	San Luis Potosi		21.9383	-101.3421
gularis	LSU	2589	Mexico	San Luis Potosi		21.8500	-101.1167
gularis	LSU	2591	Mexico	San Luis Potosi		22.8631	-100.1601
gularis	LSU	2597	Mexico	San Luis Potosi		22.0954	-98.5310
gularis	LSU	4214	Mexico	San Luis Potosi		21.9667	-100.3833
gularis	LSU	4360	Mexico	San Luis Potosi		23.6500	-100.6659
gularis	LSU	4948	Mexico	San Luis Potosi		21.9945	-99.0413
gularis	LSU	5696	Mexico	San Luis Potosi		22.3993	-99.6028
gularis	LSU	5712	Mexico	San Luis Potosi		22.1088	-100.9307
gularis	LSU	5731	Mexico	San Luis Potosi		22.3626	-99.2658
gularis	LSU	9782	USA	Texas	Hidalgo	26.2882	-98.3250
gularis	LSU	9790	USA	Texas	Maverick	29.0639	-100.6236
gularis	LSU	15027	USA	Texas	Bexar	29.3828	-98.6265
gularis	LSU	18639	USA	Texas	Hidalgo	26.0869	-98.2297
gularis	LSU	23447	USA	Texas	Kimble	30.2964	-99.8702
gularis	LSU	29371	USA	Texas	Jim Hogg	27.1020	-98.8033
gularis	LSU	29376	USA	Texas	Jim Hogg	27.0716	-98.8630
gularis	LSU	29380	USA	Texas	Starr	26.5557	-98.8925
gularis	LSU	30711	USA	Texas	Bastrop	30.0083	-97.1592
gularis	LSU	30713	USA	Texas	San Saba	30.9537	-98.6747
gularis	LSU	30721	USA	Texas	Kerr	30.2162	-99.5059
gularis	LSU	32669	USA	Texas	McMullen	28.1043	-98.3672
gularis	LSU	32670	USA	Texas	McMullen	28.1380	-98.6051
gularis	LSU	33851	USA	Texas	Cameron	25.9628	-97.2513
gularis	LSU	41915	USA	Texas	Hidalgo	26.3463	-98.3250
gularis	LSU	41951	USA	Texas	Reeves	30.9750	-103.7530
gularis	LSU	41971	USA	Texas	Crockett	30.4995	-101.1522
gularis	LSU	48752	USA	Texas	McMullen	28.2066	-98.4362
gularis	LSU	48855	USA	Texas	McMullen	28.2066	-98.4362

Spp	Inst.	Specimen#	Country	State/Province	County	Latitude	Longitude
gularis	LSU	50753	USA	Texas	Jim Hogg	27.0716	-98.8630
gularis	LSU	50754	USA	Texas	Jim Hogg	27.0716	-98.8630
gularis	LSU	50758	USA	Texas	Jim Hogg	26.9510	-98.8933
gularis	LSU	50764	USA	Texas	Bee	28.3469	-97.7228
gularis	LSU	50768	USA	Texas	Starr	26.6898	-98.8714
gularis	LSU	72976	USA	Texas	Val Verde	29.9504	-101.1458
gularis	LSU	72977	USA	Texas	Bandera	29.6465	-99.4864
gularis	LSU	72978	USA	Texas	Medina	29.6186	-99.2562
gularis	LSU	72981	USA	Texas	Maverick	28.7397	-100.4641
gularis	LSU	72982	USA	New Mexico	Lea	33.2569	-103.3172
gularis	LSU	72985	USA	Texas	Real	29.7403	-99.8185
gularis	LSU	72986	USA	Texas	Bandera	29.6465	-99.4864
gularis	LSU	73015	USA	New Mexico	Lea	33.2548	-103.2031
gularis	LSU	86679	USA	New Mexico	Eddy	32.4206	-104.2283
gularis	MCZ	4520	Mexico	San Luis Potosi		22.1557	-100.9852
gularis	MCZ	4570	USA	Texas	Webb	27.5061	-99.5072
gularis	MCZ	4573	USA	Texas	Bexar	29.4239	-98.4933
gularis	MCZ	6853	USA	Texas	Mclennan	31.5492	-97.1464
gularis	MCZ	13894	USA	Texas	Cameron	25.9014	-97.4972
gularis	MCZ	43926	USA	Texas	Williamson	30.6325	-97.6769
gularis	MCZ	114583	USA	Texas	Dickens	33.4764	-100.8379
gularis	MCZ	127365	USA	Texas	Kleberg	27.5156	-97.8558
gularis	MCZ	151718	Mexico	Queretaro		21.3761	-99.4758
gularis	MCZ	183094	USA	Texas	Starr	26.5997	-99.1185
gularis	MPM	4819	USA	Texas	Hays	30.0638	-98.0263
gularis	MPM	19175	USA	Texas	Coleman	31.7645	-99.3479
gularis	MPM	19176	USA	Texas	Llano	30.7396	-98.6335
gularis	MPM	19179	USA	Texas	Jeff Davis	30.6967	-103.8419
gularis	MPM	19180	USA	Texas	Medina	29.4877	-99.1145
gularis	MPM	25492	USA	Texas	Kinney	29.3103	-100.4841
gularis	MPM	25686	USA	Texas	Val Verde	29.4496	-100.8964
gularis	MPM	25687	USA	Texas	Mcculloch	31.0302	-99.2303
gularis	MPM	25690	USA	Texas	Kinney	29.3103	-100.4841
gularis	MPM	25703	USA	Texas	Val Verde	29.3099	-100.7339
gularis	MSU	2582	USA	Texas	Fayette	29.9056	-96.6223
gularis	MSU	3002	USA	Texas	Tom Green	31.4636	-100.4367
gularis	MSU	4401	Mexico	Tamaulipas		23.7692	-98.2055
gularis	MSU	9686	Mexico	Nueva Leon		24.7752	-100.0667
gularis	MSU	9687	Mexico	Nueva Leon		24.8025	-100.0327
gularis	MSU	9688	Mexico	Tamaulipas		22.2813	-97.8042
gularis	MVZ	12528	USA	Texas	Ellis	32.5643	-96.8969
gularis	MVZ	12703	Mexico	Tamaulipas		27.4589	-99.5630
gularis	MVZ	24371	Mexico	Nueva Leon		25.8787	-100.3085
gularis	MVZ	36729	Mexico	Nueva Leon		25.5693	-100.4595
gularis	MVZ	36730	Mexico	Nueva Leon		25.5729	-100.4579
gularis	MVZ	38194	USA	Texas	Sutton	30.6102	-100.6431
gularis	MVZ	38195	USA	Texas	Tom Green	31.4632	-100.1304
gularis	MVZ	38196	USA	Texas	Tom Green	31.3095	-100.2562
gularis	MVZ	38197	USA	Texas	Tom Green	31.4636	-100.5388
gularis	MVZ	38198	USA	Texas	Tom Green	31.7417	-100.2858
gularis	MVZ	38426	USA	Texas	Howard	32.1990	-101.4177
gularis	MVZ	38427	USA	Texas	Howard	32.2502	-101.3067
gularis	MVZ	38428	USA	Texas	Howard	32.4041	-101.2963
gularis	MVZ	52378	USA	Texas	Bastrop	30.1103	-97.3150
gularis	MVZ	52379	USA	Texas	Bastrop	30.1103	-97.3989
gularis	MVZ	52380	USA	Texas	Bastrop	30.1100	-97.5667
gularis	MVZ	52381	USA	Texas	Bee	28.2900	-97.5863
gularis	MVZ	53883	USA	Texas	Live Oak	28.2596	-98.1172

Spp	Inst.	Specimen#	Country	State/Province	County	Latitude	Longitude
gularis	MVZ	53884	USA	Texas	Caldwell	29.6655	-97.6053
gularis	MVZ	55871	USA	Texas	Atascosa	29.0307	-98.6751
gularis	MVZ	66448	USA	Texas	Fayette	29.8337	-96.5896
gularis	MVZ	76756	USA	Texas	Travis	30.2669	-97.7726
gularis	MVZ	77918	USA	Texas	Tom Green	31.4636	-100.4367
gularis	MVZ	78321	USA	Texas	Refugio	28.1817	-97.4150
gularis	MVZ	78322	USA	Texas	San Patricio	28.1453	-97.5089
gularis	MVZ	110816	USA	Texas	Terrell	30.0444	-102.2316
gularis	MVZ	129198	USA	Texas	Starr	26.4820	-99.0529
gularis	MVZ	129200	USA	Texas	Zapata	26.7392	-99.1134
gularis	MVZ	129202	USA	Texas	Cameron	25.9014	-97.5214
gularis	MVZ	129214	USA	Texas	Cameron	25.9431	-97.5418
gularis	MVZ	129221	Mexico	Tamaulipas		22.8333	-99.0237
gularis	MVZ	129229	Mexico	San Luis Potosi		22.7338	-99.9715
gularis	MVZ	129230	Mexico	San Luis Potosi		22.4667	-99.5629
gularis	MVZ	139295	USA	Texas	Williamson	30.6201	-97.7083
gularis	MVZ	139302	USA	Texas	Val Verde	29.6020	-101.0785
gularis	MVZ	139303	USA	Texas	Hays	30.1638	-97.9831
gularis	MVZ	185751	USA	Texas	Travis	30.3239	-98.1731
gularis	MVZ	185767	USA	Texas	Llano	30.4897	-98.7719
gularis	MVZ	185777	USA	Texas	Bexar	29.5475	-98.7691
gularis	MVZ	215603	USA	Texas	Terrell	30.4021	-102.2989
gularis	PSM	8251	USA	Oklahoma	Murray	34.4357	-97.1401
gularis	ROM	15344	Mexico	Zacatecas		24.6913	-101.2629
gularis	ROM	15382	Mexico	Nueva Leon		25.8726	-99.1667
gularis	SDNHM	46164	USA	Texas	Bexar	29.4479	-98.4501
gularis	SDNHM	68579	USA	Texas	Pecos	30.9907	-102.2239
gularis	TCWC	137	USA	Texas	Kerr	29.9651	-99.2349
gularis	TCWC	144	USA	Texas	Kerr	30.0472	-99.0729
gularis	TCWC	146	USA	Texas	Kerr	30.0705	-99.4214
gularis	TCWC	434	USA	Texas	Val Verde	29.6994	-101.3711
gularis	TCWC	646	USA	Texas	Jeff Davis	30.8555	-103.9855
gularis	TCWC	652	Mexico	Nueva Leon		25.3275	-99.9577
gularis	TCWC	786	Mexico	Nueva Leon		26.3664	-100.3159
gularis	TCWC	863	Mexico	Nueva Leon		25.3275	-99.9577
gularis	TCWC	1035	USA	Texas	La Salle	28.4367	-99.2347
gularis	TCWC	1093	USA	Texas	Mason	30.6905	-99.2303
gularis	TCWC	1107	USA	Texas	Kerr	30.0706	-99.3375
gularis	TCWC	2259	USA	Texas	McLennan	31.5942	-97.3075
gularis	TCWC	4535	USA	Texas	Brown	31.6366	-98.9908
gularis	TCWC	4539	USA	Texas	Brazos	30.7729	-96.3342
gularis	TCWC	4540	USA	Texas	Williamson	30.7320	-97.4425
gularis	TCWC	4544	USA	Texas	Atascosa	28.7472	-98.2525
gularis	TCWC	4552	USA	Texas	Kendall	29.9675	-98.8042
gularis	TCWC	4560	USA	Texas	Brown	31.7931	-98.8229
gularis	TCWC	5691	USA	Texas	Wharton	29.1962	-96.5189
gularis	TCWC	5692	USA	Texas	Cameron	25.9014	-97.4972
gularis	TCWC	5693	USA	Texas	Colorado	29.5894	-96.3333
gularis	TCWC	5694	USA	Texas	Jim Wells	28.0372	-97.9006
gularis	TCWC	5696	USA	Texas	Burleson	30.5311	-96.7939
gularis	TCWC	5697	USA	Texas	Brazos	30.6278	-96.4185
gularis	TCWC	5699	USA	Texas	Robertson	30.9180	-96.3658
gularis	TCWC	5700	USA	Texas	Brazos	30.5987	-96.3342
gularis	TCWC	5701	USA	Texas	Val Verde	29.7811	-101.3972
gularis	TCWC	5702	USA	Texas	Palo Pinto	32.7673	-98.3311
gularis	TCWC	5703	USA	Texas	Erath	32.1235	-98.3066
gularis	TCWC	5709	USA	Texas	Tarrant	32.7688	-97.3206
gularis	TCWC	5710	USA	Texas	Eastland	32.4700	-98.7299

Spp	Inst.	Specimen#	Country	State/Province	County	Latitude	Longitude
gularis	TCWC	6691	Mexico	Tamaulipas		24.0167	-98.7833
gularis	TCWC	6698	Mexico	Tamaulipas		25.7962	-97.5000
gularis	TCWC	6971	Mexico	Tamaulipas		22.8000	-98.6212
gularis	TCWC	6972	Mexico	Tamaulipas		22.8000	-98.7000
gularis	TCWC	7067	USA	Texas	Kenedy	26.7897	-97.7758
gularis	TCWC	7205	USA	Texas	Brazos	30.8193	-96.3697
gularis	TCWC	8924	USA	Texas	Bastrop	30.1103	-97.2647
gularis	TCWC	8925	Mexico	Tamaulipas		22.9513	-98.9500
gularis	TCWC	8932	USA	Texas	Freestone	31.8696	-96.1650
gularis	TCWC	10546	USA	Texas	Bastrop	30.0340	-97.1888
gularis	TCWC	10548	USA	Texas	Live Oak	28.4600	-98.2318
gularis	TCWC	10552	USA	Texas	Erath	32.0645	-98.3174
gularis	TCWC	10553	USA	Texas	Hays	29.8214	-98.0122
gularis	TCWC	11374	Mexico	San Luis Potosi		21.2975	-98.7502
gularis	TCWC	17116	Mexico	Nueva Leon		25.4167	-100.1178
gularis	TCWC	20804	Mexico	Tamaulipas		23.5038	-99.1361
gularis	TCWC	22097	Mexico	San Luis Potosi		23.5047	-100.6500
gularis	TCWC	30098	Mexico	Queretaro		21.2729	-99.4746
gularis	TCWC	30114	Mexico	Queretaro		21.3325	-99.4766
gularis	TCWC	30115	Mexico	Queretaro		21.4314	-99.4052
gularis	TCWC	30117	Mexico	Queretaro		21.1829	-99.2929
gularis	TCWC	31541	Mexico	Queretaro		21.3519	-99.4729
gularis	TCWC	76331	USA	Oklahoma	Carter	34.1740	-97.3538
gularis	TCWC	86517	USA	Texas	Atascosa	29.1542	-98.7399
gularis	TCWC	86518	USA	Texas	Bandera	29.7572	-99.1088
gularis	UAZ	5581	USA	Texas	Mason	30.7482	-98.9212
gularis	UAZ	5589	USA	Texas	Mason	30.7485	-99.0496
gularis	UAZ	9286	USA	Texas	Hidalgo	26.1709	-98.3830
gularis	UAZ	15794	USA	Texas	Pecos	30.8938	-103.0311
gularis	UAZ	16646	USA	Texas	Brewser	30.3583	-103.6606
gularis	UAZ	16747	USA	Texas	Bastrop	30.1103	-97.3150
gularis	UAZ	16868	USA	Texas	McCulloch	31.0939	-99.3827
gularis	UAZ	16872	USA	Texas	Pecos	30.9139	-101.8637
gularis	UAZ	17917	USA	Texas	Culberson	31.2537	-104.4324
gularis	UAZ	28247	USA	Texas	Travis	30.3445	-97.7922
gularis	UAZ	30881	USA	Texas	Jeff Davis	30.5881	-103.8942
gularis	UAZ	34109	USA	Texas	Val Verde	29.6842	-101.2065
gularis	UAZ	38336	Mexico	Coahuila		28.3129	-100.9137
gularis	UCM	14645	USA	Texas	Denton	33.3938	-97.2105
gularis	UCM	15179	USA	Texas	Taylor	32.4894	-100.1261
gularis	UCM	16938	USA	Texas	Denton	33.3938	-97.2105
gularis	UCM	16941	USA	Texas	Denton	33.4349	-97.0876
gularis	UCM	20053	USA	Texas	Brewser	30.3583	-103.6606
gularis	UCM	24225	USA	Texas	Travis	30.2669	-97.7428
gularis	UCM	27089	Mexico	Nueva Leon		25.6320	-100.4570
gularis	UCM	27093	Mexico	San Luis Potosi		22.3626	-99.2658
gularis	UCM	27104	USA	Texas	Wise	33.2341	-97.4401
gularis	UCM	27114	USA	Texas	Denton	33.2144	-97.4103
gularis	UCM	29548	USA	Texas	Garza	32.9700	-101.4200
gularis	UCM	37449	Mexico	Chihuahua		28.2614	-105.4807
gularis	UCM	37452	Mexico	Chihuahua		28.0155	-105.2915
gularis	UCM	37750	Mexico	Nueva Leon		25.8530	-100.5833
gularis	UCM	37751	Mexico	Nueva Leon		25.7833	-100.6000
gularis	UCM	37756	Mexico	Coahuila		26.6918	-101.4167
gularis	UCM	37757	Mexico	Coahuila		26.9000	-101.4997
gularis	UCM	37758	Mexico	Coahuila		27.0026	-101.7507
gularis	UCM	37759	Mexico	Coahuila		27.0500	-101.6554
gularis	UCM	37790	Mexico	Coahuila		26.9903	-102.1020

Spp	Inst.	Specimen#	Country	State/Province	County	Latitude	Longitude
gularis	UCM	39565	USA	Texas	Kleberg	27.5156	-97.8558
gularis	UCM	49407	USA	Texas	Kimble	30.6617	-99.8747
gularis	UCM	49410	USA	Texas	Pecos	30.0833	-102.6000
inornata	ASU	5486	Mexico	Coahuila		26.9268	-102.0833
inornata	CAS	7900	USA	Texas	Presidio	30.1665	-104.0284
inornata	CAS	9764	USA	Texas	Ector	31.8073	-102.3339
inornata	CAS	66281	USA	Texas	Culberson	31.0677	-104.2169
inornata	CAS	95841	Mexico	Zacatecas		24.4299	-101.4167
inornata	CAS	203880	USA	New Mexico	Hidalgo	31.9489	-108.8751
inornata	CAS	203881	USA	New Mexico	Socorro	34.0528	-106.8777
inornata	CM	43172	Mexico	Durango		26.6212	-104.1167
inornata	CM	43187	Mexico	Chihuahua		29.9000	-106.4167
inornata	CM	43193	Mexico	Coahuila		26.8616	-102.1824
inornata	CM	43200	Mexico	Coahuila		26.8616	-102.1824
inornata	CM	43204	Mexico	Coahuila		26.9936	-102.0833
inornata	CM	48186	Mexico	Coahuila		26.8781	-102.1640
inornata	CM	51154	Mexico	Coahuila		26.9500	-101.9905
inornata	CM	51159	Mexico	Coahuila		26.9500	-102.0393
inornata	CM	51160	Mexico	Coahuila		26.9500	-102.0736
inornata	CM	54891	USA	New Mexico	Chaves	33.3940	-104.7311
inornata	CM	54892	USA	New Mexico	Otero	32.7557	-106.1308
inornata	CM	75399	USA	Texas	Terrell	29.9526	-101.9995
inornata	CM	75400	USA	Texas	Terrell	30.0172	-102.0798
inornata	CM	75404	USA	Texas	Brewser	29.7118	-103.5715
inornata	CM	75410	USA	New Mexico	Otero	32.5518	-106.5961
inornata	CM	92833	USA	Texas	El Paso	31.8275	-106.1218
inornata	CM	137899	USA	New Mexico	San Juan	36.6776	-108.4694
inornata	CM	P1673	USA	New Mexico	San Miguel	35.5939	-105.2233
inornata	CU	5529	USA	New Mexico	Bernalillo	35.0844	-106.6506
inornata	CU	9052	USA	New Mexico	Otero	32.8925	-106.2158
inornata	CU	9710	Mexico	Chihuahua		29.3318	-105.2934
inornata	CU	12718	USA	New Mexico	Eddy	32.2238	-104.2435
inornata	KUNHM	12991	USA	Texas	Val Verde	29.3937	-100.9408
inornata	KUNHM	13982	USA	Texas	Brewser	29.3167	-103.6172
inornata	KUNHM	15414	USA	Texas	Terrell	30.0427	-102.1149
inornata	KUNHM	29331	Mexico	Coahuila		25.6513	-101.6455
inornata	KUNHM	33722	Mexico	Coahuila		28.4740	-103.6603
inornata	KUNHM	33724	Mexico	Coahuila		28.1609	-103.6463
inornata	KUNHM	33896	Mexico	Coahuila		28.0295	-103.8670
inornata	KUNHM	33897	Mexico	Chihuahua		29.6860	-106.3667
inornata	KUNHM	33900	Mexico	Chihuahua		29.8602	-106.3667
inornata	KUNHM	39472	Mexico	Coahuila		25.4414	-102.1747
inornata	KUNHM	47099	Mexico	Coahuila		26.9500	-102.1811
inornata	KUNHM	49589	Mexico	Chihuahua		27.1166	-105.0316
inornata	KUNHM	51907	Mexico	Chihuahua		28.4008	-105.6079
inornata	KUNHM	53749	Mexico	Coahuila		26.8048	-102.0833
inornata	KUNHM	63730	Mexico	Chihuahua		27.1167	-104.9826
inornata	KUNHM	72259	USA	Texas	Culberson	31.9366	-104.7169
inornata	KUNHM	80304	Mexico	Coahuila		26.8185	-102.1444
inornata	KUNHM	318131	USA	Texas	Brewser	30.2106	-103.1451
inornata	KUNHM	318132	USA	Texas	Brewser	30.3777	-103.5457
inornata	KUNHM	318135	USA	Texas	Terrell	30.1160	-102.3845
inornata	LACM	7550	USA	New Mexico	Otero	32.7937	-106.2034
inornata	LACM	7566	USA	New Mexico	Otero	32.8007	-106.2549
inornata	LACM	7621	USA	New Mexico	Chaves	33.1983	-104.5225
inornata	LACM	7634	USA	New Mexico	Chaves	33.3942	-104.5225
inornata	LACM	7645	USA	New Mexico	San Juan	36.5951	-107.9839
inornata	LACM	14679	USA	Arizona	Coconino	35.5211	-111.3717

Spp	Inst.	Specimen#	Country	State/Province	County	Latitude	Longitude
inornata	LACM	28441	USA	New Mexico	Dona Ana	32.2531	-106.8350
inornata	LACM	44415	Mexico	Coahuila		26.8616	-102.1824
inornata	LACM	62068	USA	New Mexico	Otero	32.7482	-106.1933
inornata	LACM	62095	USA	Texas	Val Verde	29.8717	-101.7126
inornata	LACM	62096	USA	Texas	Presidio	30.3203	-104.0866
inornata	LACM	62100	USA	Texas	Presidio	30.3203	-104.0866
inornata	LACM	66334	USA	New Mexico	De Baca	34.3905	-104.3194
inornata	LACM	66339	USA	Texas	Crockett	30.6671	-101.6968
inornata	LACM	66346	USA	Texas	Pecos	30.8913	-102.2985
inornata	LACM	66347	USA	Texas	Val Verde	29.4855	-100.9971
inornata	LACM	76181	Mexico	San Luis Potosi		22.6253	-100.7148
inornata	LACM	76200	Mexico	Coahuila		25.1702	-102.6506
inornata	LACM	76204	Mexico	Zacatecas		24.2500	-101.4300
inornata	LACM	76218	Mexico	Zacatecas		24.6600	-101.8500
inornata	LACM	76248	Mexico	Chihuahua		29.2749	-107.3625
inornata	LACM	76678	USA	Texas	Presidio	30.1696	-104.0266
inornata	LACM	99906	USA	New Mexico	Eddy	32.1756	-104.4275
inornata	LACM	99908	USA	New Mexico	Eddy	32.4358	-104.4337
inornata	LACM	99910	USA	Texas	Hudspeth	31.8405	-105.9716
inornata	LACM	99913	USA	Texas	Pecos	30.8036	-102.8330
inornata	LACM	99917	USA	Texas	Presidio	29.1645	-104.0915
inornata	LACM	99918	USA	Texas	Reeves	30.9029	-103.7910
inornata	LACM	100608	USA	New Mexico	Eddy	32.4358	-104.4337
inornata	LACM	100609	USA	Texas	Hudspeth	31.8405	-105.9716
inornata	LACM	109133	USA	Texas	Hudspeth	31.8468	-105.7822
inornata	LACM	109453	USA	New Mexico	Luna	32.3445	-107.8189
inornata	LACM	109580	USA	New Mexico	Dona Ana	32.6168	-107.2816
inornata	LACM	109581	USA	New Mexico	Chaves	33.1150	-104.3610
inornata	LACM	109583	USA	New Mexico	Chaves	33.3149	-104.5358
inornata	LACM	109587	USA	New Mexico	Dona Ana	32.3749	-106.8133
inornata	LACM	109588	USA	New Mexico	Dona Ana	32.3122	-106.7778
inornata	LACM	109589	USA	New Mexico	Dona Ana	32.3037	-106.8463
inornata	LACM	109590	USA	New Mexico	Dona Ana	32.3028	-106.8239
inornata	LACM	109596	USA	New Mexico	Dona Ana	32.3848	-106.7778
inornata	LACM	109600	USA	New Mexico	Dona Ana	32.3225	-106.8806
inornata	LACM	109601	USA	New Mexico	Grant	33.0242	-108.1415
inornata	LACM	112776	USA	New Mexico	Otero	32.8925	-106.2158
inornata	LACM	116152	Mexico	Nueva Leon		25.7941	-100.6138
inornata	LACM	116162	Mexico	Nueva Leon		25.7941	-100.6138
inornata	LACM	116251	Mexico	Coahuila		26.9200	-102.1400
inornata	LACM	116259	Mexico	Durango		25.1700	-103.7300
inornata	LACM	121635	USA	New Mexico	Dona Ana	32.6652	-107.2973
inornata	LACM	121668	USA	New Mexico	Bernalillo	35.0844	-106.6506
inornata	LACM	122408	Mexico	Chihuahua		31.3500	-106.4667
inornata	LACM	126998	USA	Texas	El Paso	31.5026	-106.1831
inornata	LACM	130635	USA	Arizona	Coconino	36.0506	-112.2192
inornata	LACM	130636	USA	Texas	Brewser	29.5713	-102.9458
inornata	LACM	131727	Mexico	Nueva Leon		25.7941	-100.6138
inornata	LACM	131748	USA	Texas	Val Verde	29.8847	-101.7252
inornata	LACM	131905	USA	New Mexico	Dona Ana	32.6652	-107.2973
inornata	LACM	132239	USA	New Mexico	Guadalupe	34.7623	-104.9691
inornata	LACM	133651	USA	New Mexico	Otero	32.7667	-106.3333
inornata	LACM	133652	USA	New Mexico	Otero	32.7667	-106.3333
inornata	LACM	133653	USA	New Mexico	Dona Ana	32.2531	-106.8350
inornata	LACM	133654	USA	New Mexico	Dona Ana	32.5107	-106.8236
inornata	LACM	134143	USA	New Mexico	Dona Ana	32.2531	-106.8350
inornata	LACM	134150	USA	New Mexico	Dona Ana	32.2531	-106.8350
inornata	LACM	134344	USA	New Mexico	Luna	32.2749	-107.7078

Spp	Inst.	Specimen#	Country	State/Province	County	Latitude	Longitude
inornata	LACM	134345	USA	Texas	Jeff Davis	30.7437	-104.6960
inornata	LACM	137192	USA	Texas	El Paso	31.8942	-106.5982
inornata	LACM	137269	USA	Arizona	Coconino	35.3739	-111.5732
inornata	LACM	137271	USA	Arizona	Coconino	35.3739	-111.5732
inornata	LACM	144790	USA	Arizona	Apache	34.8568	-109.8189
inornata	LACM	144791	USA	Arizona	Navaho	34.8278	-109.8896
inornata	LACM	146379	USA	Texas	Brewser	30.1032	-103.5936
inornata	LACM	146419	USA	Texas	Brewser	30.1032	-103.5936
inornata	LACM	146431	USA	Texas	Brewser	29.3167	-103.6172
inornata	LACM	146443	USA	Texas	Brewser	29.3180	-103.2078
inornata	LSU	9806	USA	New Mexico	Eddy	32.4205	-104.2799
inornata	LSU	9807	USA	New Mexico	Eddy	32.8103	-104.6459
inornata	LSU	9808	USA	New Mexico	Dona Ana	32.2531	-106.8350
inornata	LSU	23461	USA	Texas	Terrell	30.1649	-102.4650
inornata	LSU	41969	USA	Texas	Val Verde	29.7443	-101.2220
inornata	LSU	42835	USA	New Mexico	Eddy	32.4206	-104.2283
inornata	LSU	43013	USA	New Mexico	Torrence	34.9899	-105.8715
inornata	LSU	73052	Mexico	Coahuila		24.7783	-101.1421
inornata	LSU	73058	USA	New Mexico	Eddy	32.8422	-104.4028
inornata	LSU	73074	USA	Texas	Brewser	29.9646	-103.2599
inornata	LSU	73076	USA	New Mexico	De Baca	34.2763	-104.8994
inornata	LSU	73086	USA	Texas	Presidio	30.1337	-104.1215
inornata	LSU	73092	USA	New Mexico	Lincoln	33.6296	-105.8254
inornata	MCZ	62325	USA	New Mexico		34.0848	-104.5286
inornata	MCZ	100080	USA	New Mexico	Otero	32.8994	-105.9597
inornata	MCZ	100424	USA	New Mexico	Otero	32.8994	-105.9597
inornata	MCZ	114584	USA	New Mexico	Otero	32.8994	-105.9597
inornata	MPM	19118	Mexico	Coahuila		26.7500	-102.0167
inornata	MPM	25493	USA	Texas	Brewser	30.2142	-103.2982
inornata	MPM	25494	USA	New Mexico	Eddy	32.3590	-104.3013
inornata	MPM	25523	USA	New Mexico	Eddy	32.2973	-104.3742
inornata	MSU	184	Mexico	Durango		26.3052	-103.9635
inornata	MSU	2788	Mexico	Durango		26.4552	-104.0969
inornata	MSU	4074	USA	New Mexico	Eddy	32.2029	-104.2283
inornata	MSU	4075	USA	New Mexico	Socorro	33.8889	-106.3719
inornata	MSU	4353	Mexico	Durango		25.4038	-103.6500
inornata	MSU	7287	Mexico	Coahuila		25.5648	-101.3403
inornata	MSU	7290	Mexico	Durango		25.2858	-103.6841
inornata	MSU	9247	Mexico	Chihuahua		29.8167	-106.3667
inornata	MVZ	11240	USA	Texas	El Paso	31.0693	-104.2846
inornata	MVZ	13913	USA	New Mexico	Otero	32.9712	-106.1405
inornata	MVZ	49865	USA	New Mexico	Otero	32.8994	-105.9597
inornata	MVZ	65656	USA	New Mexico	Torrence	34.9763	-105.3781
inornata	MVZ	66075	Mexico	Chihuahua		28.7059	-106.0833
inornata	MVZ	67088	USA	New Mexico	Hidalgo	31.8353	-109.0306
inornata	MVZ	70915	Mexico	Chihuahua		29.3226	-106.4500
inornata	MVZ	200577	USA	Texas	Pecos	30.9992	-102.5033
inornata	MVZ	212179	USA	New Mexico	Hidalgo	32.0820	-109.0306
inornata	MVZ	212180	USA	New Mexico	Hidalgo	31.8208	-109.0306
inornata	OMNH	32618	USA	Texas	Culberson	31.0623	-104.3193
inornata	OMNH	41453	USA	Texas	Terrell	30.1388	-102.5450
inornata	SDNHM	40283	Mexico	Coahuila		25.4491	-100.8224
inornata	SDNHM	40284	Mexico	Coahuila		25.5063	-100.9836
inornata	SDNHM	49246	USA	Texas	Terrell	30.1380	-102.3538
inornata	TCWC	1152	USA	Texas	Brewser	29.3797	-103.0791
inornata	TCWC	16061	USA	Texas	Brewser	29.2458	-103.4123
inornata	TCWC	25714	USA	Texas	Pecos	30.9145	-102.9471
inornata	TCWC	25718	USA	Texas	Brewser	30.3170	-103.7632

Spp	Inst.	Specimen#	Country	State/Province	County	Latitude	Longitude
inornata	TCWC	25725	USA	Texas	Terrell	30.1342	-102.1180
inornata	TCWC	25740	USA	Texas	Brewser	30.1448	-103.2357
inornata	TCWC	25743	USA	Texas	Brewser	30.1119	-103.2378
inornata	TCWC	25761	USA	Texas	Pecos	30.9107	-102.8500
inornata	TCWC	25769	USA	Texas	Brewser	30.0787	-103.2703
inornata	TCWC	25900	USA	Texas	Brewser	30.2984	-103.4581
inornata	TCWC	36843	USA	Texas	Terrell	30.1299	-102.3856
inornata	TCWC	39752	USA	Texas	Pecos	30.7666	-101.8369
inornata	TCWC	39755	USA	Texas	Pecos	30.8092	-102.8344
inornata	TCWC	39848	USA	Texas	Culberson	31.1230	-104.6619
inornata	TCWC	39865	USA	Texas	Culberson	31.2941	-104.2083
inornata	TCWC	39866	USA	Texas	Culberson	31.1782	-104.2429
inornata	TCWC	43146	Mexico	Durango		26.5167	-104.1167
inornata	TCWC	43612	Mexico	Coahuila		26.4333	-101.3500
inornata	TCWC	43616	Mexico	Coahuila		26.1167	-101.3500
inornata	TCWC	43657	Mexico	Durango		25.1500	-103.7500
inornata	TCWC	44266	Mexico	Nueva Leon		25.9333	-100.6500
inornata	TCWC	46863	Mexico	Coahuila		25.3930	-101.0291
inornata	TCWC	46874	Mexico	Coahuila		26.8570	-101.7379
inornata	TCWC	47034	Mexico	Coahuila		27.3141	-102.4681
inornata	TCWC	47035	Mexico	Coahuila		27.3147	-102.5148
inornata	TCWC	47041	Mexico	Coahuila		27.3151	-102.6075
inornata	TCWC	49866	Mexico	Coahuila		25.4320	-101.1060
inornata	TCWC	49974	Mexico	Coahuila		25.5280	-102.1735
inornata	TCWC	51814	Mexico	Nueva Leon		26.0545	-100.5494
inornata	TCWC	51815	Mexico	Nueva Leon		26.1041	-100.5723
inornata	TCWC	51816	Mexico	Nueva Leon		24.0994	-99.8710
inornata	TCWC	56788	Mexico	Nueva Leon		23.8274	-100.0750
inornata	TCWC	56790	Mexico	Nueva Leon		23.8274	-100.0750
inornata	TCWC	62788	USA	Texas	Pecos	30.7145	-101.8109
inornata	TCWC	71823	USA	Texas	Terrell	30.0756	-102.2466
inornata	TCWC	72470	USA	Texas	Terrell	30.0427	-102.1149
inornata	TCWC	72508	USA	Texas	Terrell	30.0618	-102.2770
inornata	TCWC	72782	USA	Texas	Pecos	30.8990	-103.0566
inornata	TCWC	81663	USA	Texas	Terrell	30.0618	-102.2770
inornata	TCWC	87856	USA	Texas	Val Verde	29.7756	-101.1327
inornata	UAZ	14067	Mexico	Nueva Leon		25.7941	-100.6138
inornata	UAZ	14259	Mexico	Durango		25.0295	-103.8000
inornata	UAZ	16319	USA	Texas	Reeves	30.9672	-103.7535
inornata	UAZ	16579	USA	Texas	Reeves	30.9532	-103.7206
inornata	UAZ	16840	USA	Texas	Reeves	30.9906	-103.6633
inornata	UAZ	30273	USA	Texas	Reeves	30.9906	-103.6633
inornata	UAZ	30870	USA	Texas	Terrell	30.1299	-102.3856
inornata	UAZ	30886	USA	Texas	Hudspeth	31.7376	-105.1279
inornata	UAZ	30891	USA	Texas	Terrell	30.1299	-102.3856
inornata	UAZ	30894	USA	Texas	Hudspeth	31.7376	-105.1279
inornata	UAZ	30911	USA	Texas	Terrell	30.1299	-102.3856
inornata	UAZ	30914	USA	Texas	Terrell	30.1299	-102.3856
inornata	UAZ	32698	USA	Texas	Terrell	30.1058	-102.3663
inornata	UAZ	34110	USA	Texas	Val Verde	29.6981	-101.2033
inornata	UAZ	35150	Mexico	Chihuahua		29.4333	-105.0833
inornata	UCM	37801	Mexico	Chihuahua		27.0374	-104.9150
inornata	UCM	37804	Mexico	Chihuahua		26.9351	-104.9500
inornata	UCM	37884	Mexico	San Luis Potosi		23.6355	-100.6500
inornata	UCM	37886	Mexico	Coahuila		29.1702	-103.0065
inornata	UCM	37935	Mexico	Coahuila		25.6187	-100.9849
inornata	UCM	37936	Mexico	Coahuila		26.9000	-101.4997
inornata	UCM	37937	Mexico	Nueva Leon		25.6591	-100.7296

Spp	Inst.	Specimen#	Country	State/Province	County	Latitude	Longitude
inornata	UCM	49781	Mexico	Chihuahua		27.2419	-104.9147
inornata	UCM	58474	Mexico	Chihuahua		31.1123	-108.0001
inornata	UTEP	3477	USA	Texas	Terrell	30.1551	-102.5302
inornata	UTEP	15604	USA	Texas	Terrell	30.1058	-102.3663
inornata	UTEP	15622	USA	Texas	Ector	31.9158	-102.7568
inornata	YPM	7134	USA	Texas	Winkler	31.7511	-103.1594
sonorae	CAS	1511	USA	Arizona	Pima	32.2596	-110.8732
sonorae	CAS	1586	USA	Arizona	Pima	32.2596	-110.8732
sonorae	CAS	1600	USA	Arizona	Cochise	31.7323	-110.1801
sonorae	CAS	2116	USA	Arizona	Cochise	31.7589	-109.3450
sonorae	CAS	2330	USA	Arizona	Pima	32.2596	-110.8732
sonorae	CAS	2498	USA	Arizona	Pima	32.2596	-110.8732
sonorae	CAS	2612	USA	Arizona	Cochise	31.7589	-109.3450
sonorae	CAS	2617	USA	Arizona	Cochise	31.7323	-110.1801
sonorae	CAS	2645	USA	Arizona	Cochise	31.7589	-109.3450
sonorae	CAS	10105	USA	Arizona	Pima	32.3293	-110.7929
sonorae	CAS	12691	USA	Arizona	Pima	31.7994	-110.8084
sonorae	CAS	12701	USA	Arizona	Cochise	31.3928	-110.3602
sonorae	CAS	15505	Mexico	Sonora		30.7570	-108.9356
sonorae	CAS	20938	USA	Arizona	Pima	32.2596	-110.8732
sonorae	CAS	34909	USA	Arizona	Cochise	31.4625	-110.2889
sonorae	CAS	34937	USA	Arizona	Cochise	31.4625	-110.2889
sonorae	CAS	34938	USA	Arizona	Cochise	31.4625	-110.2889
sonorae	CAS	35106	USA	Arizona	Cochise	31.9347	-109.2183
sonorae	CAS	35163	USA	Arizona	Cochise	31.7323	-110.1801
sonorae	CAS	48493	USA	Arizona	Cochise	31.4625	-110.2889
sonorae	CAS	48507	USA	Arizona	Cochise	31.4268	-110.2565
sonorae	CAS	48538	USA	Arizona	Cochise	31.4733	-110.2989
sonorae	CAS	48541	USA	Arizona	Cochise	31.3819	-110.2244
sonorae	CAS	48542	USA	Arizona	Cochise	31.4788	-110.3438
sonorae	CAS	48544	USA	Arizona	Cochise	31.3457	-110.2591
sonorae	CAS	48554	USA	Arizona	Pima	31.7250	-110.8794
sonorae	CAS	48564	USA	Arizona	Santa Cruz	31.6922	-110.9529
sonorae	CAS	115030	Mexico	Sonora		30.9885	-110.8832
sonorae	CAS	152517	USA	Arizona	Santa Cruz	31.5292	-110.7435
sonorae	CAS	173542	USA	Arizona	Cochise	31.9136	-109.1408
sonorae	CAS	189075	USA	Arizona	Cochise	31.4625	-110.2889
sonorae	CAS	189076	USA	Arizona	Cochise	31.4625	-110.2889
sonorae	CAS	189077	USA	Arizona	Cochise	31.4625	-110.2889
sonorae	CAS	189078	USA	Arizona	Cochise	31.4268	-110.2565
sonorae	CAS	189080	USA	Arizona	Cochise	31.4278	-110.4559
sonorae	CAS	189081	USA	Arizona	Santa Cruz	31.4422	-111.1798
sonorae	CAS	189083	USA	Arizona	Greenlee	33.2519	-109.1962
sonorae	CAS	195831	USA	Arizona	Cochise	31.8646	-109.3953
sonorae	CM	47843	USA	Arizona	Santa Cruz	31.7212	-110.7531
sonorae	CM	51854	USA	Arizona	Santa Cruz	31.6400	-110.7067
sonorae	CM	53699	USA	Arizona	Cochise	31.9192	-109.9856
sonorae	CM	64327	USA	Arizona	Cochise	31.9057	-109.2183
sonorae	CM	65741	USA	Arizona	Santa Cruz	31.4175	-111.1482
sonorae	CM	66107	USA	Arizona	Cochise	31.8846	-109.1408
sonorae	CM	70758	USA	Arizona	Graham	32.8933	-109.4778
sonorae	CM	70785	USA	Arizona	Graham	32.5896	-109.7964
sonorae	CM	70875	USA	Arizona	Graham	32.7043	-109.7852
sonorae	CM	70896	USA	Arizona	Graham	32.7043	-109.7852
sonorae	CM	70985	USA	Arizona	Graham	32.5341	-109.8095
sonorae	CU	10047	USA	Arizona	Santa Cruz	31.4422	-111.1798
sonorae	CU	11168	USA	New Mexico	Hidalgo	31.8352	-108.8939
sonorae	CU	13755	USA	Arizona	Cochise	31.9136	-109.1921

Spp	Inst.	Specimen#	Country	State/Province	County	Latitude	Longitude
sonorae	KUNHM	6772	USA	Arizona	Cochise	31.4025	-109.9161
sonorae	KUNHM	6801	USA	Arizona	Cochise	31.3819	-110.2244
sonorae	KUNHM	6886	USA	Arizona	Cochise	31.4625	-110.2889
sonorae	KUNHM	8984	USA	Arizona	Cochise	31.4625	-110.2889
sonorae	KUNHM	13096	USA	Arizona	Pima	32.3293	-110.7929
sonorae	KUNHM	15465	USA	Arizona	Cochise	31.3457	-110.2591
sonorae	KUNHM	48357	USA	Arizona	Santa Cruz	31.7237	-111.1232
sonorae	KUNHM	48424	USA	Arizona	Santa Cruz	31.3957	-111.0906
sonorae	KUNHM	179559	USA	Arizona	Santa Cruz	31.4090	-111.2875
sonorae	LACM	14730	USA	Arizona	Santa Cruz	31.4422	-111.1798
sonorae	LACM	53343	Mexico	Sonora		31.0101	-110.4040
sonorae	LACM	53350	USA	Arizona	Pima	31.4886	-111.4988
sonorae	LACM	53351	Mexico	Sonora		30.9849	-110.2879
sonorae	LACM	62167	USA	Arizona	Santa Cruz	31.5059	-110.8066
sonorae	LACM	76385	USA	Arizona	Santa Cruz	31.4422	-111.1798
sonorae	LACM	99942	USA	Arizona	Cochise	31.4625	-110.2889
sonorae	LACM	112422	USA	Arizona	Pima	31.7350	-110.6764
sonorae	LACM	112429	USA	Arizona	Santa Cruz	31.4422	-111.1798
sonorae	LACM	112778	USA	Arizona	Cochise	31.3332	-109.0869
sonorae	LACM	112779	USA	New Mexico	Hidalgo	31.5179	-109.0145
sonorae	LACM	114673	Mexico	Sonora		29.7898	-109.6926
sonorae	LACM	114684	Mexico	Sonora		29.8061	-109.6250
sonorae	LACM	114690	Mexico	Sonora		30.1230	-109.3361
sonorae	LACM	114710	Mexico	Sonora		30.2916	-108.9374
sonorae	LACM	114716	USA	Arizona	Pinal	32.5903	-110.7946
sonorae	LACM	114840	USA	Arizona	Pinal	32.5954	-110.7886
sonorae	LACM	115677	USA	Arizona	Santa Cruz	31.4856	-111.0522
sonorae	LACM	116315	USA	Arizona	Pinal	32.5903	-110.7946
sonorae	LACM	122412	Mexico	Sonora		30.1261	-109.3339
sonorae	LACM	123459	USA	Arizona	Pinal	32.5408	-110.7089
sonorae	LACM	123464	USA	Arizona	Santa Cruz	31.3401	-111.1715
sonorae	LACM	127266	USA	Arizona	Pinal	32.5903	-110.7946
sonorae	LACM	128337	USA	Arizona	Santa Cruz	31.4422	-111.1798
sonorae	LACM	131778	USA	Arizona	Cochise	31.8471	-109.1993
sonorae	LACM	131794	Mexico	Sonora		29.9224	-109.2928
sonorae	LACM	134371	USA	Arizona	Pima	32.3383	-110.7237
sonorae	LACM	134375	USA	Arizona	Pinal	32.6108	-110.7703
sonorae	LACM	134377	USA	Arizona	Santa Cruz	31.4422	-111.1798
sonorae	LACM	134810	USA	Arizona	Pima	32.3293	-110.7929
sonorae	LACM	140510	USA	Arizona	Pima	31.9639	-111.5992
sonorae	LACM	144434	USA	Arizona	Pima	31.8578	-110.7881
sonorae	LACM	144436	USA	Arizona	Pima	32.3653	-110.8942
sonorae	LACM	153155	USA	Arizona	Pima	32.3293	-110.7929
sonorae	LACM	153158	USA	Arizona	Pima	32.3293	-110.7929
sonorae	LACM	153161	USA	Arizona		32.3293	-110.7929
sonorae	LSU	9812	USA	Arizona	Santa Cruz	31.3999	-111.0640
sonorae	LSU	9813	USA	Arizona	Pima	31.7598	-110.8654
sonorae	LSU	9814	USA	Arizona	Santa Cruz	31.4406	-111.2129
sonorae	LSU	13592	USA	Arizona	Cochise	31.9136	-109.1408
sonorae	LSU	28651	USA	Arizona	Pima	32.3196	-110.7805
sonorae	LSU	36865	USA	Arizona	Santa Cruz	31.5589	-111.3181
sonorae	LSU	72954	USA	Arizona	Pima	31.9994	-110.5794
sonorae	LSU	73190	USA	Arizona	Santa Cruz	31.4854	-110.9336
sonorae	LSU	86677	USA	Arizona	Pinal	32.7370	-110.6400
sonorae	MVZ	65685	USA	Arizona	Santa Cruz	31.6792	-110.4330
sonorae	SDNHM	5038	USA	Arizona	Santa Cruz	31.7250	-110.8794
sonorae	SDNHM	14861	USA	Arizona	Cochise	31.4625	-110.2889
sonorae	SDNHM	14880	USA	Arizona	Cochise	31.4268	-110.2565

Spp	Inst.	Specimen#	Country	State/Province	County	Latitude	Longitude
sonorae	SDNHM	14884	USA	Arizona	Cochise	31.4268	-110.2565
sonorae	SDNHM	14907	USA	Arizona	Santa Cruz	31.5612	-111.1055
sonorae	SDNHM	14913	USA	Arizona	Santa Cruz	31.6125	-111.0453
sonorae	SDNHM	15025	USA	Arizona	Pima	32.3293	-110.7929
sonorae	SDNHM	15732	USA	Arizona	Cochise	31.9683	-109.3264
sonorae	SDNHM	15747	USA	Arizona	Cochise	31.9683	-109.3264
sonorae	SDNHM	15766	USA	Arizona	Cochise	31.9347	-109.1328
sonorae	SDNHM	17927	USA	Arizona	Santa Cruz	31.3838	-110.9336
sonorae	SDNHM	17969	USA	Arizona	Santa Cruz	31.5138	-110.7857
sonorae	SDNHM	34489	USA	Arizona	Cochise	32.0280	-110.1065
sonorae	SDNHM	35260	USA	Arizona	Pima	32.3293	-110.7929
sonorae	SDNHM	56219	USA	Arizona	Cochise	31.9683	-109.3264
sonorae	SDNHM	56241	USA	Arizona	Santa Cruz	31.7250	-110.8794
sonorae	SDNHM	62727	USA	Arizona	Santa Cruz	31.4422	-111.1798
sonorae	SDNHM	62742	USA	Arizona	Santa Cruz	31.4422	-111.1798
sonorae	SDNHM	72397	USA	Arizona	Pinal	32.6108	-110.7703
sonorae	SDNHM	72399	USA	Arizona	Pinal	32.6108	-110.7703
sonorae	SDNHM	72402	USA	Arizona	Santa Cruz	31.7250	-110.8794
sonorae	SDNHM	72408	USA	Arizona	Pima	32.3293	-110.7929
sonorae	TCWC	56353	USA	New Mexico	Hidalgo	31.7542	-108.9022
sonorae	TCWC	62780	USA	New Mexico	Catron	33.2432	-108.8722
sonorae	TCWC	68324	USA	Arizona	Pima	31.7788	-110.8886
sonorae	UAZ	4937	USA	Arizona	Cochise	31.4625	-110.2889
sonorae	UAZ	4938	USA	Arizona	Cochise	31.4788	-110.3438
sonorae	UAZ	4939	USA	Arizona	Cochise	31.4788	-110.3438
sonorae	UAZ	4941	USA	Arizona	Cochise	31.4339	-110.4044
sonorae	UAZ	4953	USA	Arizona	Pima	31.7350	-110.6764
sonorae	UAZ	4954	USA	Arizona	Pima	31.7250	-110.8794
sonorae	UAZ	4955	USA	Arizona	Santa Cruz	31.4422	-111.1798
sonorae	UAZ	4956	USA	Arizona	Santa Cruz	31.3813	-110.8855
sonorae	UAZ	4958	USA	Arizona	Santa Cruz	31.4422	-111.1798
sonorae	UAZ	4961	USA	Arizona	Pima	31.5747	-111.4100
sonorae	UAZ	4962	USA	Arizona	Santa Cruz	31.4422	-111.1798
sonorae	UAZ	4964	USA	Arizona	Santa Cruz	31.4364	-110.9386
sonorae	UAZ	4966	USA	Arizona	Santa Cruz	31.6125	-111.0453
sonorae	UAZ	4967	USA	Arizona	Santa Cruz	31.3403	-110.9336
sonorae	UAZ	5046	USA	Arizona	Graham	32.4374	-110.3261
sonorae	UAZ	5047	USA	Arizona	Graham	32.4274	-110.3378
sonorae	UAZ	5049	USA	Arizona	Cochise	31.9192	-109.9856
sonorae	UAZ	5057	USA	Arizona	Graham	32.6514	-109.8039
sonorae	UAZ	5092	USA	New Mexico	Hidalgo	31.7047	-109.0306
sonorae	UAZ	5149	USA	Arizona	Cochise	31.9136	-109.1408
sonorae	UAZ	9169	Mexico	Sonora		30.7966	-109.5726
sonorae	UAZ	9248	USA	New Mexico	Grant	33.1219	-108.9556
sonorae	UAZ	9274	USA	Arizona	Santa Cruz	31.5895	-110.6547
sonorae	UAZ	9278	USA	Arizona	Pima	31.8578	-110.8222
sonorae	UAZ	10910	USA	Arizona	Pima	32.3356	-110.6958
sonorae	UAZ	10968	USA	Arizona	Pima	31.9639	-111.5992
sonorae	UAZ	11108	USA	Arizona	Pinal	32.5408	-110.7089
sonorae	UAZ	11765	USA	Arizona	Pinal	32.5903	-110.7946
sonorae	UAZ	11909	USA	Arizona	Pinal	32.5207	-110.7819
sonorae	UAZ	13823	USA	Arizona	Santa Cruz	31.3995	-111.1647
sonorae	UAZ	14277	USA	Arizona	Pima	31.9639	-111.5992
sonorae	UAZ	14411	USA	Arizona	Pima	31.9639	-111.5992
sonorae	UAZ	14952	USA	Arizona	Pima	32.3293	-110.7929
sonorae	UAZ	15541	USA	Arizona	Pima	32.3293	-110.7929
sonorae	UAZ	15555	USA	Arizona	Pima	31.9639	-111.5992
sonorae	UAZ	18157	USA	Arizona	Pinal	32.5903	-110.7946

Spp	Inst.	Specimen#	Country	State/Province	County	Latitude	Longitude
sonorae	UAZ	19875	USA	Arizona	Pinal	32.7705	-110.7703
sonorae	UAZ	20677	USA	Arizona	Pima	32.3196	-110.7805
sonorae	UAZ	24756	USA	Arizona	Cochise	31.8345	-110.3601
sonorae	UAZ	24797	USA	Arizona	Santa Cruz	31.4422	-111.1798
sonorae	UAZ	24827	USA	Arizona	Cochise	31.8345	-110.3601
sonorae	UAZ	30087	USA	Arizona	Pima	32.3196	-110.7805
sonorae	UAZ	30089	USA	Arizona	Pima	32.2773	-110.6335
sonorae	UAZ	30682	USA	Arizona	Pima	32.3542	-110.9381
sonorae	UAZ	32128	USA	Arizona	Pinal	32.6207	-110.9917
sonorae	UAZ	36115	USA	Arizona	Santa Cruz	31.4091	-111.1868
sonorae	UAZ	36117	USA	Arizona	Santa Cruz	31.4683	-111.2165
sonorae	UAZ	36254	USA	Arizona	Santa Cruz	31.4290	-111.0005
sonorae	UAZ	36439	USA	Arizona	Santa Cruz	31.4676	-110.8399
sonorae	UAZ	36638	USA	Arizona	Pima	32.3293	-110.7929
sonorae	UAZ	39090	USA	Arizona	Cochise	31.9192	-109.9856
sonorae	UAZ	43667	USA	Arizona	Cochise	31.4712	-110.2889
sonorae	UAZ	43742	USA	Arizona	Pima	31.9154	-110.6811
sonorae	UAZ	44967	USA	Arizona	Pima	32.3293	-110.7929
sonorae	UAZ	44968	USA	Arizona	Pima	32.3293	-110.7929
sonorae	UAZ	47304	USA	Arizona	Pima	31.7639	-110.8007
sonorae	UAZ	50049	USA	Arizona	Cochise	31.4339	-110.4044
sonorae	UAZ	50121	USA	Arizona	Pima	31.5885	-111.5087
sonorae	UAZ	50258	USA	Arizona	Pima	31.4932	-111.5518
sonorae	UAZ	50260	USA	Arizona	Pima	31.4702	-111.5127
sonorae	UAZ	50641	USA	Arizona	Pima	31.5885	-111.5087
sonorae	UAZ	50813	USA	Arizona	Pima	31.9639	-111.5992
sonorae	UAZ	50814	USA	Arizona	Pima	31.9639	-111.5992
sonorae	UAZ	51079	USA	Arizona	Pima	31.7639	-110.8007
sonorae	UAZ	51780	USA	Arizona	Cochise	31.7666	-110.4278
sonorae	UAZ	51782	USA	Arizona	Cochise	31.8682	-110.3940
sonorae	UAZ	51784	USA	Arizona	Cochise	31.8682	-110.3940
sonorae	UAZ	51786	USA	Arizona	Cochise	31.8828	-110.4109
sonorae	UAZ	51788	USA	Arizona	Pima	31.8537	-110.4784
sonorae	UAZ	51789	USA	Arizona	Cochise	31.8102	-110.3772
sonorae	UAZ	51865	USA	Arizona	Cochise	32.2889	-110.1740
sonorae	UAZ	51873	USA	Arizona	Pima	32.0874	-110.5082
sonorae	UAZ	51876	USA	Arizona	Pima	32.1447	-110.4572
sonorae	UAZ	51879	USA	Arizona	Pima	32.1591	-110.4742
sonorae	UAZ	51976	USA	Arizona	Pima	31.5834	-111.6306
sonorae	UAZ	51987	USA	Arizona	Santa Cruz	31.5897	-111.0881
sonorae	UAZ	51991	USA	Arizona	Pima	32.3356	-110.6958
sonorae	UAZ	51992	USA	Arizona	Pima	32.3356	-110.6958
sonorae	UAZ	51993	USA	Arizona	Pima	32.3356	-110.6958
sonorae	UAZ	51999	USA	Arizona	Pima	31.7666	-111.5517
sonorae	UAZ	52124	USA	Arizona	Santa Cruz	31.4422	-111.1798
sonorae	UAZ	52155	USA	Arizona	Pima	32.0420	-111.8089
sonorae	UAZ	52464	USA	Arizona	Cochise	31.6181	-109.4726
sonorae	UAZ	52470	USA	Arizona	Cochise	31.4163	-110.4338
sonorae	UAZ	52729	USA	New Mexico	Grant	32.7706	-108.6209
sonorae	UAZ	52735	USA	New Mexico	Grant	32.7706	-108.6209
sonorae	UAZ	52737	USA	New Mexico	Grant	32.7706	-108.6209
sonorae	UAZ	52738	USA	New Mexico	Grant	32.7706	-108.5180
sonorae	UAZ	52742	USA	Arizona	Greenlee	33.2152	-109.1955
sonorae	UAZ	52745	USA	New Mexico	Grant	32.7561	-108.5180
sonorae	UAZ	52747	USA	New Mexico	Grant	32.7706	-108.6209
sonorae	UAZ	52761	USA	Arizona	Cochise	31.4339	-110.4044
sonorae	UAZ	52764	USA	Arizona	Cochise	31.3421	-109.0495
sonorae	UAZ	52766	USA	Arizona	Cochise	31.4921	-109.3717

Spp	Inst.	Specimen#	Country	State/Province	County	Latitude	Longitude
sonorae	UAZ	55351	USA	Arizona	Pima	32.3293	-110.7929
sonorae	UAZ	55430	USA	Arizona	Pima	32.2217	-110.9258
sonorae	UAZ	55455	USA	Arizona	Cochise	32.0044	-109.3561
sonorae	UAZ	55456	USA	Arizona	Cochise	32.0044	-109.3561
sonorae	UAZ	56687	USA	Arizona	Pinal	32.6108	-110.7703
sonorae	UCM	42082	Mexico	Sonora		30.4175	-109.7010
sonorae	UCM	56291	USA	Arizona	Santa Cruz	31.5981	-110.4524
sonorae	UCM	56292	USA	Arizona	Santa Cruz	31.5793	-110.4856
sonorae	UCM	56293	USA	Arizona	Santa Cruz	31.5673	-110.4162
sonorae	UCM	56298	USA	Arizona	Santa Cruz	31.5793	-110.4856
sonorae	UCM	61740	USA	Arizona	Cochise	31.9192	-109.9856
sonorae	UCM	61743	USA	Arizona	Cochise	31.9455	-109.9425
sonorae	UCM	61835	USA	Arizona	Cochise	31.9192	-109.9856
sonorae	UTEP	16184	USA	New Mexico	Grant	32.8577	-108.9637
sonorae	YPM	1417	USA	Arizona	Santa Cruz	31.7250	-110.8794
uniparens	ASU	5309	Mexico	Chihuahua		30.0657	-107.6089
uniparens	CAS	1614	USA	Arizona	Cochise	31.7323	-110.1801
uniparens	CAS	35113	USA	Arizona	Cochise	31.9347	-109.2183
uniparens	CAS	35164	USA	Arizona	Cochise	31.7323	-110.1801
uniparens	CAS	39846	USA	Arizona	Cochise	31.3444	-109.5447
uniparens	CAS	39848	USA	Arizona	Cochise	31.4186	-109.8794
uniparens	CAS	48512	USA	Arizona	Cochise	31.4268	-110.2565
uniparens	CAS	173540	USA	Arizona	Cochise	31.9136	-109.1408
uniparens	CAS	203889	USA	Arizona	Cochise	31.6923	-110.0428
uniparens	CAS	203890	USA	Arizona	Cochise	31.6923	-110.0428
uniparens	CAS	203891	USA	Arizona	Cochise	31.6923	-110.0428
uniparens	CAS	203893	USA	Arizona	Cochise	31.3660	-109.8733
uniparens	CAS	203898	USA	Arizona	Cochise	31.7127	-109.9305
uniparens	CAS	203899	USA	Arizona	Cochise	31.7127	-109.9305
uniparens	CAS	203964	USA	Arizona	Cochise	31.4667	-109.7235
uniparens	CAS	203966	USA	Arizona	Cochise	31.7128	-110.0669
uniparens	CAS	203967	USA	Arizona	Santa Cruz	31.6794	-110.5490
uniparens	CAS	203968	USA	Arizona	Cochise	31.6792	-110.4211
uniparens	CAS	203969	USA	New Mexico	Hidalgo	31.9488	-108.9435
uniparens	CAS	203971	USA	Arizona	Cochise	31.4383	-110.0972
uniparens	CM	18210	USA	New Mexico	Hidalgo	31.4169	-108.9292
uniparens	CM	18239	USA	New Mexico	Dona Ana	32.4865	-106.9842
uniparens	CM	18254	USA	New Mexico	Dona Ana	32.4865	-106.9842
uniparens	CM	43205	Mexico	Chihuahua		29.9000	-106.4167
uniparens	CM	43231	USA	New Mexico	Grant	33.1823	-108.8239
uniparens	CM	48461	USA	New Mexico	Dona Ana	32.6653	-107.1697
uniparens	CM	48709	USA	Arizona	Graham	32.7043	-109.7852
uniparens	CM	48790	USA	New Mexico	Sierra	32.8964	-107.2911
uniparens	CM	51879	USA	Arizona	Graham	32.7043	-109.7852
uniparens	CM	54938	USA	Arizona	Cochise	32.3620	-109.6201
uniparens	CM	54957	USA	Arizona	Graham	32.5629	-109.7267
uniparens	CM	54966	USA	New Mexico	Hidalgo	32.4842	-108.8415
uniparens	CM	54973	USA	New Mexico	Grant	32.5903	-107.9753
uniparens	CM	58116	USA	Arizona	Cochise	32.1514	-109.4527
uniparens	CM	64331	USA	Arizona	Cochise	31.9136	-109.0211
uniparens	CM	64348	USA	Arizona	Cochise	31.9426	-109.1408
uniparens	CM	65797	USA	Arizona	Yavapai	34.7711	-112.0572
uniparens	CM	65798	USA	Arizona	Gila	34.3627	-111.4544
uniparens	CM	65799	USA	Arizona	Yavapai	34.2658	-112.1037
uniparens	CM	65803	USA	Arizona	Yavapai	34.6776	-112.0841
uniparens	CM	65972	USA	Arizona	Cochise	31.9136	-109.1750
uniparens	CM	69716	USA	Arizona	Cochise	31.9136	-109.0553
uniparens	CM	70568	USA	New Mexico	Sierra	33.1933	-106.6222

Spp	Inst.	Specimen#	Country	State/Province	County	Latitude	Longitude
uniparens	CM	70665	USA	Arizona	Graham	32.7043	-109.7852
uniparens	CM	70802	USA	Arizona	Graham	32.5341	-109.8095
uniparens	CM	70988	USA	Arizona	Graham	32.5341	-109.8095
uniparens	CM	71263	USA	Arizona	Graham	32.4556	-109.9027
uniparens	CM	71592	USA	Arizona	Graham	32.7043	-109.7852
uniparens	CM	75505	USA	New Mexico	Hidalgo	31.9213	-108.8067
uniparens	CM	75527	USA	New Mexico	Hidalgo	31.9489	-108.8580
uniparens	CM	75542	USA	New Mexico	Hidalgo	31.9489	-108.8768
uniparens	CM	83698	USA	Arizona	Graham	32.8339	-109.7069
uniparens	CM	90166	USA	Arizona	Yavapai	34.4924	-112.6206
uniparens	CM	137898	USA	New Mexico	Dona Ana	32.2785	-106.6407
uniparens	KUNHM	6804	USA	Arizona	Cochise	31.3819	-110.2244
uniparens	KUNHM	12798	USA	Arizona	Cochise	31.4624	-110.1528
uniparens	KUNHM	44251	USA	New Mexico	Grant	32.1911	-108.2948
uniparens	KUNHM	47380	Mexico	Chihuahua		31.5667	-107.6167
uniparens	KUNHM	48474	USA	Arizona	Cochise	31.4383	-110.0972
uniparens	KUNHM	49555	USA	Arizona	Cochise	31.9025	-109.1092
uniparens	KUNHM	49574	USA	New Mexico	Grant	32.7700	-108.2797
uniparens	KUNHM	49576	USA	New Mexico	Grant	32.7700	-108.2797
uniparens	KUNHM	49577	USA	New Mexico	Sierra	32.9754	-107.5148
uniparens	KUNHM	49596	USA	New Mexico	Luna	32.0487	-108.3197
uniparens	KUNHM	50198	USA	New Mexico	Grant	32.7699	-108.4350
uniparens	KUNHM	72282	USA	New Mexico	Hidalgo	32.3503	-108.7081
uniparens	KUNHM	73298	USA	New Mexico	Hidalgo	31.3951	-108.5624
uniparens	KUNHM	300588	USA	New Mexico	Luna	32.2680	-108.1357
uniparens	KUNHM	318169	USA	Arizona	Pima	32.3392	-110.9089
uniparens	KUNHM	318171	USA	Arizona	Pima	32.3542	-110.9381
uniparens	KUNHM	318172	USA	Arizona	Pima	32.3542	-110.9381
uniparens	LACM	7642	USA	New Mexico	Dona Ana	32.2700	-106.8346
uniparens	LACM	7646	USA	New Mexico	Hidalgo	31.9488	-108.9435
uniparens	LACM	7702	USA	New Mexico	Hidalgo	32.0886	-108.9731
uniparens	LACM	7704	USA	New Mexico	Hidalgo	31.7439	-108.3198
uniparens	LACM	7708	USA	New Mexico	Hidalgo	31.5100	-109.0431
uniparens	LACM	7709	USA	New Mexico	Grant	32.6847	-108.1314
uniparens	LACM	7711	USA	New Mexico	Dona Ana	32.5107	-106.8236
uniparens	LACM	53312	USA	Arizona	Pima	31.4886	-111.4988
uniparens	LACM	53313	USA	Arizona	Pima	31.5746	-111.5123
uniparens	LACM	53314	Mexico	Sonora		31.2900	-109.6900
uniparens	LACM	53316	Mexico	Sonora		31.2621	-109.9483
uniparens	LACM	76172	USA	New Mexico	Luna	31.8055	-107.7027
uniparens	LACM	76402	USA	New Mexico	Grant	32.4910	-108.4875
uniparens	LACM	76419	USA	New Mexico	Sierra	32.7667	-107.2872
uniparens	LACM	100621	USA	New Mexico	Dona Ana	32.6653	-107.1318
uniparens	LACM	100624	USA	New Mexico	Hidalgo	31.9488	-108.6852
uniparens	LACM	100627	USA	New Mexico	Hidalgo	31.9010	-108.8067
uniparens	LACM	100632	USA	New Mexico	Hidalgo	31.9489	-108.7554
uniparens	LACM	100633	USA	New Mexico	Hidalgo	31.9489	-108.7211
uniparens	LACM	100642	USA	New Mexico	Luna	32.2686	-107.7958
uniparens	LACM	100647	USA	New Mexico	Sierra	32.7685	-107.5664
uniparens	LACM	107270	USA	Arizona	Pima	32.2773	-110.6335
uniparens	LACM	108875	USA	New Mexico	Grant	32.5351	-108.0023
uniparens	LACM	109454	USA	New Mexico	Luna	32.3483	-107.8228
uniparens	LACM	109455	USA	New Mexico	Luna	32.4327	-107.9109
uniparens	LACM	112786	USA	New Mexico	Socorro	33.8055	-106.8891
uniparens	LACM	112788	USA	New Mexico	Hidalgo	31.5179	-109.0145
uniparens	LACM	115676	USA	Arizona	Cochise	31.3443	-109.3578
uniparens	LACM	121454	USA	New Mexico	Hidalgo	31.9488	-108.9435
uniparens	LACM	126966	USA	New Mexico	Hidalgo	32.0385	-109.0306

Spp	Inst.	Specimen#	Country	State/Province	County	Latitude	Longitude
uniparens	LACM	126967	USA	Arizona	Cochise	31.6998	-109.6864
uniparens	LACM	128372	USA	New Mexico	Hidalgo	31.8353	-109.0306
uniparens	LACM	130659	USA	Arizona	Yavapai	34.8958	-112.4800
uniparens	LACM	131800	USA	Arizona	Pinal	32.6480	-110.7242
uniparens	LACM	133677	USA	New Mexico	Hidalgo	32.3500	-108.4504
uniparens	LACM	133678	USA	New Mexico	Dona Ana	32.4250	-106.5748
uniparens	LACM	133682	USA	New Mexico	Dona Ana	32.5107	-106.8236
uniparens	LACM	134394	USA	New Mexico	Hidalgo	32.2456	-108.9695
uniparens	LACM	134396	USA	New Mexico	Luna	32.2686	-107.7581
uniparens	LACM	134835	USA	Arizona	Pima	32.3293	-110.7929
uniparens	LACM	135888	Mexico	Chihuahua		29.8600	-107.4400
uniparens	LACM	153347	USA	Arizona	Pima	31.8578	-110.7881
uniparens	LSU	13590	USA	Arizona	Cochise	31.8726	-109.0925
uniparens	LSU	28652	USA	Arizona	Pima	32.3196	-110.7805
uniparens	LSU	30841	USA	Arizona	Yavapai	34.8001	-112.0572
uniparens	LSU	30854	USA	Arizona	Yavapai	34.3639	-112.7383
uniparens	LSU	30858	USA	Arizona	Gila	34.2206	-111.3120
uniparens	LSU	30862	USA	Arizona	Yavapai	34.6725	-111.9280
uniparens	LSU	30866	USA	Arizona	Yavapai	34.5300	-112.1613
uniparens	LSU	31182	USA	Arizona	Gila	34.3627	-111.4544
uniparens	LSU	31187	USA	Arizona	Coconino	34.8842	-111.7603
uniparens	LSU	31192	USA	Arizona	Yavapai	34.7392	-112.0092
uniparens	LSU	31223	USA	Arizona	Yavapai	34.6722	-111.9754
uniparens	LSU	36835	USA	Arizona	Yavapai	34.4924	-112.6206
uniparens	LSU	50786	USA	Arizona	Coconino	34.8697	-111.7444
uniparens	LSU	73283	USA	Arizona	Cochise	31.7464	-110.1143
uniparens	MVZ	7894	USA	Arizona	Cochise	32.0156	-109.6128
uniparens	MVZ	7900	USA	Arizona	Cochise	32.0011	-109.6128
uniparens	MVZ	7903	USA	Arizona	Cochise	32.1137	-109.5400
uniparens	MVZ	7906	USA	Arizona	Cochise	32.0829	-109.5037
uniparens	MVZ	42576	USA	New Mexico	Grant	32.7700	-108.2797
uniparens	MVZ	42577	USA	New Mexico	Grant	32.7700	-108.2797
uniparens	MVZ	42579	USA	New Mexico	Grant	33.0750	-108.4760
uniparens	MVZ	46676	Mexico	Chihuahua		30.5333	-106.9667
uniparens	MVZ	70905	Mexico	Chihuahua		29.4667	-106.3167
uniparens	MVZ	70913	Mexico	Chihuahua		29.3226	-106.4500
uniparens	MVZ	97066	USA	New Mexico	Hidalgo	32.0886	-108.9731
uniparens	SDNHM	4898	USA	Arizona	Cochise	31.7125	-110.3229
uniparens	SDNHM	14878	USA	Arizona	Cochise	31.4733	-110.2989
uniparens	SDNHM	14919	USA	Arizona	Santa Cruz	31.6125	-111.0453
uniparens	SDNHM	14924	USA	Arizona	Cochise	31.4383	-110.1993
uniparens	SDNHM	14958	USA	Arizona	Cochise	31.4383	-110.0632
uniparens	SDNHM	15730	USA	Arizona	Cochise	31.9683	-109.3264
uniparens	SDNHM	15734	USA	Arizona	Cochise	31.9683	-109.3264
uniparens	SDNHM	22914	USA	Arizona	Pinal	32.6108	-110.7703
uniparens	SDNHM	32362	USA	Arizona	Cochise	31.9677	-110.4650
uniparens	SDNHM	72464	USA	New Mexico	Luna	32.2686	-107.7581
uniparens	TCWC	35451	USA	New Mexico	Hidalgo	31.9488	-108.9435
uniparens	TCWC	35453	USA	New Mexico	Hidalgo	32.0824	-108.9767
uniparens	TCWC	56344	USA	New Mexico	Hidalgo	31.8784	-108.2103
uniparens	TCWC	56346	USA	New Mexico	Hidalgo	31.9295	-108.9916
uniparens	TCWC	56356	USA	New Mexico	Grant	31.9181	-108.3197
uniparens	TCWC	56370	USA	New Mexico	Grant	31.9179	-108.5249
uniparens	TCWC	56377	USA	New Mexico	Hidalgo	31.8513	-108.3197
uniparens	TCWC	56403	USA	New Mexico	Luna	31.8275	-107.6394
uniparens	TCWC	56410	USA	New Mexico	Luna	32.2684	-107.5435
uniparens	TCWC	62757	USA	New Mexico	Hidalgo	31.8353	-109.0476
uniparens	TCWC	63589	USA	New Mexico	Hidalgo	31.8353	-109.0476

Spp	Inst.	Specimen#	Country	State/Province	County	Latitude	Longitude
uniparens	UAZ	5125	Mexico	Sonora		30.9832	-110.3013
uniparens	UAZ	5157	USA	Arizona	Cochise	31.9018	-109.8157
uniparens	UAZ	5158	USA	Arizona	Cochise	31.6903	-109.0549
uniparens	UAZ	5161	USA	Arizona	Cochise	31.4625	-110.2889
uniparens	UAZ	5169	USA	Arizona	Cochise	31.4625	-110.2889
uniparens	UAZ	5176	USA	Arizona	Cochise	31.6051	-109.2318
uniparens	UAZ	5180	USA	Arizona	Cochise	31.3426	-109.9684
uniparens	UAZ	5203	USA	Arizona	Cochise	31.9136	-109.1750
uniparens	UAZ	5208	USA	New Mexico	Hidalgo	31.7347	-108.9122
uniparens	UAZ	5209	USA	Arizona	Santa Cruz	31.6125	-111.0453
uniparens	UAZ	5213	USA	New Mexico	Hidalgo	32.4856	-108.5477
uniparens	UAZ	5226	USA	New Mexico	Hidalgo	32.4856	-108.5477
uniparens	UAZ	5230	USA	New Mexico	Hidalgo	32.0824	-108.9767
uniparens	UAZ	5232	USA	New Mexico	Grant	32.9935	-108.5431
uniparens	UAZ	5268	USA	Arizona	Cochise	31.7323	-110.1801
uniparens	UAZ	5278	USA	Arizona	Cochise	31.7323	-110.1801
uniparens	UAZ	5303	USA	New Mexico	Socorro	33.7000	-106.9867
uniparens	UAZ	5324	USA	Arizona	Cochise	31.5875	-110.2583
uniparens	UAZ	5326	USA	Arizona	Cochise	31.4625	-110.2889
uniparens	UAZ	5331	USA	Arizona	Cochise	31.4625	-110.2889
uniparens	UAZ	5334	USA	Arizona	Pima	31.8263	-110.5934
uniparens	UAZ	9171	Mexico	Sonora		30.7933	-109.5733
uniparens	UAZ	9181	Mexico	Sonora		31.0328	-109.5722
uniparens	UAZ	9285	USA	Arizona	Pima	31.8578	-110.8222
uniparens	UAZ	10502	USA	New Mexico	Grant	33.1219	-108.9556
uniparens	UAZ	10889	USA	Arizona	Graham	32.5595	-109.7665
uniparens	UAZ	10892	USA	Arizona	Graham	32.5692	-109.8129
uniparens	UAZ	10912	USA	Arizona	Graham	32.5595	-109.7665
uniparens	UAZ	11005	USA	Arizona	Cochise	31.3443	-109.7317
uniparens	UAZ	11072	USA	Arizona	Graham	32.5962	-109.8957
uniparens	UAZ	11180	USA	Arizona	Santa Cruz	31.5394	-110.7590
uniparens	UAZ	11221	USA	Arizona	Graham	32.5692	-109.8129
uniparens	UAZ	15414	USA	Arizona	Santa Cruz	31.6794	-110.7229
uniparens	UAZ	15783	USA	New Mexico	Grant	32.6266	-108.1314
uniparens	UAZ	15819	USA	Arizona	Yavapai	34.5636	-111.8536
uniparens	UAZ	17234	USA	Arizona	Santa Cruz	31.6167	-110.5872
uniparens	UAZ	18521	USA	New Mexico	Sierra	32.8529	-107.2911
uniparens	UAZ	30080	USA	Arizona	Maricopa	33.5478	-112.2774
uniparens	UAZ	31019	USA	New Mexico	Catron	33.2441	-108.8825
uniparens	UAZ	33039	USA	Arizona	Cochise	32.0054	-109.4406
uniparens	UAZ	34531	Mexico	Chihuahua		31.1767	-107.9051
uniparens	UAZ	35763	USA	Arizona	Graham	32.8384	-110.2184
uniparens	UAZ	36129	Mexico	Chihuahua		30.0705	-107.5799
uniparens	UAZ	36308	Mexico	Chihuahua		30.8521	-108.1577
uniparens	UAZ	39097	USA	New Mexico	Hidalgo	31.4639	-108.6961
uniparens	UAZ	39776	Mexico	Sonora		30.6847	-109.5986
uniparens	UAZ	40232	USA	New Mexico	Hidalgo	32.5266	-108.9170
uniparens	UAZ	42788	USA	Arizona	Greenlee	32.5496	-109.1597
uniparens	UAZ	42789	USA	Arizona	Greenlee	32.6074	-109.1768
uniparens	UAZ	42792	USA	New Mexico	Hidalgo	32.5965	-108.9637
uniparens	UAZ	42795	USA	Arizona	Graham	32.5496	-109.2280
uniparens	UAZ	42798	USA	Arizona	Greenlee	32.8818	-109.0914
uniparens	UAZ	42799	USA	Arizona	Cochise	31.8102	-110.1916
uniparens	UAZ	42800	USA	Arizona	Greenlee	32.8673	-109.1085
uniparens	UAZ	42805	USA	Arizona	Cochise	32.1514	-109.4527
uniparens	UAZ	42806	USA	Arizona	Cochise	32.1514	-109.4527
uniparens	UAZ	43621	USA	Arizona	Yavapai	34.3139	-112.8583
uniparens	UAZ	43622	USA	New Mexico	Hidalgo	31.3504	-108.3192

Spp	Inst.	Specimen#	Country	State/Province	County	Latitude	Longitude
uniparens	UAZ	43636	USA	New Mexico	Hidalgo	31.4660	-108.6258
uniparens	UAZ	43646	USA	New Mexico	Socorro	33.9318	-107.1185
uniparens	UAZ	43651	USA	New Mexico	Hidalgo	31.3937	-108.3022
uniparens	UAZ	43655	USA	New Mexico	Hidalgo	31.4516	-108.3874
uniparens	UAZ	43662	Mexico	Sonora		30.7207	-109.5862
uniparens	UAZ	43677	USA	Arizona	Cochise	31.4625	-110.2889
uniparens	UAZ	44854	USA	Arizona	Cochise	31.9547	-109.0925
uniparens	UAZ	48833	USA	Arizona	Cochise	32.1336	-109.5609
uniparens	UAZ	50607	USA	Arizona	Pima	31.5885	-111.5087
uniparens	UAZ	50640	USA	Arizona	Pima	31.5885	-111.5087
uniparens	UAZ	51751	USA	Arizona	Cochise	31.8102	-110.3772
uniparens	UAZ	51754	USA	Arizona	Cochise	31.8774	-111.3262
uniparens	UAZ	51860	USA	Arizona	Cochise	32.2889	-110.1911
uniparens	UAZ	52135	USA	Arizona	Pima	31.6877	-111.4282
uniparens	UAZ	52136	USA	Arizona	Pima	31.6877	-111.4282
uniparens	UAZ	52689	USA	Arizona	Cochise	31.3444	-109.4512
uniparens	UAZ	52716	USA	New Mexico	Grant	32.8286	-108.6037
uniparens	UAZ	52720	USA	New Mexico	Grant	32.9697	-108.5861
uniparens	UAZ	52724	USA	New Mexico	Grant	32.7125	-108.7237
uniparens	UAZ	53436	USA	New Mexico	Hidalgo	31.8784	-108.2103
uniparens	UAZ	53473	USA	Arizona	Cochise	32.0049	-109.2484
uniparens	UAZ	54493	USA	New Mexico	Hidalgo	32.2397	-108.9522
uniparens	UAZ	55593	USA	New Mexico	Socorro	34.1167	-107.2030
uniparens	UAZ	56688	USA	Arizona	Yavapai	34.5400	-112.4678
uniparens	UCM	27205	USA	New Mexico	Dona Ana	32.3943	-106.6806
uniparens	UCM	29671	USA	Arizona	Cochise	31.6657	-109.4292
uniparens	UCM	35675	USA	Arizona	Cochise	31.3752	-109.5808
uniparens	UCM	41624	USA	New Mexico	Hidalgo	31.9487	-109.0290
uniparens	UCM	41629	USA	Arizona	Cochise	31.6184	-109.0472
uniparens	UCM	41630	USA	Arizona	Cochise	31.9136	-109.1750
uniparens	UCM	57852	USA	Arizona	Santa Cruz	31.5793	-110.4856
uniparens	UCM	57854	USA	Arizona	Santa Cruz	31.6597	-110.5810
uniparens	UCM	58348	USA	New Mexico	Sierra	33.1486	-107.1443
uniparens	YPM	7906	USA	Arizona	Cochise	31.4625	-110.2889
velox	CAS	10868	USA	Arizona	Yavapai	34.5400	-112.4678
velox	CAS	10869	USA	Arizona	Yavapai	34.5400	-112.3973
velox	CAS	35286	USA	Arizona	Coconino	34.9134	-111.7286
velox	CAS	55028	USA	Utah	Washington	37.3417	-113.2743
velox	CAS	189050	USA	Arizona	Apache	34.3134	-109.3564
velox	CAS	189055	USA	Arizona	Navaho	34.5772	-110.3775
velox	CAS	189057	USA	Arizona	Gila	33.8112	-110.8884
velox	CAS	189062	USA	Utah	San Juan	37.3727	-109.9395
velox	CM	39349	USA	Colorado	Montrose	38.4455	-108.8616
velox	CM	39351	USA	Colorado	Mesa	38.6594	-108.9582
velox	CM	39353	USA	Colorado	Mesa	38.5378	-108.8977
velox	CM	43240	USA	Colorado	Mesa	39.3840	-108.7406
velox	CM	65698	USA	Arizona	Coconino	35.0789	-111.0318
velox	CM	65808	USA	Arizona	Yavapai	34.6776	-112.0841
velox	CM	65809	USA	Arizona	Coconino	35.0789	-111.0318
velox	CM	90156	USA	Arizona	Coconino	34.9961	-111.0225
velox	CM	P1617	USA	New Mexico	San Miguel	35.5939	-105.2233
velox	CU	5609	USA	New Mexico	McKinley	35.2960	-108.7419
velox	CU	5614	USA	New Mexico	McKinley	35.3461	-108.1536
velox	CU	5626	USA	New Mexico	McKinley	35.3010	-108.2228
velox	CU	5675	USA	New Mexico	McKinley	35.3155	-108.2228
velox	CU	5679	USA	Utah	San Juan	37.2844	-109.5511
velox	KUNHM	12741	USA	New Mexico	Rio Arriba	36.4013	-106.1881
velox	KUNHM	12743	USA	New Mexico	McKinley	35.5281	-108.7419

Spp	Inst.	Specimen#	Country	State/Province	County	Latitude	Longitude
velox	KUNHM	50811	USA	Utah	Washington	37.3060	-113.4331
velox	KUNHM	106146	USA	Colorado	Montezuma	37.1996	-108.5426
velox	KUNHM	106148	USA	Colorado	Montezuma	37.2595	-108.4945
velox	KUNHM	318174	USA	New Mexico	San Juan	36.2859	-108.1926
velox	LACM	7712	USA	New Mexico	Sandoval	35.9062	-106.9578
velox	LACM	7928	USA	Arizona	Coconino	36.3322	-112.3567
velox	LACM	7935	USA	Arizona	Coconino	36.3322	-112.3567
velox	LACM	7937	USA	Colorado	Delta	38.8246	-108.3795
velox	LACM	7938	USA	New Mexico	Rio Arriba	36.1589	-105.9742
velox	LACM	7939	USA	New Mexico	McKinley	35.4219	-108.9933
velox	LACM	14656	USA	New Mexico	Santa Fe	35.8758	-106.1419
velox	LACM	28893	USA	New Mexico	San Miguel	35.3354	-105.4503
velox	LACM	100650	USA	Arizona	Coconino	35.0281	-111.0225
velox	LACM	123505	USA	Arizona	Apache	34.5980	-109.6517
velox	LACM	128376	USA	Utah	Washington	37.1857	-112.9886
velox	LACM	134383	USA	New Mexico	Bernalillo	35.1455	-106.3772
velox	LACM	134385	USA	New Mexico	Socorro	34.1505	-107.2024
velox	LACM	135941	USA	New Mexico	Los Alamos	35.8881	-106.3064
velox	LACM	137211	USA	New Mexico	Bernalillo	35.0082	-106.0444
velox	LACM	137272	USA	Arizona	Coconino	35.3739	-111.5732
velox	LACM	178620	USA	Arizona	Yavapai	34.8856	-112.4675
velox	LSU	50787	USA	Arizona	Yavapai	34.6521	-112.0092
velox	LSU	50789	USA	Arizona	Yavapai	34.5736	-112.0411
velox	LSU	73269	USA	Arizona	Gila	34.1014	-110.9631
velox	LSU	73274	USA	Arizona	Gila	34.1014	-110.9631
velox	MCZ	114592	USA	New Mexico	Taos	36.4072	-105.6266
velox	MVZ	16026	USA	Arizona	Coconino	35.2050	-111.4075
velox	MVZ	17873	USA	Arizona	Navaho	36.7278	-110.2539
velox	MVZ	17875	USA	Arizona	Navaho	36.6858	-110.5267
velox	MVZ	17876	USA	Arizona	Navaho	36.7273	-110.5796
velox	MVZ	18209	USA	New Mexico	Rio Arriba	36.1572	-106.6285
velox	MVZ	49855	USA	Arizona	Navaho	34.8297	-110.1575
velox	MVZ	59451	USA	Utah	Washington	37.2569	-112.9461
velox	MVZ	65666	USA	Arizona	Coconino	35.8903	-111.4122
velox	MVZ	65805	USA	New Mexico	McKinley	35.4801	-108.9086
velox	MVZ	75902	USA	Arizona	Yavapai	34.4498	-112.5355
velox	MVZ	180233	USA	Arizona	Navaho	36.7277	-110.3570
velox	SDNHM	2089	USA	Arizona	Coconino	36.1350	-111.2392
velox	SDNHM	5366	USA	Arizona	Yavapai	34.2499	-112.4678
velox	SDNHM	5372	USA	Arizona	Navaho	34.9457	-110.1575
velox	SDNHM	5373	USA	Arizona	Navaho	35.0473	-110.1575
velox	SDNHM	5958	USA	Arizona	Coconino	35.5583	-111.3528
velox	SDNHM	5963	USA	Arizona	Coconino	35.2549	-111.4310
velox	SDNHM	9087	USA	New Mexico	Valencia	34.8253	-106.8381
velox	SDNHM	9090	USA	Arizona	Apache	35.1242	-109.5375
velox	SDNHM	9103	USA	Arizona	Coconino	35.0867	-110.9042
velox	SDNHM	22980	USA	Utah	Kane	37.2955	-112.6383
velox	SDNHM	24747	USA	Utah	Kane	37.0789	-111.6642
velox	SDNHM	25548	USA	New Mexico	Cibola	35.0265	-107.3167
velox	SDNHM	26701	USA	Utah	Kane	37.3178	-112.5972
velox	SDNHM	29087	USA	Arizona	Coconino	35.1628	-111.1169
velox	SDNHM	29196	USA	Arizona	Yavapai	34.8856	-112.4675
velox	SDNHM	35716	USA	Arizona	Yavapai	34.5913	-112.4055
velox	SDNHM	35869	USA	Arizona	Coconino	34.8697	-111.7603
velox	SDNHM	57865	USA	New Mexico	Catron	34.4464	-108.3708
velox	SDNHM	64447	USA	Utah	Garfield	37.8252	-111.4241
velox	SDNHM	72473	USA	New Mexico	Taos	36.4072	-105.5725
velox	TCWC	9419	USA	Arizona	Mohave	35.0875	-113.8887

Spp	Inst.	Specimen#	Country	State/Province	County	Latitude	Longitude
velox	TCWC	71090	USA	Utah	San Juan	37.6096	-110.0232
velox	UAZ	5335	USA	Utah	Kane	37.0475	-112.5263
velox	UAZ	5350	USA	Utah	Kane	37.1163	-112.5274
velox	UAZ	5352	USA	Utah	Kane	37.0487	-112.4747
velox	UAZ	5356	USA	Utah	Kane	37.0456	-112.5561
velox	UAZ	5357	USA	Utah	Kane	37.1321	-112.5674
velox	UAZ	5358	USA	Utah	Kane	37.1127	-112.5639
velox	UAZ	5359	USA	Arizona	Yavapai	34.7784	-112.0572
velox	UAZ	5382	USA	Arizona	Mohave	36.8629	-112.7405
velox	UAZ	5387	USA	Arizona	Coconino	36.1350	-111.2392
velox	UAZ	5394	USA	Arizona	Coconino	36.9456	-112.5258
velox	UAZ	5395	USA	Arizona	Coconino	36.9891	-112.5258
velox	UAZ	5396	USA	Arizona	Navaho	35.8764	-110.6397
velox	UAZ	5399	USA	Arizona	Navaho	35.8764	-110.6397
velox	UAZ	5400	USA	Arizona	Navaho	35.8764	-110.6397
velox	UAZ	5403	USA	Arizona	Yavapai	34.3139	-112.8583
velox	UAZ	5410	USA	Arizona	Navaho	35.8764	-110.6397
velox	UAZ	5414	USA	Arizona	Yavapai	35.2250	-112.4833
velox	UAZ	5418	USA	Arizona	Yavapai	34.8147	-112.6333
velox	UAZ	5420	USA	Arizona	Yavapai	34.9036	-112.5594
velox	UAZ	9291	USA	Arizona	Yavapai	34.6147	-112.4175
velox	UAZ	10791	USA	Arizona	Apache	34.3569	-109.3564
velox	UAZ	10796	USA	Arizona	Mohave	35.2305	-113.8346
velox	UAZ	10799	USA	Arizona	Yavapai	34.5399	-112.2917
velox	UAZ	14208	USA	Arizona	Yavapai	34.4682	-112.3806
velox	UAZ	14533	USA	Arizona	Mohave	36.3981	-113.0556
velox	UAZ	34549	USA	Arizona	Mohave	35.0875	-113.8887
velox	UAZ	36307	USA	Arizona	Apache	34.5058	-109.3603
velox	UAZ	37204	USA	Arizona	Apache	34.1914	-109.2853
velox	UAZ	43698	USA	Arizona	Yavapai	34.5636	-111.8536
velox	UAZ	43701	USA	Arizona	Coconino	35.0075	-111.7603
velox	UAZ	43706	USA	Arizona	Yavapai	34.3139	-112.8583
velox	UAZ	43707	USA	Arizona	Yavapai	34.5980	-112.4678
velox	UAZ	43709	USA	New Mexico	Santa Fe	35.2883	-105.8956
velox	UAZ	48188	USA	Arizona	Apache	34.4086	-109.5595
velox	UAZ	48235	USA	Arizona	Navaho	34.7379	-110.0428
velox	UAZ	51066	USA	Arizona	Coconino	34.5871	-110.7780
velox	UAZ	54515	USA	New Mexico	Guadalupe	34.8408	-104.9442
velox	UAZ	54669	USA	Colorado	Montezuma	37.3205	-108.6761
velox	UAZ	55589	USA	New Mexico	Socorro	34.1167	-107.2433
velox	UAZ	55590	USA	New Mexico	Socorro	34.1167	-107.2030
velox	UAZ	56057	USA	Arizona	Apache	34.9541	-109.7941
velox	UCM	451	USA	Colorado	San Miguel	37.9393	-108.8259
velox	UCM	1313	USA	Colorado	Montezuma	37.1532	-108.7933
velox	UCM	1335	USA	Colorado	Montrose	38.4118	-108.7358
velox	UCM	1357	USA	Colorado	Montrose	38.3683	-108.7358
velox	UCM	1385	USA	Colorado	Montrose	38.3617	-108.7507
velox	UCM	3182	USA	Colorado	Montrose	38.3633	-108.5681
velox	UCM	4320	USA	Colorado	San Miguel	38.1247	-108.8388
velox	UCM	4321	USA	Colorado	San Miguel	38.0440	-108.7086
velox	UCM	4323	USA	Colorado	San Miguel	38.0222	-108.7086
velox	UCM	4331	USA	Colorado	Montezuma	37.3205	-108.6761
velox	UCM	6095	USA	New Mexico	Catron	33.8711	-108.5736
velox	UCM	6562	USA	Utah	San Juan	37.7330	-109.4088
velox	UCM	6563	USA	Colorado	Mesa	38.6722	-108.9613
velox	UCM	7138	USA	Colorado	Delta	38.9427	-107.9785
velox	UCM	7250	USA	New Mexico	San Juan	36.7241	-107.6981
velox	UCM	7263	USA	New Mexico	Rio Arriba	36.1875	-106.4660

Spp	Inst.	Specimen#	Country	State/Province	County	Latitude	Longitude
velox	UCM	10405	USA	Colorado	Montezuma	37.1808	-108.4950
velox	UCM	11825	USA	Colorado	Montezuma	37.4894	-108.7728
velox	UCM	13186	USA	Arizona	Yavapai	34.2319	-112.7591
velox	UCM	13187	USA	New Mexico	San Miguel	35.4050	-105.5318
velox	UCM	17332	USA	Colorado	Montrose	38.3991	-109.0009
velox	UCM	17357	USA	Colorado	Montrose	38.3150	-108.8903
velox	UCM	17358	USA	Colorado	Montrose	38.3005	-108.8903
velox	UCM	18643	USA	Colorado	Montezuma	37.2995	-108.4204
velox	UCM	19698	USA	Colorado	Garfield	39.6066	-107.6556
velox	UCM	19699	USA	Colorado	Garfield	39.6217	-107.7825
velox	UCM	19823	USA	Colorado	Delta	38.7972	-108.3217
velox	UCM	20503	USA	Colorado	Mesa	39.0638	-108.6994
velox	UCM	21069	USA	Colorado	Delta	38.8246	-108.3795
velox	UCM	21549	USA	Colorado	La Plata	37.2753	-107.8794
velox	UCM	22136	USA	Colorado	Mesa	38.9911	-108.4528
velox	UCM	22817	USA	New Mexico	Sandoval	35.6143	-106.3375
velox	UCM	23345	USA	Arizona	Apache	35.1656	-109.3331
velox	UCM	23352	USA	New Mexico	Socorro	33.8449	-106.9489
velox	UCM	24831	USA	New Mexico	Sandoval	35.6143	-106.3375
velox	UCM	24898	USA	New Mexico	Sandoval	35.6143	-106.3375
velox	UCM	24899	USA	New Mexico	Socorro	33.8515	-106.9087
velox	UCM	25815	USA	Colorado	Delta	38.7510	-107.7811
velox	UCM	27244	USA	Colorado	Delta	38.7972	-108.3217
velox	UCM	29457	USA	New Mexico	Santa Fe	35.9090	-106.1814
velox	UCM	29458	USA	New Mexico	Sandoval	35.7883	-106.3022
velox	UCM	29470	USA	New Mexico	Santa Fe	35.9090	-106.1814
velox	UCM	29538	USA	New Mexico	Santa Fe	35.5564	-105.9372
velox	UCM	29666	USA	Colorado	Mesa	39.1299	-108.7283
velox	UCM	30141	USA	Colorado	Dolores	37.7604	-108.7755
velox	UCM	36396	USA	Colorado	Delta	38.7972	-108.3217
velox	UCM	36398	USA	Colorado	Mesa	39.0383	-108.6639
velox	UCM	36399	USA	Colorado	Mesa	39.0574	-108.7283
velox	UCM	36400	USA	Colorado	Mesa	39.1615	-108.2842
velox	UCM	36401	USA	Colorado	Mesa	38.9911	-108.4528
velox	UCM	51993	USA	Colorado	Montezuma	37.3488	-108.7494
velox	UCM	55572	USA	Arizona	Navaho	34.8597	-110.1572
velox	UCM	56610	USA	Colorado	Ouray	38.2942	-107.8184
velox	UCM	61704	USA	New Mexico	Sandoval	35.7883	-106.3022
velox	UCM	61737	USA	Colorado	Delta	38.7728	-107.7811
velox	UCM	61845	USA	New Mexico	Sandoval	35.5743	-107.7478
velox	UTEP	15061	USA	UTAH	San Juan	38.3124	-109.3472
velox	UTEP	18682	USA	New Mexico	Cibola	35.0968	-107.7730

APPENDIX B:

Definition of WorldClim variables.

Variable	Definition
BIO1	Annual Mean Temperature
BIO2	Mean Diurnal Range (Mean of monthly (max temp - min temp))
BIO3	Isothermality (BIO2/BIO7) (* 100)
BIO4	Temperature Seasonality (standard deviation *100)
BIO5	Max Temperature of Warmest Month
BIO6	Min Temperature of Coldest Month
BIO7	Temperature Annual Range (BIO5-BIO6)
BIO8	Mean Temperature of Wettest Quarter
BIO9	Mean Temperature of Driest Quarter
BIO10	Mean Temperature of Warmest Quarter
BIO11	Mean Temperature of Coldest Quarter
BIO12	Annual Precipitation
BIO13	Precipitation of Wettest Month
BIO14	Precipitation of Driest Month
BIO15	Precipitation Seasonality (Coefficient of Variation)
BIO16	Precipitation of Wettest Quarter
BIO17	Precipitation of Driest Quarter
BIO18	Precipitation of Warmest Quarter
BIO19	Precipitation of Coldest Quarter

APPENDIX C:

Pairwise Pearson correlation coefficient for 19 WorldClim variables. Coefficients are based on values extracted from all *Aspidoscelis* specimen locations, and highly correlated variables ($R > 0.75$) are shown in bold.

	BIO1	BIO2	BIO3	BIO4	BIO5	BIO6	BIO7	BIO8	BIO9	BIO10	BIO11	BIO12	BIO13	BIO14	BIO15	BIO16	BIO17	BIO18
BIO2	-0.54																	
BIO3	0.31	0.24																
BIO4	-0.63	0.37	-0.80															
BIO5	0.68	-0.05	-0.06	0.02														
BIO6	0.95	-0.63	0.44	-0.80	0.46													
BIO7	-0.72	0.69	-0.52	0.91	-0.02	-0.90												
BIO8	0.75	-0.23	0.18	-0.30	0.69	0.65	-0.39											
BIO9	0.47	-0.06	0.43	-0.44	0.39	0.54	-0.41	0.45										
BIO10	0.88	-0.44	-0.08	-0.19	0.89	0.71	-0.36	0.78	0.37									
BIO11	0.96	-0.51	0.52	-0.81	0.51	0.99	-0.85	0.68	0.54	0.72								
BIO12	0.44	-0.58	0.23	-0.58	-0.02	0.58	-0.66	0.11	0.23	0.20	0.52							
BIO13	0.49	-0.44	0.50	-0.73	-0.01	0.65	-0.74	0.24	0.38	0.19	0.63	0.88						
BIO14	0.05	-0.45	-0.51	0.17	0.02	0.02	-0.01	-0.15	-0.32	0.14	-0.05	0.48	0.08					
BIO15	0.35	0.14	0.73	-0.60	0.05	0.41	-0.44	0.36	0.40	0.09	0.48	0.10	0.51	-0.62				
BIO16	0.47	-0.40	0.55	-0.74	-0.04	0.63	-0.73	0.21	0.35	0.16	0.61	0.87	0.98	0.04	0.52			
BIO17	0.05	-0.48	-0.51	0.15	0.00	0.03	-0.04	-0.17	-0.25	0.12	-0.04	0.51	0.10	0.98	-0.63	0.06		
BIO18	0.39	-0.36	0.48	-0.63	-0.08	0.54	-0.65	0.21	0.31	0.12	0.52	0.77	0.93	-0.02	0.53	0.94	-0.01	
BIO19	-0.13	-0.24	-0.31	0.13	-0.08	-0.02	-0.01	-0.16	0.25	-0.06	-0.12	0.44	0.17	0.53	-0.44	0.10	0.61	0.08

APPENDIX D:

Maxent AIC, AICc and BIC model scores calculated as variables are iteratively removed.

The row label indicates the WorldClim variables removed (separated by commas) and the resulting scores are shown for each species with overall sum and average scores.

Coloration indicates high (dark) to low (light) model scores, with the top three scores for each species in white text. Bold and underlined values indicate the full and reduced variable sets used in subsequent Maxent modeling.

<u>AIC:</u>		b	e	f	g	i	s	u	v	sum	ave
	Full	2947	4838	1344	6711	5188	3558	5418	4133	34137	4267
	7, 10, 13	2991	4780	1348	6651	5224	3567	5405	4121	34088	4261
	7, 10, 13, 17	2950	4772	1338	6663	5198	3592	5397	4122	34033	4254
	6, 7, 11, 13, 16	2987	4798	1351	6702	5268	3600	5366	4111	34183	4273
	3, 7, 10, 13, 17	2992	4785	1328	6707	5210	3585	5411	4116	34134	4267
	7, 10, 11, 13, 17	2985	4795	1352	6686	5217	3591	5379	4111	34116	4264
	7, 10, 13, 16, 17	2943	4787	1332	6717	5196	3569	5398	4091	34033	4254
	3, 7, 10, 11, 13, 17	2989	4784	1349	6681	5230	3604	5438	4134	34209	4276
	3, 7, 10, 13, 16, 17	2978	4777	1337	6682	5187	3581	5408	4109	34058	4257
	7, 10, 11, 13, 16, 17	2993	4777	1338	6650	5209	3561	5389	4089	34005	4251
	3, 7, 10, 11, 13, 16, 17	2998	4783	1353	6664	5240	3590	5411	4102	34141	4268
	6, 7, 10, 11, 13, 16, 17	3009	4817	1353	6702	5199	3591	5382	4126	34177	4272
	3, 6, 7, 10, 11, 13, 16, 17	2969	4824	1355	6723	5254	3571	5385	4134	34216	4277
	3, 6, 7, 10, 11, 12, 13, 16, 17	3037	4823	1358	6706	5244	3589	5405	4141	34302	4288
	3, 6, 7, 10, 11, 13, 16, 17, 18	2991	4834	1345	6684	5195	3582	5424	4176	34231	4279
	3, 7, 8, 10, 11, 12, 13, 16, 17	3000	4775	1325	6684	5247	3595	5411	4142	34179	4272
	3, 6, 7, 8, 10, 11, 12, 13, 16, 17	3007	4826	1346	6693	5257	3577	5419	4130	34255	4282

<u>AICc:</u>		b	e	f	g	i	s	u	v	sum	ave
	Full	2986	4881	1367	6773	5250	3568	5442	4241	34509	4314
	7, 10, 13	3064	4817	1374	6690	5275	3586	5433	4182	34420	4302
	7, 10, 13, 17	3020	4803	1364	6690	5258	3616	5420	4183	34354	4294
	6, 7, 11, 13, 16	3059	4839	1375	6740	5312	3616	5384	4165	34489	4311
	3, 7, 10, 13, 17	3029	4815	1347	6753	5257	3599	5433	4160	34394	4299
	7, 10, 11, 13, 17	3029	4825	1368	6719	5271	3615	5403	4162	34393	4299
	7, 10, 13, 16, 17	3012	4833	1343	6766	5242	3588	5414	4136	34334	4292
	3, 7, 10, 11, 13, 17	3049	4812	1366	6707	5296	3621	5464	4198	34513	4314
	3, 7, 10, 13, 16, 17	3082	4804	1352	6714	5224	3601	5425	4157	34360	4295
	7, 10, 11, 13, 16, 17	3072	4812	1359	6674	5250	3576	5407	4136	34286	4286
	3, 7, 10, 11, 13, 16, 17	3102	4828	1387	6694	5298	3607	5429	4168	34514	4314
	6, 7, 10, 11, 13, 16, 17	3066	4848	1366	6734	5234	3609	5398	4194	34449	4306
	3, 6, 7, 10, 11, 13, 16, 17	3029	4860	1384	6758	5298	3584	5399	4186	34496	4312
	3, 6, 7, 10, 11, 12, 13, 16, 17	3081	4853	1384	6734	5271	3601	5425	4197	34546	4318
	3, 6, 7, 10, 11, 13, 16, 17, 18	3020	4870	1371	6711	5224	3594	5441	4246	34477	4310
	3, 7, 8, 10, 11, 12, 13, 16, 17	3031	4805	1344	6712	5288	3610	5429	4210	34429	4304
	3, 6, 7, 8, 10, 11, 12, 13, 16, 17	3049	4863	1358	6727	5288	3595	5435	4168	34482	4310

BIC:	b	e	f	g	i	s	u	v	sum	ave
Full	3078	5049	1400	7017	5444	3658	5612	4392	35651	4456
7, 10, 13	3158	4978	1406	6900	5460	3701	5611	4328	35541	4443
7, 10, 13, 17	3114	4956	1396	6878	5451	3739	5584	4329	35448	4431
6, 7, 11, 13, 16	3153	5006	1407	6951	5489	3721	5531	4308	35567	4446
3, 7, 10, 13, 17	3120	4966	1379	6978	5438	3699	5598	4297	35475	4434
7, 10, 11, 13, 17	3122	4976	1399	6920	5459	3739	5573	4304	35492	4436
7, 10, 13, 16, 17	3107	5005	1372	6993	5421	3700	5559	4275	35431	4429
3, 7, 10, 11, 13, 17	3144	4961	1398	6890	5493	3731	5636	4345	35597	4450
3, 7, 10, 13, 16, 17	3169	4950	1384	6912	5394	3718	5573	4296	35396	4425
7, 10, 11, 13, 16, 17	3166	4971	1391	6851	5424	3679	5558	4276	35314	4414
3, 7, 10, 11, 13, 16, 17	3189	4998	1418	6887	5490	3717	5580	4316	35594	4449
6, 7, 10, 11, 13, 16, 17	3160	5001	1397	6932	5399	3721	5544	4343	35497	4437
3, 6, 7, 10, 11, 13, 16, 17	3124	5018	1416	6961	5476	3681	5535	4328	35539	4442
3, 6, 7, 10, 11, 12, 13, 16, 17	3173	5004	1416	6922	5423	3696	5584	4342	35560	4445
3, 6, 7, 10, 11, 13, 16, 17, 18	3107	5029	1403	6896	5378	3692	5589	4395	35490	4436
3, 7, 8, 10, 11, 12, 13, 16, 17	3119	4955	1377	6900	5461	3715	5580	4359	35466	4433
3, 6, 7, 8, 10, 11, 12, 13, 16, 17	3141	5024	1388	6928	5447	3708	5577	4300	35512	4439

APPENDIX E:

Model fit scores for full, reduced and environmental change data sets. High values are highlighted by darker colors. Area under the curve (AUC) scores were calculated by Maxent based on both training (75% of the data points) and test (25% of data points) data. The AIC, AICc and BIC scores were calculated using ENMTools.

Training AUC:

	b	e	f	g	i	s	u	v	sum	average
Full	0.9837	0.9689	0.9912	0.9348	0.9581	0.9894	0.978	0.9706	7.7747	0.971838
Full DC	0.9849	0.9728	0.9899	0.9408	0.9621	0.9908	0.9802	0.976	7.7975	0.974688
Full DM	0.9863	0.9746	0.9906	0.9449	0.9631	0.9897	0.98	0.974	7.8032	0.9754
Reduce	0.9792	0.9632	0.9896	0.9256	0.9485	0.9882	0.9775	0.9628	7.7346	0.966825
Reduce DC	0.9824	0.9715	0.9911	0.9318	0.9556	0.9887	0.9796	0.9727	7.7734	0.971675
Reduce DM	0.9855	0.9718	0.9899	0.9361	0.9576	0.9893	0.9793	0.9724	7.7819	0.972738

Test AUC:

	b	e	f	g	i	s	u	v	sum	average
Full	0.9699	0.9484	0.9889	0.8996	0.9318	0.9859	0.9684	0.9408	7.7747	0.971838
Full DC	0.9706	0.9549	0.9874	0.904	0.9296	0.9881	0.9706	0.9495	7.7975	0.974688
Full DM	0.9698	0.9544	0.9869	0.9099	0.9249	0.9859	0.97	0.9492	7.8032	0.9754
Reduce	0.9638	0.948	0.9869	0.8984	0.9199	0.9861	0.9688	0.9426	7.7346	0.966825
Reduce DC	0.9694	0.9518	0.9881	0.8988	0.9281	0.9859	0.9706	0.9532	7.7734	0.971675
Reduce DM	0.9709	0.952	0.9876	0.9059	0.9322	0.9866	0.9699	0.9515	7.7819	0.972738

AIC:

	b	e	f	g	i	s	u	v	sum	ave
Full	2946.619	4837.896	1343.958	6711.483	5188.019	3557.797	5417.992	4132.95	34136.71	4267.089
Full DC	2803.243	4659.245	1349.183	6553.374	5198.279	3527.749	5363.702	3996.205	33450.98	4181.373
Full DM	2857.505	4681.878	1318.749	6590.582	5149.953	3498.782	5291.001	3993.663	33382.11	4172.764
Reduce	3036.531	4823.323	1358	6706.069	5243.708	3588.824	5404.777	4141.246	34302.48	4287.81
Reduce DC	2847.789	4713.576	1347.603	6643.674	5175.809	3502.488	5343.935	4028.337	33603.21	4200.401
Reduce DM	2851.944	4671.104	1311.903	6588.084	5163.082	3528.546	5333.215	4035.482	33483.36	4185.42

AICc:

		b	e	f	g	i	s	u	v	sum	ave
Full		2986.219	4881.119	1367.488	6772.798	5250.111	3568.131	5442.349	4240.984	34509.2	4313.65
Full	DC	2865.879	4747.635	1375.183	6616.756	5278.303	3561.107	5406.357	4061.701	33912.92	4239.115
Full	DM	3064.718	4757.425	1342.278	6705.729	5260.353	3525.147	5325.568	4078.438	34059.66	4257.457
Reduce		3080.654	4853.28	1384	6733.89	5270.769	3600.689	5425.279	4197.275	34545.84	4318.229
Reduce	DC	2916.858	4782.095	1371.132	6686.334	5219.636	3525.147	5377.257	4107.226	33985.68	4248.211
Reduce	DM	2961.418	4716.001	1329.014	6653.289	5253.329	3542.069	5370.358	4129.697	33955.17	4244.397

BIC:

		b	e	f	g	i	s	u	v	sum	ave
Full		3077.595	5049.448	1399.896	7016.549	5444.499	3658.353	5612.312	4392.323	35650.98	4456.372
Full	DC	2956.578	4943.626	1407.451	6861.887	5482.867	3698.693	5613.019	4209.614	35173.74	4396.717
Full	DM	3090.457	4948.919	1374.686	6984.587	5473.189	3652.967	5518.32	4230.054	35273.18	4409.147
Reduce		3173.461	5003.663	1416.268	6921.847	5422.893	3696.083	5584.432	4341.521	35560.17	4445.021
Reduce	DC	3007.022	4970.212	1403.54	6903.865	5397.155	3646.618	5567.587	4258.162	35154.16	4394.27
Reduce	DM	3040.665	4886.124	1360.848	6900.314	5461.723	3642.509	5567.867	4281.722	35141.77	4392.722

APPENDIX F:

Variable importance for each species, including paleoclimate PCA calculations for CCSM and MIROC. Metrics used to indicate variable importance during Maxent model building is indicated in column title for each species: contribution (c), permutation (p), jackknife with variable as the only variable used (w/), and jackknife with variable omitted (w/o). Variables important using the full set of variables indicated by an “F,” variables important using the reduced set of variables indicated by “r.” Variables used in the reduced set are indicated by bold row headings. ¹Does not include models that used MIROC PCA. ²Only models that include CCSM PCA variables.

	burti				exsanguis				flagellicauda				gularis				
	c	p	w/	w/o	c	p	w/	w/o	c	p	w/	w/o	c	p	w/	w/o	
WorldClim	BIO1					r	r							Fr	Fr	Fr	
	BIO22																
	BIO3																
	BIO4	Fr	Fr	Fr	Fr	r	r										
	BIO5																
	BIO6					F	F	F	F								
	BIO7																
	BIO8																
	BIO9	Fr	Fr	Fr	Fr					Fr	Fr		Fr				
	BIO10																
	BIO11																
	BIO12																
	BIO13																
	BIO14	Fr												Fr	Fr		Fr
	BIO15					Fr¹	Fr¹	Fr¹	Fr¹	Fr	Fr		Fr				
	BIO16																
	BIO17													F	F		
	BIO18																
	BIO19									Fr	Fr	F					
CCSM	PC1																
	PC2					Fr	Fr	Fr	Fr								
	PC3																
	PC5																
MIROC	PC1																
	PC2					Fr	Fr	Fr									
	PC3					Fr	Fr	Fr	Fr								
	PC5																

	inornata				sonorae				uniparens				velox				
	c	p	w/	w/o	c	p	w/	w/o	c	p	w/	w/o	c	p	w/	w/o	
WorldClim	BIO1													Fr	Fr	Fr	Fr
	BIO22																
	BIO3									F	F						
	BIO4					Fr	Fr	Fr	Fr	Fr	Fr	Fr	Fr				
	BIO5																
	BIO6																
	BIO7																
	BIO8	F															
	BIO9	F								F	F						
	BIO10																
	BIO11																
	BIO12																
	BIO13																
	BIO14					Fr ²	Fr ²										
	BIO15																
	BIO16																
	BIO17																
	BIO18	r	r	r	r									Fr	Fr	Fr	
	BIO19	Fr	Fr	Fr	Fr	Fr	Fr	Fr	Fr					Fr	Fr		Fr
CCSM	PC1																Fr
	PC2																
	PC3																Fr
	PC5																
MIROC	PC1									Fr							
	PC2					Fr	Fr		Fr					Fr	Fr	Fr	Fr
	PC3	Fr	Fr		Fr	Fr	Fr										
	PC5																

APPENDIX G:

Specimens of *A. uniparens* and *A. velox* collected across Arizona, Colorado, New Mexico and Utah. Specimen collection number, Las Vegas tissue collection number, species name, state, county, latitude, longitude, and written locality description are given.

Specimen #	Tissue #	Species	Country	State	County	Location	Latitude	Longitude	Locality Info
ABL00004	LVT09021	uniparens	USA	AZ	Pinal	Pepper	32.53736	-110.72133	5 mi S, 3 mi E of Oracle: Peppersauce campground
ABL00007	LVT09024	uniparens	USA	AZ	Pima	Cinegas	31.76203	-110.61953	Las Cinegas; 5 mi E of HW 83
ABL00013	LVT09030	uniparens	USA	AZ	Green Lee	Duncan	32.77304	-109.25142	3.5 mi S, 8.5 mi W of Duncan
ABL00014	LVT09031	uniparens	USA	AZ	Green Lee	Duncan	32.77304	-109.25142	3.5 mi S, 8.5 mi W of Duncan
ABL00015	LVT09032	uniparens	USA	AZ	Green Lee	Duncan	32.77304	-109.25142	3.5 mi S, 8.5 mi W of Duncan
ABL00016	LVT09033	uniparens	USA	AZ	Green Lee	Duncan	32.77304	-109.25142	3.5 mi S, 8.5 mi W of Duncan
ABL00017	LVT09034	uniparens	USA	AZ	Green Lee	Duncan	32.77304	-109.25142	3.5 mi S, 8.5 mi W of Duncan
ABL00021	LVT09038	uniparens	USA	AZ	Pima	Green	31.79808	-110.80010	3.8 mi S, 11.5 mi E of Green Valley
ABL00023	LVT09040	uniparens	USA	AZ	Cochise	Tombstone	31.85121	-110.00358	9.3 mi N, 3.7 mi E of Tombstone
ABL00024	LVT09041	uniparens	USA	AZ	Cochise	Tombstone	31.85121	-110.00358	9.3 mi N, 3.7 mi E of Tombstone
ABL00026	LVT09043	uniparens	USA	AZ	Cochise	Tombstone	31.85121	-110.00358	9.3 mi N, 3.7 mi E of Tombstone
ABL00027	LVT09044	uniparens	USA	AZ	Cochise	Tombstone	31.85121	-110.00358	9.3 mi N, 3.7 mi E of Tombstone
ABL00029	LVT09046	uniparens	USA	AZ	Pima	Tucson	32.34807	-110.54076	8.8 mi N, 21 mi E Tucson
ABL00032	LVT09049	uniparens	USA	AZ	Pima	Tucson	32.35091	-110.54040	8.8 mi N, 21 mi E Tucson
ABL00033	LVT09050	uniparens	USA	AZ	Pima	Tucson	32.35091	-110.54040	8.8 mi N, 21 mi E Tucson
ABL00034	LVT09051	uniparens	USA	AZ	Pima	Tucson	32.35091	-110.54040	8.8 mi N, 21 mi E Tucson
ABL00035	LVT09052	uniparens	USA	AZ	Pima	Tucson	32.35091	-110.54040	8.8 mi N, 21 mi E Tucson
ABL00036	LVT09053	uniparens	USA	AZ	Graham	Clifton	33.09705	-109.53458	13 mi N, 13.8 mi W of Clifton
ABL00037	LVT09054	velox	USA	AZ	Coconino	Williams	35.39376	-112.54567	9.8 mi N, 20 mi W of Williams
ABL00038	LVT09055	velox	USA	AZ	Coconino	Williams	35.39376	-112.54567	9.8 mi N, 20 mi W of Williams
ABL00039	LVT09056	velox	USA	AZ	Coconino	Williams	35.39376	-112.54567	9.8 mi N, 20 mi W of Williams
ABL00040	LVT09057	velox	USA	AZ	Coconino	Williams	35.39376	-112.54567	9.8 mi N, 20 mi W of Williams
ABL00041	LVT09058	velox	USA	AZ	Coconino	Williams	35.39376	-112.54567	9.8 mi N, 20 mi W of Williams
ABL00042	LVT09059	velox	USA	AZ	Coconino	Winslow	34.68342	-110.72118	23 mi S of Winslow
ABL00043	LVT09060	velox	USA	AZ	Coconino	Winslow	34.68342	-110.72118	23 mi S of Winslow
ABL00044	LVT09061	velox	USA	AZ	Coconino	Winslow	34.68342	-110.72118	23 mi S of Winslow
ABL00045	LVT09062	velox	USA	AZ	Coconino	Winslow	34.68342	-110.72118	23 mi S of Winslow

Specimen #	Tissue #	Species	Country	State	County	Location	Latitude	Longitude	Locality Info
ABL00046	LVT09063	velox	USA	AZ	Coconino	Winslow	34.68342	-110.72118	23 mi S of Winslow
ABL00047	LVT09064	velox	USA	AZ	Coconino	Flagstaff	35.43245	-111.53940	16.1 mi N, 6 mi E of Flagstaff
ABL00048	LVT09065	velox	USA	AZ	Coconino	Flagstaff	35.43245	-111.53940	16.1 mi N, 6 mi E of Flagstaff
ABL00049	LVT09066	velox	USA	AZ	Coconino	Flagstaff	35.43245	-111.53940	16.1 mi N, 6 mi E of Flagstaff
ABL00050	LVT09070	uniparens	USA	AZ	Pima	Cinegas	31.76203	-110.61953	Las Cinegas; 5 mi E of HW 83
ABL00051	LVT09067	uniparens	USA	AZ	Pima	Cinegas	31.76203	-110.61953	Las Cinegas; 5 mi E of HW 83
ABL00052	LVT09068	uniparens	USA	AZ	Pima	Cinegas	31.76203	-110.61953	Las Cinegas; 5 mi E of HW 83
ABL00053	LVT09069	uniparens	USA	AZ	Pima	Cinegas	31.76203	-110.61953	Las Cinegas; 5 mi E of HW 83
ABL00054	LVT09072	uniparens	USA	AZ	Pima	Arivaca	31.59810	-111.36815	3.66 mi NW of Arivaca
ABL00055	LVT09073	uniparens	USA	NM	Hildago	Hachita	31.76972	-108.36761	10.59 mi SSW of Hachita
ABL00056	LVT09074	uniparens	USA	NM	Hildago	Hachita	31.76972	-108.36761	10.59 mi SSW of Hachita
ABL00057	LVT09075	uniparens	USA	AZ	Pima	Arivaca	31.59810	-111.36815	3.66 mi NW of Arivaca
ABL00058	LVT09076	uniparens	USA	AZ	Pima	Arivaca	31.59810	-111.36815	3.66 mi NW of Arivaca
ABL00059	LVT09077	uniparens	USA	AZ	Yavapai	Bridgeport	34.65916	-111.98496	4.32 mi S of Bridgeport
ABL00060	LVT09078	uniparens	USA	AZ	Yavapai	Bridgeport	34.65916	-111.98496	4.32 mi S of Bridgeport
ABL00061	LVT09079	uniparens	USA	AZ	Yavapai	Bridgeport	34.65916	-111.98496	4.32 mi S of Bridgeport
ABL00062	LVT09080	uniparens	USA	AZ	Yavapai	Bridgeport	34.66259	-111.98804	4.32 mi S of Bridgeport
ABL00063	LVT09081	uniparens	USA	AZ	Yavapai	Bridgeport	34.66259	-111.98804	4.32 mi S of Bridgeport
ABL00064	LVT09082	uniparens	USA	AZ	Yavapai	Bridgeport	34.66259	-111.98804	4.32 mi S of Bridgeport
ABL00065	LVT09083	uniparens	USA	AZ	Yavapai	Bridgeport	34.66259	-111.98804	4.32 mi S of Bridgeport
ABL00066	LVT09084	velox	USA	AZ	Apache	Springer	34.15183	-109.21302	2.6 mi ENE of Springerville
ABL00068	LVT09086	uniparens	USA	NM	Sandoval	Ysidro	35.49235	-106.84924	5.5 mi SW of San Ysidro
ABL00070	LVT09088	velox	USA	NM	Sandoval	Ysidro	35.49235	-106.84924	5.5 mi SW of San Ysidro
ABL00071	LVT09089	velox	USA	NM	Sandoval	Ysidro	35.49235	-106.84924	5.5 mi SW of San Ysidro
ABL00072	LVT09090	velox	USA	NM	Sandoval	Ysidro	35.50051	-106.8691	5.5 mi SW of San Ysidro
ABL00073	LVT09091	velox	USA	NM	Sandoval	Ysidro	35.50051	-106.8691	5.5 mi SW of San Ysidro
ABL00074	LVT09092	velox	USA	NM	Sandoval	Ysidro	35.49887	-106.84733	5.5 mi SW of San Ysidro

Specimen #	Tissue #	Species	Country	State	County	Location	Latitude	Longitude	Locality Info
ABL00076	LVT09094	velox	USA	NM	Sandoval	Ysidro	35.49887	-106.84733	5.5 mi SW of San Ysidro
ABL00077	LVT09095	velox	USA	NM	Sandoval	Ysidro	35.49887	-106.84733	5.5 mi SW of San Ysidro
ABL00078	LVT09096	velox	USA	NM	Sandoval	Ysidro	35.49887	-106.84733	5.5 mi SW of San Ysidro
ABL00079	LVT09097	velox	USA	NM	Santa Fe	SantaFe	35.61259	-106.13969	2.5 mi W of Santa Fe Munciple Airport
ABL00080	LVT10100	velox	USA	NM	Santa Fe	SantaFe	35.61259	-106.13969	2.5 mi W of Santa Fe Munciple Airport
ABL00081	LVT10101	velox	USA	NM	Santa Fe	SantaFe	35.61259	-106.13969	2.5 mi W of Santa Fe Munciple Airport
ABL00082	LVT10102	velox	USA	NM	Santa Fe	SantaFe	35.61259	-106.13969	2.5 mi W of Santa Fe Munciple Airport
ABL00083	LVT10103	velox	USA	NM	Santa Fe	SantaFe	35.61259	-106.13969	2.5 mi W of Santa Fe Munciple Airport
ABL00086	LVT10106	uniparens	USA	NM	Sierra	Monticello	33.44805	-107.38435	5.1 mi NE of Monticello
ABL00087	LVT10107	uniparens	USA	NM	Sierra	Monticello	33.44805	-107.38435	5.1 mi NE of Monticello
ABL00088	LVT10108	uniparens	USA	NM	Sierra	Monticello	33.44805	-107.38435	5.1 mi NE of Monticello
ABL00089	LVT10109	uniparens	USA	NM	Sierra	Monticello	33.44805	-107.38435	5.1 mi NE of Monticello
ABL00090	LVT10110	uniparens	USA	NM	Sierra	Monticello	33.44805	-107.38435	5.1 mi NE of Monticello
ABL00091	LVT10111	uniparens	USA	NM	Hildago	Hachita	31.76972	-108.36761	10.59 mi SSW of Hachita
ABL00092	LVT10112	uniparens	USA	NM	Hildago	Hachita	31.76972	-108.36761	10.59 mi SSW of Hachita
ABL00093	LVT10113	uniparens	USA	NM	Luna	Deming	32.42871	-107.5913	15mi NE of Deming
ABL00094	LVT10114	uniparens	USA	NM	Luna	Deming	32.42871	-107.5913	15mi NE of Deming
ABL00095	LVT10115	uniparens	USA	NM	Luna	Deming	32.42871	-107.5913	15mi NE of Deming
ABL00096	LVT10116	uniparens	USA	NM	Luna	Deming	32.42871	-107.5913	15mi NE of Deming
ABL00097	LVT10117	uniparens	USA	NM	Luna	Deming	32.42871	-107.5913	15mi NE of Deming
ABL00098	LVT10118	velox	USA	UT	Kane	Kanab	37.16544	-112.35601	13.1mi NE of Kanab
ABL00099	LVT10119	velox	USA	UT	Kane	Kanab	37.1686	-112.34995	13.1mi NE of Kanab
ABL00100	LVT10120	velox	USA	UT	Kane	Kanab	37.1686	-112.34995	13.1mi NE of Kanab
ABL00101	LVT10121	velox	USA	UT	Kane	Kanab	37.1686	-112.34995	13.1mi NE of Kanab
ABL00102	LVT10122	velox	USA	UT	Garfield	Escalante	37.73607	-111.50279	5.9mi ESE of Escalante
ABL00103	LVT10123	velox	USA	UT	Garfield	Escalante	37.73607	-111.50279	5.9mi ESE of Escalante
ABL00104	LVT10124	velox	USA	UT	Garfield	Escalante	37.73607	-111.50279	5.9mi ESE of Escalante

Specimen #	Tissue #	Species	Country	State	County	Location	Latitude	Longitude	Locality Info
ABL00105	LVT10125	velox	USA	UT	Garfield	Escalante	37.73607	-111.50279	5.9mi ESE of Escalante
ABL00106	LVT10126	velox	USA	UT	Garfield	Escalante	37.73607	-111.50279	5.9mi ESE of Escalante
ABL00107	LVT10127	velox	USA	UT	San Juan	Bridge	37.59702	-109.92271	3.1mi ESE from Natural Bridges National Monument
ABL00108	LVT10128	velox	USA	UT	San Juan	Bridge	37.59702	-109.92271	3.1mi ESE from Natural Bridges National Monument
ABL00109	LVT10129	velox	USA	UT	San Juan	Bridge	37.59702	-109.92271	3.1mi ESE from Natural Bridges National Monument
ABL00110	LVT10130	velox	USA	UT	San Juan	Bridge	37.59702	-109.92271	3.1mi ESE from Natural Bridges National Monument
ABL00111	LVT10131	velox	USA	UT	San Juan	Bridge	37.59702	-109.92271	3.1mi ESE from Natural Bridges National Monument
ABL00113	LVT10133	velox	USA	NM	San Juan	Bloomfield	36.54359	-107.86199	13.4mi SE of Bloomfield
ABL00114	LVT10134	velox	USA	NM	San Juan	Bloomfield	36.54359	-107.86199	13.4mi SE of Bloomfield
ABL00115	LVT10135	velox	USA	NM	San Juan	Bloomfield	36.54359	-107.86199	13.4mi SE of Bloomfield
ABL00116	LVT10136	velox	USA	NM	San Juan	Bloomfield	36.54359	-107.86199	13.4mi SE of Bloomfield
ABL00117	LVT10137	velox	USA	NM	McKinley	Church	35.46676	-108.46759	9mi SE of Church Rock
ABL00118	LVT10138	velox	USA	NM	McKinley	Church	35.46676	-108.46759	9mi SE of Church Rock
ABL00119	LVT10139	velox	USA	NM	McKinley	Church	35.46676	-108.46759	9mi SE of Church Rock
ABL00120	LVT10140	velox	USA	NM	McKinley	Church	35.46676	-108.46759	9mi SE of Church Rock
ABL00121	LVT10141	velox	USA	NM	McKinley	Church	35.46676	-108.46759	9mi SE of Church Rock
ABL00122	LVT10146	velox	USA	NM	Cibola	Grants	34.97037	-107.81017	12.5mi SSE of Grants
ABL00123	LVT10147	uniparens	USA	NM	Cibola	Magdalena	34.16576	-107.22326	3.5mi NNE of Magdalena
Specimen #	Tissue #	Species	Country	State	County	Location	Latitude	Longitude	Locality Info
ABL00124	LVT10148	uniparens	USA	NM	Socorro	Magdalena	34.16576	-107.22326	3.5mi NNE of Magdalena
ABL00125	LVT10149	velox	USA	NM	Socorro	Magdalena	34.16576	-107.22326	3.5mi NNE of Magdalena
ABL00126	LVT10150	velox	USA	NM	Socorro	Magdalena	34.16576	-107.22326	3.5mi NNE of Magdalena
ABL00127	LVT10262	uniparens	USA	NM	Socorro	Magdalena	34.16576	-107.22326	3.5mi NNE of Magdalena
ABL00128	LVT10263	velox	USA	NM	Socorro	Jacob	36.45152	-112.00338	21.5 mi SSE of Jacob Lake
ABL00129	LVT10264	velox	USA	AZ	Coconino	Jacob	36.45152	-112.00338	21.5 mi SSE of Jacob Lake

Specimen #	Tissue #	Species	Country	State	County	Location	Latitude	Longitude	Locality Info
ABL00130	LVT10265	velox	USA	AZ	Coconino	Jacob	36.45152	-112.00338	21.5 mi SSE of Jacob Lake
ABL00131	LVT10266	velox	USA	AZ	Coconino	Jacob	36.45152	-112.00338	21.5 mi SSE of Jacob Lake
ABL00132	LVT10267	velox	USA	AZ	Coconino	Jacob	36.45152	-112.00338	21.5 mi SSE of Jacob Lake
ABL00133	LVT10268	velox	USA	AZ	Coconino	Flagstaff	35.43245	-111.53940	16.1 mi N, 6 mi E of Flagstaff
ABL00134	LVT10269	velox	USA	AZ	Coconino	Flagstaff	35.43245	-111.53940	16.1 mi N, 6 mi E of Flagstaff
ABL00135	LVT10270	velox	USA	AZ	Coconino	Springer	34.1201	-109.21081	4.4mi ESE of Springerville
ABL00136	LVT10271	velox	USA	AZ	Apache	Springer	34.1201	-109.21081	4.4mi ESE of Springerville
ABL00137	LVT10272	velox	USA	AZ	Apache	Springer	34.1201	-109.21081	4.4mi ESE of Springerville
ABL00138	LVT10273	velox	USA	AZ	Apache	Springer	34.1201	-109.21081	4.4mi ESE of Springerville
ABL00139	LVT10274	velox	USA	AZ	Apache	Pilar	36.35283	-105.82237	6mi NNW of Pilar
ABL00140	LVT10275	velox	USA	NM	Taos	Pilar	36.35283	-105.82237	6mi NNW of Pilar
ABL00141	LVT10276	velox	USA	NM	Taos	Pilar	36.35283	-105.82237	6mi NNW of Pilar
ABL00142	LVT10142	velox	USA	NM	Cibola	Grants	34.97037	-107.81017	12.5mi SSE of Grants
ABL00143	LVT10143	velox	USA	NM	Cibola	Grants	34.97037	-107.81017	12.5mi SSE of Grants
ABL00144	LVT10144	velox	USA	NM	Cibola	Grants	34.97037	-107.81017	12.5mi SSE of Grants
ABL00145	LVT10145	velox	USA	NM	Cibola	Grants	34.97037	-107.81017	12.5mi SSE of Grants
ABL00146	LVT10281	velox	USA	CO	Montrose	Naturita	38.19804	-108.58636	1.7mi SW of Naturita
ABL00149	LVT10277	velox	USA	NM	Taos	Pilar	36.35283	-105.82237	6mi NNW of Pilar
ABL00150	LVT10278	velox	USA	NM	Taos	Pilar	36.35283	-105.82237	6mi NNW of Pilar
ABL00151	LVT10279	velox	USA	NM	Taos	Naturita	38.19804	-108.58636	1.7mi SW of Naturita
ABL00152	LVT10280	velox	USA	CO	Montrose	Naturita	38.19804	-108.58636	1.7mi SW of Naturita

BIBLIOGRAPHY

- Amos, W. & Balmford, A. (2001) When does conservation genetics matter? *Heredity*, **87**, 257-265.
- AMVA (2000) Report of the AMVA Panel on Euthanasia. *Journal of the American Veterinary Medical Association*, **218**, 669-696.
- Anderson, R.A., Wright, J.W. & Vitt, L.J. (1993) An analysis of foraging in the lizard, *Cnemidophorus tigris*. In: *Biology of Whiptail Lizards (Genus Cnemidophorus)* (eds. J.W. Wright and L.J. Vitt), pp. 83-116. Oklahoma Museum of Natural History, Norman, Oklahoma.
- Anderson, R.P., Peterson, A.T. & Gomez-Laverde, M. (2002) Using niche-based GIS modeling to test geographic predictions of competitive exclusion and competitive release in South American pocket mice. *Oikos*, **98**, 3-16.
- Arrigo, N., Tuszyński, J.W., Ehrich, D., Gerdes, T. & Alvarez, N. (2009) Evaluating the impact of scoring parameters on the structure of intra-specific genetic variation using RawGeno, an R package for automating AFLP scoring. *BMC Bioinformatics*, **10**, 1-14.
- Barton, N.H. (2001) The role of hybridization in evolution. *Molecular Ecology*, **10**, 551-568.
- Bell, G. (1982) *The Masterpiece of Nature: The Evolution and Genetics of Sexuality*. University of California Press, Berkeley.
- Bell, L.E. (2003) *Maternity analysis and phylogeography of the plateau striped whiptail (Aspidoscelis velox complex): interspecies sex and its consequences*. MS, San Diego State University, San Diego.
- Braconnot, P. (1999) PMIP, Paleoclimate Modeling Intercomparison Project (PMIP): proceedings of the third PMIP workshop. Canada.
- Braconnot, P., Otto-Bliesner, B., Harrison, S., Joussaume, S., Peterchmitt, J.Y., Abe-Ouchi, A., Crucifix, M., Driesschaert, E., Fichefet, T., Hewitt, C.D., Kageyama, M., Kitoh, A., Loutre, M.F., Marti, O., Merkel, U., Ramstein, G., Valdes, P., Weber, L., Yu, Y. & Zhao, Y. (2007a) Results of PMIP2 coupled simulations of the Mid-Holocene and last glacial maximum - Part 2: Feedbacks with emphasis on the location of the ITCZ and mid- and high latitudes heat budget. *Climate of the Past*, **3**, 279-296.

- Braconnot, P., Otto-Bliesner, B., Harrison, S., Joussaume, S., Peterchmitt, J.Y., Abe-Ouchi, A., Crucifix, M., Driesschaert, E., Fichefet, T., Hewitt, C.D., Kageyama, M., Kitoh, A., Laîné, A., Loutre, M.F., Marti, O., Merkel, U., Ramstein, G., Valdes, P., Weber, S.L., Yu, Y. & Zhao, Y. (2007b) Results of PMIP2 coupled simulations of the Mid-Holocene and last glacial maximum - part 1: experiments and large-scale features. *Climate of the Past*, **3**, 261-277.
- Brennan, T.C. & Holycross, A.T. (2006) *Amphibians and Reptiles in Arizona*. Arizona Game and Fish Department, Phoenix.
- Bromham, L. & Penny, D. (2003) The modern molecular clock. *Nature Reviews Genetics*, **4**, 216-224.
- Brown, J.H. (1984) On the relationship between abundance and distribution of species. *The American Naturalist*, **124**, 255-279.
- Cain, S.A. (1944) *Foundations of Plant Geography*. Harper & Brothers, New York.
- Carstens, B.C. & Richards, C.L. (2007) Integrating coalescent and ecological niche modeling in comparative phylogeography. *Evolution*, **61**, 1439-1454.
- Case, T.J. (1990) Patterns of coexistence in sexual and asexual species of *Cnemidophorus lizards*. *Oecologia*, **83**, 220-227.
- Castoe, T.A., Spencer, C.L. & Parkinson, C.L. (2007) Phylogeographic structure and historical demography of the western diamondback rattlesnake (*Crotalus atrox*): A perspective on North American desert biogeography. *Molecular Phylogenetics and Evolution*, **42**, 193-212.
- Charlesworth, D. & Charlesworth, B. (1987) Inbreeding depression and its evolutionary consequences. *Annual Review of Ecology and Evolution*, **18**, 237-268.
- Cole, C.J., Hardy, L.M., Dessauer, H.C., Harry, L. & Townsend, C.R. (2010) Laboratory hybridization among North American whiptail lizards, including *Aspidoscelis inornata arizonae* x *A. tigris marmorata* (Squamata: Teiidae), ancestors of unisexual clones in nature. *American Museum Novitates*, **3698**, 1-43.
- Cuellar, O. (1977) Animal parthenogenesis. *Science*, **197**, 837-843.
- Cuellar, O. (1993) On competition and natural history of coexisting parthenogenetic and bisexual whiptail lizards. In: *Biology of Whiptail Lizards (Genus Cnemidophorus)* (eds. J.W. Wright and L.J. Vitt), pp. 345-370. Oklahoma Museum of Natural History, Norman, Oklahoma.

- Cullum, A.J. (1997) Comparisons of physiological performance in sexual and asexual whiptail lizards (Genus *Cnemidophorus*): implications for the role of heterozygosity. *The American Naturalist*, **150**, 24-47.
- Cullum, A.J. (2000) Phenotypic variability of physiological traits in populations of sexual and asexual whiptail lizards (genus *Cnemidophorus*). *Evolutionary Ecology Research*, **2**, 841-855.
- Degenhardt, W.G., Painter, C.W. & Price, A.H. (2005) *Amphibians and Reptiles of New Mexico*. University of New Mexico Press, Albuquerque.
- Densmore III, L.D., Moritz, C.C., Wright, J.W. & Brown, W.M. (1989) Mitochondrial-DNA analyses and the origin and relative age of parthenogenetic lizards (genus *Cnemidophorus*). IV. Nine *sexlineatus*-group unisexuals. *Evolution*, **43**, 969-983.
- Després, L., Gielly, L., Redoutet, B. & Taberlet, P. (2003) Using AFLP to resolve phylogenetic relationships in a morphologically diversified plant species complex when nuclear and chloroplast sequences fail to reveal variability. *Molecular Phylogenetics & Evolution*, **27**, 185-196.
- Dessauer, H.C. & Cole, C.J. (1986) Clonal inheritance in parthenogenetic whiptail lizards: biochemical evidence. *Journal of Heredity*, **77**, 8-12.
- Dessauer, H.C. & Cole, C.J. (1989) Diversity between and within nominal forms of unisexual Teiid lizards. In: *Evolution and Ecology of Unisexual Vertebrates* (eds. R.M. Dawley and J.P. Bogart), pp. 49-71. New York State Museum Bulletin 466, Albany, NY.
- Drummond, a.J., Rambaut, a., Shapiro, B. & Pybus, O.G. (2005) Bayesian coalescent inference of past population dynamics from molecular sequences. *Molecular Biology and Evolution*, **22**, 1185-1192.
- Elith, J., Graham, C., Anderson, R., Dudík, M., H. Graham, C., P. Anderson, R., Dudík, M., Ferrier, S., Guisan, A., J. Hijmans, R., Huettmann, F., R. Leathwick, J., Lehmann, A., Li, J., G. Lohmann, L., A. Loiselle, B., Manion, G., Moritz, C., Nakamura, M., Nakazawa, Y., McC. M. Overton, J., Townsend Peterson, A., J. Phillips, S., Richardson, K., Scachetti-Pereira, R., E. Schapire, R., Soberón, J., Williams, S., S. Wisz, M., E. Zimmermann, N., Elith, J., Graham, H., Anderson, P., Hijmans, J., Leathwick, R., Lohmann, G., Loiselle, A., Overton, C.M., Phillips, J., Schapire, E., Soberon, J., Wisz, S. & Zimmermann, E. (2006) Novel methods improve prediction of species' distributions from occurrence data. *Ecography*, **29**, 129-151.

- Excoffier, L., Smouse, P.E. & Quattro, J.M. (1992) Analysis of molecular variance inferred from metric distances among DNA haplotypes: application to human mitochondrial DNA restriction data. *Genetics*, **131**, 479-491.
- Falush, D., Stephens, M. & Pritchard, J.K. (2007) Inference of population structure using multilocus genotype data: dominant markers and null alleles. *Molecular Ecology Notes*, **7**, 574-578.
- Fielding, A.H. & Bell, J.F. (1997) A review of methods for the assessment of prediction errors in conservation presence/absence models. *Environmental Conservation*, **24**, 38-49.
- Franklin, I.R. (1980) Evolutionary change in small populations. In: *Conservation Biology: An Evolutionary-Ecological Perspective* (eds. M.E. Soulé and B.A. Wilcox), pp. 135-149. Sinauer Associates, Inc., Sunderland, MA.
- Garcia-Ramos, G. & Kirkpatrick, M. (1997) Genetic models of adaptation and gene flow in peripheral populations. *Evolution*, **51**, 21-28.
- Glesener, R.R., Tilman, D., Naturalist, T.A. & Aug, N.J. (1978) Sexuality and the Components of Environmental Uncertainty : Clues from Geographic Parthenogenesis in Terrestrial Animals. *The American Naturalist*, **112**, 659-673.
- Gray, M.M. & Weeks, S.C. (2001) Niche breadth in clonal and sexual fish (*Poeciliopsis*): a test of the frozen niche variation model. *Canadian Journal of Fisheries and Aquatic Sciences*, **58**, 1313-1318.
- Haack, L., Simon, J.C., Gauthier, J.P., Plantegenest, M. & Dedryver, C.A. (2000) Evidence for predominant clones in a cyclically parthenogenetic organism provided by combined. *Molecular Ecology*, **9**, 2055-2066.
- Haag, C.R. & Ebert, D. (2004) A new hypothesis to explain geographic parthenogenesis. *Ann. Zool. Fennici*, **41**, 539-544.
- Hamilton, W.D. (1980) Sex versus non-sex versus parasite. *Oikos*, **35**, 282-290.
- Hasumi, H. & Emori, S. (2004) K-1 Coupled GCM (MIROC) Description. In. Center for Climate System Research (CCSR), Tokyo.
- Hijmans, R.J., Guarino, L. & Mathur, P. (2012) *DIVA-GIS v.7.5*. Available at: <http://www.diva-gis.org/>.
- Hijmans, R.J., Cameron, S.E., Parra, J.L., Jones, P.G. & Jarvis, A. (2005) Very high resolution interpolated climate surfaces for global land areas. *International Journal of Climatology*, **25**, 1965-1978.

- Hugall, A., Moritz, C., Moussalli, A. & Stanistic, J. (2002) Reconciling paleodistribution models and comparative phylogeography in the Wet Tropics rainforest land snail *Gnarosiphia bellendenkerensis* (Brazier 1875). *Proceedings of the National Academy of Sciences of the United States of America*, **99**, 6112-7.
- Hunter, K.L., Betancourt, J.L., Riddle, B.R., Van Devender, T.R., Cole, K.L. & Spaulding, W.G. (2001) Ploidy race distributions since the Last Glacial Maximum in the North American desert shrub, *Larrea tridentata*. *Global Ecology and Biogeography*, **10**, 521-533.
- Hutchinson, G.E. (1957) Concluding Remarks. *Population Studies: Animal Ecology and Demography. Cold Spring Harbor Symposia on Quantitative Biology*, **22**, 127-415.
- IUCN (2010) *IUCN Red List of Threatened Species. Version 2010.1*. Available at: www.icunredlist.org (accessed 10/11/2010).
- Jensen, L.H., Enghoff, H., Frydenberg, J., Parker Jr., E.D. & Parker, E.D. (2002) Genetic diversity and the phylogeography of parthenogenesis: comparing bisexual and thelytokous populations of *Nemasoma varicorne* (Deplopoda: Nemasomatidae) in Denmark. *Hereditas*, **136**, 184-194.
- Jiménez-Valverde, A. & Lobo, J.M. (2007) Threshold criteria for conversion of probability of species presence to either–or presence–absence. *Acta Oecologica*, **31**, 361-369.
- Kearney, M. (2005) Hybridization, glaciation and geographical parthenogenesis. *Trends in Ecology & Evolution*, **20**, 495-502.
- Kearney, M. & Shine, R. (2004) Morphological and physiological correlates of hybrid parthenogenesis. *The American Naturalist*, **164**, 803-813.
- Kearney, M., Fujita, M.K. & Ridenour, J. (2009) Lost Sex in the Reptiles: Constraints and Correlations. *Lost Sex: The Evolutionary Biology of Parthenogenesis* (ed. by I. Schön, K. Martens and P. Dijk), pp. 447-474. Springer Netherlands, Dordrecht.
- Kearney, M.R., Moussalli, A., Strasburg, J., Kindenmayer, D. & Moritz, C. (2003) Geographic parthenogenesis in the Australian arid zone I. A climatic analysis of the *Heteronotia binoei* complex (Gekkonidae). *Evolutionary Ecology Research*, **5**, 953-976.
- Keller, L.F. & Waller, D.M. (2002) Inbreeding effects in wild populations. *Trends in Ecology & Evolution*, **17**, 230-241.
- Knowles, L.L. & Maddison, W.P. (2002) Statistical phylogeography. *Molecular Ecology*, **11**, 2623-2635.

- Knowles, L.L., Carstens, B.C. & Keat, M.L. (2007) Coupling genetic and ecological-niche models to examine how past population distribution contribute to divergence. *Current Biology*, **17**, 940-946.
- Leaché, A.D. & Reeder, T.W. (2002) Molecular systematics of the eastern fence lizard (*Sceloporus undulatus*): a comparison of parsimony, likelihood, and Bayesian approaches. *Systematic biology*, **51**, 44-68.
- Leaché, A.D. & Mulcahy, D.G. (2007) Phylogeny, divergence times and species limits of spiny lizards (*Sceloporus magister* species group) in western North American deserts and Baja California. *Molecular Ecology*, **15**, 5216-5233.
- Levin, D.A. (1975) Pest pressure and recombination systems in plants. *American Naturalist*, **109**, 437-451.
- Liu, C., Berry, P.M., Dawson, T.P. & Pearson, R.G. (2005) Selecting thresholds of occurrence in the prediction of species distributions. *Ecography*, **28**, 385-393.
- Loiselle, B.A., Howell, C.A., Graham, C.H., Goerck, J.M., Brooks, T., Smith, K.G. & Williams, P.H. (2003) Avoiding pitfalls of using species distribution models in conservation planning. *Conservation Biology*, **17**, 1591-1600.
- Lutes, A.A., Neaves, W.B., Baumann, D.P., Wiegraebe, W. & Baumann, P. (2010) Sister chromosome pairing maintains heterozygosity in parthenogenetic lizards. *Nature*, **464**, 283-286.
- Lynch, M. (1984) Destabilizing hybridization, general-purpose genotypes and geographic parthenogenesis. *Quarterly Review of Biology*, **59**, 257-290.
- Marshall, N.R. & Reeder, T. (2005) *Phylogenetics and Historical Biogeography of the Tiger Whiptail Lizard, *Aspidoscelis tigris**. San Diego State University, San Diego.
- Maynard Smith, J. (1978) *The Evolution of Sex*. Cambridge University Press, MA.
- Moore, W.S. (1984) Evolutionary ecology of unisexual fishes. In: *Evolutionary Genetics of Fishes* (ed. B.J. Turner), pp. 329-398. Plenum Press, New York.
- Moritz, C. & Bi, K. (2011) Spontaneous speciation by ploidy elevation: Laboratory synthesis of a new clonal vertebrate. *Proceedings from the National Academy of Sciences of the United States of America*, **108**, 9733-9734.
- Moritz, C.C., Wright, J.W. & Brown, W.M. (1989) Mitochondrial-DNA analyses and the origin and relative age of parthenogenetic lizards (genus *Cnemidophorus*). III. *C. velox* and *C. exsanguis*. *Evolution*, **43**, 958-968.

- Mulcahy, D.G. (2008) Phylogeography and species boundaries of the western North American Nightsnake (*Hypsiglena torquata*): Revisiting the subspecies concept. *Molecular Phylogenetics and Evolution*, **46**, 1095-1115.
- Otto-Bliesner, B.L., Marshall, S.J., Overpeck, J.T., Miller, G.H., & Hu, A. (2006) Simulating Arctic climate warmth and icefield retreat in the last Interglaciation. *Science*, **311**, 1751-1753.
- Otto, S. & Whitton, J. (2000) Polyploid incidence and evolution. *Annual review of genetics*, **34**, 401-437.
- Parker Jr., E.D., Selander, R.K., Hudson, R.O. & Lester, L.J. (1977) Genetic diversity in colonizing parthenogenetic cockroaches. *Evolution*, **31**, 836-842.
- Paulissen, M. (2001) Ecology and behavior of lizards of the parthenogenetic *Cnemidophorus laredoensis* complex and their gonochoristic relative *Cnemidophorus gularis*: Implications for coexistence. *Journal of Herpetology*, **35**, 282-292.
- Pearson, R.G., Raxworthy, C.J., Nakamura, M. & Townsend Peterson, A. (2007) Predicting species distributions from small numbers of occurrence records: a test case using cryptic geckos in Madagascar. *Journal of Biogeography*, **34**, 102-117.
- Peck, J., Yearsley, J. & Waxman, D. (1998) Explaining the geographic distributions of sexual and asexual populations. *Nature*, **391**
- Pellmyr, O., Segraves, K.A., Althoff, D.M., Balcazar-Lara, M. & Leebens-Mack, J. (2007) The phylogeny of yuccas. *Molecular Phylogenetics and Evolution*, **43**, 493-501.
- Peterson, A.T. & Nyári, A.S. (2007) Ecological niche conservatism and Pleistocene refugia in the Thrush-like Mourner, *Schiffornis* sp., in the neotropics. *Evolution*, **62**, 173-83.
- Phillips, S.J. & Dudik, M. (2008) Modeling of species distributions with Maxent: new extensions and a comprehensive evaluation. *Ecography*, **31**, 161-175.
- Phillips, S.J., Anderson, R.P. & Schapire, R.E. (2006) Maximum entropy modeling of species geographic distributions. *Ecological Modelling*, **190**, 231-259.
- Price, A.H., Lapointe, J.L. & Atmar, J.W. (1993) The ecology and evolutionary implications of competition and parthenogenesis in *Cnemidophorus*. In: *Biology of the Whiptail Lizards (Genus Cnemidophorus)* (eds. J.W. Wright and L.J. Vitt), pp. 371-410. Oklahoma Museum of Natural History, Norman, Oklahoma.
- Pritchard, J.K., Stephens, M. & Donnelly, P. (2000) Inference of population structure using multilocus genotype data. *Genetics*, **155**, 945-959.

- Pulliam, H.R. (2000) On the relationship between niche and distribution. *Ecology Letters*, **3**, 349-361.
- Real, L.A., Levin, S.A. & Brown, J.H. (1991) The role of theory in the rise of modern ecology. In: *Foundations of Ecology: Classic Papers with Commentaries*, pp. 177-191. The University of Chicago Press, Chicago.
- Reeder, T.W., Cole, C.J. & Dessauer, H.C. (2002) Phylogenetic relationships of whiptail lizards of the genus *Cnemidophorus* (Squamata: Teiidae): a test of monophyly, reevaluation of karyotypic evolution, and review of hybrid origins. *American Museum Novitates*, **3365**, 1-61.
- Rios, N.E. & Bart, J., Henry L. (2010) *GEOLocate. Georeferencing software for natural history collections*. Tulane University Museum of Natural History.
- Rissler, L.J. & Apodaca, J.J. (2007) Adding more ecology into species delimitation: ecological niche models and phylogeography help define cryptic species in the black salamander (*Aneides flavipunctatus*). *Systematic Biology*, **56**, 924-942.
- Rondinini, C., Wilson, K.a., Boitani, L., Grantham, H. & Possingham, H.P. (2006) Tradeoffs of different types of species occurrence data for use in systematic conservation planning. *Ecology letters*, **9**, 1136-45.
- Schultz, R.J. (1969) Hybridization, unisexuality, and polyploidy in the Teleost *Poeciliopsis* (*Poeciliidae*) and other vertebrates. *The American Naturalist*, **103**, 605-619.
- Semlitsch, R.D., Hotz, H. & Guex, G.-D. (1997) Competition among tadpoles of coexisting hemiclones of hybridogenetic *Rana esculenta* : support for the Frozen Niche Variation model. *Evolution*, **51**, 1249-1261.
- Simon, J., Delmotte, F., Rispe, C. & Crease, T. (2003) Phylogenetic relationships between parthenogens and their sexual relatives: the possible routes to parthenogenesis in animals. *Biological Journal of the Linnean Society*, **79**, 151-163.
- Soberón, J. & Peterson, A.T. (2005) Interpretation of models of fundamental ecological niches and species' distributional areas. *Biodiversity Informatics*, **2**, 1-10.
- Soulé, M.E. (1980) Thresholds for survival: maintaining fitness and evolutionary potential. In: *Conservation Biology: An Evolutionary-Ecological Perspective* (eds. M.E. Soulé and B.A. Wilcox), pp. 151-169. Sinauer Associates, Inc., Sunderland, MA.
- Stebbins, R.C. (2003) *Western Reptiles and Amphibians. Peterson Field Guides*. Houghton Mifflin Company, New York.

- Sullivan, B.K., Hamilton, P.S., Kwiatkowski, M.A., Arizona, T. & Whiptail, S. (2005) The Arizona Striped Whiptail : Past and Present. pp. 145-148. USDA Forest Service Proceedings RMRS-P-36
- Swofford, D.L. (2002) *PAUP* phylogenetic analysis using parsimony (*and other methods)*. Sinauer Associates.
- Templeton, A.R. (2004) Statistical phylogeography: methods of evaluating and minimizing inference errors. *Molecular Ecology*, **13**, 789-809.
- Thompson, R.S. & Anderson, K.H. (2000) Biomes of western North America at 18,000, 6000 and 0 14C yr bp reconstructed from pollen and packrat midden data. *Journal of Biogeography*, **27**, 555-584.
- Thompson, R.S., Whitlock, C., Bartlein, P.J., Harrison, S.P. & Spaulding, W.G. (1994) Climatic Changes in the Western United States since 18,000 yr B.P. In: *Global Climates Since the Last Glacial Maximum* (eds. H. Wright Jr., J. Kutzbach, T. Webb Iii, W. Ruddiman, F. Street-Perrott and P. Bartlein), pp. 468-513. University of Minnesota Press, Minneapolis, Minnesota.
- Van Doninck, K., Schön, I., De Bruyn, L. & Martens, K. (2002) A general purpose genotype in an ancient asexual. *Oecologia*, **132**, 205-212.
- Vandel, A. (1928) La parténogenèse géographique. Contribution à l'étude biologique et cytologique de la parténogenèse naturelle. *Bulletin Biologique de la France et de la Belgique*, **62**, 164-281.
- VanDerWal, J., Shoo, L.P., Graham, C. & Williams, S.E. (2009) Selecting pseudo-absence data for presence-only distribution modeling: How far should you stray from what you know? *Ecological Modelling*, **220**, 589-594.
- Vekemans, X., Beauwens, T., Lemaire, M. & Roldán-Ruiz, I. (2002) Data from amplified fragment length polymorphism (AFLP) markers show indication of size homoplasy and of a relationship between degree of homoplasy and fragment size. *Molecular ecology*, **11**, 139-51.
- Vrijenhoek, R.C. (1989) Genetic and ecological constraints on the origins and establishment of unisexual vertebrates. In: *Evolution and Ecology of Unisexual Vertebrates* (eds. R.M. Dawley and J.P. Bogart), pp. 24-31. New York State Museum, Albany, NY.
- Vrijenhoek, R.C. (2006) Polyploid Hybrids: Multiple Origins of a Treefrog Species. *Current Biology*, **16**, R245-R247.
- Vrijenhoek, R.C.R. (1998) Animal clones and diversity. *Bioscience*, **48**, 617-628.

- Waltari, E., Hijmans, R.J., Townsend Peterson, A., Nyári, Á.S., Perkins, S.L. & Guralnick, R.P. (2007) Locating Pleistocene refugia: comparing phylogenetic and ecological niche model predictions. *PLoS Biology*, **2**, e563.
- Warren, D.L. & Seifert, S.N. (2011) Ecological niche modeling in Maxent: the importance of model complexity and the performance of model selection criteria. *Ecological applications*, **21**, 335-342.
- White, M.J.D. (1978) *Modes of Speciation*. W. H. Freeman, San Francisco.
- Whitlock, M.C., Ingvarsson, P.R.K. & Hatfield, T. (2000) Local drift load and the heterosis of interconnected populations. *Heredity*, **84**, 452-457.
- Wolf, P. (2000) *AFLP Protocol*. Available at:
http://bioweb.usu.edu/wolf/aflp_protocol.htm (accessed August 30 2012).
- Wright, J.W. & Lowe, C.H. (1968) Weeds, polyploids, parthenogenesis, and the geographical and ecological distribution of all-female species of *Cnemidophorus*. *Copeia*, **1968**, 128-138.
- Wright, J.W. & Lowe, C.H. (1993) Synopsis of the subspecies of the Little Striped Whiptail Lizard, *Cnemidophorus inornatus* Baird. *Journal of the Arizona-Nevada Academy of Science*, **27**, 129-157.
- Wright, J.W. & Vitt, L.J. (1993) Evolution of the lizards of the genus *Cnemidophorus*. In: *Biology of the Whiptail Lizards (Genus Cnemidophorus)* (eds. J.W. Wright and L.J. Vitt), pp. 27-81. Oklahoma Museum of Natural History, Norman, Oklahoma.

CURRICULUM VITAE

Adam Bohrer Leland

School of Life Sciences
Graduate College
University of Nevada, Las Vegas
adam.leland@gmail.com

Education:

Ph.D. Candidate in Biology, University of Nevada, Las Vegas.

Dissertation: A comprehensive research framework for geographic parthenogenesis in whiptail lizards (genus *Aspidoscelis*)

Advisor: Dr. Brett Riddle

Committee Member: Dr. Dan Thompson

Committee Member: Dr. David Bradford

Graduate College Representative: Dr. Matthew Lachniet

Master of Science in Biology, San Diego State University; May 2007.

Dissertation: The population genetics of the orange-throated whiptail, *Aspidoscelis hyperythra*

Advisor: Dr. Leroy McClenaghan

Bachelor of Science in Biological Sciences, Bachelor of Arts in Physical Anthropology, University of California, San Diego; March 2002.

Research Experience:

Ecological niche congruence among co-distributed taxa in the Great Basin: Ecological niche model building and statistical assessment of similarity, GIS, statistics (PCA, MANOVA).

PhD Dissertation Research: Collection & preparation of specimens, DNA extraction and amplification, AFLP protocol, GIS, niche modeling, genetic and statistical analysis.

Master of Science Dissertation: Collection of reptile specimens, DNA extraction and amplification, genetic and statistical analysis. Sep 2002 to Jul 2005.

Primate Study: Dry Tropical Field Station, Ralleighvallen National Reserve, Suriname. Oct 1999 to Feb 2000.

Archeological Field School: Social Archeology and Early Metallurgy, Jebel Hamrat Fidan, Jordan, Jun 1999 to Aug 1999.

Professor: Dr. Tom Levy, Dept. of Anthropology, University of California, San Diego.

Teaching Experience:

TA: Federal GS-401 Fire Program for BLM rangeland firefighters, UNLV. Sep 2005 to May 2012.

Instructor: SAGE (Summer Advanced Gifted Education) Academy, UNLV (High school education). Global Topics in Biology (Course Name). Course design, instruction, and student evaluation. Jul 2007.

TA: SAGE (Summer Advanced Gifted Education) Academy, UNLV. Summer science course for high school students. Credit: 3 UNLV Honors Seminar units. Jul 2006.

TA: BIOL189 (Fundamentals of Life Science) Lab, UNLV. Jun 2006 and Jun 2007.

GA: Undergraduate Organismal Biology Lab Setup, SDSU. Sep 2002 to May 2005.

Funding:

UNLV Graduate & Professional Student Association Grants 07-09 (Total \$3,325); UNLV Graduate College Summer Session Fellowship 08 (Stipend \$6,000); ASIH Gaige Award 08 (\$500).

Abstracts, Publications and Presentations:

Leland, A. and B. R. Riddle. Geographic Parthenogenesis in Whiptail Lizards (genus *Aspidoscelis*). Presented to Federal GS-401 Fire Program, Mar 2011 & 2012.

Leland, A. and B.R. Riddle. Geographic Parthenogenesis in Whiptail Lizards (genus *Aspidoscelis*). Presented at the UNLV GPSA Symposium, Mar 2008.

Leland A., R. Fisher, and L. McClenaghan. The Population Genetics of the Orange-throated Whiptail *Aspidoscelis hyperythra*. Master's Thesis, San Diego State University. Spring, 2007.

Leland A., R. Fisher, and L. McClenaghan. Population Genetics of the Orange-throated Whiptail, *Aspidoscelis hyperythra*. Poster presentation at the 53rd annual meeting of the Southwestern Association of Naturalists in Colima, Col. Mexico. April 13-15, 2006.

Leland, A., R. Fisher, and L. McClenaghan. Population and Conservation Genetics of the Orange-throated Whiptail, *Aspidoscelis hyperythra*, in a Fragmented Landscape. Presented at the UNLV BIOS Symposium. November 5, 2005.